

NUMERICAL INVESTIGATION OF TOP-SEAT ANGLE  
CONNECTIONS AT ELEVATED TEMPERATURES

LEONG SIONG HEAN

UNIVERSITY OF MALAYA

THESIS SUBMITTED IN FULFILLMENT OF THE  
REQUIREMENTS FOR THE DEGREE OF  
MASTER OF ENGINEERING SCIENCE

FACULTY OF ENGINEERING  
UNIVERSITY OF MALAYA  
KUALA LUMPUR

2013

# UNIVERSITI MALAYA

## ORIGINAL LITERARY WORK DECLARATION

Name of Candidate: *LEONG SIONG HEAN* (I.C/Passport No:

Registration/Matric No: *KGA 080083*

Name of Degree: *MASTER OF ENGINEERING SCIENCE*

Title of Project Paper/Research Report/Dissertation/Thesis ("this Work"):  
*NUMERICAL INVESTIGATION OF TOP-SEAT ANGLE CONNECTIONS  
AT ELEVATED TEMPERATURES*

Field of Study: *STEEL STRUCTURE*

I do solemnly and sincerely declare that:

- (1) I am the sole author/writer of this Work;
- (2) This Work is original;
- (3) Any use of any work in which copyright exists was done by way of fair dealing and for permitted purposes and any excerpt or extract from, or reference to or reproduction of any copyright work has been disclosed expressly and sufficiently and the title of the Work and its authorship have been acknowledged in this Work;
- (4) I do not have any actual knowledge nor do I ought reasonably to know that the making of this work constitutes an infringement of any copyright work;
- (5) I hereby assign all and every rights in the copyright to this Work to the University of Malaya ("UM"), who henceforth shall be owner of the copyright in this Work and that any reproduction or use in any form or by any means whatsoever is prohibited without the written consent of UM having been first had and obtained;
- (6) I am fully aware that if in the course of making this Work I have infringed any copyright whether intentionally or otherwise, I may be subject to legal action or any other action as may be determined by UM.

Candidate's Signature

Date

Subscribed and solemnly declared before,

Witness's Signature

Date

Name:

Designation:

## ABSTRACT

Significant studies have been conducted for beams and columns in fire. However, studies of connections in fire is comparatively less, although being the more critical component in a steel structure. In addition, the behavior of top-seat angle connection type is still not fully understood in an elevated temperature conditions and subsequently the effect of axial loadings due to steel expansion in fire have also yet to be studied. Very limited experimental data was available for top-seat angle at elevated temperature, which resulted in limited design guideline for this type of connection.

Thus, a finite element model for top-seat angle connection at elevated temperature is developed in this study using ANSYS Workbench and validated with existing test results. Models geometry was developed in Solidworks, which was then imported into Hypermesh for the meshing process, followed by detail analysis in ANSYS Workbench. Non-linear behavior of the materials was modeled with the definition of elastic-plastic multi-linear properties and frictional contact between surfaces is included to simulate actual connection behavior. 3D Solid Elements was used in the model. Elevated temperature models are analyzed using the Static Structural option which is shown to be able to simulate elevated temperature conditions.

The validation of the ambient temperature models shows that the parameters and techniques used are accurate and in good agreement with experimental results. The validated ambient temperature models are further used for parametric studies on the effect of seat angles, gaps and angle length.

Comparison of models at elevated temperature with experimental data shows that the model is in good agreement with existing behavior results of top-seat angle connection tests and therefore the model is used for further study on the effect of axial restraints towards connection behavior. For ambient temperature conditions, Increase in axial restraints has been shown to increase connection capacity while the stiffness remains similar for low axial levels, where at 10% axial restraint, the corresponding moment capacity is increased by 89% and 10% in axial release relates to the same amount in capacity reduction. On the other hand, the shrinkage of the beam, may lead to axial releases, causing axial “pulling” on the connection caused by the catenary action of beams under loads, resulting in higher deformation and different deformation patterns of the connection.

Axial release under anisothermal conditions leads to a 28% reduction in resistive temperatures for 10% in axial release levels. In terms of isothermal conditions, the axial restraints are increased by 60% at the lowest temperature for 10% axial restraint and 300% increase of moment capacity under elevated temperature of 600°C. Comparisons with the guidelines provided by EC3 has also been made and the study show that the design guidelines needs further verifications, on parameters including the gap effect, seat angle effect, axial loading design and the angle section length used.

## ABSTRAK

Penyiasatan serta kajian yang menyeluruh telah pernah dijalankan terhadap rasuk dan tiang keluli dalam keadaan suhu yang tinggi iaitu dalam kebakaran, namun, penyelidikan mengenai sambungan keluli adalah kurang jika dibandingkan, walaupun sambungan keluli tersebut adalah komponen yang dikira kritikal untuk struktur keluli. Tambahan pula, kelakuan bagi sambungan angle connections atau sambungan yang menggunakan bahagian berbentuk 'L' masih tidak difahami sepenuhnya dalam kes kebakaran dan ini membawa pula bahawa kelakuan angle connections kesan daripada beban aksi daripada kesan pengembangan besi juga masih belum dikaji.

Dengan itu, model finite-element telah dalam keadaan suhu tinggi telah dibangunkan menggunakan perisian ANSYS Workbench dan telah disahkan dengan hasil ujikaji yang telah dijalankan oleh penkaji yang lain. Model terlebih dahulu dibangunkan dalam perisian Solidworks yang kemudian dieksport ke perisian Hypermesh bagi tujuan *meshing* dan seterusnya diikuti pula dengan pengeksportan model ke perisian ANSYS Workbench. Kelakuan bahan keluli yang mulur telah diambil kira dengan definasi bahan yang merangkumi bahagian elastik dan plastik bahan keluli tersebut serta pekali geseran antara permukaan seperti yang berlaku dalam keadaan sebenarnya. Analisis model dalam keadaan suhu tinggi telah dijalankan menggunakan *Static Structural* dan ini telah ditunjuk dapat mensimulasi keadaan suhu tinggi sebenar.

Model yang dibangunkan disahkan dapat mensimulasi keadaan ujikaji yang sebenar dan ini menunjukkan bahawa parameter dan anggapan yang digunakan adalah sesuai. Model yang telah disahkan itu juga digunakan bagi mengkaji kesan bentuk 'L' bawah sambungan terhadap kelakuan sambungan termasuk kesan ketebalan, panjang yang digunakan serta kesan ruang antara rasuk dan tiang. Hasil kajian menunjukkan pengagihan daya dalam sambungan tersebut memerlukan penyelidikan yang lebih lanjut.

Setelah model disahkan dalam keadaan suhu persekitaran, model tersebut diubahsuai dan memenuhi keadaan yang telah dilaporkan untuk ujikaji sambungan dalam keadaan suhu tinggi. Perbandingan kelakuan model menunjukkan bahawa kelakuan dalam ujikaji serta model adalah sesuai. Ini pula diteruskan dengan penyelidikan mengenai kesan beban paksi terhadap jenis sambungan yang dimaksudkan. Dalam keadaan suhu persekitaran, peningkatan dalam beban paksi menyebabkan kekerasan awal kelakuan sambungan serta kapasiti momen turut meningkat sebanyak 89% dengan peningkatan beban paksi sebanyak 10%.

Dalam keadaan *anisothermal*, suhu yang dapat ditanggung berkurang sebanyak 28% bagi beban paksi positif 10%. Perbandingan turut dijalankan dengan garis panduan oleh EC3 dan telah ditunjukkan bahawa parameter seperti kesan ruang, kesan 'L' bawah sambungan, kesan beban paksi serta panjang yang digunakan memerlukan pengesahan lanjut.

## ACKNOWLEDGEMENT

During this study, countless parties have assisted the author, whether in terms of moral support, financial or knowledge sharing. First and foremost, would like to express gratitude to my supervisor for this study, Dr Norhafizah Ramli Bt. Sulong. It is with her knowledge and expertise that I may complete this study successfully. With her guide, this study is improved and made more valuable for the colleagues in this field. Her teaching is greatly appreciated and remembered.

Second, would like to express gratitude to all the colleagues during the course of this study especially: Mahdi Shahriati, Yew Ming Chian and Noraini Ajit. They have provided with all the information, knowledge and some, assisting in completing the minor tasks involved in the completion of this study.

Also to my parents who have supported my studies morally throughout these years. Their advice and support has given me the perseverance to complete the study all these years. Lastly to all parties who have also provided me with assistance through the duration of the study, but not mentioned here, I would like to express my thanks.

## TABLE OF CONTENTS

<b>TITLE PAGE</b>	
<b>ORIGINAL WORK DECLARATION</b>	ii
<b>ABSTRACT</b>	iii
<b>ABSTRAK</b>	v
<b>ACKNOWLEDGEMENT</b>	vii
<b>TABLE OF CONTENTS</b>	viii
<b>LIST OF TABLES</b>	xi
<b>LIST OF FIGURES</b>	xii
<b>LIST OF SYMBOLS</b>	xvii
<b>CHAPTER 1: INTRODUCTION</b>	
1.1 Introduction	1
1.2 Problem Statement	3
1.3 Scope of Study	4
1.4 Research Objectives	5
1.5 Layout of the Thesis	5
1.6 Significance of Study	7
<b>CHAPTER 2: LITERATURE REVIEW</b>	
2.1 Introduction	9
2.2 Design of Joints in EC3: Part 1-8	12
2.3 Steel Material Behavior at Elevated Temperatures	18
2.4 Previous Studies on Connections at Ambient Temperature	22
2.4.1 Experimental Studies	23
2.4.2 Empirical Models	26
2.4.3 Analytical Models	28
2.4.4 Component Based Method	30
2.4.5 Finite Element Models	33
2.5 Connection in Elevated Temperature Studies	38
2.5.1 Experimental Studies at Elevated Temperatures	38
2.5.2 Finite Element Studies for Elevated Temperature	40
2.5.3 Analytical Studies	45
2.5.4 Component Method	48

2.6	Concluding Remarks	52
-----	--------------------	----

### **CHAPTER 3: METHODOLOGY**

3.1	Introduction	54
3.2	Geometrical Models - Solidworks	56
3.2.1	Creating Parts	57
3.2.2	Parts Assembly	58
3.3	Meshing in Hypermesh	60
3.3.1	Hypermesh Models	61
3.4	ANSYS Workbench Basics	63
3.4.1	Material Properties Considerations	67
3.4.2	Ambient Temperature Models	67
3.4.3	Elevated Temperature Models	69
3.5	Element Types	72
3.5.1	SOLID187	73
3.5.2	SOLID186	73
3.5.3	SOLID185	74
3.5.4	CONTA174 and TARGE170	74
3.5.5	PRETS179	75
3.6	Contacts Definition	76
3.6.1	Coefficient of Friction	76
3.6.2	Contact Settings	77
3.7	Loading Conditions	80
3.7.1	Direct Loads	81
3.7.2	Applying Pretension Loads	81
3.7.3	Temperature Loads	84
3.8	Boundary Condition	85
3.9	Model Simplifications	87
3.10	Analysis Convergence Method	88
3.11	Post-processing	90

### **CHAPTER 4: RESULTS & DISCUSSION**

4.1	Introduction	91
4.2	Validation Studies	91
4.2.1	Ambient Temperature Conditions	91

4.2.1.1	T-Stub Models	92
4.2.1.2	Connection model based on Azizinamini (1982)	97
4.2.1.3	Connection model based on Komuro et al. (2003)	104
4.2.1.4	Connection model based on Kukreti and Abomaali (1999)	108
4.2.2	Elevated Temperature Models	112
4.2.2.1	Beam Behavior at Elevated Temperatures	113
4.2.2.2	Validation of Joint Model at Elevated Temperatures	117
4.3	Parametric Studies at Ambient Temperature	128
4.3.1	Effect of Seat Angle	134
4.3.1.1	Effect of Seat Angle Thickness	135
4.3.1.2	Effect of Seat Angle Gauge Length	137
4.3.1.3	Effect of Seat Angle Bolt Rows	139
4.3.2	Effect of Gap	140
4.3.3	Effect Angle Length	143
4.3.4	Effect of Coefficient of Friction	145
4.3.5	Effect of Contact Settings	146
4.3.6	Effect of Axial Loadings At Ambient Temperature	149
4.4	Parametric Studies at Elevated Temperature	154
4.4.1	Connection Behavior at Isothermal Conditions	154
4.4.2	Effect of Axial Loadings	161
4.4.2.1	Anisothermal Temperature Conditions	161
4.4.2.2	Isothermal Temperature Conditions	168
4.4.3	Effect of Pretension Loads	172
4.5	Design Implications	176
4.5.1	Seat Angle Design Effect	177
4.5.2	Axial Loading Design Effect	180
4.5.3	Angle Length Design Effect	183
4.5.4	Gap Design Effect	185
4.5.5	Implications on Designs Summary	187
4.6	Concluding Remarks	189
<b>CHAPTER 5: CONCLUSION &amp; RECOMMENDATIONS</b>		
5.1	Conclusion	191
5.2	Recommendations	194
<b>REFERENCES</b>		196

## LIST OF TABLES

<b>Table</b>	<b>Title</b>	<b>Page</b>
2.1	Example of basic Components for a Connection	15
2.2	Components considered for top-seat angle analysis	16
2.3	Temperature distribution ratio for components at elevated temperatures.	21
2.4	Reduction factors for steel at various temperatures	22
3.1	Elements used in previous studies	60
3.2	Reduction factors for steel at various temperatures	70
3.3	Material curve definition formula	70
4.1	Geometrical Properties of the T-Sub Validation Model	94
4.2	Mechanical properties of steel materials for T-stub Model	94
4.3	Mesh criteria for model	94
4.4	Geometrical properties of steel materials for Model	98
4.5	Mesh criteria for model	99
4.6	Steel Members for the model	104
4.7	Mechanical properties of steel materials for the model	104
4.8	Mesh criteria for model	107
4.9	Steel members for the model	108
4.10	Mechanical properties of steel materials for the model	108
4.11	Mesh criteria for model	109
4.12	Material properties of concrete used in the model	115
4.13	Details of the models in elevated temperatures	118
4.14	Mesh criteria for models	123
4.15	Summary of angle length study models	143
4.16	Contact Settings Locations	148
4.17	Reduction factors under elevated temperatures	160
4.18	T-Stub Failure Mode Computation for Angle Connections	184
4.19	Moment capacity of Joints with different angle lengths	185
4.20	Implications of the model results to EC3	187

## LIST OF FIGURES

<b>Table</b>	<b>Title</b>	<b>Page</b>
2.1	Common Steel Connection Configurations	11
2.2	Typical moment-rotation curves for various connections type	12
2.3	Simplified bi-linear graph of moment-rotation curves	13
2.4	Flange angle analysis as T-stub	16
2.5	T-stub failure modes	17
2.6	Determination of $e_{min}$ and $m$ .	18
2.7	Relative Elongation of carbon steels as a function of temperatures	19
2.8	Thermal Conductivity of steels as a function of temperature	20
2.9	EC3 Component Model	32
2.10	Example of Finite Element Model	33
2.11	Analysis results of Finite Element Model	41
2.12	Dog-bone shaped beam deformation	45
2.13	An example of component model	49
2.14	General force-deformation graph for connection components	50
3.1	General flow of Modeling Procedure	55
3.2	General Flow of Study	56
3.3	Modeling solids in Solidworks	58
3.4	Example of connecting parts selection in Solidworks	59
3.5	Complete Bolted Connection Assembly in Solidworks	59
3.6	Meshing Differences	62
3.7	Meshing of bolt using Hypermesh	62
3.8	Main Window screen of ANSYS Workbench	64
3.9	Analysis Component List	65

<b>Table</b>	<b>Title</b>	<b>Page</b>
3.10	Main analysis setup interface and critical interface aspects	66
3.11	Typical Stress-strain behavior of steel material.	67
3.12	Typical initial stress-strain curve of Steel Behavior	68
3.13	Trilinear Material Properties Adopted	68
3.14	Stress-strain curve for steel in elevated temperatures	71
3.15	Comparison of EC3: Part 1-2 and material model of this study	71
3.16	Representation of SOLID187 element	73
3.17	Representation of SOLID 186 element	73
3.18	Representation of CONTA174 element	74
3.19	Representation of TARGE170 element	75
3.20	Representation of PRETS179 element	76
3.21	Selection methods bolt pretension	83
3.22	Coordinate systems for pretension of bolts	84
3.23	Options for pretension definitions	84
3.24	Default ANSYS Support options	86
3.25	Model symmetry applications	88
3.26	Newton-Rhapson method used by ANSYS	89
3.27	Example force convergence plot of ANSYS Workbench	89
4.1	Geometrical Reference of the T-Sub Validation Model	95
4.2	Boundary and loading conditions of the T-stub validation model.	95
4.3	Mesh pattern of the model	96
4.4	Comparison of the model and Specimen S4	96
4.5	Mechanical properties of steel materials for the model	98
4.6	Geometrical properties of steel sections for the model	99
4.7	Boundary and loading conditions of the model	101

<b>Table</b>	<b>Title</b>	<b>Page</b>
4.8	Mesh pattern of the model	101
4.9	Behavior of model compared to Specimen AS1	102
4.10	Plastic strain distributions at the top angle of model	102
4.11	Deformation of Components and Stress distribution of the model	103
4.12	Geometrical properties of steel materials for the model	105
4.13	Boundary conditions and displacement load for the model	106
4.14	Resulting mesh pattern for the model	106
4.15	Behavior of model compared to Specimen W00	107
4.16	Geometrical properties of steel materials for model	109
4.17	Loading and boundary conditions of the model	110
4.18	Meshing pattern result for the model	111
4.19	Behavior of model and TS6	111
4.20	Stress pattern comparison for bolts	112
4.21	Material properties of steel used in the model	115
4.22	Mesh pattern of the model	116
4.23	Loading and Boundary Conditions of the model	116
4.24	Comparison between the model and test results	117
4.25	Material Models for Elevated Temperature Models of Steel	119
4.26	Material Models for Elevated Temperature Models of Steel Bolts	119
4.27	Sample of the simplified material properties adopted in the model	120
4.28	Meshing result for bolts	121
4.29	Meshing results Steel Sections	121
4.30	Typical boundary conditions of elevated temperature models	122
4.31	Typical thermal loading areas applied on the models	123
4.32	Behavior of Model ELM3 compared to test S3	125

<b>Table</b>	<b>Title</b>	<b>Page</b>
4.33	Behavior of Model ELM4 compared to test S4	125
4.34	Behavior of Model ELM9 compared to test S9	126
4.35	Stress pattern for ELM3 at 600°C	127
4.36	Top angle bolt stress for models at elevated temperature	129
4.37	Top Angle Plastic Deformation patterns of models at elevated temperatures	130
4.38	Top Angle Stress patterns of Models at elevated temperatures	131
4.39	Bottom Angle Stress patterns of models at elevated temperature	132
4.40	Bottom angle bolt stress of models at elevated temperatures	133
4.41	Illustration of the effect of seat angle concept	134
4.42	Effect of Bottom Angle Thickness	136
4.43	Effect of Increased Gage Length at Bottom Angle	138
4.44	Effect of Decreased Gage Length at Bottom Angle	138
4.45	Reduced Bolt Row comparisons	139
4.46	Effect of Reduced Bolt Row at Seat Angle	140
4.47	Effect of Gap values on the behavior of connection	141
4.48	Deformation of Seat Angle for reduced gap (6.35mm) model	142
4.49	Comparison of top angle deformation for effect of gap	142
4.50	Effect of Angle Length on Connection Behavior	144
4.51	Plastic Deformation Pattern due to Effect of Angle Length	145
4.52	Effect of Coefficient of Friction	146
4.53	Effect of Contact Settings on connection	148
4.54	Slip of bottom angle – column leg bolt under frictionless contact	149
4.55	Plastic Deformation at Ambient Models under 10% Axial Loadings	152
4.56	Effect of Axial Restraint on Model AMS1	153

<b>Table</b>	<b>Title</b>	<b>Page</b>
4.57	Effect of Axial Release on Model AMS1	153
4.58	Model ELM3 Response under Isothermal conditions	155
4.59	Plastic Deformation Pattern under Isothermal Conditions	157
4.60	Stress Distribution Pattern under Isothermal Conditions	158
4.61	Comparison of isothermal behavior with Saedi and Yahyai	159
4.62	Effect of axial restraints on the connection with Method 1	163
4.63	Effect of axial release on the connection with Method 1	163
4.64	Effect of axial release on the connection with Method 2	164
4.65	Top Angle stress concentration of model ELM3 due to effect of axial loadings	166
4.66	Bottom Angle stress concentration of model ELM3 due to effect of axial loadings	167
4.67	Deformations of Angles at 10% Axial Release Method 2	168
4.68	Effect of axial restraints on Isothermal Model at 22°C	170
4.69	Effect of axial restraints on Isothermal Model at 600°C	171
4.70	Effect of axial restraints on Isothermal Model at 400°C	171
4.71	Behavior of Isothermal Models at 10% Axial Restraints	172
4.72	Plastic Regions for isothermal models at 10% Axial Restraints	173
4.73	Effect of Pretension on Anisothermal Model ELM3	175
4.74	Effect of Pretension on Ambient Temperature Models	175
4.75	Moment load distribution to EC3: Part 1-8 for flange cleat connections.	178
4.76	Determination of parameters $e_{min}$ and $m$	186

## LIST OF SYMBOLS

$d$	Beam-end displacement
$d_b$	Beam section depth
$\delta_t$	Beam displacement at top flange (y-direction)
$\delta_b$	Beam displacement at bottom flange (y-direction)
$E$	Elastic Modulus
$E_{a,\theta}$	Elastic Modulus of steel material at temperature $\theta$
$f_y$	Yield strength of steel material
$f_{y,\theta}$	Yield strength at temperature $\theta$
$f_{u,\theta}$	Ultimate strength at temperature $\theta$
$F_{Rd}$	Resistance Force
$k_i$	Component for component method as per EC3: Part 1-8
$k_{y,\theta}$	Reduction factor for yield strength
$k_{u,\theta}$	Reduction factor for ultimate strength
$L$	Length of beam
$t_a$	Thickness of angle section
$t_f$	Thickness of T-stub considered
$r_a$	Root radius of angle section
$\theta$	Rotation of joint

# CHAPTER 1

## INTRODUCTION

### 1.1 Introduction

Steel connections and members that are involved in an industrial structure are constantly exposed to the risk of fire. Steel being a good heat conductor and combined with reduction of steel strength with increasing heat, the design of the steel connections under elevated temperatures are relatively different. The possible failures could be different in fire compared to the connection behavior in ambient temperature due to the difference in material properties and behavior. A better understanding of the behavior of bare steel connections under elevated temperatures is vital for a more effective design of fire-protection system and thus leading to a more cost effective protection coverage.

For the same reason of construction cost effectiveness, a better understanding would also lead to less dependability on fire-protection systems and relying more on the capability of the structure itself, thus resulting in lower overall costs. The fire protection system serves as the additional deterrent to fire, further delaying failure times. Capability of the structure refers to continuity of the action between members in resisting loads while its strength is being degraded by fire. However, studies have shown that the connection is the among the weakest link for failure of a structure under fire conditions, as evident in the report by FEMA (2002). This highlights the basic need for a greater understanding for any type of steel connections that is being used in industrial structures where there is a risk of fire.

Effects of fire on steel connections are addressed in Eurocode 3 (EC3) by means of material degradation factors of the steel but relatively less on the connection design under anisothermal conditions. Further studies and research being conducted to understand connection behaviors under elevated temperatures such as those by Wang et al. (2007), Yu et al. (2009) and Mao et al. (2009).

For top-seat angle connection, crane time can be reduced as the member can be placed in position for the workers to complete the connection, while the crane is used elsewhere. Comparatively, the end-plate connections require that all bolts to be correctly fitted and tightened before the crane can be utilized for other members. In the construction point of view, this concept offers cost saving due to the less usage of crane time per connection and thus saving of the overall rental of the crane for the whole project. However, literature review shows that the available experimental tests on top-seat angle connections under elevated temperature conditions is limited to the study done by Saedi and Yahyai (2009a). Effect of axial restraints on the behavior of top seat angle connections, on the other hand, has not been done to date.

With the reasoning, this study focuses on the behavior of angle connections particularly the top-seat angle connections under fire conditions. Models are produced and validated against available experimental test results, at ambient temperature models and elevated temperature models. In an attempt to first understand the behavior of the connection, the validated models are used for further studies on the effect of seat angles, followed by the study on the effect of axial restraints.

## 1.2 Problem Statement

Fire poses a major critical effect to be considered for steel connections due to the relative rapid degradation of steel materials at high temperatures. Extensive studies have been conducted for steel beams and columns at elevated temperatures, however, studies have shown that there is still a considerable lack of studies for joints at elevated temperatures. Without doubt, there are various types of connection types possible with steel members due to flexibility of combination of bolts, plates and welding to form the connection to suit the purpose and site conditions. However, in comparison to the other common connection types, the angle connection, specifically the top-seat angle connection is relatively less understood as it is less studied. [ (Saedi and Yahyai, 2009a); (Saedi and Yahyai, 2009b); Yuan et al. (2011) ]

At elevated temperatures, a major effect to be considered includes the axial restraint of the beam and joints due to the surrounding adjacent members. Coupling of axial and moment at elevated temperature will reduce the capacity of the beam and joint. This results in the joint to govern the behavior of the beam, which justifies the study of the effect of axial restraints on the connection to be critical (Li et al, 2012). The best direction to cater for these gaps would be to conduct studies experimentally as actual testing mirrors the actual behavior of the connection. However, the cost to conduct these tests are often the main issue and therefore, the alternative would be to make use of computerized methods to simulate previous tests and conduct further studies from the verified models.

### 1.3 Scope of Study

With the gap in the code on the angle connections and on axial restraints in elevated temperatures, the research would focus on using Finite-Element Analysis (FEA) software to simulate the top-seat angle connections behavior. With correct modeling techniques and parameters, the finite element method is able to accurately simulate actual conditions. Behavior in elevated temperature condition involves an additional factor, temperature which has non-linear complexity by itself.

Therefore, to ensure that proper modeling has been used, a connection model is first verified with previous ambient temperature experimental tests. A FEA model is produced based on the available experimental test parameters and geometrical properties where the behavior is compared against the available results. Verified ambient temperature models are assumed to conclude that the methods, procedures, parameters and assumptions are considered to be applicable.

Procedures from the verified ambient model is then applied to a model with elevated temperatures according to experimental tests and compared with the experimental results to verify for the elevated temperature modeling procedures and methods. Geometrics of the verified model would be different from the elevated temperature model as it is uncommon to conduct elevated temperature tests that include ambient temperature models in the same study. Final verified model is applied with axial restraints at different levels and behavior of connection is studied as well as the variation of parameters. Following that, comparisons are being made with the results of the analysis and EC3 design guidelines.

#### **1.4 Research Objectives**

Main objective of study is to model top-seat angles connections under elevated temperatures and also to study the effect of axial restraints. Specifically, the objectives of this study are:-

1. To model the behavior of top-seat angle connections at elevated temperatures, including anisothermal and isothermal conditions using finite element analysis and validate with existing experimental results.
2. To examine the effect of different levels of axial restraints on top-seat angle connections behavior at elevated temperatures in anisothermal and isothermal conditions.
3. To investigate on the effect of various parameters on the connection behavior at ambient and elevated temperature conditions through parametric studies.
4. To relate the implication of the models with EC3 design guidelines.

#### **1.5 Layout of Thesis**

This thesis is divided into five main chapters, in which, Chapter One outlines the basis and foundations of the study. The introduction to the study, background of the study and also the objectives that the study is designed to achieve is laid out and explained in the chapter. This chapter also highlights the scope of works and the significance of the study being conducted.

Meanwhile, the summary of the previous studies and also the theoretical knowledge involved the study are covered in Chapter Two. Focus for the previous studies are on the conceptual and experimental works conducted. As there are various modeling techniques available for analysis of steel connections, the available techniques are discussed through individual sub-chapter/section. Considering that Finite Element analysis is mainly used in the study, the major part of the literature studies shall be on angle connections with finite element analysis, reviewing on the components for the finite element analysis and the application.

The process of modeling and procedures of modifications using the ANSYS software are reviewed in Chapter Three for the ambient and elevated temperature models. This would cover the geometrical modeling, meshing aspect, elements used, loading placement, thermal loads application and other aspects involved in the modeling while using ANSYS. As the chapter would be discussing on the procedural works, the results of the study can be attributed to the steps taken and therefore, any procedural / assumption error can then be modified in future studies.

Chapter Four aims to provide a clear understanding on the results obtained. Discussions on the results obtained from the analysis and the difference with the experimental results compared is made. Validation of the modeled connections is done through comparison with available data, from previous studies. Assumptions, graphs, and theories that were not part of the original models are also discussed in further detail in the chapter. Effect of axial restraints and the effect of seat angle geometry variations are also thoroughly discussed. Besides that, the comparison of the results obtained with the guidelines provided by EC3 on top-seat angle connection is also discussed.

Conclusion for the study is then located at Chapter Five. A summary of study with the main findings are discussed in the chapter. This includes the discussion on the factors that may have affected the results produced from testing and modeling, discussion on the various possibilities to improve the study, and future recommendations for other similar studies. Further study topics are also discussed in this chapter.

## **1.6 Significance of Study**

The completion of this study would generate several benefits and contributions to the field. One of the benefits would obviously be the increase in understanding of the top-seat angle connections. Due to the fact that the major amount of the studies for steel connection are on end-plate connections and relatively less on the angle connections, future studies would generally benefit from another examination on the top-seat angle connections as reference.

Not only that, as elevated temperatures are also beginning to gain more attention, studies on the angle connections in elevated temperatures can be used to also understand the behavior of connections under elevated temperatures, possibly resulting in a more detailed guideline being developed for designing steel connections in elevated temperatures. Besides, this study may also serve as one of the studies to further reinforce and improve Eurocode 3, considering the fact that this study makes a number of references towards the code, whether directly or either through other studies that has the code as reference. Undoubtedly, with the code improved, designers and engineers would be able to design more robust structures.

The other field that would benefit from this study would be the mathematical finite-element field and also its related software. The successful verification of the finite-element models with actual previous studies would further prove that the finite-element is indeed suitable as simulation software for analyzing real-life applications. With the use of software, extended studies from previously completed may no longer require further actual specimens to be fabricated for testing so as long as the models have been verified with experimental results of previous studies and therefore save costs and resources. Accuracy of the finite-element modeling can be assumed to be limited only by the parameters involved and assumed in the analysis. With this, the loads and stress can be simulated accordingly and the results would improve the actual application especially when considered in the design stage.

Not only that, with the verification of the finite-element method models and hence the modification of the component method to a greater accuracy, this would be useful to the design engineers. Relatively, the component method is rather simplistic and therefore does not require much computational effort. A simpler method reduces design time and therefore designs can be produced efficiently and is definitely ideal for basic designs of steel connection especially in design offices. In turn, construction can start earlier and subsequently add speed to the development of the area.

## CHAPTER 2

### LITERATURE REVIEW

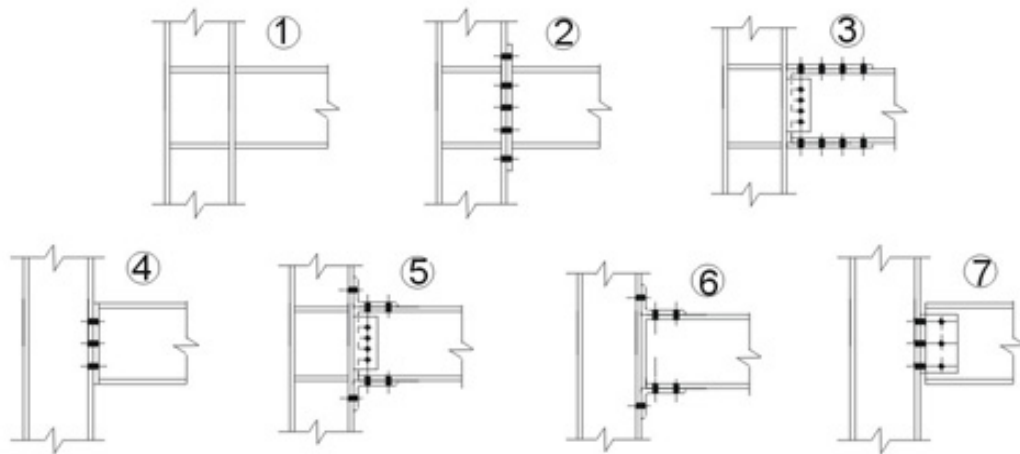
#### 2.1 Introduction

Structural steel connections are the main system of a steel structure that holds the whole structure in place. Whether between beam and column or beam and beams, any form of system that connects two steel members that forms a frame is a structural steel connection. Although joint has been defined in Eurocode 3(2005): Part 1-8 (EC3: Part 1-8) as the zone where two members interconnect. For design purposes it is the assembly of all the basic components required to represent the behavior during the transfer of the relevant internal forces and moments between the connected members. A beam-to-column joint consists of a web panel and either one connection (single sided joint configuration) or two connections (double sided joint configuration)

Meanwhile, connection is defined as location at which two or more elements meet. For design purposes, it is the assembly of the basic components required to represent the behavior during the transfer of the relevant internal forces and moments at the connection. In the context of this study to represent the collective assembly of components used to transfer loads from one steel member to the other or as a support for either. These components can be consisted of, but not limited to, steel plates, bolts, sections of members and welds.

A variety of connection configurations currently exist, including those that were fabricated in-situ as a solution for case-to-case basis due to limitations encountered at the site, such as clashing with pipes, utilities and spacing issues. Some of the common steel connection configurations are as shown in Figure 2.1. End plate connections can be divided into flush end-plates, extended end-plate or flexible end plates / partial depth end plates. In this connection type, a plate connected is welded to the beam end and bolted onto the supporting member in a column-beam case. Meanwhile, angle connections can be further divided into double angle web connections, top and seat angle connection and the top and seat with double web angle connection. In angle connections, angle members are cut into lengths and bolted to connect the members.

One of the main basic concepts of connection design is to design an assembly of joint components to resist the applied loads onto a structural member such as a beam. This is preceded first by the basis assumption of the connection as the support for the beam, either pinned or rigid. Assuming pinned support would result in a larger beam size due to no moment transfer at the connections. A rigid support would result in having to distribute the moment loads on to the connections to be resisted by the components, resulting in additional checks on the connection and higher fabrication costs.



*Key:- (1) – Welded Connections, (2) – Extended End-Plate. (3) – Top and Flange Splice  
 (4) – Flush End Plate, (5) – Top, Seat and Double Web Angles, (6) – Top and Seat  
 Angles, (7) – Double Web Angles*

Fig 2.1 Common Steel Connection Configurations (Galambos, 1988)

The simplification of the connection to either rigid or pinned has been replaced with the more current concept of semi-rigid connections. Where previously assumed to be purely pinned joints, have been found to be able to resist limited levels of rotational loads and meanwhile, rigid connections have been found to be displaying deformation behavior under loadings, which is in contrast to the simplified assumption earlier. As depicted in Figure 2.2, in the simplified concept, pinned joints are assumed to be not able resist much moment loads, and would display large deformations under nominal moment loads.

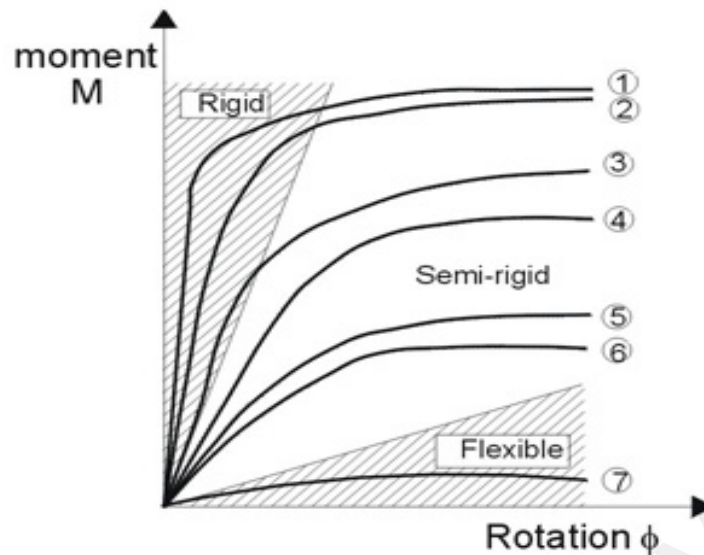


Figure 2.2 Typical moment-rotation curves for various connections type.  
(Galambos, 1988)

## 2.2 Design of Joints in EC3: Part 1-8

In Eurocode 3 (2005): Part 1-8, (EC3: Part 1-8) rotation capacity is defined as the angle through which the joint can rotate for a given resistance level without failing while rotation stiffness the moment that is required to produce a unit rotation in a joint. Meanwhile, moment loads are the forces that cause the system to bend at an axis in an angle. The main representation of the behavior of connections is the moment-rotation graph as shown in figure 2.3, where the major parameters would be the rotation stiffness  $S_{j,ini}$ , moment resistance of joint,  $M_{j,Rd}$  and joint rotation,  $\Phi$ . The moment-rotation curve can be obtained through actual experimental testing of the joint, empirical methods or computer based modeling.

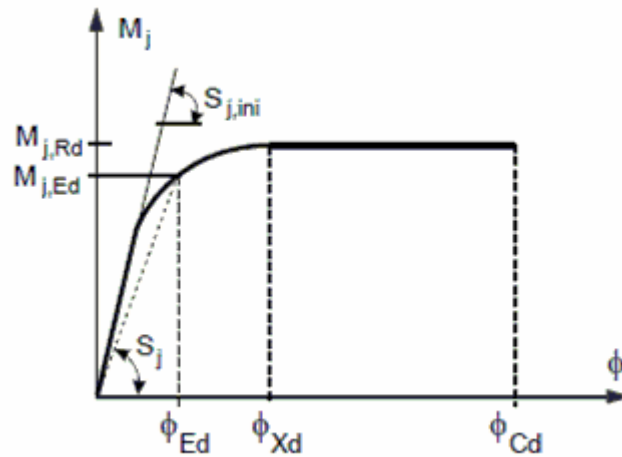


Fig 2.3 Simplified bi-linear graph of moment-rotation curves.  
(EC3 :Part 1-8, 2005)

Rotational stiffness of a joint is denoted by  $S_j$ , which can be determined numerically using equation 2.1 as shown in EC3: Part 1-8. In the equation,  $z$  denotes the lever arm,  $k$  as the stiffness factor for the component involved and parameter  $\mu$  is the stiffness ratio that depends on the ratio between an applied moment and the maximum moment designed for the connection, where clause 6.3.1 (6) in EC3: Part 1-8 can be used to calculate the value of parameter  $\mu$ . The equivalent stiffness,  $k_i$  can be determined using the multiple spring systems theory as according to Hooke's law, with the analogy that each component is a spring and have a limited stiffness value. The spring analogy is being used in EC3: Part 1-8 and stiffness clause in the code for various components is as shown in Table 2.1.

$$S_j = \frac{Ez^2}{\mu \sum_i \frac{1}{k_i}}$$

Equation 2.1

In terms of angle connections design based on EC3: Part 1-8, the focus is on the top-seat angle connections as there were no components defined for web angles. The lever arm of the connection is determined to be the distance between the top bolt of the angle section in tension at the column leg and the center line of thickness for the beam leg of the angle section in compression. Meanwhile, the components recommended for the analysis of top-seat angle connection as detailed in Table 6.9 in EC3: Part 1-8 of the code: beam-to-column joint with bolted angle flange cleat connections, as shown in Table 2.2.

On the other hand, the design moment resistance of the joint  $M_{j,Rd}$ , the code mentioned that the value can be determined according to Table 6.15 in the code. However, a review of EC3: Part 1-8 (2005) shows that there were no proper guidelines defined and only the determination of the lever arm value  $z$  and parameter  $F_T$ , the design resistance force was provided, as shown in Figure 2.4. The design resistance has to be determined from the most critical component as listed from Table 2.2 and multiplied by the lever arm to obtain moment resistance value for the connection.

Design resistance of angle in bending is similar to the behavior of a T-stub where the analogy is illustrated as shown in Figure 2.4. The  $l_{eff}$  used to determine the strength is also shown by Figure 2.4 where  $l_{eff}$  is equivalent to the half of the angle depth. The T-stub resistance determination is governed by three modes of behavior, where Mode 1 being the complete yielding of the angle, Mode 2 with the yielding of the angle and bolt failure while only bolt failures is considered to be Mode 3. Graphical representation and actual failure of each mode is as shown in Figure 2.5, as provided in the study by Spyrou et al. (2004a).

Table 2.1: Example of basic Components for a Connection  
( EC3: Part 1-8, 2005 )

Component			Reference to application rules		
			Design Resistance	Stiffness coefficient	Rotation capacity
1	Column web panel in shear		6.2.6.1	6.3.2	6.4.2 and 6.4.3
2	Column web In transverse compression		6.2.6.2	6.3.2	6.4.2 and 6.4.3
3	Column web in transverse tension		6.2.6.3	6.3.2	6.4.2 and 6.4.3
4	Column flange in bending		6.2.6.4	6.3.2	6.4.2 and 6.4.3
5	End-plate in bending		6.2.6.5	6.3.2	6.4.2
6	Flange cleat in bending		6.2.6.6	6.3.2	6.4.2

Table 2.2: Components considered for top-seat angle analysis.

Stiffness number	Component
$k_1$	Column web panel in shear
$k_2$	Column web in transverse compression
$k_3$	Column web in transverse tension
$k_4$	Column flange in bending
$k_6$	Flange cleat in bending
$k_{10}$	Bolts in tension
$k_{11}$	Bolts in shear
$k_{12}$	Bolts in bearing

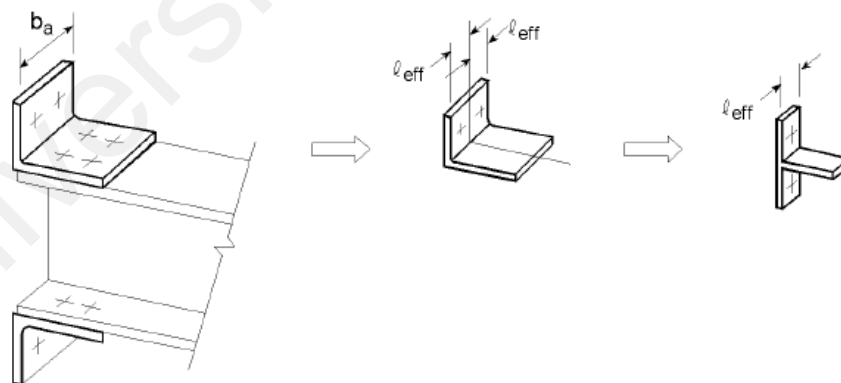


Figure 2.4: Flange angle analysis as T-stub (EC3: Part 1-8)

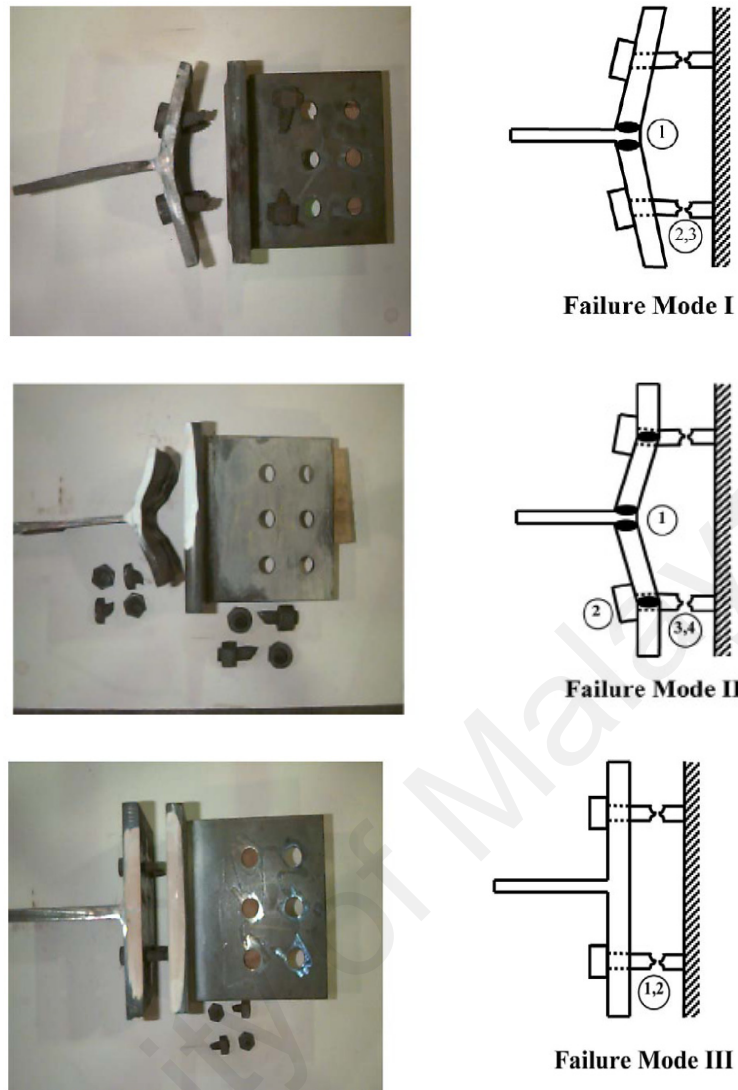


Figure 2.5 T-stub failure modes. (Spyrou et al., 2004a)

Depending on the gap between the column flange and the beam end, the values of the length  $e_{\min}$  and parameter  $m$  can be determined as according to Figure 2.6, where Figure 2.6(a) is for gap less or equal to  $0.4 t_a$  while for gaps more than  $0.4 t_a$  is as shown in Figure 2.6(b). From the figure, reduction in gap distances reduces the  $m$  parameter while maintaining the  $e_{\min}$  value.

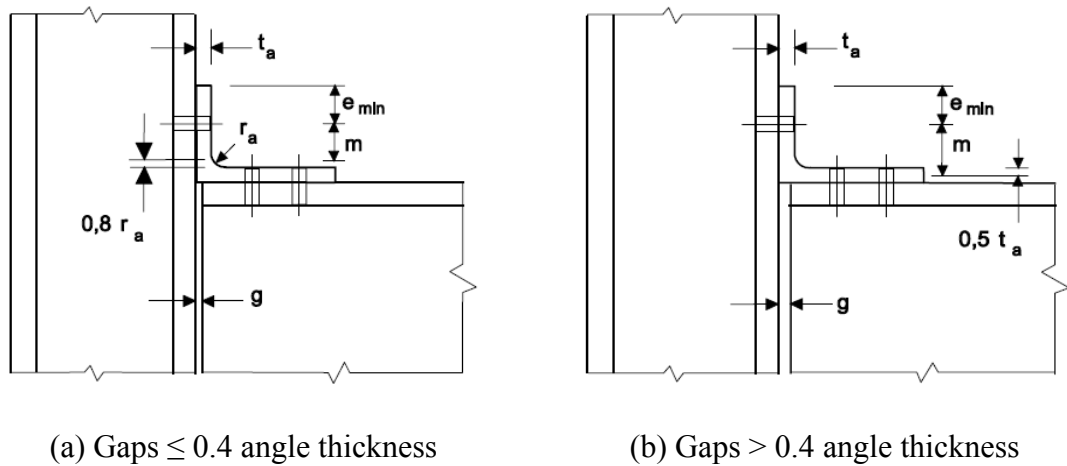


Figure 2.6: Determination of  $e_{min}$  and  $m$ .

### 2.3 Steel Material Behavior at Elevated Temperatures

Steel materials behave differently at elevated temperature compared to at ambient condition. According to Eurocode 3 (2005): Part 1-2 (EC3: Part 1-2), the thermal elongation / expansion behavior of carbon steels can be established with the formulas as shown in expressions 2.7(a), (b) and (c) in EC3: Part 1-2. Figure 2.7 below clearly illustrates the summary resultant from the expressions 2.7 in EC3: Part 1-2 for the relative elongation of steel as a function of increasing temperature.

From the graph, it is discovered that the elongations of steels between temperatures of  $750^{\circ}\text{C}$  to  $850^{\circ}\text{C}$  have no differences and remain flat, which constitutes that in the range of temperatures, the steel connection does not suffer from an increase in stresses due the elongation of steels under temperatures. The basis for measurement is at  $20^{\circ}\text{C}$ , which would result in an elongation due to the local temperatures of anywhere between  $30^{\circ}\text{C}$  and  $35^{\circ}\text{C}$  as the basis of ambient temperatures, but the change as seen in Figure 2.7 is relatively minor and negligible.

Relatively, the change in length with respect to the temperature involved has a linear behavior. Although this, the effect of thermal expansion was not included in the study by Silva et al., 2001. The effect of thermal elongation is not a complicated phenomenon to be considered in the analysis, however, the actual elongation of each of the components is not relatively known and therefore further calibration is needed. This study did not include the effect of thermal expansion for the sake of simplicity and to avoid further considerations that complicates the behavior.

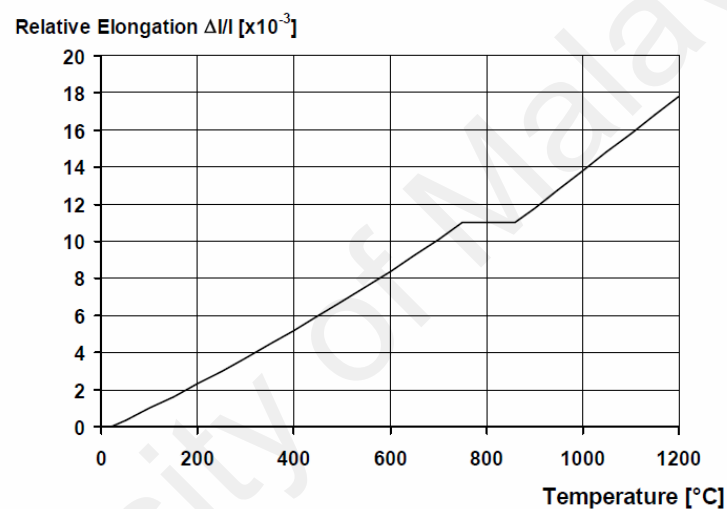


Figure 2.7 Relative Elongation of carbon steels as a function of temperatures. (EC3: Part 1-2, 2005)

Meanwhile, thermal conductivity of carbon steel is governed by the graph shown in Figure 2.8. From the graph, thermal conductivity of steels decreases as temperatures increase and continues to remain constant after 800°C but no thermal conductivity is defined for temperatures after 1200°C, as the temperature results in a strength ratio approaching zero. Proposed analysis method for the thermal distributions in steel connections is covered in sections of 4.3.1 and 4.3.2 of EC3: Part 1-2.

Generally, the consideration on analysis shall be relevant thermal actions and variation of strength with temperature. A large number of studies have ignored this property in the analysis, with the assumption that the temperatures are uniform throughout the connection for simplifications. Although this, variation of the temperatures to be used at the joints has been proposed as according to Table 2.3 as the study done by Silva et. al. (2001), which is particularly useful for individual connection component studies.

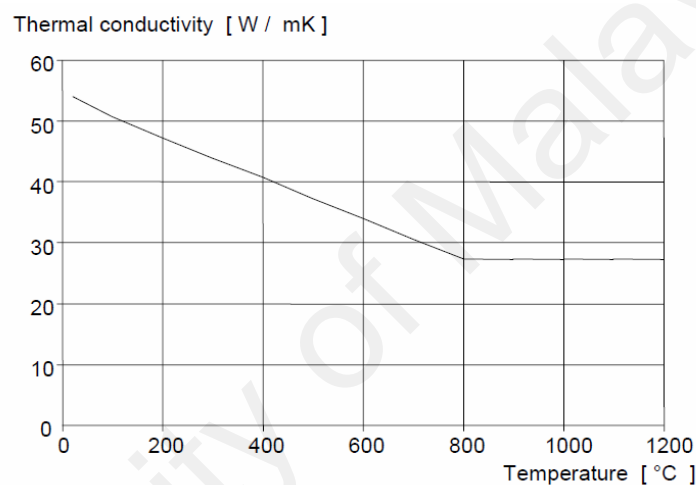


Fig 2.8 Thermal Conductivity of steels as a function of temperature. (EC3: Part 1-2, 2005)

The component method rely heavily on the force-deformation graph or the stress strain diagram and application of the thermal expansion properties into the models would generally involve considering the additional factors due to elevated temperatures. With consideration to the thermal elongation, together with the stress generated due the expansion, is limited by nearby members which are a case-to-case basis. This consideration is largely dependent on extensive research due to the various possibilities of where the elongation may cause additional stress to the components.

In most studies, such as those by Saedi and Yahyai (2009a) and Silva et al. (2001), the thermal elongations are not considered and where in the case of Silva et al. (2001), it was not considered due to a lack in calibration of thermal elongations data and not being that it is not possible. Major properties of steel to be considered in an elevated-temperatures condition would be the reduction factors for the degradation of the strength, Young's modulus and the proportional limit of the material. In EC3: Part 1-2, the material reduction factors of steel depending on the temperature are as shown in Table 2.4. For temperatures in between those specified, e.g at 550°C, the factors can be linearly interpolated factored.

Table 2.3 Temperature distribution ratio for components at elevated temperatures. (Silva et.al. 2001)

Element	Temperature
	Ratio
Beam Bottom	1.00
Beam Top	1.02
Beam Web	1.06
Bottom Bolt	1.01
Middle Bolt	1.03
Top Bolt	1.04
Column Web	1.14
Column Flange	1.03
End-Plate	1.03

Table 2.4 Reduction factors for steel at various temperatures.  
(EC3: Part 1-2, 2005)

Steel Temperature $\theta_a$	Reduction factors at temperature $\theta_a$ relative to the value of $f_y$ or $E_a$ at 20°C		
	Reduction factor (relative to $f_y$ ) for effective yield strength $k_{y,\theta} = f_{y,\theta}/f_y$	Reduction factor (relative to $f_y$ ) for proportional limit $k_{p,\theta} = f_{p,\theta}/f_y$	Reduction factor (relative to $E_a$ ) for the slope of the linear elastic range $k_{E,\theta} = E_{a,\theta}/E_a$
20°C	1,000	1,000	1,000
100°C	1,000	1,000	1,000
200°C	1,000	0,807	0,900
300°C	1,000	0,613	0,800
400°C	1,000	0,420	0,700
500°C	0,780	0,360	0,600
600°C	0,470	0,180	0,310
700°C	0,230	0,075	0,130
800°C	0,110	0,050	0,090
900°C	0,060	0,0375	0,0675
1000°C	0,040	0,0250	0,0450
1100°C	0,020	0,0125	0,0225
1200°C	0,000	0,0000	0,0000

## 2.4 Previous Studies on Connection at Ambient Temperature

To analyze the behavior of a connection, there is no doubt that the recommended solution would be to conduct an actual specimen testing. Due to variation in connection configuration, with various different possible dimensions, too much resource has to be consumed in order to conduct connections testing.

Therefore, the alternative would be to analyze the connection as a model as it is widely accepted that a proper model would generally be considered as the representative of the connection under analysis. This is applicable if the method of modeling has been verified with previous results of tests that has similar pattern to the cases studied.

Where cases that the connection type has never existed, multiple Model parameters would be easier to modify and evaluate as compared to having to fabricate a variety of new specimens for testing. Among the more common modeling techniques includes analytical models, finite-element models, component based models and empirical models. Reviews on previous studies on connections with different approaches are explained in the following sub-sections.

#### **2.4.1 Experimental Studies**

The main purpose for conducting an experimental study on connections is to obtain data on an actual connection behavior, including all imperfections and material behaviors under the loading conditions. Essentially, due to this, the test result data can be used to verify further / future modeling and analysis results or as the basis for design procedure formulation. Considering there are extensive experimental studies on different connections, only angle connection is reviewed here.

Rathburn (1936) are among the earliest researchers studying on the double angle connections. In the study, rivets were used and therefore render the results of the study obsolete in today's term as high strength bolts are currently used to replace rivets in connections. Azizinamini (1982) conducted 18 experimental tests on angle connections in ambient temperatures, with and without web angles. Variation of parameters such as angle thickness is studied and due to the extensive study and the number of experimental results, numerous modeling studies on angle connections have used the experimental results obtained to verify the models.

Cyclic loadings are similar to earthquake loadings where structures are subjected to load reversal. These loads cause the connection to resist tension and compression loads in both directions of the loading axis. For angle connections, the cyclic energy dissipation was found to be relatively high when compared to the energy in monotonic loadings of the same connection as investigated by Shen and Astanteh (1999). With this, it is understood that the behavior of bolted connections in an earthquake is more favorable in comparison to welded connections. Angle thickness is highlighted as one of the main contributing factors of increasing connection capacity.

Another test on cyclic loadings has been by Kukreti and Abomaali (1999) which was then compared with proposed analytical models, such as Ramber-Osgood, bilinear, and elasto-plastic models. This study confirms that the top-seat angle connection behaves and can be classified as a semi-rigid connection. Considering the results of the comparison, the modified bilinear model has been proposed to be included in any finite-element software to predict the behavior under cyclic loads. Meanwhile, the elasto-plastic model is the least conservative model.

Where double web angles connections are concerned, Yang et al. (2000) conducted experimental tests on double web angle connections that were bolted to the column and welded to the beam. Axially loaded, the angles have displayed higher stresses near the heel of the angle, while in shear loads; the stresses are also concentrated near the heel of the angle. In the study, one of the main points was that the thickness of the angle has a significant effect over the behavior of the connection. Thicker angles lead to higher stiffness and capacity behavior.

Calado et. al (2000) studied on the response of semi-rigid top, seat and double web angle connection configurations for monotonic and cyclic loads. Variation of the parameter is three different sizes of the connected column. Cyclic loads have shown to have reduced the ultimate moment and rotational capacity significantly due to reversal of loadings. However, cyclic loadings prove to have less effect on the stiffness of the connection. Flange angle cleat is found to be the main contributor to the stiffness and strength of the connection due to the higher post-yield behavior.

Another series of angle connection tests has been conducted by Komuro et al. (2003) in effort to understand the effect of web angle dimensions. Three specimens were tested; with one specimen on top-seat angles while the other with web angles. Both monotonic and cyclic loadings were applied to the connections and results from the experiments have been compared with Kishi-Chen (ref???) models. It is shown that the Kishi-Chen model referred in the study has been able to predict the stiffness and moment capacity to an accurate degree. On the other hand, the envelope of cyclic test result curves is representative of the response of the connection under monotonic loadings.

## 2.4.2 Empirical Models

Empirical is the study of connection behaviors based on observation without any form of postulations, or earlier knowledge of the behavior. Usually, this is applied in earlier studies of the connection. This is due to limited knowledge available on a particular connection type.

Derivation of the empirical models require no previous knowledge of the analyzed problem and therefore, analysis are mostly based the moment-rotation graph where empirical equations are developed to best reflect the shape of the graph produced from specimen testing. From literature review, the more often used method is the regression analysis of the results. The common empirical model exists in a number of types: linear, polynomial, power and exponential models.

The earliest linear model was proposed by Rathburn (1936) from a ratio of rotation and moment representing  $Z$ , the semi-rigid connection factor. No doubt that this can only be applied to the regression graph only due to the linear line involved. From the linear models, improvements over the model has been made by introducing polynomial models as done by Sommer (1969) and referred to by Frye and Morris (1975). The polynomial model reflected closer to the actual graph when compared to the linear model as the actual curve has slight curve in the elastic-plastic zone. Equation for the model is as shown below in Equation 2.1 below:-

$$\theta = C_1(KM) + C_2(KM)^3 + C_3(KM)^5 \quad \text{Eqn. 2.1}$$

Meanwhile, Ang and Morris (1984) used another improved model over Sommer's proposal. The Ramberg-Osgood model when compared with the study by Sommer shows that the model is fairly similar, but the format has changed into a ratio form as shown in Equation 2.2, where  $K$  is the standardization factor concerning with the geometry and connection configuration and  $n$  is the curve sharpness factor.

$$\frac{\theta}{\theta_o} = \frac{KM}{(KM)_o} \left[ 1 + \left( \frac{KM}{(KM)_o} \right)^{n-1} \right] \quad \text{Eqn. 2.2}$$

This model is then modified by Liu and Chen (1986) to better reflect the test results, into Equation 2.3 by considering the cubic B-spline method by Jones (1981). This involves in the strain hardening connection stiffness,  $K_p$ . The model, although fairly accurate, is limited by sharp curves on the moment rotation graph. Which then lead to the model above being improved by Kishi and Chen (1986) into Equation 2.4 for accommodating any sharp changes in the moment-rotation curve.

$$M = M_o + \sum_{j=1}^n C_j \left[ 1 - \exp\left(\frac{\theta}{-2j\alpha}\right) \right] + \sum_{k=1}^n D_k (\theta - \theta_k) H[\theta - \theta_k] \quad \text{Eqn. 2.3}$$

$$M = M_o + \sum_{j=1}^n C_j \left[ 1 - \exp\left(\frac{\theta}{-2j\alpha}\right) \right] + M_o + R_{kf} \cdot \theta \quad \text{Eqn. 2.4}$$

In Lee and Mun (2002) , the proposed empirical model for defining the moment-rotation graph of a semi-rigid connection should be, where  $n$  and  $\alpha$  is the shape parameters. The model does not consider on the stiffness, strength nor standardization factor, but relies on the  $n$  and  $\alpha$  constants, derived from the results of 75 experimental data, with the inclusion of the initial stiffness ( $k_i$ ) and plastic stiffness ( $k_p$ ), which is as shown in Equation 2.5.

$$M = \alpha[\ln(n \cdot 1000 \cdot \theta + 1)]^n \quad \text{Eqn. 2.5}$$

Without doubt, the empirical models have application in situations where the testing conditions and configurations are similar to the experimental studies done for the derivation of the models. Clearly, the use of empirical models as a generalized form of solution for obtaining the moment-rotation graph or any form of steel connection behavioral analysis is certainly not recommended as the models rarely consider the material properties or the variation of the steel connection configuration parameter accurately. Non-linearity of steel connection behavior also is another factor pressing against the use of empirical methods. The simplicity of the model although is agreed and achieves acceptable accuracy when compared to experimental results, but nevertheless, it should be taken as the governing formula in analysis of steel connections.

### 2.4.3 Analytical Models

Analytical models are based models on analysis considering fixed equations. The equations, developed from empirical models, have fixed parameters in which, by using the relevant parameters and combined with suitable calculations would produce required results. This modeling technique generally considers a couple of fixed parameters of the connection and is much more reliable when compared to empirical models as the effects from material properties, structural factor and component behavior is catered for. In some cases, the derived analytical model is a result of logical and detailed application of structural theories and assumption, in which it is combined to form an analysis model to understand the connection better.

Yang and Lee (2000) proposed on the initial stiffness and ultimate moment for double angle connections using analytical models. The proposed model analyses were compared to the models from Frye-Morris (1975), and Ang-Morris (1984). The comparison results show that the Wu-Chen model (ref??) reflect closer to the actual behavior of the tested joint, with the condition that the initial stiffness and ultimate moment to be accurately predicted first. Derivation is made from the model and the final proposed model was found to be a more accurate than the Wu-Chen model, with error of less than 7.8%. The initial rotational stiffness of a double angle connection proposed is given by equation 2.6.

$$K_{e, double} = 2 \cdot \left[ \frac{bEt^3 \left[ b^2 + 2(1-\nu)a^2 \right] \frac{1}{\eta}}{9(1-\nu^2)a^3} \right] \quad \text{Eqn. 2.6}$$

Heidarpour et al. (2008) detailed on the failures of the T-stub component and each possibilities of failure. Derivation of the analytical equation for the first yield point and subsequent yield points involves in assumption that the deformation of the bolts is fully affected by the deformation of the end-plate or column flange only. The bolt has an infinitely stiff stratum although the bolts was assumed to be non-preloaded in the analysis. The resulting load displacement graph is observed to be having noticeable difference with the theoretical results which was attributed to strain hardening and post-yield strength that was not considered in the theoretical approach.

There is no doubt that studies of this manner has cleared up on the claims by the previous versions of the Eurocode 3. Claims that the steel connections need not any consideration on elevated temperatures failure due to the concentration of mass at the connection would generally result in a higher heat distribution, therefore lowering the effect of temperatures, which have been found to be untrue.

The analytical method, although may seem to be a viable method, requires detailed understanding of each of the analytical method, the derivation and a proper application of each of the required parameters. As with every other method, the model can be manipulated accordingly to suit for the available parameters but lacking of important parameters would generally render the model being not applicable any further. As the analytical method varies from studies to studies, and no standard was universally agreed upon and neither does it have any proper / standard guidelines, therefore, the variation is undeniably larger than compared to the component method or the finite-element method.

#### 2.4.4 Component-based Method

The basis of component models are that each of the area in the connection that may contribute to the stiffness of the connection is represented by a spring, in which when combined and analyzed, will result in the total stiffness of the connection in whole. This method is highlighted in Eurocode 3: Part 1-8 Chapter 6, where a table of basic components and guidelines of analyzing the design resistance of basic components is provided.

In the design of connections, connections to the flange of the column has been extensively studied, however, connections to the web of column has not been given much attention. Studies by Steenhuis et al. (1998) cater for this gap using end-plate connections and the component method. New components for the connections to column web have been proposed, including stiffness for column web bending and punching, compression and for slender columns. Further studies are required to validate these proposed components.

Through cyclic loading of the connection, Shen and Astanteh (1999) developed the component models for the angle connections. The derivation of the model was based on the experimental results of the first of the test, where the angles are actually tested with cyclic loads. This study has summarized that bolted angle connections have very low yielding strength but instead an almost double the yielding strength for the ultimate strength, due to material strain hardening.

In the practical fieldwork, it is common to encounter 3D-based loadings, where loadings are applied in both axis of the connection, at the minor axis and major axis. Connections at the minor axis are also studied by Cabrero and Bayo (2007). Components for the column web in terms of additional plates bending are proposed, which also caters for 3D loadings. Component arrangements for both minor and major axis connections are also shown. The results of the study suggests that the guidelines provided by EC3 computes values which overestimates the stiffness of the connection.

Del Savio et al. (2009) studied on the axial interaction of end-plate connections using the component method. The basis of axial loadings inclusion into the analysis is the stationery potential energy principle. In this study, it is highlighted that the lever arm  $d$  strongly influences the connection stiffness. Proposed method is in close agreement with the experimental test results of Lima et al. (2004).

Meanwhile, the local steel sections, Perwaja Steel have been studied by Tahir et al. (2009) with the end-plate connections, using the component method. The justification for this study is that the EC3 guidelines caters for British Standards Steel and therefore for steels other than BS:Steel, the component method must be verified for applicability.

Studies show that in end-plate connections, the deformation of the connection is dependent on the column flange thickness and not the column size. On the other hand, failure modes of the connection are affected by the thickness of the end-plate used.

Lemonis and Gantes (2009) proposed a modification to the Eurocode 3: Part 1-8 proposed component model. The modification is located at the upper-most row where the common practice would be to ‘align’ all the relevant components for the tension zone into the same row as the top bolt row. The modification is where the relevant levels of the component are modeled in the actual condition. In other words, the components considered are placed in linear with the component level of the connection during model production. A clear illustration is provided as in Figure 2.9 where the difference is undeniably prominent. The results of analysis show that the non-aligned model has a higher accuracy.

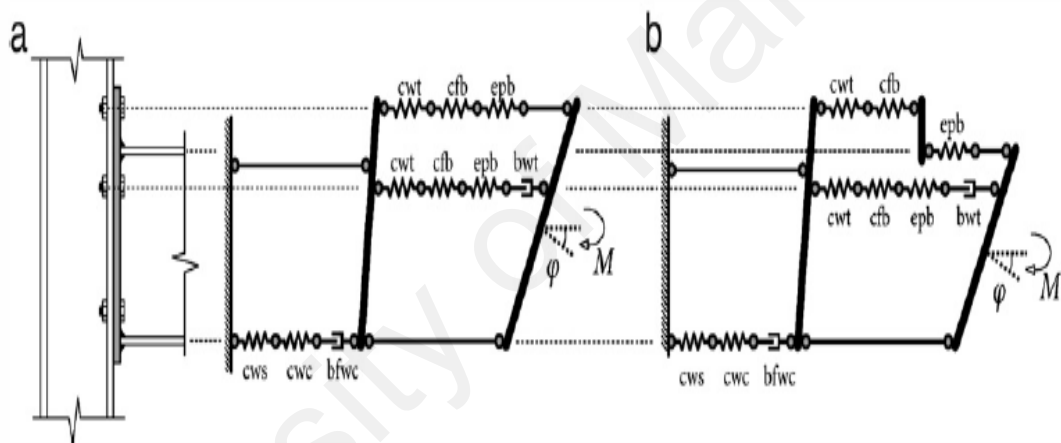


Figure 2.9 EC3 Component Model (Lemonis and Gantes, 2009)

a) Aligned Model b) Non-Aligned Model

It is fairly clear that the component method caters for most of the structural components in the steel connection. It is also versatile as additional components that were found to have an effect on the connection can easily be adapted into previous models. As much as the number of components-springs can be increased, so can it be decreased accordingly. This generally would increase the accuracy of the model as it is improved over time as a result from previous studies. Due to its simplicity, manual calculations are possible and therefore reduce computational costs.

### 2.4.5 Finite Element Models

Finite Element Modeling for steel connections has started since the early 1970's to solve the analysis of the connection. A number of studies have been conducted since, in which, the studies have shown that the finite element analysis is capable of analyzing complex calculations and yet comply accurately with actual values. Advance on computer specifications and hardware has made the finite element analysis easier to be conducted, and more accessible to the larger population and able to be analyzed within a short amount of time.

The basis of the finite element modeling was the process of turning a continuous object into discrete elements for simpler analysis procedures. There is no doubt that, through this way, the accuracy of the analysis may be lost, but this can be compensated by considering a larger amount of smaller sized discrete element. ANSYS and ABAQUS are among the more commonly used software to conduct finite-element modeling and analysis. An example of finite element model is as shown in Figure 2.10

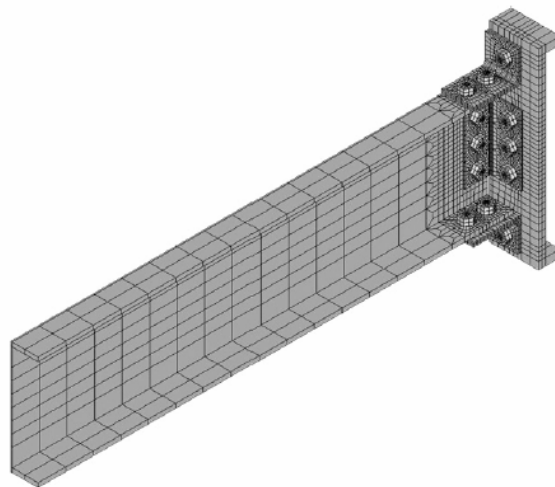


Figure 2.10: Example of Finite Element Model of Top, Seat and Double Web Angle Connection (Pirmoz et.al., 2008)

Bahaari and Sherbourne (1994) modeled the beam-column endplate connections using ANSYS. Plastic quadrilateral elements of STIF43 were used to model the main larger components of the connection. Bolt head were modeled using the eight-node isoperimetric elements STIF45. Contact elements between the column-flange and the end-plate were modeled with the STIF52 element.

Researchers such as Yang et.al (2000), have done a more recent research on steel connections using finite element modeling on the behavior of double angle connections with shear forces and applied axial load. The angle is connected to the column with bolts while welded to the beam web area. Brick elements are used for most of the members of the connection besides the welds which utilizes triangular prism elements. Model was verified with the experimental tests conducted in the same study and the results show that the model can be used to simulate double angle connections under axial loadings. A mechanical model was also proposed consisting of springs and beams.

Ali Ahmed et.al. (2001) conducted studies on prying forces in angle connections. The bolts are applied with additional forces due to prying from the top angle vertical leg deformation during bending behavior when moment loads are applied onto the connection. Azizinamini (1982) experimental test without web angles is used for verifications of the finite-element model. Parameters such as higher material properties, smaller angle thickness, higher gage length and larger bolt diameters lead to a higher prying force. In this test particularly, the geometrical and material properties were clearly shown but there were no indication of where and how the data for the moment-rotation graph were obtained from.

Hong et.al (2002) studied on the moment rotation behavior of double angle connections, similar in type as in the study by Yang et. al (2000), subjected to shear load. A number of parametric studies have been discussed, largely involving with the model definitions in ABAQUS and also on the simplification of the model, to investigate on the effects on the behavior. In comparison to the study by Yang et. al., this study conducted experimental tests for the effect of shear forces which was previously only modeled through finite-element. Richard's regression formula (ref??) is used to analyze the test results and the author claims that the moment rotation curve can be easily drawn by using the regression formula as it incorporates the curve sharpness factor, initial stiffness and plastic stiffness.

Azizinamini's (1982) studies are commonly referred to as the verification for the finite element models, this includes studies by Danesh et al. (2007) on the top, seat and double web angle connection with shear loads. The initial stiffness of the connection was reduced with the reduction in the web angles length??. Lower shear capacity of the web angles would lead to a lower yield moment capacity. A regression based equation is proposed to determine the reduction factor for the initial stiffness of top and seat angles with web angles under the influence of shear loads.

With the results of tests in Komuro et al. (2003), numerical models are produced by Komuro et al. (2004) with the usage contact algorithms, bolt pretension and solid elements. Results from the finite-element model show that the increase in web angle length coupled with the increased number of bolts at the web angle has resulted in an increase of connection moment capacity. Comparison of the strain measurements and both model and experimental tests, have shown acceptable match.

Pirmoz et. al (2008) conducted studies through finite element analysis on the angle connections with both shear force and moment loads for top and seat angle connections with double web angles. According to Pirmoz, previous studies have not considered the effect of gravitational loads that result in internal shear forces. The software used was ANSYS. Members were modeled using the eight node first order element of SOLID 45 while bolts were using SOLID 64.

Element SOLID 64 apparently is able to cater for thermal gradient, which is particularly useful for considering thermal loads on the connection. As to avoid any penetration on the steel members during loadings, the contact elements were modeled using CONTA 174 and TARGE 170. Friction coefficient was taken lightly with only 0.1, which value is a third of the recommended value. A method for predicting the deterioration of the initial stiffness due to shear was also proposed.

On three-dimensional finite-element modeling through nonlinear elastic-plastic conducted by Reinoso et. al (2008), the tests 8S1 and 8S2 of Azizinamini's study is reproduced. Modeling is based on the concept of symmetrical which therefore results in a quarter of the connection being modeled. Angle connection configuration used is the top, seat and double web angle. Eight node brick elements with full integration and incompatible modes are used. Contact element is explicitly modeled. Bolt pretension is modeled at a value of 150 kN.m. This study shows that the bolt pretension and friction has minor effect on the connection. Again, this study has shown that the angle thickness plays an important role in connection response coupled together with the prying action. Bending in angles directly affects the joint resistance, which is governed by the parameter  $m$ , or the distance between the plastic hinge in the failure mechanism of the connection.

Little is known of the role of the seat angle in the connection behavior, which lead Pirmoz (2009b) to conduct a study to understand this role. Using the same model as previously presented in Pirmoz (2008), instead of the seat angle being varied, the length of the beam is used as a variable parameter where the behavior is shown through a moment-rotation graph. It is found that as the beam length increases, the capacity of the connection decreases, which is directly attributed to the role of the seat angle. Although, more tests and data are required to verify this, couple with other factors such as variation of angle thickness, gage length and gaps.

Cafer (2009) conducted verification of top and seat with and without web angles models based on Azizinamini (1982) for top and seat with web angles, while top and seat angle without web angles model verified using results in the study by Kukreti and Abolmaali (1999). The software used was the ANSYS Workbench and is among the first to use the software. In addition, analytical methods have also been proposed. Both model and method have been seen to provide good correlations but improvements are still possible. Polynomial models have been concluded to provide the greatest accuracy among the methods tested.

The importance of the gauge length at the top angle of a top-seat angle connection has been shown by Yang et al. (2011) through the modeling of the top-seat angle connection with the variation of angle thickness and gauge length at the column leg of the flange angle. Using ABAQUS, the value for initial stiffness accuracy is higher in comparison to the models proposed by Yang and Jeon (2009) and Chen-Kishi in Chen and Lui (1991), while plastic moment values are more accurate when compared to the model proposed by Faella et al. (2000) and Yang and Jeon (2009).

In comparison, the component model can also be considered to be a form of finite-element analysis due to the simplification of an actual connection to its basic elements and using the matrix method to translate forces into connection behavior. In order to provide distinct difference for reference in this study, finite element models refers to models using 3-dimensional models where the model is volume meshed and split into smaller elements, while the component method refers to analysis using simplified 2-dimensional models using connection component representations for each part in a connection and combined into a arranged system.

## **2.5 Connection in Elevated Temperature Studies**

In comparison to ambient temperature analysis, elevated temperature condition studies require additional consideration such as the degradation of materials with temperatures. For model or analytical based studies, validation with ambient temperature models are initially needed, followed by the validation with elevated temperatures, to reduce the considerations associated with ambient temperature study.

### **2.5.1 Experimental Studies at Elevated Temperature**

An experimental study on the modeling of extended end-plate joints in fire using spring component has recently been undertaken by Wang et al. (2007). Reduction of steel properties in the context of elevated temperatures is according to Chinese Standard for steel plates.

The components taken into consideration includes:- column web in tension, flexure zone in column flange, flexure zone in end-plate, column web in compression and also the shear zone of the column web. Other components, such as the bolt in tension are not considered. ISO834 temperature curve was utilized to provide the elevated temperature condition but due to the small variation in temperature in which the difference is considered to be insignificant, the heating is considered to be uniform throughout the connection location.

With angle of loading,  $\alpha$  of,  $35^\circ$ ,  $45^\circ$  and  $55^\circ$ , shear forces and tying forces are the resulting loads from the distribution to the axis and thus, Yu et al. (2008) investigated four types of connections including web cleats, end plate connections and fin plate connection types. Results obtained from the study show that the web cleat connections have high rotational capacity. Behavior of fin plate connections on the other hand is governed by the capacity of bolt shear.

Experimental tests and studies on top and seat angle connections have been conducted by Saedi and Yahyai (2009a). Twelve configurations were utilized in the study and the results show the thermal strength of the connection relies heavily on the angle thickness and temperature restraint bolts. Increasing these values would generally lead to increase of thermal stiffness. Furthermore, angle connections will not be able to withstand elevated temperatures of more than  $900^\circ\text{C}$ . At a temperature of  $900^\circ\text{C}$ , the connection stiffness can almost be ignored. It is also emphasized that the bolts are one of the most important components in a bolted connection as the premature failure of bolts would prevent the connection from achieving its maximum capacity.

Elevated temperature tests on various connections, including on the fin plate connection, web cleat connection, and end-plate connection types has been conducted by Wang et al. (2011). This study has revealed a multitude of possible connection failures, which are vital for further validation studies or design studies. Highlights of the study includes that connections with shallower depths has been found to be able to reach higher connection rotations which is different to the common conception that deeper connections would be able to resist more. At fix joints, the catenary effect of the beam would result in the failure of the connection, while the catenary effect on pinned connections, especially web cleat connections, show high resistance. Therefore, the web cleat connection is recommended for further studies.

### **2.5.2 Finite Element Studies for Elevated Temperature**

Using the results in Saedi and Yahyai (2009a), Saedi and Yahyai (2009b) conducted modeling on angle connections in elevated temperatures, which includes top-seat angle connections, specimens S3 and S9. Main purpose of the study was to investigate on the failure mechanism in top-seat angle connections. The behavior of the models was compared to the experimental tests and the model results have shown that the model is in good agreement with the experimental tests. Degradation of the material has been according to the guides set out by EC3. One of the result models is as shown in Figure 2.11

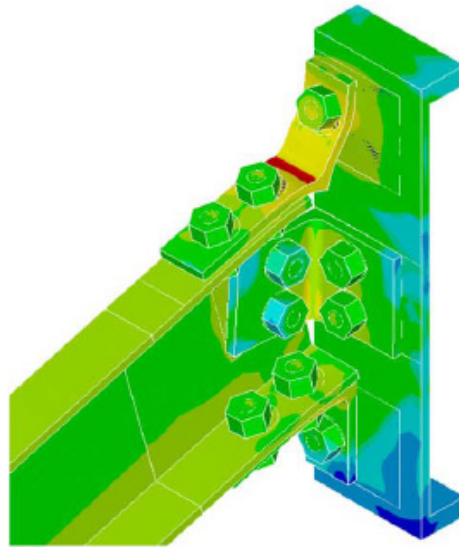


Fig. 2.11 Analysis results of Finite Element Model for Saedi and Yahyai (2009b).

Mao et.al. (2009) studied on the response of steel beam-column connections, especially fin plate, under fire loads by conducting experimental tests and attempts to model the exact response in the finite element software, ANSYS, in which the validated methods is used to model for other connections of interest. In terms of the thermal loading, the an-isothermal and isothermal method is used. In the finite element model shown as the result, it is observed that the bolt row from the fin-plate at the beam web is not modeled in finite element.

Another latest finite-element model studies is as conducted by Diaz (2011) on end plate connections. Several effects of various loads / forces are studied with the finite element model, namely: effect of thermal expansion, effect of transverse load pattern of beam, effect of axial load on column, effect of applied moment of beam, of shear force of beam and of axial force of beam. Effects from the shear force of beam and of transverse load pattern of beam is minor.

Meanwhile, effect of axial force on beam towards the stiffness of the connection is only significant in the plastic region and minor in the elastic region, which is for cases where the temperature is constant while the load increases. When the load is constant and temperature increases, the axial force instead do not affect the connection stiffness. There was no doubt that the thermal expansion was necessary in determining the connection stiffness

Michal et al. (2011) has conducted a study on the column web component at elevated temperatures using the finite-element and analytical method. Based on the experimental investigation conducted, the end-plate connection was modeled and the result show good agreement after adjustments has been made to the model to ensure maximum column web effect. The material properties were defined according to EC3 (2005): Part 1-2.

In terms of axial restraints, major studies have been conducted on the effect of axial restraints towards the behavior of beams in elevated temperatures. These studies include those by Liu et.al. (1996) which has also conducted modeling of end-plate connections with the effect of axial restraints. From the results of the study, fire resistance of any structural beams is enhanced with fixed end moment connections. It also shows the possibility of using finite element to simulate elevated temperature condition models. The study by Heidarpour and Bradford (2009) focuses on the empirical modeling of the connection behavior and the results have shown that the proposed concept has higher accuracy in comparison to finite-element software analysis, which is recommended for future analysis connections in elevated temperature conditions.

Studies by Dai et al. (2010) have shown that the static analysis is sufficient for analysis of elevated temperature conditions. A number of proposals on increasing the fire performance of a shear plate or fin plate connection type, including to increase bolt grades, matching web thickness of the shear plate, additional plates on the web and utilizing larger bolts holes has been suggested by Selamet and Garlock (2010) from the results of the finite-element analysis of the fin plate connections.

From various studies, it is shown that the temperatures in the furnace do not necessarily be the temperature of the component in the connection due to various factors such as the heat transmission, heat transfer and the phases of the gasses. Therefore, a finite-element model is produced with the software FD5 with validations of a test on a fully-welded-spliced connection at elevated temperatures by Lee et al. (2011). The FD5 software was able to simulate the heat transfers and accurately simulate the result of the connection components temperature and subsequently the failure mode of the connection. With the results from this study, it is expected that further studies would continue to use this method proposed to predict the connection temperatures and thus, assist in achieving greater model accuracy.

A finite element model has been developed for the flush end plate connections at elevated temperatures in a study done by Li et al. (2012). An experimental test was conducted for the basis of the finite-element model. Besides that, two models, at 352.5°C and 751.5°C was applied with axial loadings. Response of the connection, in comparison with experimental results show acceptable accuracy and the effect of axial restraints have lowered the moment capacity and stiffness of the connection. At the same time, the ductility of the model has also been reduced.

Pakala et al. (2012) using the ANSYS Software has modeled the behavior of the fin plate connections at elevated temperatures. Validations of the model are with the studies by Yu et al. (2009b). Various parameters have been studied such as the bolt hole diameter, beam web thickness and edge distance.

From the results of the parametric studies, several items have been suggested that affects the performance of the fin plate connections at elevated temperatures including gaps, sizes of bolts holes, and web thickness. Although this, the addition of top-seat angles is presumed to be able to help with the connection performance due to the higher ductility but have been found that there are limited literature available on this topic.

For end-plate connections, the robustness of the connection at elevated temperature conditions can be increased by utilizing the spaced extended end-plate, channel bolted extended end plate or by the usage of a “dog-boned” shaped beam, as shown in Figure 2.12, in a study by Wang and P.Wang (2013). Robustness is determined by the higher rotational capacity that the connection would respond under loads. Bolt size increase has been determined to be ineffective in increasing the resisting temperature of the connection. Other end-plate connections under fire studies using finite element has also been conducted by Chen and Wang (2012).

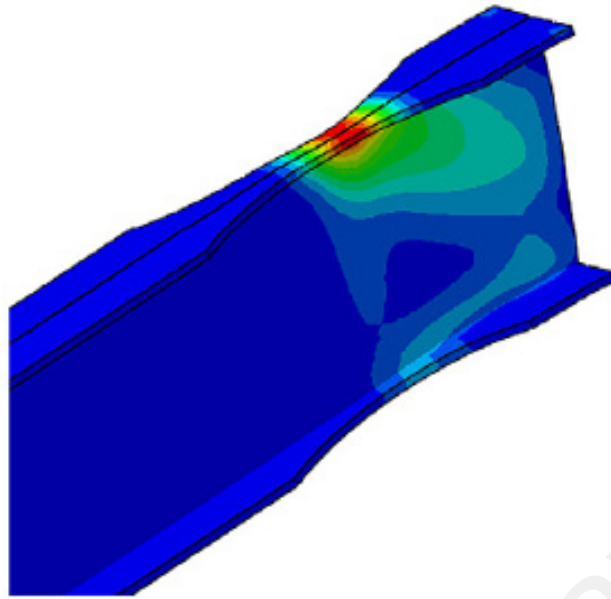


Figure 2.12 Dog-bone shaped beam deformation. (Wang and P.Wang, 2013)

### 2.5.3 Analytical Studies

With the Ramberg-Osgood method, Al-Jabri et al. (2004) conducted studies to predict the degradation of the connection at elevated temperatures. With ambient temperature connection response results, the method proposed is able to predict with high accuracy on the non-linear behavior of end-plate connections. The moment capacity of the connection and the initial stiffness of the connection were taken as the major coefficient to be applied into the formula.

Producing column web stiffeners would result in additional costs towards construction and this would also increase in material usage which is not recommended in this age of sustainable construction. Therefore, Spyrou et. al. (2004b) has conducted a study to not only eliminate the usage of stiffeners, but also to increase understanding in the effects of transverse compressive forces on the column which may affect the capacity of a connection.

Failure modes of the column web are compared between the British Standard 5950 (BS 5950) code and EC3: Annex J. BS 5950 covers two failures, including crushing and buckling while EC3 covers an additional failure: web crippling. Guides by both codes are rejected by the author, that was claimed to be conservative and combined with the results of another study, it shows that the plotted graphs by both codes is too scattered. An experimental investigation is first carried out and a formula is derived for the ultimate compressive force of the column web with the effects of temperature.

The proposed equation given in Eqn. 2.7 shows better comparison to experimental results than of Eurocode 3 and BS 5950, where;  $\beta$  = development width of the bearing zone,  $t_{wc}$  = column web thickness,  $E_{wc}$  = Young's Modulus of the column web,  $t_{fc}$  = flange thickness of the column,  $c$  = uniform distributed patch length,  $d_{wc}$  = depth of column between fillets.

$$P_u = t_{wc}^2 \sqrt{E_{wc} \sigma_{wc}} \sqrt{\frac{t_{fc}}{t_{wc}}} \left\{ 0.65 + \left[ \left( \frac{1.6c}{d_{wc}} \right) \left( \frac{2\beta}{2\beta + c} \right) \right] \right\} \quad \text{Eqn. 2.7}$$

Besides at the compression zone of the connection, Spyrou et. al. (2004) also studied on the tension zone of the connection. Focus of the study was on the T-stub component. T-stub component has been introduced by Zoetemeijer (1974) and implemented in Eurocode 3, and subsequently adopted by various researchers. T-stub is a method of modeling several components in tension zone of the connection, thus simplifying the modeling process and analysis of the connection. Three failure modes has been proposed and the analytical formulas, based on the concept of elastic, plastic flexure of flange of end plate / flange and the plastic elastic elongation of the bolts.

A semi-analytical model was proposed by Akbar Pirmoz et. al (2009). It is shown from previous study that the gage of the flange angle and thickness of the flange angle are among the most important factors that determine the moment-rotation performance of an angle connection. This study has provided a method in which the nonlinear stiffness of the connection can be determined.

In terms of stiffness, it is found that the stiffness of connections drops to almost 50% of the ambient stiffness at a temperature of 500°C and to a quarter at 650°C (Yang et.al, 2009). As fires may reach up to 2000°C, this study reveals that steel connection would probably not be able to maintain structural integrity in a fire and continue to resist loads. Undoubtedly, failure of a member may lead to a ‘domino’ effect and cause the failure of the whole structure.

Proposals on the stiffness of steel structural connections at elevated temperature conditions have been made by Mao et al. (2010) using ANSYS software. With the connection type being a fully-welded beam to column connection, parameters such as the effect yield stress, column flange width, column thickness, plate thickness and beam parameters have been studied. Following the studies, a formula is presented to predict the stiffness of a connection under a four-sided heating. However, from the validations, the formula proposed has been found to be relatively conservative and therefore, further modifications are required with additional studies.

In terms of end-plate connections, 23 different experimental test results were used to validate the proposal by Huang (2011). With a 2 node model, the end-plate connection at elevated temperatures is studied and the result of this study have shown that at elevated temperature conditions, the axial restraint levels have significant effect over the moment capacity of the connection. While for axial restraints, the model proposed is able to predict with good accuracy. Values for axial tension resistances are still conservative with accordance to the EC3: Part 1-8 extension to elevated temperature conditions.

#### **2.5.4 Component Method**

The component method or the equivalent spring stiffness model has been used by Al-Jabri (2004) for his studies on end-plate connections at elevated temperatures. Using the proposals from various sources, such as Agerskov (1976) for the bolts and Jaramillo (1950) for the column flange, the resulting connection response has shown good agreement with the experimental results. A trilinear graph model has been defined, where the early initial stiffness of the model valued at  $k$ , has subsequent stiffness at the elasto-plastic region as  $0.05k$  and the ultimate regions as  $0.01k$ . This method would generally be applied to analysis software due to its simplicity and effectiveness.



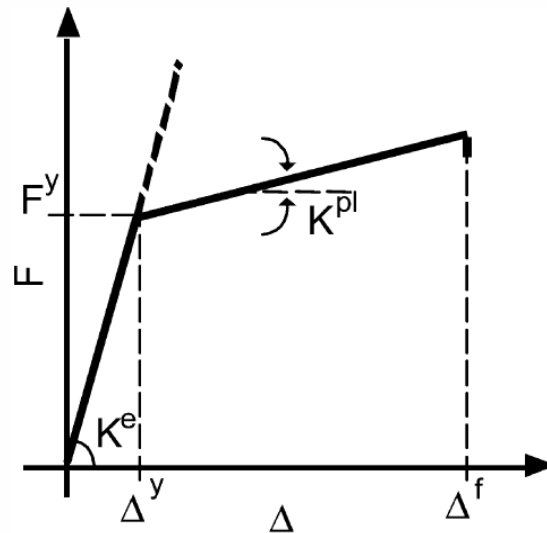


Fig 2.14: General force-deformation graph for connection components (Silva et al., 2004)

Developed by Izzudin (1991), the non-linear finite element analysis software ADAPTIC was used by Ramli Sulong (2005) which developed a new model of connection using component-based approach. Validation works are carried on five connections types under monotonic and cyclic loading at ambient and elevated temperatures condition including angle connections, extended end plate connections and fin plate connections at elevated temperatures. Experimental testing validations for the component method utilized includes tests by Leston-Jones et al. (1997) and Al-Jabri (1999). For the top-seat angle connection validations, experimental tests by Davison et al. (1987) and Shen and Astanaheh (1999) were used.

Studies on fin-plate connections have been done experimentally by Yu et.al. (2009), although the main aim of the study is to develop a component based model for fin-plate connections. Fourteen specimens were used where twelve specimens utilized a single column of bolts at the beam web side, while another two has two columns of bolts. It is observed that at elevated temperatures, the bolts tend to be governed by shear alone and relatively less bearing deformation on the beam web even if the fin plate has a higher thickness compared to the beam web. At the points where the bolt with the bolt holes and when the beam flange with the column flange is in contact, the resistance of the connection increases. Components such as the plates in bearing and bolts in shear was being referred to the mathematical models by Sarraj (2007).

According to Qian et.al (2009), there are two types of component modeling, modified rotational model and general connection element, in which, the modified model involves in axial thermal restraint which is applied indirectly while the other method is rather conventional, where the rotational stiffness is not specified and the components are free to deform accordingly to achieve the overall global rotational stiffness when assembled as a single connection element. The second method is more commonly used in the current studies.

The first method was used by Qian et.al. (2009) in the study. The study by Faella et.al. (2000) has been taken as basis of the component model. Finite element models are also used for the analysis of the end plate connections. Two groups were tested, where the first group has thermal restraint while the other has none. Results are verified against experimental data collected by Qian et.al. (2008). The results of either with or without thermal restraint show good correlations with the experimental data.

Meanwhile, for the effect of axial restraints on the connection, a study has been conducted by Pirmoz et al.(2011) in ambient temperatures for angle connections, showing that the axial tensional force with moment loads reduces connection moment capacity and initial stiffness in ambient temperatures.

Meanwhile, Qian et al. (2009) studied the effect on end plate connections in elevated temperatures. A component model for the analysis is developed and the results show that the behavior of the model is in good agreement with the experimental results. From literature, no studies have been conducted on the effect of the axial restraints on the top seat angle connections at elevated temperature condition.

## **2.6 Concluding Remarks**

Steel connections have been previously assumed to be either pinned or rigid but previous studies have shown otherwise. Connections that were assumed to be rigid displays some flexible characteristics while connections assumed pinned are able to resist an amount of the applied rotation loads. This has lead to the term semi-rigid connections. Most connections can be classified as semi-rigid connections as the connection behavior lies between the rigid and flexible behavior.

This also rises from the fact that it is not possible to have a pure shear loading, only that the connection rotation would be too small and is assumed to be negligible due to the connection stiffness. Due to the complexity of the behavior of steel connections, many studies have been conducted to obtain the relationship between various parameters that affect the behavior of a steel connection.

Results from experimental studies is used to develop further methods, such as the analytical, empirical, component / mechanical and also finite element method. Although the finite element method calculation basis itself requires no further development, the parameters assumed, the elements used in the model, refinement of model mesh size, contact element between components are among the issues that can be improved further to achieve a higher level of accuracy.

For a three-dimensional finite-element modeling, the required computational effort has resulted in numerous attempts to simplify the models for easier design process. One of the more common methods includes the component method. As the component method requires proper elements for each of the connection parts, each element must be considered for analysis as either component. Attempts in modeling for the finite-element verification and improving accuracy for the current component method software is as highlighted in the subsequent chapters.

An overall literature study reveals that previous studies on angle connections were found to be in low amount as compared to end-plate based (either flexible end-plate or extended end-plate) connections, which is likely to be caused by the increased in interest in extended and flush end-plate connections due to its reliability and widespread use. There have been sufficient studies on angle connections in ambient temperatures; however the study of top-seat angle connections in elevated temperatures is severely limited and this therefore reinforce the need for either further experimental tests or numerical modeling to cater for this specialized area.

## CHAPTER 3

### METHODOLOGY

#### 3.1 Introduction

This chapter discusses on the development of the top-and seat angle connection at ambient and elevated temperature. The main analysis software used in this study is the ANSYS Finite-Element Software, specifically the ANSYS Workbench branch of the software. ANSYS software can be divided into the Classic Interface or the Workbench interface. In comparison, the Workbench interface has several advantages over the Classic interface, being more user-friendly, faster model checking and easier definitions of surface contacts, boundary conditions, definitions of material properties and the analysis methods. Undoubtedly, there are limitations posed by the overall easier interface, such as having no control over the element types which is defined by default, applications of loads are limited to types that are visible on the model e.g. on the edges of beam and not being able to apply as a line load on centre of the beam flange surface.

As with all finite-element analysis, the geometrical models must be meshed with elements before any analysis can proceed. Completion of the meshing would then be followed by the application of the boundary conditions, definitions of material properties, loads and subsequently applying non-linear strategies followed by the completion of the analysis. Subsequently, the post-processing is conducted to obtain the results required for comparison in the study.

The resulting behavior is then compared to experimental test results and if the model analysis is unable to converge, modifications would have to be applied, e.g. definitions of parameters to enable the analysis to converge to a result. The basic flow of the modeling procedure is as shown in Figure 3.1.

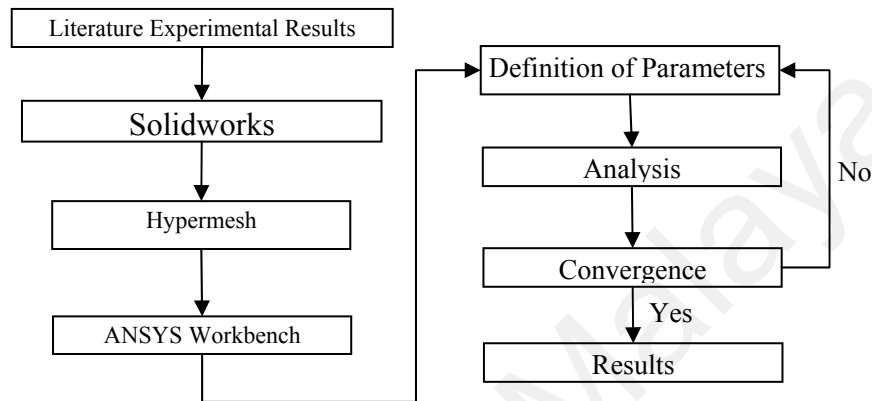


Figure 3.1 General flow of Modeling Procedure.

Generally, two models were studied, first being the ambient temperature model and subsequently the elevated temperature model. Ambient temperature models serve the purpose of reducing issues that may be encountered during the analysis elevated temperature models. Verifications of the ambient temperature model would justify the procedures in preparing the model for elevated temperature analysis. In elevated temperature models, the variation of materials with elevated temperatures has to be considered which increases the complexity of the analysis, in addition to the proper temperature loading procedure where the usage of static or dynamic analysis have to be decided. The procedural flow of the study is as shown in Figure 3.2 below. First three parts of the study are verifications of the modeling procedures and assumptions while the other are on the objectives of the study.

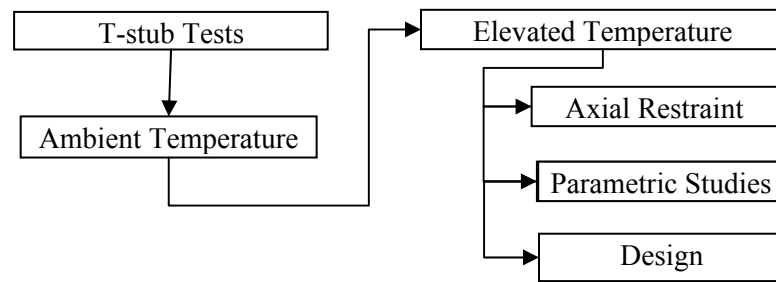


Figure 3.2 General Flow of Study.

In general, different software has each own advantages and strong points which is the reason for the selection of Hypermesh for the meshing procedure and Solidworks for the geometrical modeling stage. Utilizing the softwares would relatively reduce the amount of work required to prepare the model for analysis and therefore, increasing productivity due to the ease of these specialized software in comparison to ANSYS Workbench default modules. It has been found that the ANSYS Workbench Meshing module is comparatively suited for automatic tetrahedral meshing, while difficulties in correcting mistakes when modeling geometrical models in ANSYS Design Modeler has led to the selection of Solidworks as the alternative geometrical modeler.

### 3.2 Geometrical Model - Solidworks

Developed by Dassault Systèmes SolidWorks Corp. as an easy to use 3D CAD software and first released in 1995 where Solidworks is a parasolid based modeling software. The main concept of modeling is on the parameters, such as the length that defines the geometrical model, instead of having solids to define the dimensions where the limits of the model are defined when the model is created.

In comparison of Solidworks to the default ANSYS Workbench geometrical modeler which is the Design Modeler module, errors in the Design Modeler is much more complicated to correct due to the nature of the model being a 'single' solid rather than an assembly of components.

It is common for users to have trial and error modeling before the model can be suitable for analysis and geometrically correct. With the modeling concept of Solidworks, models of bolt shanks attached to the bolt head can be length modified without having to remodel the whole bolt while still remain attached to the bolt head. To complete the geometrical model, parts (e.g beams, bolts, columns and plates) have to be modeled and assembled in Solidworks.

### **3.2.1 Creating Parts**

Generally, modeling in Solidworks mainly involves in using lines and points to create cross sections that would be extruded to form a solid. Due to the fact that Solidworks has structural steel sections defined in its default library, the beam and column members are selected from the library as a cross section which is then extruded to the required lengths. Although a connection wizard is available for bolts where suitable bolt sizes and types can be inserted into the model accordingly, but the issue is that the geometrics provided are too complex for analysis purposes and generally would require extensive time and work to enable proper analysis convergence of the model.

In order to export the model to Hypermesh, bolt holes must first be modeled in the part creation stage. Without the bolt holes or if the bolt holes are added in the assembly stage, the Hypermesh software ignores the bolt holes created and meshes the model without any consideration to the holes. In basic, the 'simple hole' function is selected to place relevant bolt holes at the general area of required locations. No pre-drawn locations required due to the setting dimensions such as the distance from an edge can be defined and modified using the 'Smart Dimension' function which relocates the hole based on the dimensions defined, resulting in a simpler process of creating these holes. An example of parts modeling process is as shown in Figure 3.3.

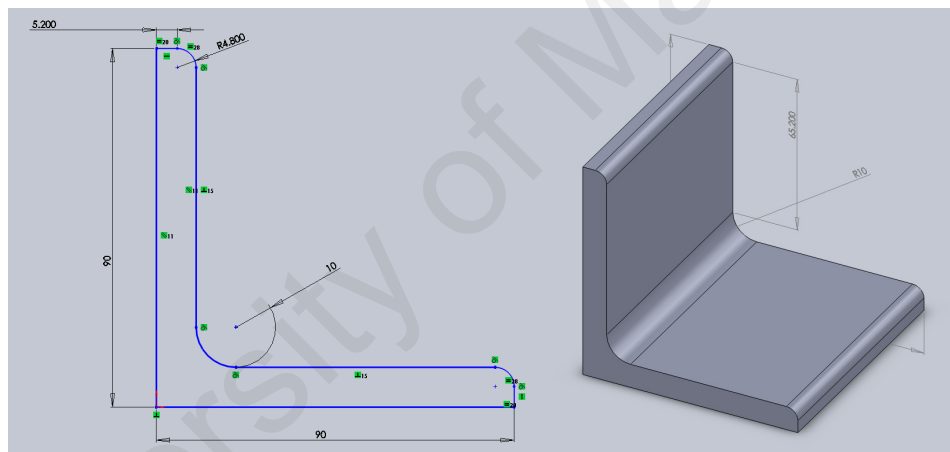


Figure 3.3 Modeling solids in Solidworks

### 3.2.2 Parts Assembly

Assembly at this stage only involves the column, angle and the beam. To complete the connection geometrical model, some procedures are followed. With the bolt holes in place, the bolts are first assembled, by 'mating' the surface of the connecting member, as shown in Figure 3.4, where in this example would be the angle section surface and the bottom surface of the bolt head, which results in both surfaces to be on the same plane.

After the location plane has been established, 'mate' is selected for the bolt hole edges and bolt shank surface, causing both parts to have concurrent centers of diameter and having the bolt to be 'connected', bolting both the angle and plate. With the same concept, the bolt nut is joined to the column / beams other side of the head and the inner wall of the nut is joined to the bolt shank, resulting in a geometrical model that resembles a bolted connection, as shown in Figure 3.5.

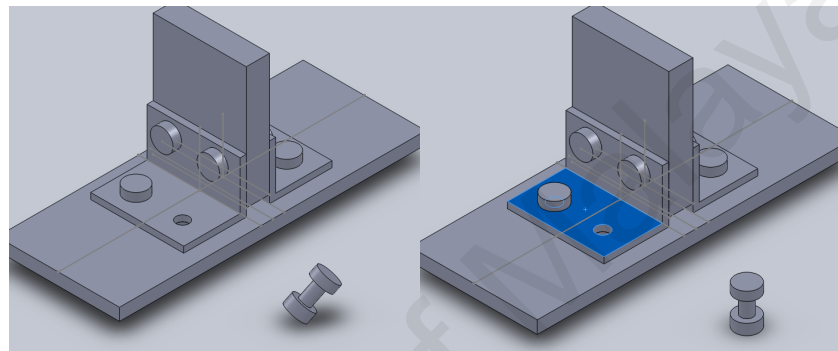


Figure 3.4: Example of connecting parts selection in Solidworks

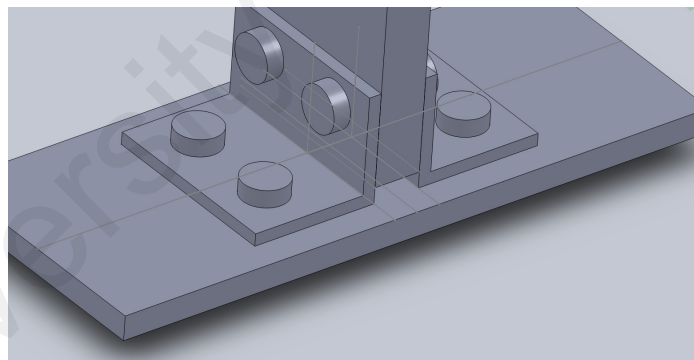


Figure 3.5: Complete Bolted Connection Assembly in Solidworks

### 3.3 Meshing In Hypermesh

Hypermesh is the main software used for the meshing procedures in this study. Developed by Altair Engineering and released in 1999, Hypermesh is part of the module under the main software package of Hyperworks, which is a product design and development software. The main concept of meshing would be to replace the geometrical model with equivalent elements of size and shape relevant to the study. One of the major issues in the meshing procedure would be on the element types and hexahedral or tetrahedral shaped meshing.

From previous studies, where the documented elements being used are as shown in Table 3.1, the elements used are commonly 8 node elements, which each node having three degrees of freedom. ANSYS software utilizes the SOLID elements while the ABAQUS software utilizes the C-series elements. Most studies utilize the hexahedral shaped mesh, where it is assumed to be due to the decreased number of nodes covering an area, therefore reducing stiffness of elements in comparison to higher number nodes created with tetrahedral elements.

Table 3.1 Elements used in previous studies

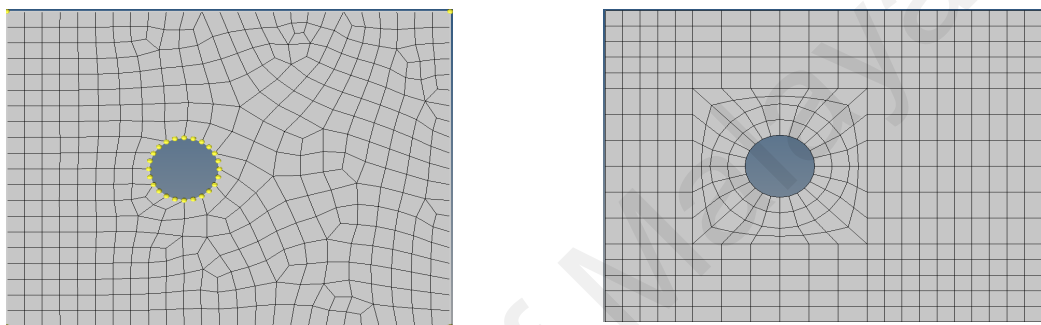
Author	Connection Type / Study	Element Used
Yang et al. (2000)	Web Angles, Welding at beam leg	C3D8, CC3D20
N.Kishi et al. (2001)	Top-seat with web angles	C3D8
Hong et al. (2002)	Web Angles, Welding at beam leg	C3D8, CC3D20
Pirmoz et al. (2008)	Top-seat with web angles	SOLID45, SOLID64
Cafer (2009)	Top-seat with web angles	SOLID186
Saedi and Yahyai 2009b)	Top-seat angle	SOLID64

### 3.3.1 Hypermesh Methods

One of the main procedures in producing hexahedral meshing would be the splitting of the geometrical model into smaller parts, which includes the faces of the geometry or sectioning of the geometry into parts which can be easily 'mapped'. To highlight on the importance in application of meshing techniques, an example is as shown in Figure 3.6 for the difference in automatic hexahedral meshing and meshing of the same geometry without sectioning. It is clear that sectioning provides a more efficient and uniform meshing in comparison to the automatic method. Proper control across the geometrical model produces an arranged mesh which provides a platform for easier convergence of the surface contacts in the analysis at later stages.

On the other hand, using the concept of extrusion as a meshing technique, hexahedral meshing can be produced out of 2D surface elements by extruded into 3D equivalent elements. The same concept can also be applied to convert 1D element to 2D elements, thus simplifying the meshing process into knowing how to utilize the methods for a hexahedral meshing. An example is as shown in Figure 3.7, for modeling of a hex bolt, including the shanks, head and nut. In the figure, the process from (a) geometry to (c) fully meshed bolt show extrusion of the 2D mesh from top of bolt head to bottom of bolt, into a 3D hexahedral mesh.

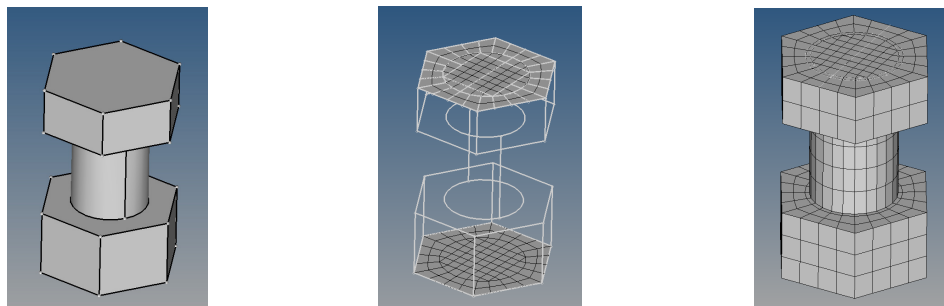
Completion of the meshing in Hypermesh would require for the model to be modified before exporting the mesh into ANSYS Workbench. The modifications required includes the deletion of the “free” nodes that are not involved in any of the mesh elements, nodes created to assist in sectioning the geometry for meshing and assigning elements types to the mesh elements created. Any mesh that is not 3D has to be removed for the mesh to be properly imported by ANSYS Workbench.



(a) Hypermesh Automatic Meshing (b) Sectioning Method Applied Mesh

Figure 3.6 Meshing Differences

To be imported into ANSYS Workbench, mesh has to be processed by the ‘Finite-Element Modeler’ module which converts the exported codes into ANSYS Workbench model. It is crucial that the mesh to be uniformed and meshed as a single solid as so to result in full solid. The processed meshing will be linked to the ‘Model’ Component of the analysis system to create the model for analysis.



(a) Solidworks model (b) Top and Bottom Mesh (c) Mesh Extrusion – 3D

Figure 3.7 Meshing of bolt using Hypermesh.

### 3.4 ANSYS Workbench Basics

At the current version of ANSYS, two platforms are available, either the ANSYS Classic or the Workbench interface. ANSYS Workbench has been selected for this study due to its user-friendly interface and the ease of importing CAD models directly from Solidworks model files. From literature review, most analysis studies have been conducted using the Classical interface and relatively less studies have been conducted using ANSYS Workbench. Therefore, having a study in ANSYS Workbench provides a point where comparisons can be made on the limitations and advantages between the two interfaces. Considering that ANSYS Workbench is fairly easy to work with, it would definitely be beneficial if Workbench can be used for various situations and analysis without any loss of accuracy.

ANSYS Workbench favors a drag-and-drop interface at the main layout of the program. The main layout example is as shown in Figure 3.8, where ANSYS Workbench has several default analysis systems fulfilling needs depending on the analysis requirements. Several analyses can be placed in the main layout, resulting in a collective analysis, possibly with different parameters / settings and results. This collective is saved as a project. After an analysis system is selected, the output is an “Analysis Component List”, as shown in Figure 3.9, which outlines the components which must be defined in order to analyze the model. In the direct order, the Engineering Data component defines the material properties and the Geometry component for model imports or modeling using the Design Modeler module. Meanwhile, the “Setup”, “Results” and “Solution” component is related to the definition of loads and boundary conditions.

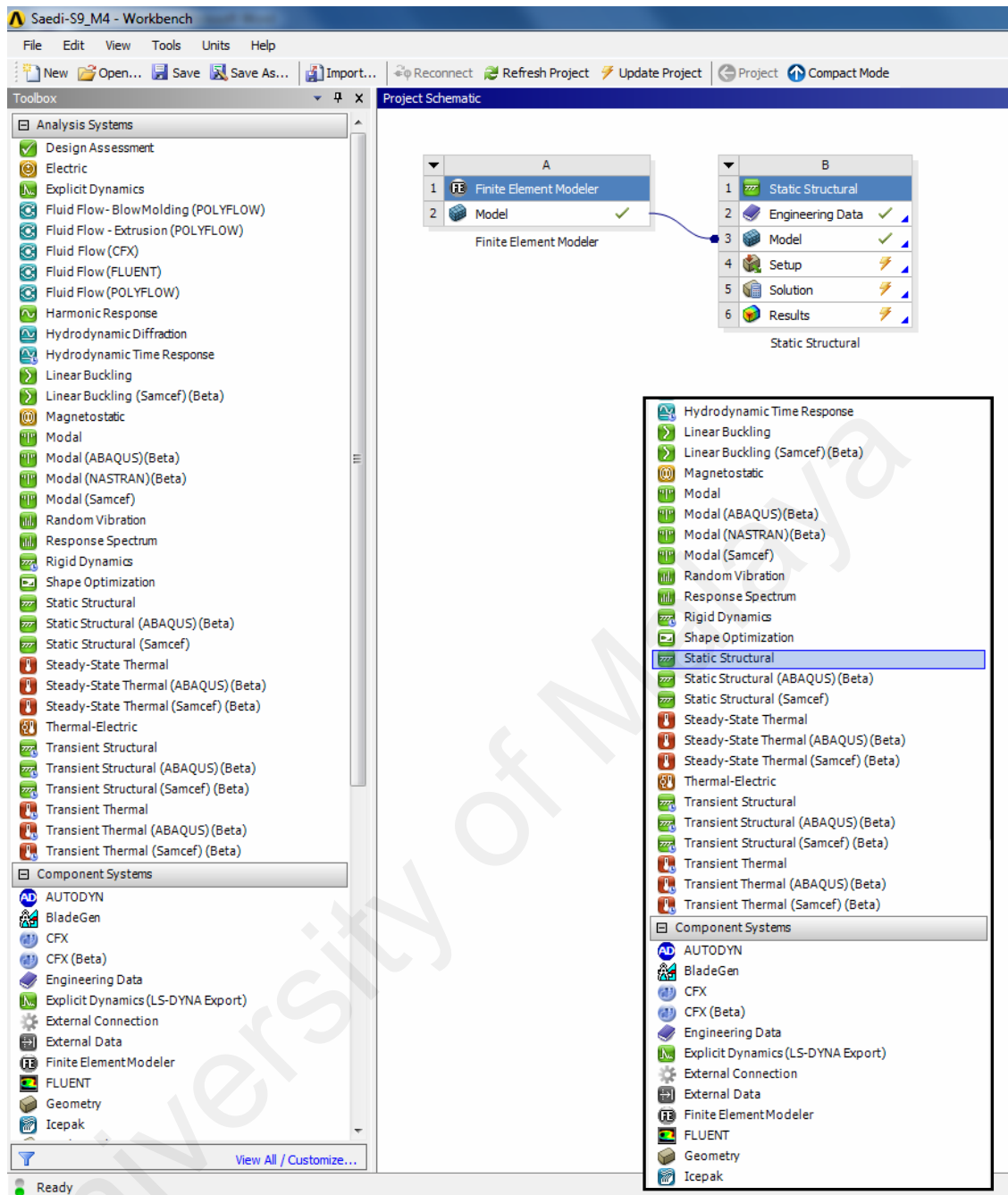


Figure 3.8 Main Window screen of ANSYS Workbench  
(Inset) Various Analysis Systems

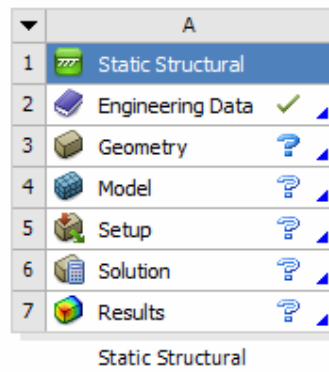


Figure 3.9: Analysis Component List

Files and data can be linked by dragging and placing one over the other, or resulting in cases where the results data for static structural analysis can be used for further analysis e.g. thermal stresses. Importing from Hypermesh involves in the “Finite Element Modeler” system where the Hypermesh (.cdb file) is processed by the “Finite Element Modeler” system and linked with the “Model” component of the “Static Structural” System. Linking both the mesh files and analysis systems eliminates the geometry component as the Finite Element Modeler system converts available mesh into geometrical solids. A comparison can be made between Figure 3.8 and 3.9 where the former has imported the mesh from Hypermesh, while the later is the default list for the same analysis system.

The “Setup” component is one the main components in any analysis using ANSYS Workbench. All loads, supports, definitions of different material properties for each solids, and results are defined from the “Setup” component. Figure 3.10 shows the interface of the “Setup” component, where the model view, analysis definitions, tabular data / load steps and definition options are located.

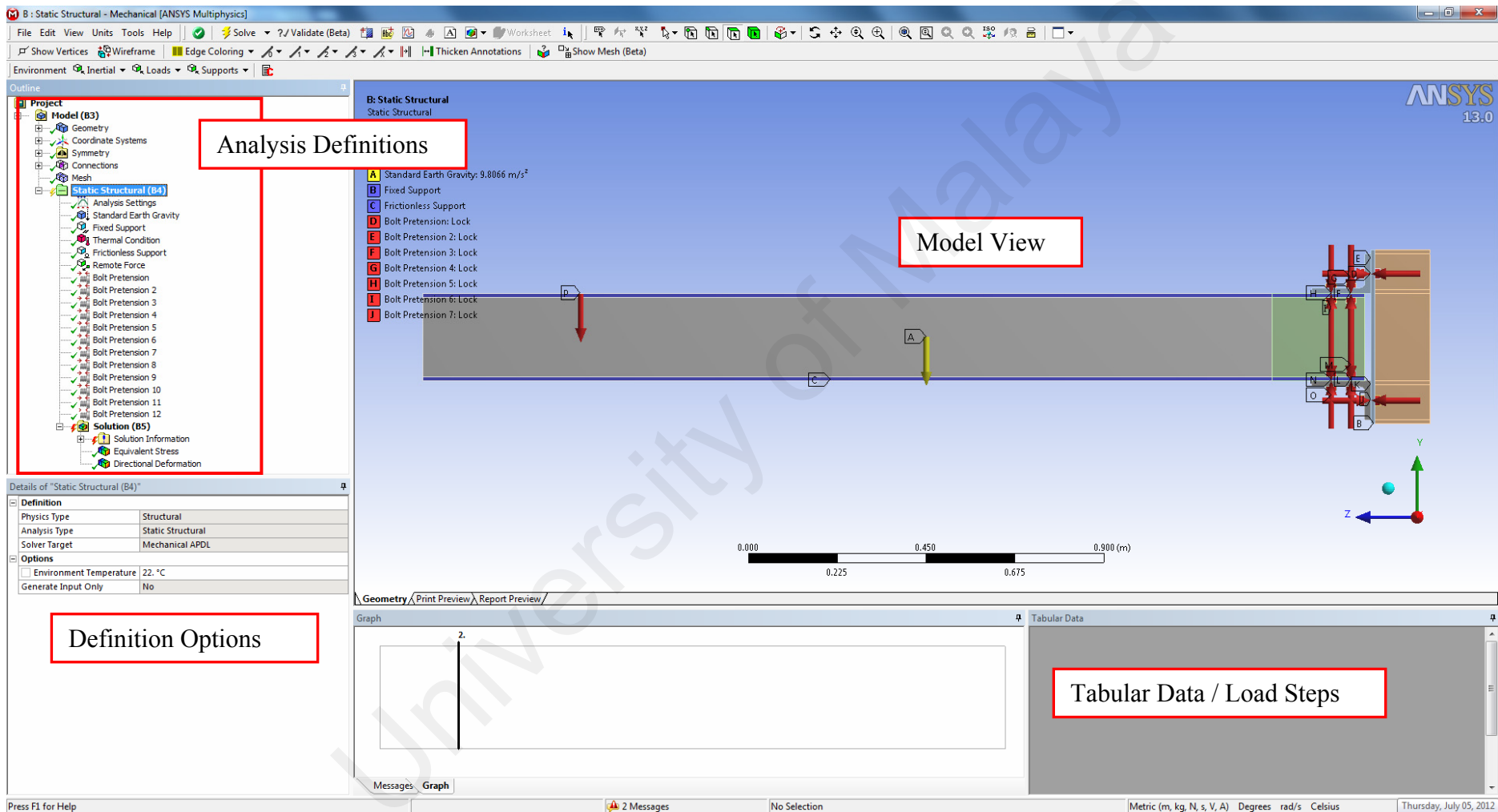


Figure 3.10 Main analysis setup interface and critical interface aspects.

### 3.4.1 Material Properties Considerations

Steel material is usually uniform and therefore, little variation can be found due to the standardized process of producing steel sections. The common properties of steel to be considered includes the yield stress, ultimate stress and the Modulus of Elasticity. The typical stress-strain graph is as shown in Figure 3.11 as documented by Cafer (2009). Strains of 0.002 in elongation length ratio are still considered to be in the elastic range while the ultimate stress lies between the 0.2 and 0.3 elongation length ratio.

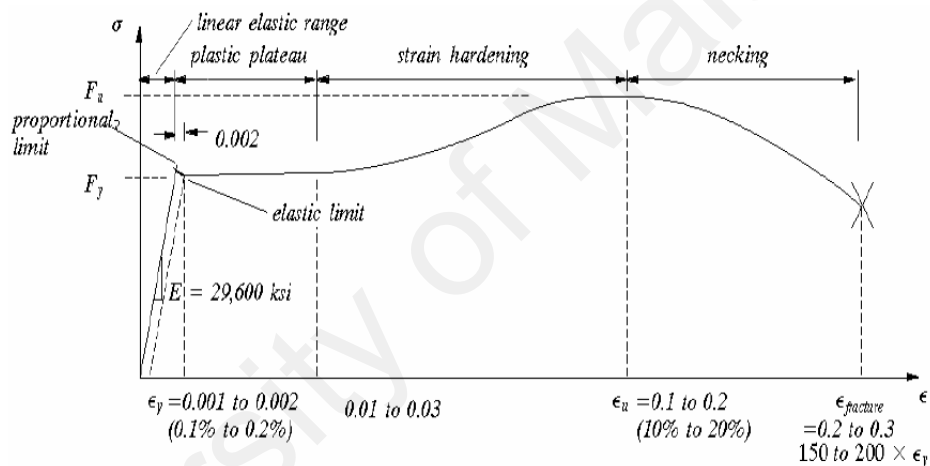


Figure 3.11 Typical Stress-strain behavior of steel material.

### 3.4.2 Ambient Temperature Materials

For ambient temperature models, the initial behavior of a steel material is as shown in Figure 3.11. In actual, Figure 3.12 shows the behavior of ASTM A541, ASTM A441 and ASTM A36 steels as a typical stress-strain graph. For consideration in a finite-element analysis, simplifications of the behavior have been considered in various studies, such as by Pirmoz (2009), N.Kishi (2001) and Saedi (2009).

The results from the models have shown good agreement with the respective experimental results being simulated, where the material behavior is simplified to a multilinear graph, encompassing the yield and the ultimate stress value. An example of the simplification of the behavior by using trilinear material model as shown in Figure 3.13 and is considered for the steel material in this study.

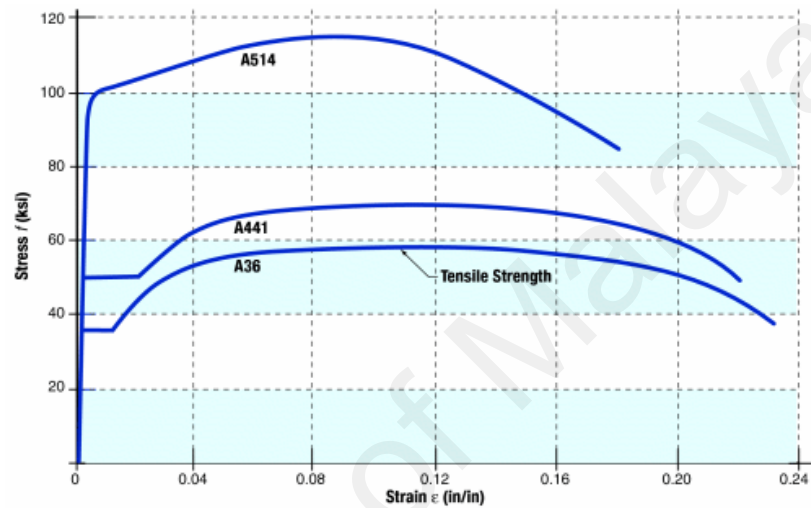


Figure 3.12 Typical initial stress-strain curve of Steel Behavior.

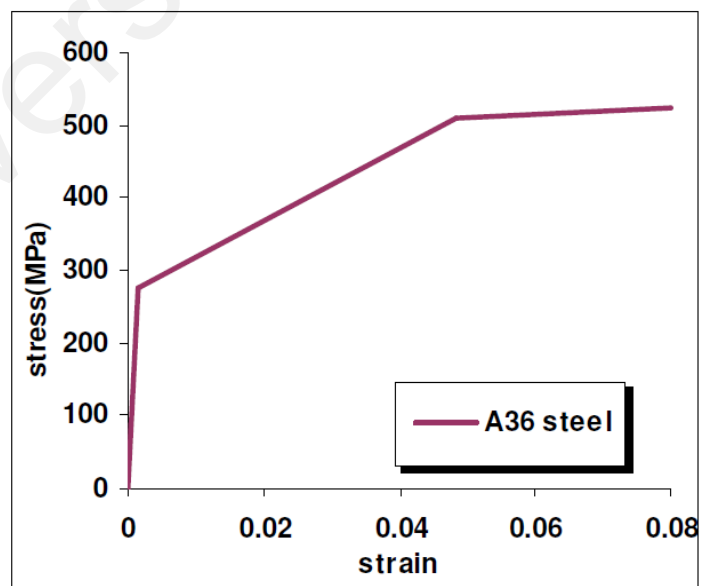


Figure 3.13 Trilinear Material Properties Adopted.

### 3.4.3 Elevated Temperature Material Models

In comparison to the ambient temperature models, the major difference in the consideration for the material properties would be the degradation factors of steel with the variation of temperatures. EC3: Part 1-2 provided the degradation factors and the stress-strain curve for steel, defining the slope of the elastic area, the curve after the proportional limits and the limitation strain for the behavior under elevated temperature. Degradation factor values are as shown in Table 3.2 while the definition of the curves is as shown in Table 3.3. The typical stress-strain curve for steel in elevated temperature is as shown in Figure 3.14 as defined in EC3:Part 1-2. Both steel members and bolts used the same definition as have been outlined.

The material models used in the analysis are based on the material models defined by EC3: Part 1-2 and simplified to a multilinear material model, where the major points of the material model curve are at the starting point, the proportional limit point, and yield stress at 0.02 strains and at 0.15 strains. A comparison is made between the proposed material models in EC3: Part 1-2 and those used for this study as shown in Figure 3.15. It should be noted that the Multilinear Isotropic Hardening material model does not allow for decrease in material properties, therefore, model in ANSYS is only up to the 0.15 strains level as beyond 0.15, the strain levels increases while the stress levels decreases, which would lead to material failure.

Table 3.2 Reduction factors for steel at various temperatures.  
(EC3: Part 1-2, 2005)

Steel Temperature $\theta_a$	Reduction factors at temperature $\theta_a$ relative to the value of $f_y$ or $E_a$ at 20°C		
	Reduction factor (relative to $f_y$ ) for effective yield strength $k_{y,\theta} = f_{y,\theta}/f_y$	Reduction factor (relative to $f_y$ ) for proportional limit $k_{p,\theta} = f_{p,\theta}/f_y$	Reduction factor (relative to $E_a$ ) for the slope of the linear elastic range $k_{E,\theta} = E_{a,\theta}/E_a$
20°C	1,000	1,000	1,000
100°C	1,000	1,000	1,000
200°C	1,000	0,807	0,900
300°C	1,000	0,613	0,800
400°C	1,000	0,420	0,700
500°C	0,780	0,360	0,600
600°C	0,470	0,180	0,310
700°C	0,230	0,075	0,130
800°C	0,110	0,050	0,090

Table 3.3 Material curve definition formula

Strain range	Stress $\sigma$	Tangent modulus
$\varepsilon \leq \varepsilon_{p,\theta}$	$\varepsilon E_{a,\theta}$	$E_{a,\theta}$
$\varepsilon_{p,\theta} < \varepsilon < \varepsilon_{y,\theta}$	$f_{p,\theta} - c + (b/a) [a^2 - (\varepsilon_{y,\theta} - \varepsilon)^2]^{0.5}$	$\frac{b(\varepsilon_{y,\theta} - \varepsilon)}{a [a^2 - (\varepsilon_{y,\theta} - \varepsilon)^2]^{0.5}}$
$\varepsilon_{y,\theta} \leq \varepsilon \leq \varepsilon_{t,\theta}$	$f_{y,\theta}$	0
$\varepsilon_{t,\theta} < \varepsilon < \varepsilon_{u,\theta}$	$f_{y,\theta} [1 - (\varepsilon - \varepsilon_{t,\theta}) / (\varepsilon_{u,\theta} - \varepsilon_{t,\theta})]$	-
$\varepsilon = \varepsilon_{u,\theta}$	0,00	-
Parameters	$\varepsilon_{p,\theta} = f_{p,\theta} / E_{a,\theta}$ $\varepsilon_{y,\theta} = 0,02$	$\varepsilon_{t,\theta} = 0,15$ $\varepsilon_{u,\theta} = 0,20$
Functions	$a^2 = (\varepsilon_{y,\theta} - \varepsilon_{p,\theta})(\varepsilon_{y,\theta} - \varepsilon_{p,\theta} + c / E_{a,\theta})$ $b^2 = c(\varepsilon_{y,\theta} - \varepsilon_{p,\theta})E_{a,\theta} + c^2$ $c = \frac{(f_{y,\theta} - f_{p,\theta})^2}{(\varepsilon_{y,\theta} - \varepsilon_{p,\theta})E_{a,\theta} - 2(f_{y,\theta} - f_{p,\theta})}$	

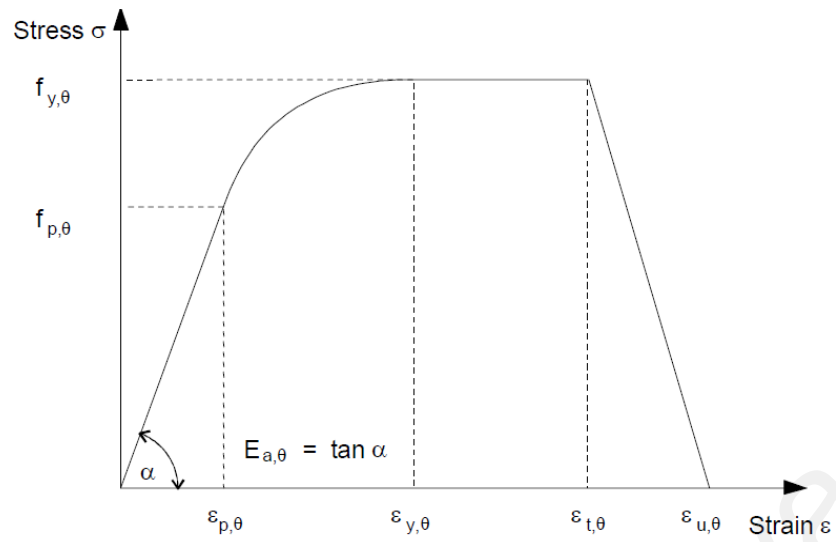


Figure 3.14 Stress-strain curve for steel in elevated temperatures

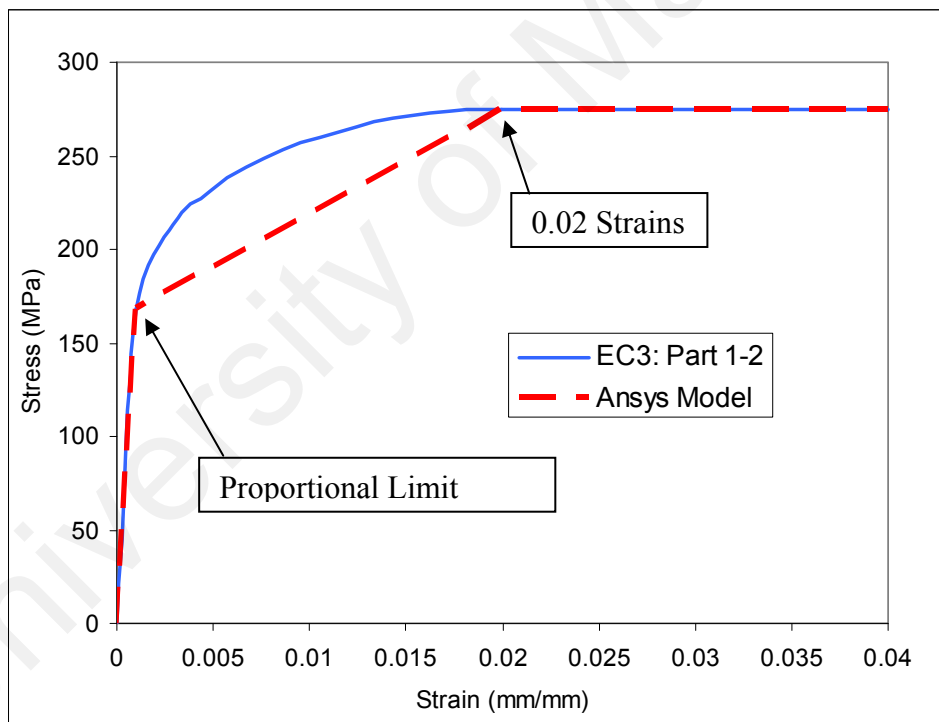


Figure 3.15 Comparison of EC3: Part 1-2 and material model of this study

### **3.5 Element Types**

In comparison to the ANSYS Classic interface, unfortunately no element types can be selected nor modified for the model. Element selection has been automated depending on the mesh settings defined within the mesh setting or defined according in Hypermesh. The common elements used are SOLID185, SOLID186 and SOLID187, while for the element default for pretension is PRET179. In terms of contact elements CONTA174 and TARGE170 is commonly pre-defined. Comparing with other finite-element software, these elements are also available with different names. An example would be that the SOLID185 is the C3D8 element in ABAQUS. In effort of simplifications, the bolts and steel members both used the same element types, in the sense that for triangular shaped elements, either SOLID186 or SOLID187 is used while the SOLID185 is used for hexagonal elements defined using Hypermesh.

#### **3.5.1 SOLID187**

The SOLID187 element, as represented in figure 3.16, is described as a 10-node element having quadratic displacement behavior. This element is suitable for the case where model mesh are irregular especially in geometrical models imported from CAD software such as Solidworks. Each node has a 3 degree of freedom in the x,y and z axis. The element has capabilities for the simulation of early incompressible elasto-plastic materials, and fully incompressible hyper-elastic materials. Besides that this element has plasticity, hyper-elasticity, creep, stress stiffening, large deflection, and large strain capabilities. When using tetrahedral meshing, this element will be higher in number in comparison to the other elements that were also generated in default.

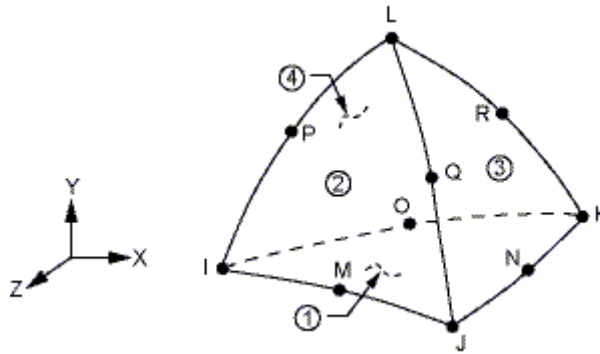


Figure 3.16 Representation of SOLID187 element

### 3.5.2 SOLID186

In comparison to SOLID187, SOLID186 is a 20-node hexahedral element that has similar capabilities with the SOLID187 element. Representation of SOLID186 element is as shown in Figure 3.17. Analysis has shown that the SOLID186 has lower deformation stiffness in comparison to SOLID185 due to the mid-side nodes. The existence of the mid-side nodes classifies this element as the 2nd order elements and requires higher computational effort in comparison to 1st order elements.

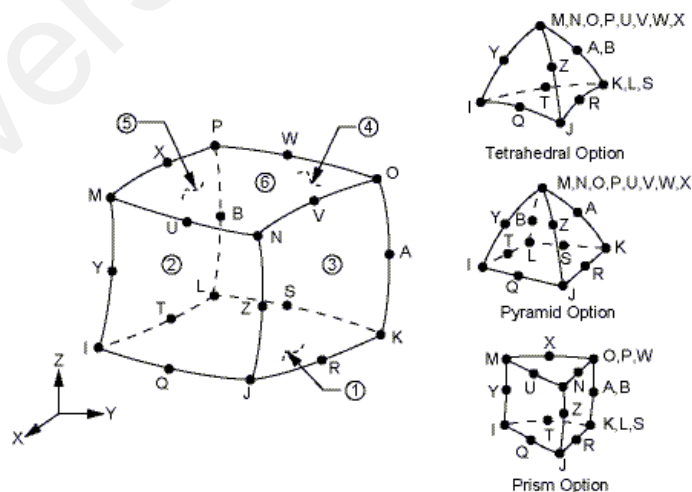


Figure 3.17 Representation of SOLID 186 element

### 3.5.3 SOLID185

SOLID185 and SOLID186 differs only in the number of nodes involved, from 20-node to 8-node. Therefore, the SOLID185 element is classified as a first-order element and comparatively, has lower degrees of freedom. Definition of mesh with Hypermesh would default to SOLID185 in ANSYS Workbench for any first order hexagonal elements defined.

### 3.5.4 CONTA174 and TARGE170 elements

For contact between two surfaces or one edge with one surface, ANSYS Workbench utilizes both elements of CONTA174 and TARGE170 as the elements on top of the solid elements as shown in Figure 3.18 and Figure 3.19. Depending on the order of the elements, either CONTA173 or CONTA174 elements are used where CONTA174 is the corresponding contact element for 2nd order solid elements while the other is for the 1st order elements.

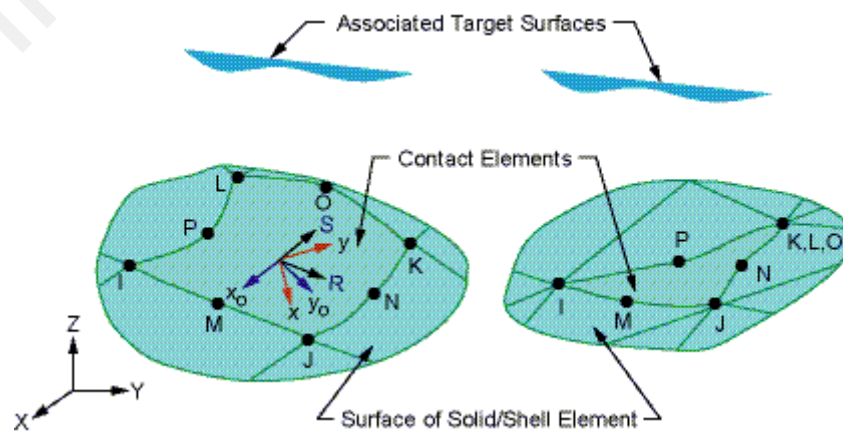


Figure 3.18 Representation of CONTA174 element

### 3.5.5 PRETS179

For bolts applied with pretension loads, a single element is generated in the bolt axis which is the PRETS179, given in Figure 3.20, the element specifically only for pretension. This element can only deform in the direction which the pretension was specified and will only react under tension loads, ignoring other forms of loads. When represented in analysis, the optimum procedure would be to define the pretension as first load step and continue with other loads in the second step due to the ignorance of other loads.

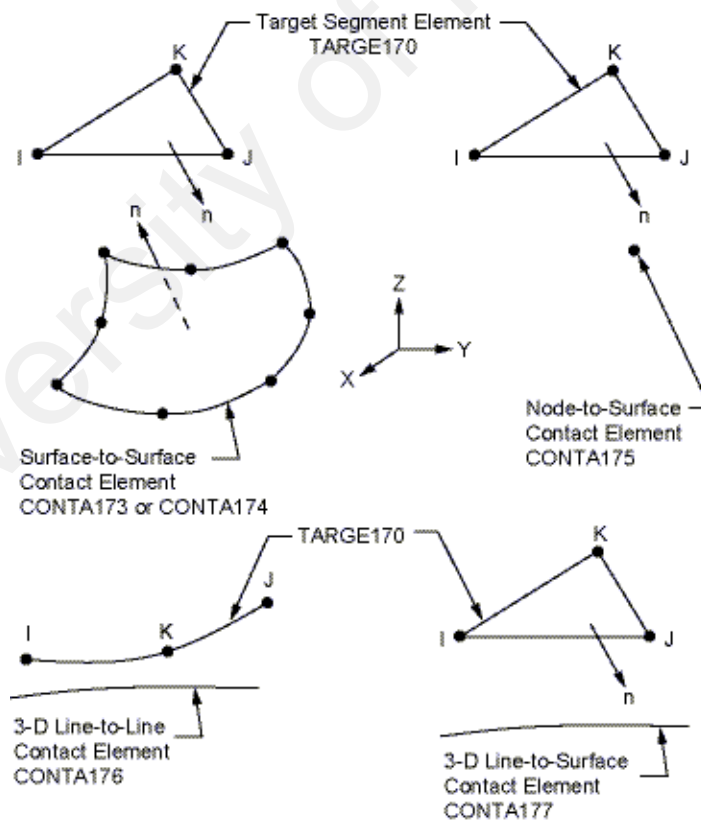


Figure 3.19 Representation of TARGE170 element

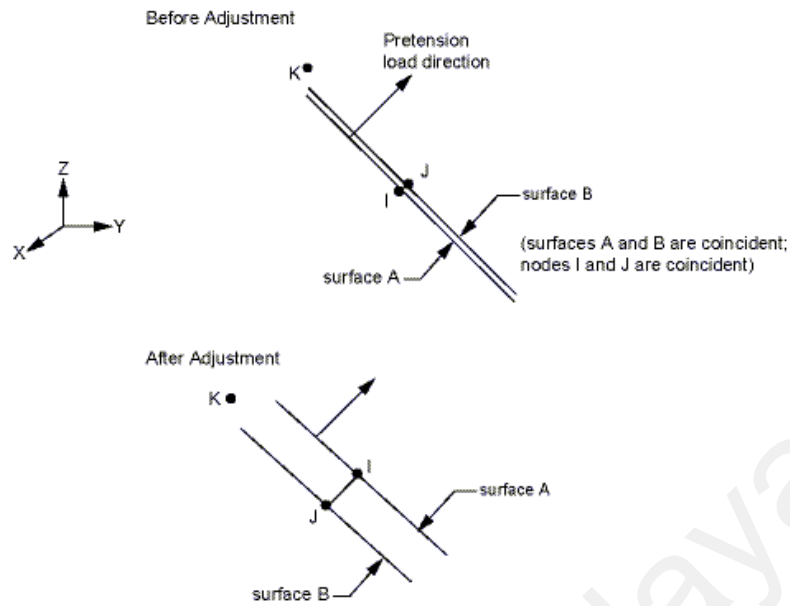


Figure 3.20 Representation of PRETS179 elements.

### 3.6 Contact Definition

For both ambient and elevated temperatures, several parameters continue to remain unchanged as these parameters are not affected by the variation in temperature. Among the parameters under this category includes the density of steel, coefficient of friction, and the parameters set for the contact interactions.

#### 3.6.1 Coefficient of Friction

Coefficient of friction is the dimensionless Coulomb friction value between two surfaces, which can be described as the ratio of tangential force and the force normal to the surface. In studies, such as those by N.Kishi et. al. (2001) the value of 0.1 has been considered.

Guidelines provided by AISC (Manual for Steel Construction) mentions that the value of 0.33 for class 'A' surfaces, where class 'A' refers to clean mill surfaces. Value of 0.25 has been considered in the study by Saedi (2009) where sensitivity studies conducted have shown that it has better agreement with experimental results.

### **3.6.2 Contact Settings**

The contact settings between parts have been defined as bonded settings in default after the model is imported into ANSYS. This setting imposes that both parts do not separate at the contact areas and therefore behave as a single part when system transfers loads and deform. Usually this setting is useful for parts that have high bonds between each other or where it is assumed to have minimal separation between them. As an example, between a nut and a bolt thread area, where the nut is assumed to be fully locked against the bolt thread and therefore, for simplicity, is assumed to be bonded. This setting does not simulate actual conditions for most cases including for this study which results in only some contact settings are defined as bonded. Besides the bonded contact settings, other contact settings include the following:-

- a) No Separation - Similar to bonded but sliding is allowed. Therefore, both surfaces are still able to deform parallel to each other but the perpendicular direction deformation is assumed to be locked in place.

- b) Frictional - It is common for this setting to be utilized throughout the model as this setting closely represents the actual interaction between materials / parts. A frictional coefficient has to be defined which is either determined by experimental or theory. Both parts are able to slide against each other but with limitations due to the friction between them.
- c) Frictionless – This setting is used with the assumption that no friction exists between the parts and are free to slide against each other. Possible cases includes that a thin film of liquid exists between them therefore, friction is minimum which is almost frictionless.
- d) Rough – For cases where the friction between the parts is unknown but yet an amount of friction exists and is known to provide significant amount of limitations on the movements due to the interactions between both parts. This setting can be used for validation purposes and later modifications. It is assumed that both parts can have minor slides against each other but not so much as to behave similar to the bonded settings.

In the same contact setting area, the other parameter to highlight would be the analysis formulation method for the contact defined. The formulation method selected will affect the convergence in solving the model, where the issues of convergence are commonly governed by the stiffness and the penetration of the contact areas. Among them, the MPC method, which is the method for connecting components without having to share nodes, especially in connections with small gaps, is usually defined for bonded contact settings and therefore is not thoroughly studied. Meanwhile, the other formulation method includes:-

- a) Pure Penalty – Virtual work is increased when the contact is deformed and some small amount of penetration is required to satisfy the equations. Models are solved as it is where there are no additional degrees of freedom posed by the other methods. This therefore results in minimal over-constraining issues.
- b) Pure Lagrange - Does not rely on the stiffness of the contacts. Additional degrees of freedom posed by the Lagrange multipliers may cause the model to increase in size and computational effort. Convergence has been found to be the best among the other settings.
- c) Augmented Lagrange – In comparison to the pure Lagrange method, the augmented Lagrange method does rely on the stiffness of the contact. Although this, it relies less on the stiffness of the contact when compared to the pure penalty method. Therefore, this method allows for some penetration to occur between contacts and therefore convergence of the analysis is relatively easier.

Due to the fact that stiffness of the contact directly affects the penetration of the contact and subsequently the convergence, the stiffness of the formulation can be defined to be updated at every equilibrium points, sub-step or none at all. Minor penetration may occur if the stiffness is low but, the stress values generated does not change which therefore produces accurate stress contour and results. It is assumed that minor penetration does occur in actual specimens and the possible reason it is not detected is that the penetration is not measured. Although this, the assumption have to be paired with the suitable method of formulation.

In another issue, the other parameter that can be defined would be the determination of area of contact and area of target. ANSYS Manual (2010) states that the defined region being fixed as the area of contact, is constrained against penetrating the target element. This is usually the case when asymmetric contact parameter is selected. Meanwhile symmetric contact parameter is not affected by this definition as it is assumed that both sides have equal contacts when asymmetric contact denotes that the contacts both have different behaviors. In addition, the asymmetric definition would also raise another issue of concern especially in cases where the “actual” contact behavior is not determined. Assumptions of contact and target sides may lead to behaviors that are not according to actual cases unless an experimental was previously available for comparison.

### **3.7 Loading Conditions**

The study on connection in basic, involves in the connection behavior under various loads. These loads are transferred from the floor to the beams and to the connections, causing deformations and failures of components. In experimental studies, the loads are commonly applied using a load-cell and hydraulic loader while in finite-element analysis; the loads are simulated by pure forces acting in the direction specified or the moment loads in an axis. In elevated temperature analysis, the other form of load to be applied would be from the temperatures due the fire condition.

### **3.7.1 Direct Loads**

In ANSYS Workbench the application of forces can be done using two methods, either on geometrical elements such as on the edge, face, or point, while the other method involves remote forces. One of the limitations found in ANSYS Workbench is that the application of loads cannot be applied onto geometrics which have no edges or point clearly defined. This limitation applies to loads which are applied in the middle of a surface where there are no edges defined due the geometrical model being as a single solid, which therefore requires improvisation of the remote forces function. The original intention of the remote forces was to provide forces beyond the geometrical boundaries of the model, enabling simplifications of the model and reducing analysis time, but the function can be used to define forces that have to geometrical associations.

### **3.7.2 Applying Pretension Loads**

It is common practice in bolted connections that the bolts are tightened using either normal wrenches or torque controlled wrenches. For torque controlled tightened bolts, it is generally agreed that a force is generated by the bolt internally due to the shank being clamped by both the bolt head and nut simultaneously, where this force is known as the pretension force in the bolts. Preloading or pretension in the bolts would cause the bolts to rely on the clamping and friction between the bolts and washers with the surface of the connection to resist any shear forces applied. Same concept also applies for normal wrench tightened bolts where it can also be assumed to have generated pretension due to the tightening of the bolt to a certain degree and may even match the torque controlled wrenches.

Undoubtedly, it is concluded here that for any bolted connections, there is pretension forces in the bolts to certain amount or level. From literature studies, especially on the component method type of analysis, having bolt pretension would increase the resistance of the shear and bearing check of the bolt. The level of resistance has even been assumed to be infinite in the component method and the failure need not be considered if the bolts have been preloaded. With this reasoning, the effect of bolt pretension should be included in the finite-element models as the effect could be the major influence in a bolted connection behavior.

In comparison with ANSYS Classic, ANSYS Workbench utilizes the geometrical selection to apply the pretension force. Two methods are available for applying pretension, where one is convenient for cylindrical shaped geometrics while the other applies for geometrics that are otherwise non-cylindrical shaped (square bolt assumptions) or separately meshed, being two geometric components assumed to be as one bolt, especially in model simplifications. Geometrical models meshed using Hypermesh uses the 2nd technique as the bolt shank is no longer cylindrical but is a polygon with 24 or more sides depending on the meshing done. However, direct import of geometrics from Solidworks is considered as a cylinder.

ANSYS Workbench provides two geometry selection method for the two cases described. For the first method involving cylindrical or full cylinder bolt shanks, the procedure is basically selecting the “face” of the bolt shank while the other method involves in selecting all the geometries or solids being considered as a single bolt. Both selection methods are as shown in Figure 3.21.

In the first method, no definitions of the axis is necessary but a definition is required for the second method as pretension is only applied in the z-axis, and considering that in an top-seat angle connection, bolts center axis faces two directions, at the column flange and the beam flange. Figure 3.22 shows the various coordinate systems defined for the column and beam bolts.

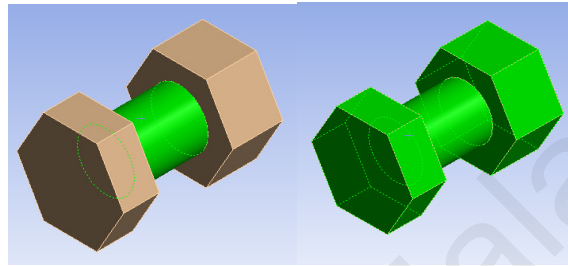


Figure 3.21 Selection methods bolt pretension

Specifications for the pretensions loads are located under the definition sub-component. It is common practice to define the pretension as force under the first load-step and subsequent load-steps to be configured to the 'lock' option to fix the pretension deformations. The other option 'open', as shown in an example in Figure 3.23, clears the pretension and removes any loads applied. Although this, utilizing the 'open' option has resulted in non-convergence of the analysis but the option should be studied further in tests to understand the behavior.

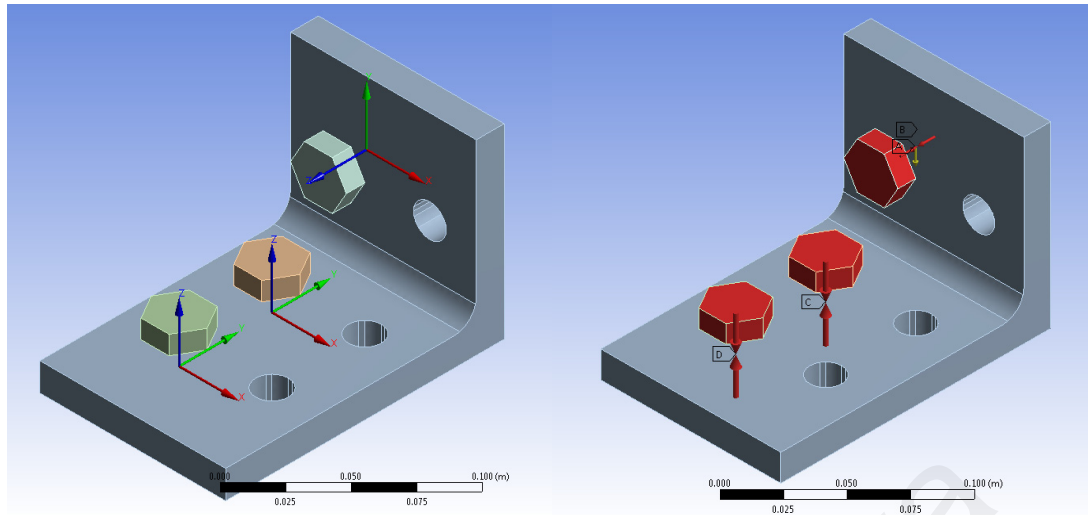


Figure 3.22: Coordinate systems for pretension of bolts and the direction of force.

Tabular Data				
	Steps	<input checked="" type="checkbox"/> Define By	<input checked="" type="checkbox"/> Preload [N]	<input checked="" type="checkbox"/> Adjustment [m]
1	1.	Load	20000	N/A
2	2.	Lock	N/A	N/A
3	3.	Lock	N/A	N/A
4	4.	Lock	N/A	N/A
*		Lock		
		Open		

Figure 3.23: Options for pretension definitions.

### 3.7.3 Temperature Loads

In comparison to the pretension loads or the direct forces, temperature loads are applied on the bodies as whole solid by definitions of temperatures. Temperature loadings that are defined do not follow any standard fire curves with the concept that the behavior is not dependent on time factor. At constant moment load levels, the response of the connection at a particular temperature would not be affected by the amount of time which has passed.

Therefore, for anisothermal conditions, the temperature loading definition can be defined at 100°C value increments at each load steps instead of having to define the relevant temperatures at each second according to fire curves. This justifies the use of the static structural systems as it is not a dynamic behavior where dynamic analysis is dependent on the time factor. On the other hand, for isothermal analysis, the temperatures are defined as a constant value across the load steps.

As a model simplifications procedure, the temperatures are defined as a uniform temperature throughout the solid and does not consider on the variation of temperature which requires a further thermal analysis and consideration to thermal conductivity and the specific heat values of steel. In ANSYS Workbench, thermal loads are applied by selecting the target solids and defining the relevant temperatures in the load steps. The temperatures may also have to be dependent on the convergence of the analysis where increased amount of load steps with smaller temperature increments to be implemented.

### **3.8 Boundary Conditions**

In any structural analysis, the three common supports are pinned, roller and fixed supports. These supports are essential for any finite element analysis and therefore can be defined in ANSYS Workbench using the default supports options. Figure 3.24 shows the default supports available in ANSYS Workbench, including the fixed support option and the frictionless support as the roller support option. On the other hand, pinned support, although is not a default option, can be defined using two methods, either using the displacement support option or the cylindrical support option.

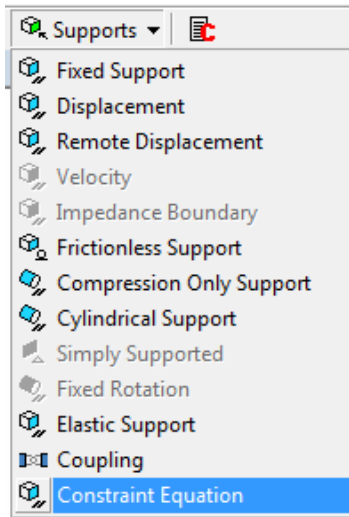


Figure 3.24: Default ANSYS Support options

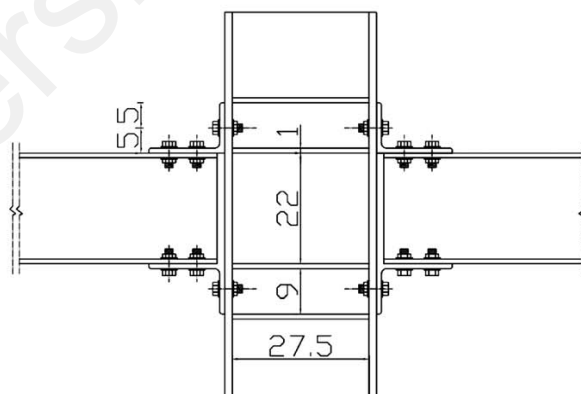
The displacement support option can be used to define pinned supports due to concept of pinned supports where one horizontal and one vertical reactions at the support and able to rotate in the remaining of the three main 3D axis. This therefore can be simulated depending on the selected geometrical component type, e.g for edges, both axis should be fixed in place while the other, using the surface, should only be fixed on one axis while in the other axis, is free to deform.

Although the supports can be defined, but these supports cannot be removed for one load step and replaced in another load step. To disable the displacements for one axis, the displacements must be set to the value of zero. Setting the displacements to the 'free' option would release the support in the axis specified, and the option between 'free' and zero is not interchangeable. On the other hand, cylindrical supports can also be used to define pinned supports but the geometrical model have to be modeled with a hole representing where the pinned support will go through. The cylindrical supports acts as though a physical pin with the diameter specified is available fitted at the hole, thus, enabling rotation but resisting displacements in two axes, horizontal and vertical.

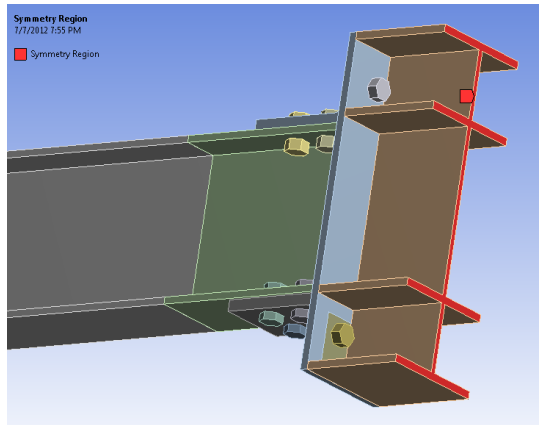
### 3.9 Model Simplifications

Models used for finite-element analysis usually undergo modifications to reduce analysis time and computational effort. Often for connection studies, the geometrical model is simplified using the concept that if the connection can be modeled as a mirror, only one half of the connection is modeled and in ANSYS Workbench, the ‘Symmetry’ option is defined at the mirror line.

Radial symmetry can also be defined for the simplifications of radial models. The basic definition in the symmetry option is the selection and definition of the area connecting to the other symmetry half and the definition of the axis normal to the symmetry surface. A comparison is made between the original experimental test connection and the geometrical model, highlighting the symmetry area is shown in Figure 3.25(b)



(a) Actual Specimen Configuration



(b) Symmetry definition to half-model

Figure 3.25: Model symmetry applications

### 3.10 Analysis Convergence Method

In ANSYS, the Newton-Rhapson method is being used for the analysis of models. Iteratively, the calculation is computed where the product of the stiffness at certain points and the displacement caused is equivalent to the forces applied deducting the residual forces, where the simplification is addressed by Thomas (2004), shown in Figure 3.26. Under perfect conditions, no residual forces would be encountered, which would mean that the behavior corresponds accurately to the material properties and geometry. However due to the nature of imperfections and the sensitivity of the model, there is usually some minor residual stress,

On the other hand, to aid with convergence of the analysis, using the force convergence plot / diagram, with an example as shown in Figure 3.27, the progress of the analysis can be checked. With non-convergence, there are possible solutions, such as refining mesh, reducing contact stiffness and to define increased number of loads steps between where the non-convergence occur in the previous particular load-step. The common method applied in this study would be to decrease the contact stiffness to acceptable levels, to allow for minor penetrations for example, at  $10^{-5}$ m.

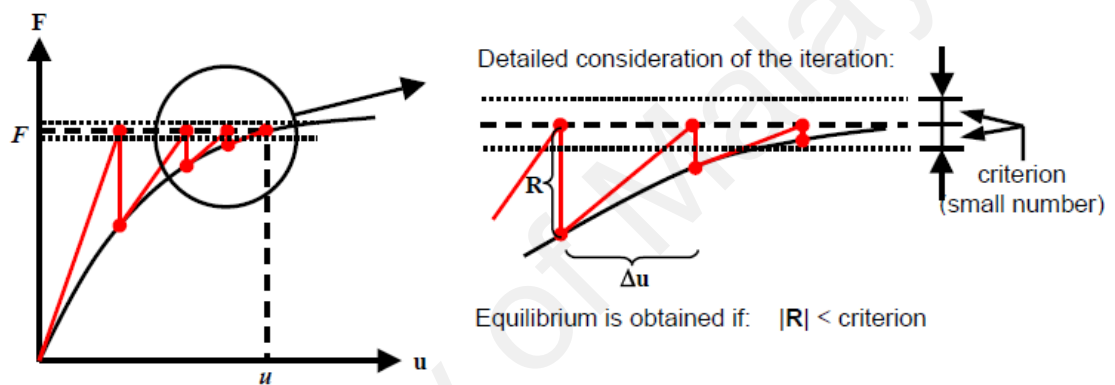


Figure 3.26 Newton-Raphson method used by ANSYS (Thomas, 2004)

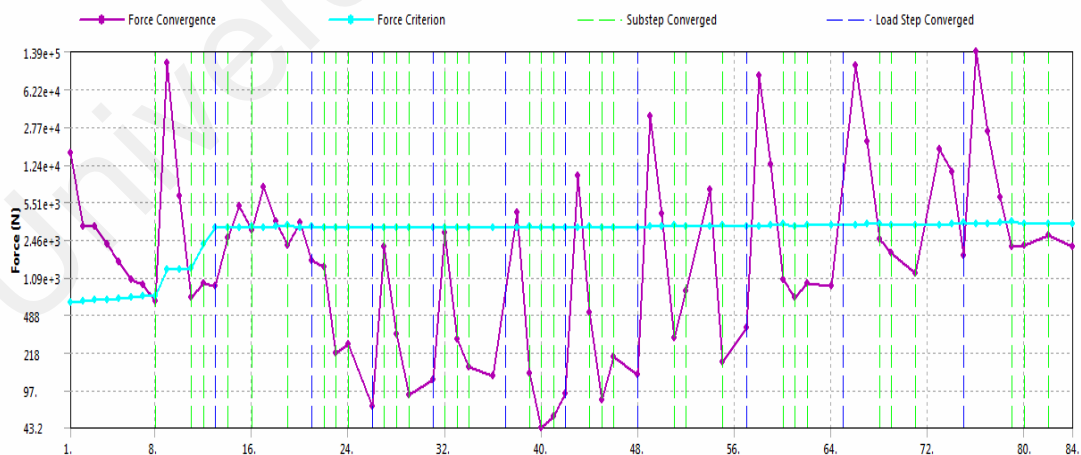


Figure 3.27 Example force convergence plot of ANSYS Workbench

### **3.11 Post Processing**

After the analysis has been completed, the results are extracted from the software in forms of reaction forces or displacement values. For where displacement values are applied as the controlling load for the model, the reaction forces are taken as the result, while in terms of moment loadings being applied, the displacement values are extracted accordingly. Whether in terms of stress or plastic deformation patterns, no other post-processing is done and taken as is shown.

University of Malaya

## CHAPTER 4

### RESULTS AND DISCUSSION

#### 4.1 Introduction

The models are divided into ambient temperature conditions models and the elevated temperature conditions models. The models are presented in the order of ambient temperature models, being the T-stub model followed by the full connection model. Elevated temperature model validations are presented next. The results are compared with available experimental test results and attempts will be made to explain the possible reason for the differences between the results together on the behavior of the models. Parametric studies that were conducted, including seat angle effect, isothermal condition behavior are presented next and the discussions on the design guidelines provided by EC3: Part 1-8 is presented last.

#### 4.2 Validation Studies

##### 4.2.1 Ambient Temperature Conditions

Due to the fact that elevated temperature models have additional factors to be considered, the validations of ambient temperature models are vital to ensure that further procedures and assumptions of the models produce results with good agreement with the experimental results to eliminate these modeling considerations. T-stub models are validated first to familiarize with the software.

In comparison to the T-stub models, actual full connection models are more closely related to the models of the objectives in this study in terms of geometrical properties. Therefore, validation of different ambient temperature models with components that match the actual conditions would eliminate any additional factors that may have been caused by the differences between the T-stub models and top-seat angle models at ambient temperatures.

Three models of top-seat angle connections were created and validated against experimental test, which are specimens AS1 conducted by Aziznamini (1984) and documented by various studies including Pirmoz et al. (2009a) and Ali Ahmed et al. (2001), test W00 in the study by Komuro et al. (2004) and also specimen TS6 in the study conducted by Kukreti and Abolmaali (1999).

#### **4.2.1.1 T-Stub Models**

T-stub is one of the basic connection components and in the case of top-seat angle connections, have been assumed to be representative behavior of the connection type, as shown in the design guidelines provided by EC3: Part 1-8. Due to this simplification, early studies to validate the T-stub would be critical in understanding the behavior of the basic components in angle connection without the additional considerations found in a full connection. Study on the behavior of the connection under hysteretic loadings done by Shen-Astaneh (1999) is selected for validation purposes.

The original study was on the hysteretic behavior of bolted angle connections. However, a test was also conducted in the study with monotonic loadings for behavior comparison, which is reported as Specimen S4. Consisting of two plates to represent the beam and the column flange respectively, the study is focused on the deformation of the angle sections when subjected to axial forces on the beam.

Geometrical and material properties of the model are as shown in Table 4.1 while the representation of the specimen for the geometrical properties reference is as shown in Figure 4.1. On the other hand, the mechanical properties of the material assumed as shown in Table 4.2. Boundary conditions around the 20mm thick plate representing the column is fixed on the perimeter edge surfaces as shown in Figure 4.2. Loads are applied in the form of gradually increasing displacement values on the 38mm thick plate representing the beam, in “upwards” direction for the section view. A pretension load of 125kN is applied on to each of the bolts as documented by Shen-Astaneh (1999). The resulting mesh of the model is as shown in Figure 4.3 where the resulting mesh criteria is as recorded in Table 4.3. All of the 44456 elements used are the SOLID185 with a total of 58189 nodes.

Results of the analysis, as depicted in Figure 4.4, indicate that the model is in good agreement with the experimental results, except differences on the behavior at the post-yielding areas. The differences are assumed to have been caused by the simplification of models such as the removal of the angle root. Although differences were observed, the basic methods and parameters assumed for the analysis has been validated from the results shown, which is then continued to be used in the validation process of the other models in this study.

Table 4.1: Geometrical Properties of the T-Sub Validation Model

Pretension Force:- 125 kN							
Properties	Angle Thickness, t	Beam Leg Length, a	Beam Leg Gauge Length, g2	Column Leg Length, b	Column Leg Gauge Length, g1	Bolt Diameter, d	Gap, C
Value (mm)	10	89	64	102	66	19	13

Table 4.2: Mechanical properties of steel materials for T-stub model

Component	Member	Bolts
Yield Stress	250 N/mm <sup>2</sup>	660 N/mm <sup>2</sup>
Ultimate Stress	400 N/mm <sup>2</sup>	880 N/mm <sup>2</sup>
Elastic Modulus	2.0 x 10 <sup>5</sup> N/mm <sup>2</sup>	

Table 4.3: Mesh criteria for model

Criteria	Minimum	Maximum	Average
Skewness	1.31	0.875	0.04
Jacobian Ratio	1.29	58.23	1.44
Aspect ratio	1.03	452.3	4.06
Element Quality	0.12	0.99	0.91

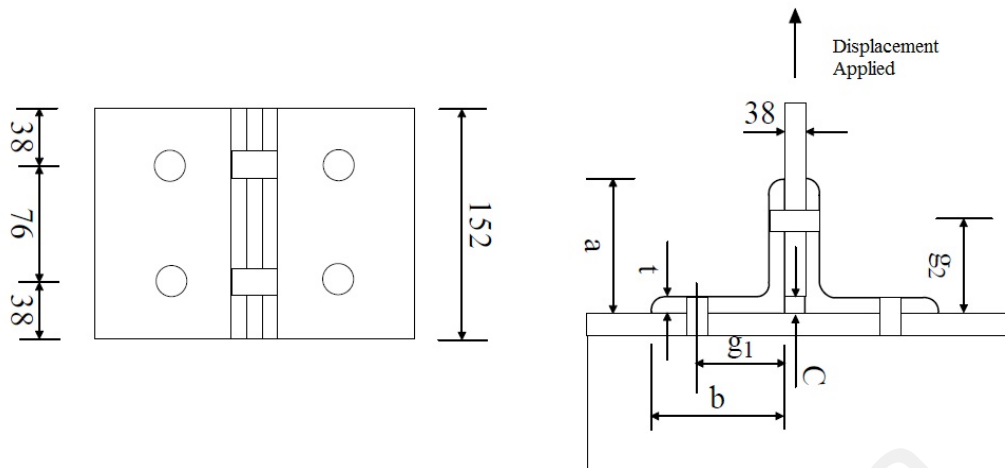


Figure 4.1: Geometrical Reference of the T-Sub Validation Model

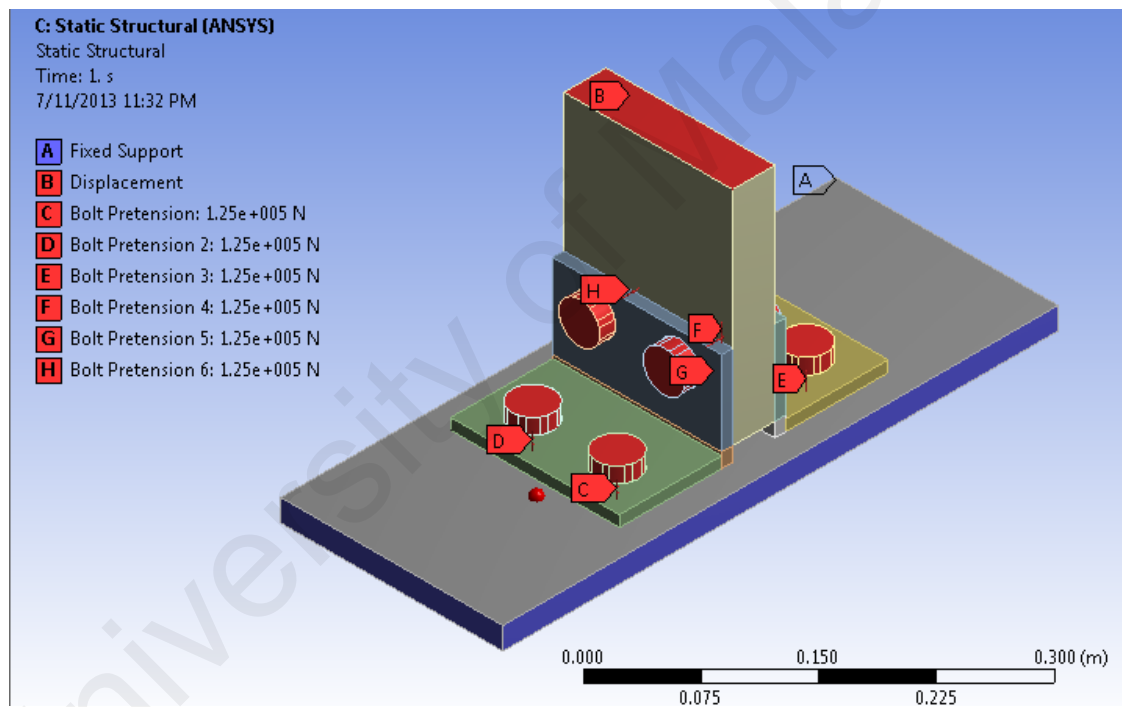


Figure 4.2 Boundary and loading conditions of the T-stub validation model.

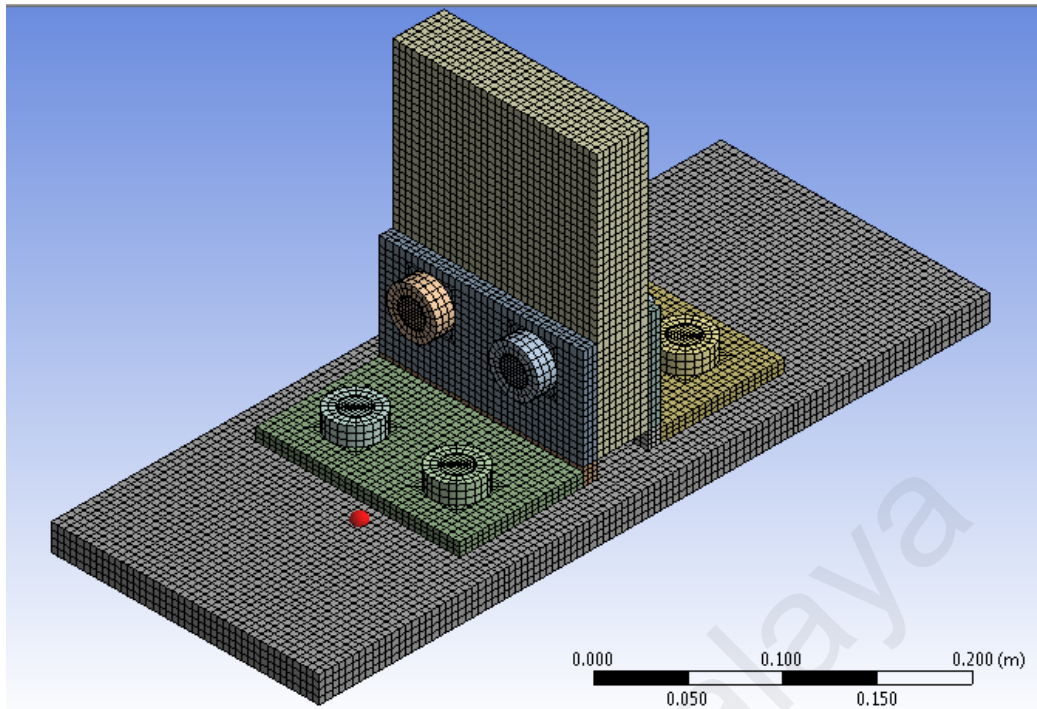


Figure 4.3 Mesh pattern of the model

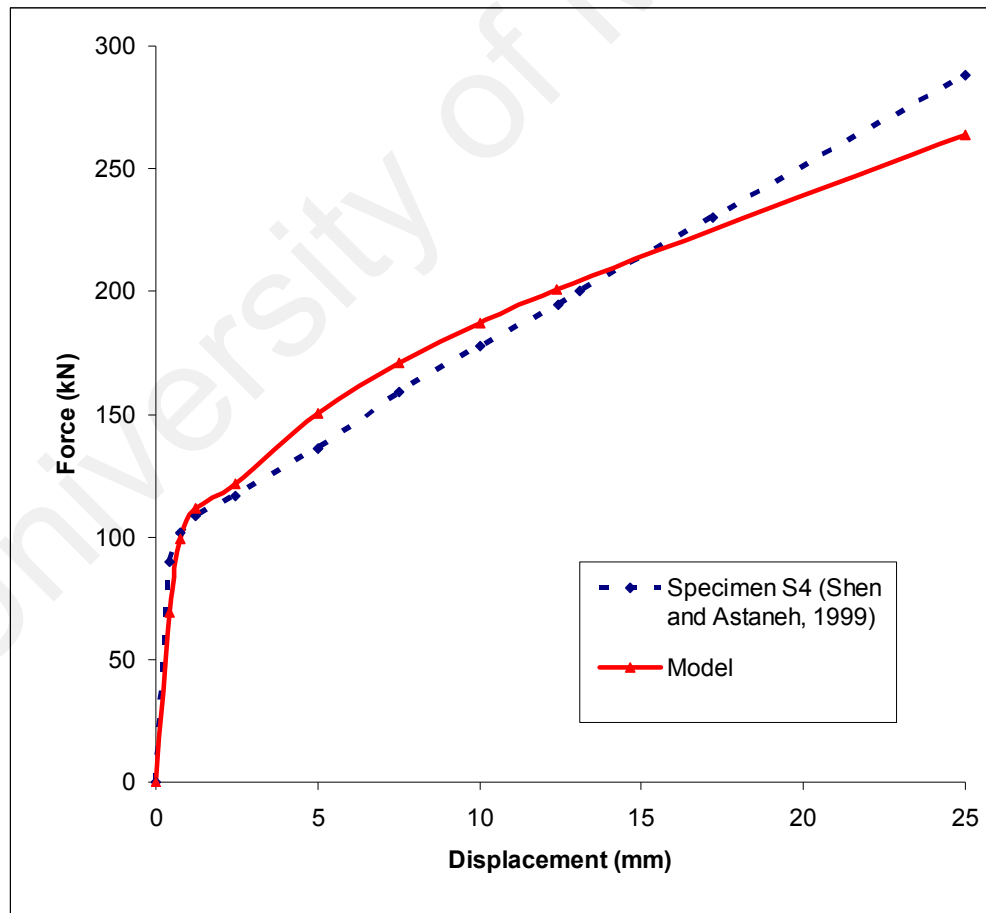


Figure 4.4 Comparison of the Model and Specimen S4 (Shen and Astaneh, 1999)

#### 4.2.1.2 Connection Models Based on Azizinamini (1982)

Although two tests, being tests AS1 and AS2 were top-seat angle specimens, only specimen AS1 from Azizinamini (1982) were used for the validation. Material properties considered are as shown in Figure 4.5. Yield stress for steel members is set at  $365 \text{ N/mm}^2$  and ultimate stress value of  $525 \text{ N/mm}^2$  at 8% strain and  $510 \text{ N/mm}^2$  at 4.85% strain. On the other hand, the geometrical properties (in ANSI inches) and steel sections of the models are as shown in Table 4.4. Dimensions such as the gauges distances, bolt distances for specimens AS1 are shown in Figure 4.6.

Loads are applied on the beam ends as a series of displacements on the beam and the displacements, being the controlling factor, provides the necessary rotation on the connection. To achieve the level of displacement specified, a certain amount of force is required, which is measured as the reaction force,  $F$  from the results of the analysis which will be converted to the applied moment force.

Overall loading and boundary conditions of the model is as shown in Figure 4.7. Mesh for the model is done using the automatic meshing in ANSYS Workbench and the resulting mesh is as shown in Figure 4.8 while in terms of the mesh metrics, the values for the criteria as shown in Table 4.5 is recorded. 36806 elements with 69978 nodes has been recorded with the element used being SOLID186. Determination of the rotation for the connection is based on the formula presented as Equation 4.1 while the corresponding moment force is computed using Equation 4.2.

Table 4.4: Geometrical properties of the steel sections for model

Pretension Force	178 kN
Column	W12x96
Beam	W14x38
Angle	L6x4
Angle Thickness	3/8 in. (9.5 mm)

In comparison to the method described by Pirmoz and Danesh (2009b), Equation 4.1 directly converts the displacement of the beam end into rotation values. In the equations, the moment,  $M$  is the product of the force at the cantilever point,  $F$  and the distance from column flange to cantilever point,  $L$  while the rotation is the value obtained by the displacement caused by the loading,  $d$  over the distance  $L$ . Fixed value of 1.5m, similar to the distance between the column flange to the beam edge as documented has been used for the computations for this particular model.

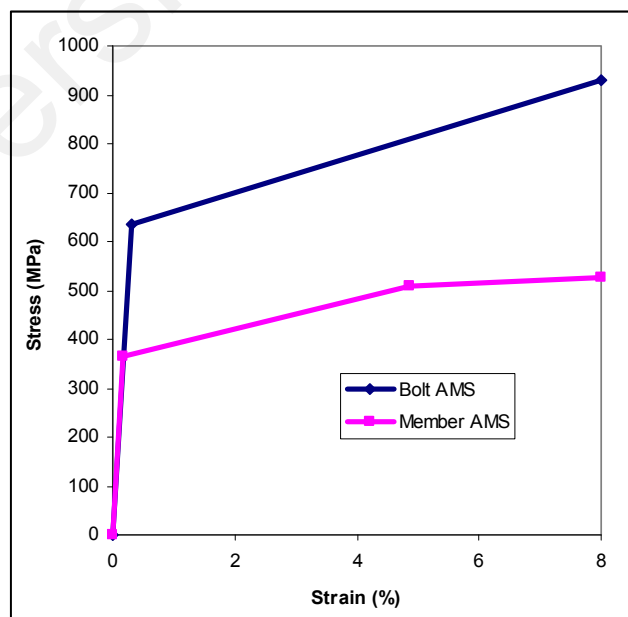


Figure 4.5 Mechanical properties of steel materials for model

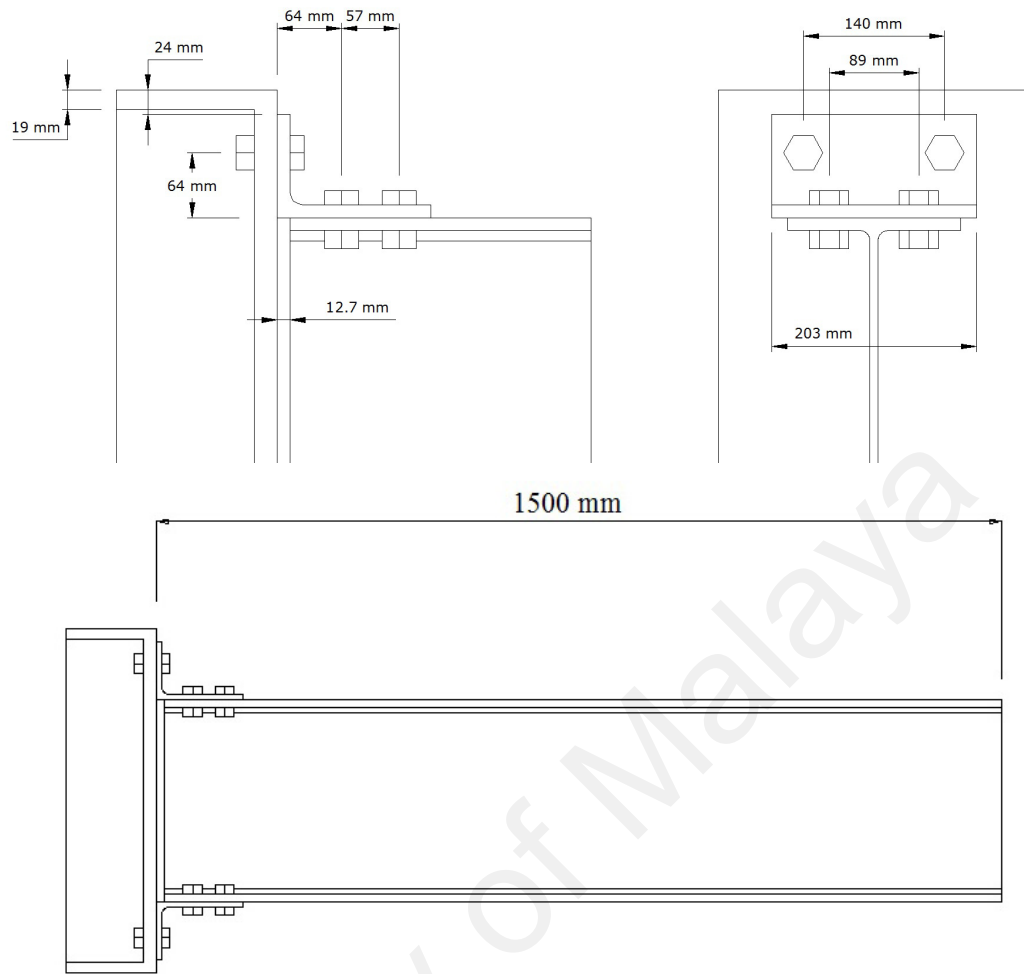


Figure 4.6: Geometrical properties for model

Table 4.5: Mesh criteria for model

Criteria	Minimum	Maximum	Average
Skewness	1.31	0.98	0.41
Jacobian Ratio	1.0	37.74	1.11
Aspect ratio	1.18	8.8	2.35
Element Quality	0.16	0.99	0.70

Behavior of model compared with the experimental results of Azizinamini (1982) is as shown in Figure 4.9. The behavior shows that model behaves relatively close to the experimental test results other than the end behavior which deviates slightly. This shows that the model is in good agreement with the experimental results. In terms of connection failure, the plastic strain distribution is concentrated at the top angle and as shown in Figure 4.10.

Plastic strain is concentrated at the column leg bolt areas and the “heel” area at the beam leg of the top angle. Distribution at the beam leg is in a fairly linear fashion across the length of the angle section. This correlates with the failure mode of the connection where the top angle fractures near the root radius of the angle section of the beam leg, caused by the tensional forces generated by the moment loads due to the lever arm combined with the bending force of the angle generated by the ‘downward’ force of the loadings.

On the other hand, the deformation on the bolt areas at the column leg of the angle section is caused by the clamping action by the bolts that have higher material properties. Stress distribution of the connection is as shown in Figure 4.11 with the top figure for the top angle and bottom figure for the seat angle stress. Stress concentration on the bottom angle focuses on the area right after the heel of the section.

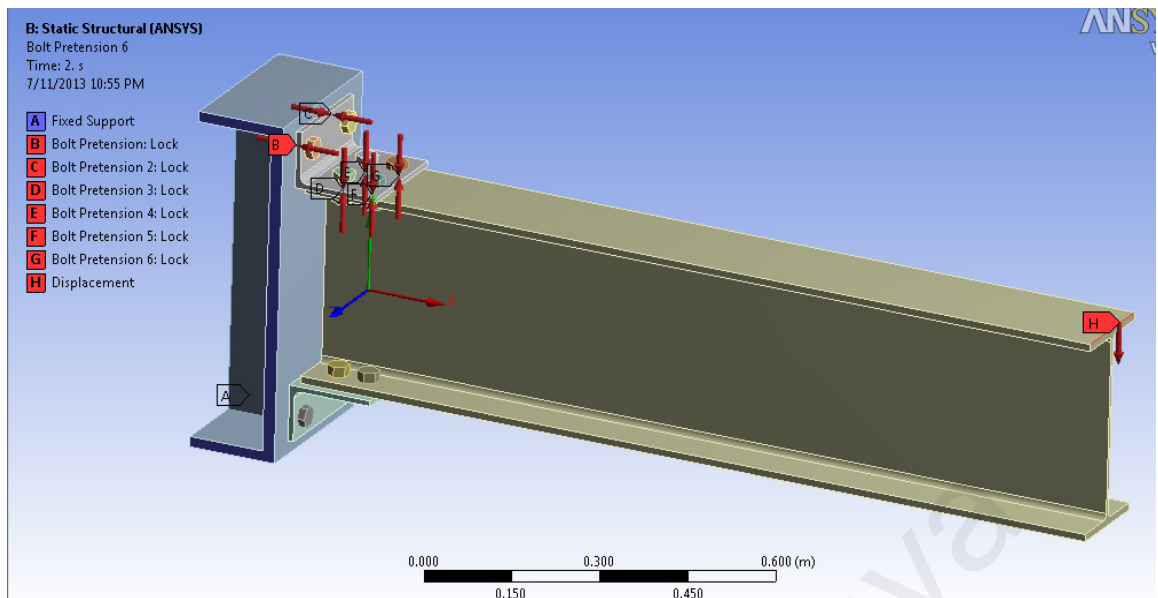


Figure 4.7 Boundary and loading conditions of the model

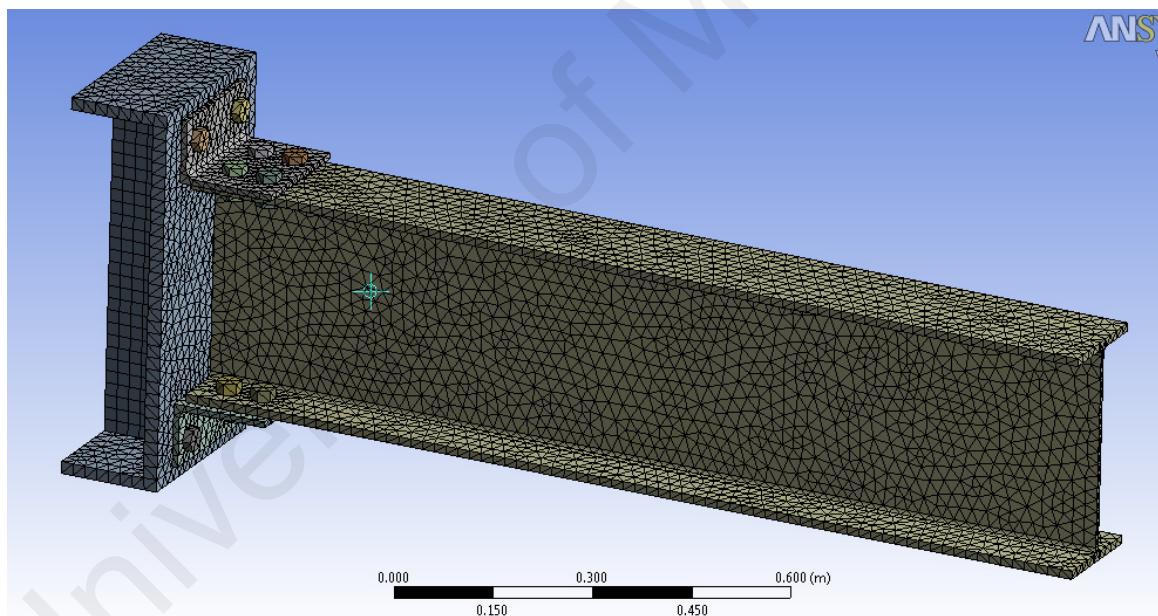


Figure 4.8 Mesh pattern of the model

$$M = F.L \quad (\text{Eqn 4.1})$$

$$\theta = \frac{d}{L} \quad (\text{Eqn 4.2})$$

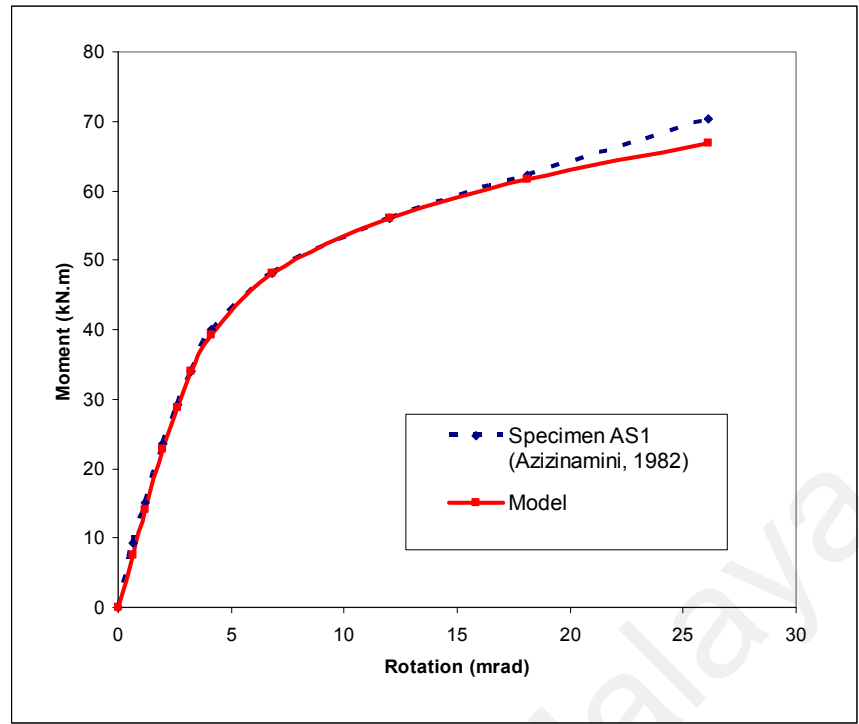


Figure 4.9 Behavior of model compared to Specimen AS1 (Azizinamini, 1982)

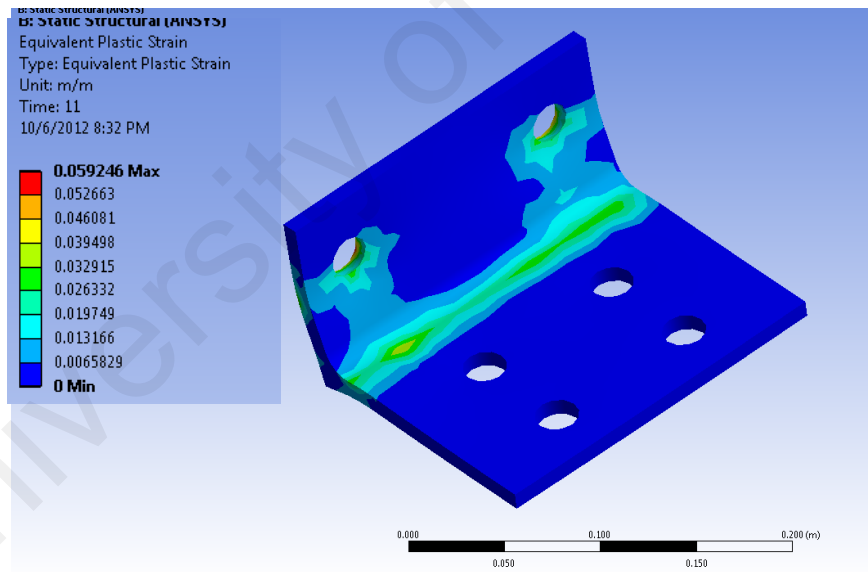
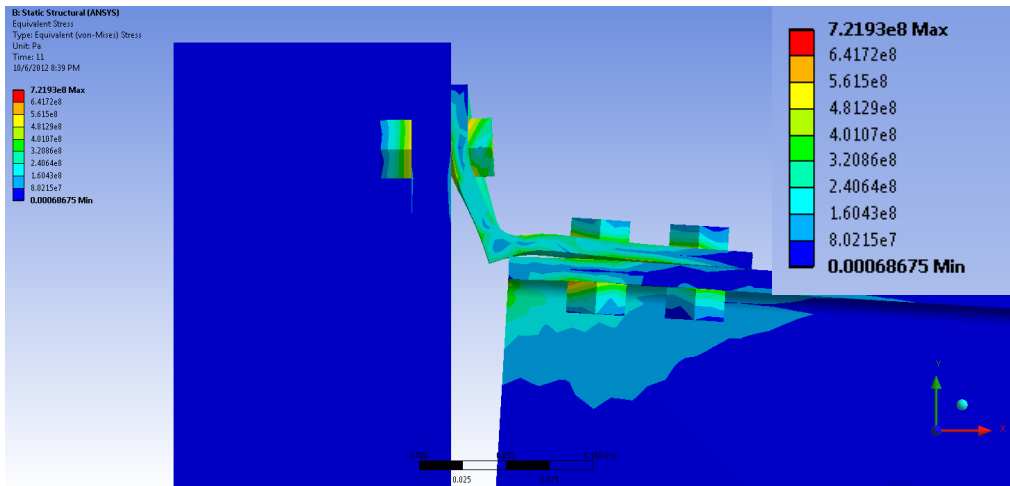
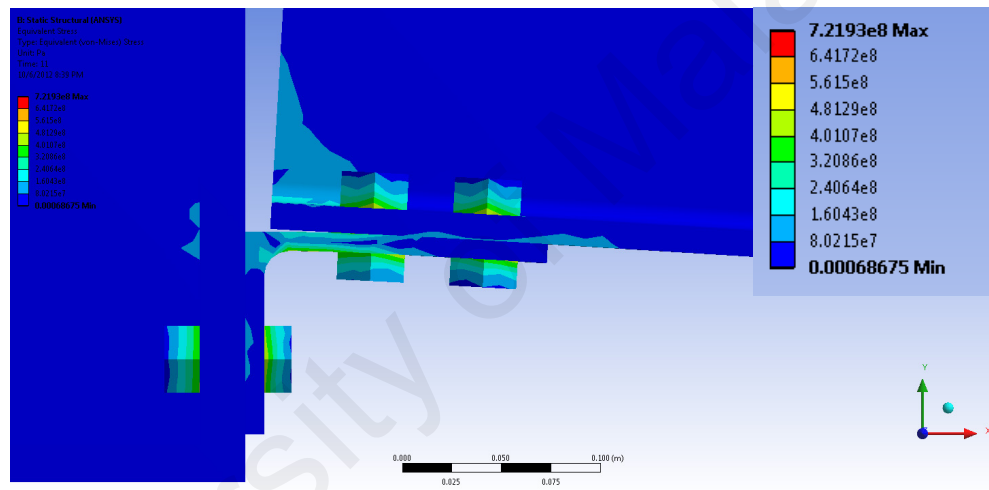


Figure 4.10 Plastic strain distributions at the top angle of model



(a) Top angle stress pattern and deformation



(b) Seat angle stress pattern and deformation

Figure 4.11 Deformation of Components and Stress distribution of model

(Inset) Stress Pattern Legend

#### 4.2.1.3 Connection Model Based on Komuro et al. (2003)

Validations of the model are also conducted against the tests conducted by Komuro et al. (2003) using tests W00. While three experimental tests have been conducted in the study (Komuro et al., 2003), however the other two tests are of the top-seat angle with web angles type. The sections for the members used in the study are as shown in Table 4.6 while the geometrical dimensions shown in Figure 4.12. Material properties used in the model are as shown in Table 4.7.

Table 4.6 Steel members for the model

Component	Section
Column	H408x408x21x21
Beam	H400x200x13x8
Angle	L150x100x12

Table 4.7: Mechanical properties of steel materials for the model

Component	Member	Bolts
Yield Stress	200 N/mm <sup>2</sup>	1060 N/mm <sup>2</sup>
Ultimate Stress	449 N/mm <sup>2</sup>	1098 N/mm <sup>2</sup>
Elastic Modulus	2.1 x 10 <sup>5</sup> N/mm <sup>2</sup>	

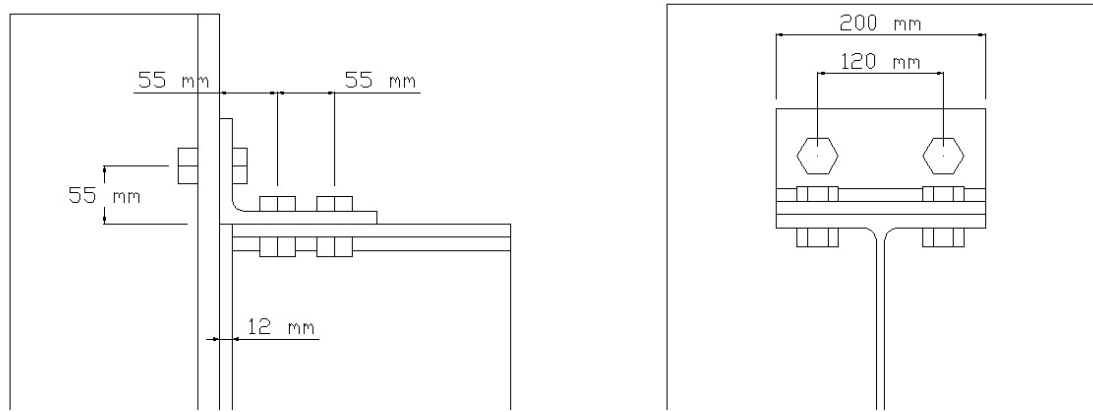


Figure 4.12 Geometrical properties for the model

As shown in Figure 4.13, loadings are applied via displacement control to obtain the reaction forces which would be computed into moment loads. Rotation of the connection is obtained by dividing the difference in displacements of the beam top edge displacement and beam bottom edge displacements in the horizontal direction by the depth of the beam section, as summarized in Equation 4.3, where  $\delta$  is the horizontal displacements and  $d$  is the depth of beam section. Moment loads are calculated with the same concept as Equation 4.1. With the mesh metric as shown in Table 4.8, the mesh pattern for this model is with respect to Figure 4.14 where 22655 elements were used and 45496 nodes on the model.

$$\theta = \frac{\delta_t - \delta_b}{d_b} \quad (\text{Eqn 4.3})$$

Figure 4.15 shows the comparison between the model response and experimental results, initial stiffness of the model is in good correlations with the experimental tests, however the post elasto-plastic region, the behavior of the model deviates from the test results. In general the model shows that the behavior of the model corresponds to the experimental results. Differences in the behavior might be caused by the geometrical differences between the model and experimental test results.

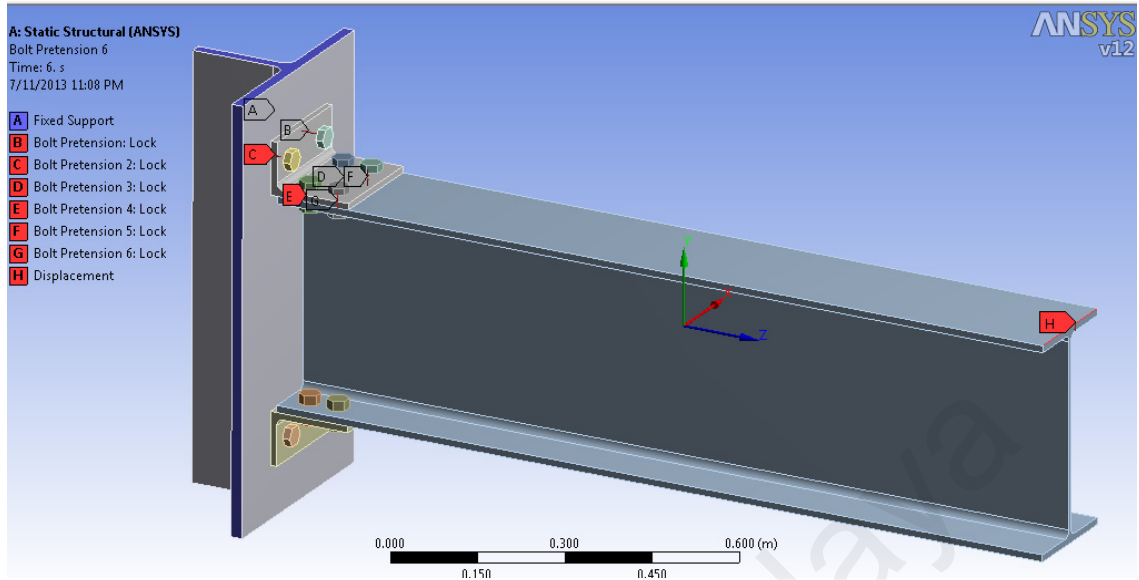


Figure 4.13 Boundary conditions and displacement load for the model

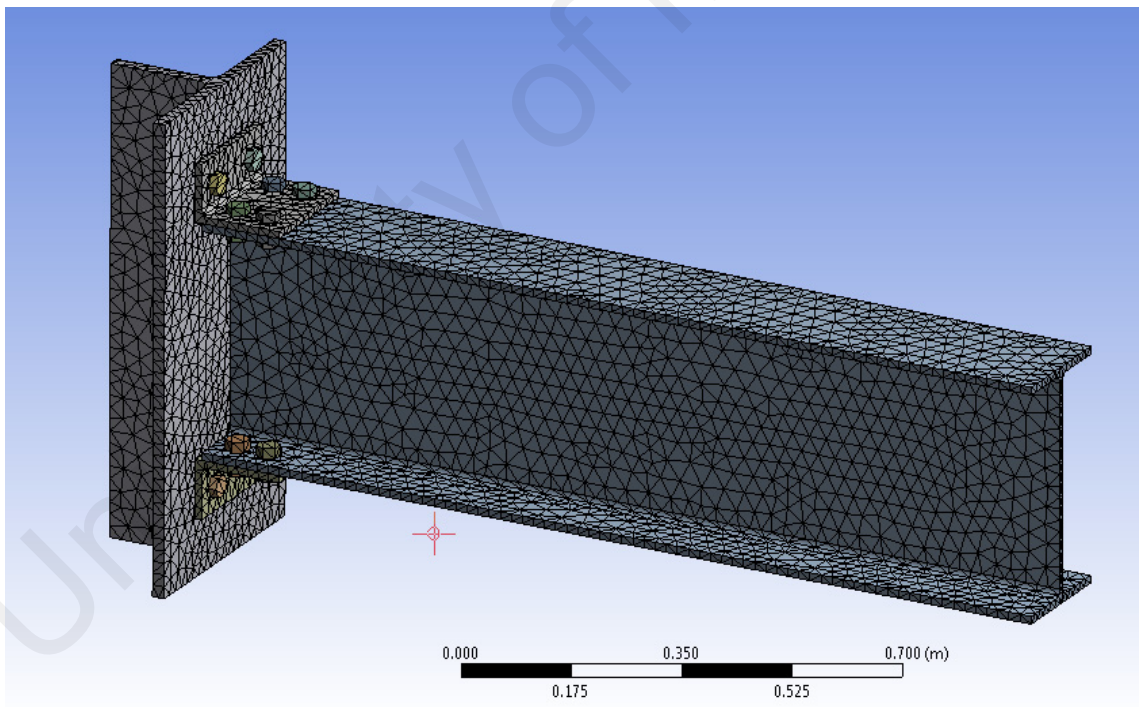


Figure 4.14 Resulting mesh pattern for the model

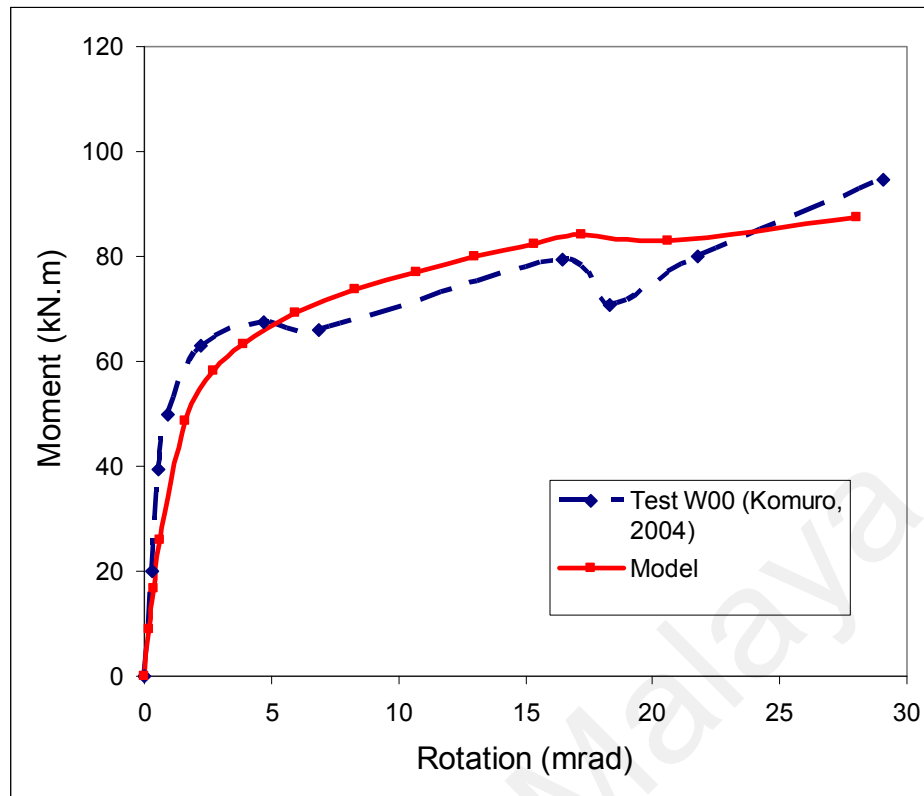


Figure 4.15 Behavior of model compared to Specimen W00 (Komuro, 2004)

Table 4.8: Mesh criteria for model

Criteria	Minimum	Maximum	Average
Skewness	4.87	0.99	0.52
Jacobian Ratio	1	29.68	1.14
Aspect ratio	1.19	26.35	2.85
Element Quality	0.99	5.59	0.61

#### 4.2.1.4 Connection Model Based on Kukreti & Abomaali (1999)

Another model is created for further validation of the ambient temperature models. Cyclic loadings were the original objective in the study by Kukreti and Abomaali (1999). However, the envelope behavior of test TS6 (Kukreti and Abomaali, 1999) was extracted by Cafer (2009). Geometrical properties (in ANSI inches) are as shown in Table 4.9 and Figure 4.16 respectively. Material properties utilized for the model are as outlined in Table 4.10. A pretension force of 135 kN was specified for all bolts of this model.

Table 4.9 Steel members for the model

Component	Section
Column	W8x67
Beam	W14x43
Angle	L6x4x0.5

Table 4.10: Mechanical properties of steel materials for the model

Component	Member	Bolts
Yield Stress	325 N/mm <sup>2</sup>	634 N/mm <sup>2</sup>
Ultimate Stress	550 N/mm <sup>2</sup>	830 N/mm <sup>2</sup>
Elastic Modulus	2.1 x 10 <sup>5</sup> N/mm <sup>2</sup>	

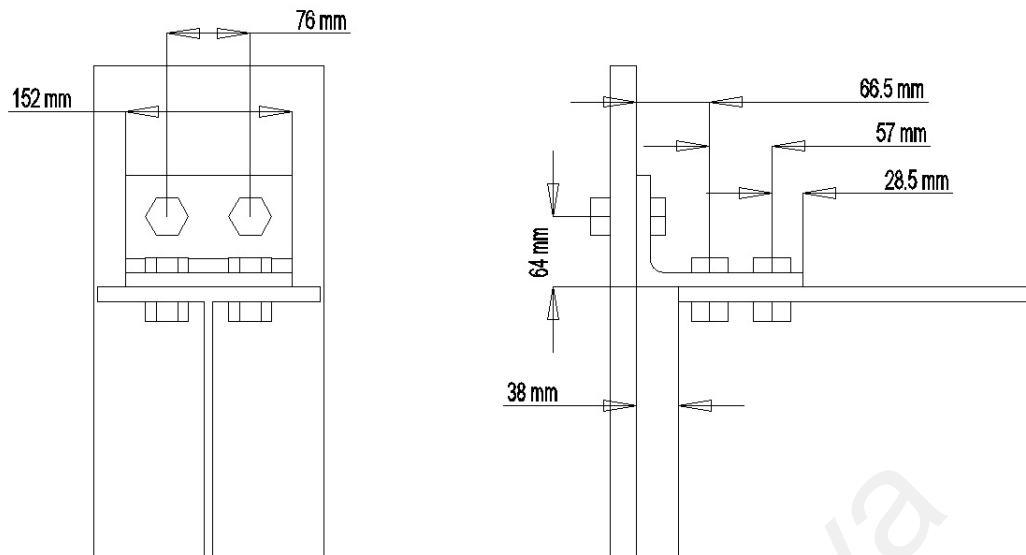


Figure 4.16: Geometrical properties of steel materials for model

The distance value between the column face to the edge of the beam for the test, where the value would be necessary to compute the moment force applied onto the connection that results in the deformation documented was not provided in the study. Length of the beam, although provided in the document (Kukreti and Abomaali, 1999) as 978 mm (38.5 in.), the value is incomplete without as there is no gap distance reported. Value of 1016 mm (40 in.) is utilized with the assumption that a round-off value would be common. Overall boundary conditions and displacement loads similar to previous validations models together with the mesh pattern is as shown in Figure 4.17 and Figure 4.18 respectively. Mesh criteria values is as indicated in Table 4.11.

Table 4.11: Mesh criteria for model

Criteria	Minimum	Maximum	Average
Skewness	1.31	0.99	0.32
Jacobian Ratio	1.0	133.48	1.08
Aspect ratio	1.13	21.83	2.03
Element Quality	8.6	0.99	0.77

In terms of model behavior, a comparison is made and is as shown in Figure 4.19. From the figure, the behavior of the model is in good agreement with the testing results with only minor variations in between. A slight deviation has been found at the end-behavior area but the stiffness of both results is in particularly good agreement.

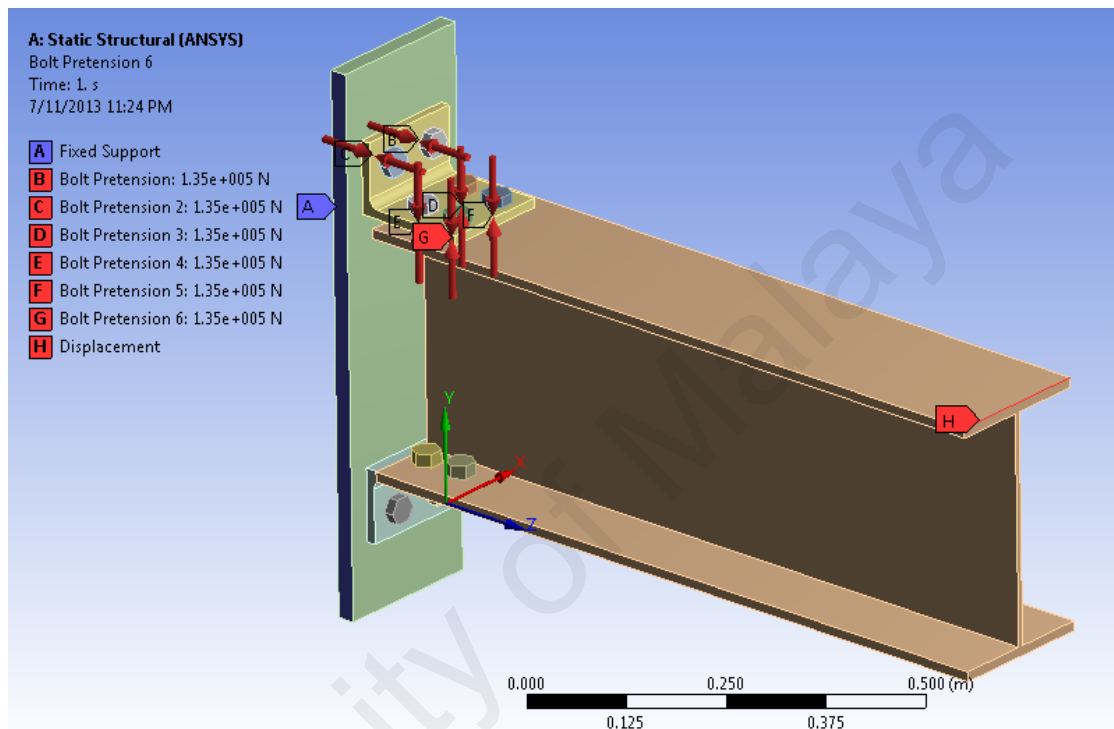


Figure 4.17 Loading and boundary conditions of the model

Deformation of model validated with Kukreti and Abomaali (1999) is similar to the model validated with Azizinamini (1982) where plastic strains are focused on the beam leg of the top angle near the root of the section. Bolts on the beam leg and the bottom angle is still in elastic state while the bolts at the column leg on the top angle displays plastic behavior and is caused by the prying forces of the angle due to tensile action of the top angle as a result of the moment loads applied. However, the stress in the bolts is comparatively different.

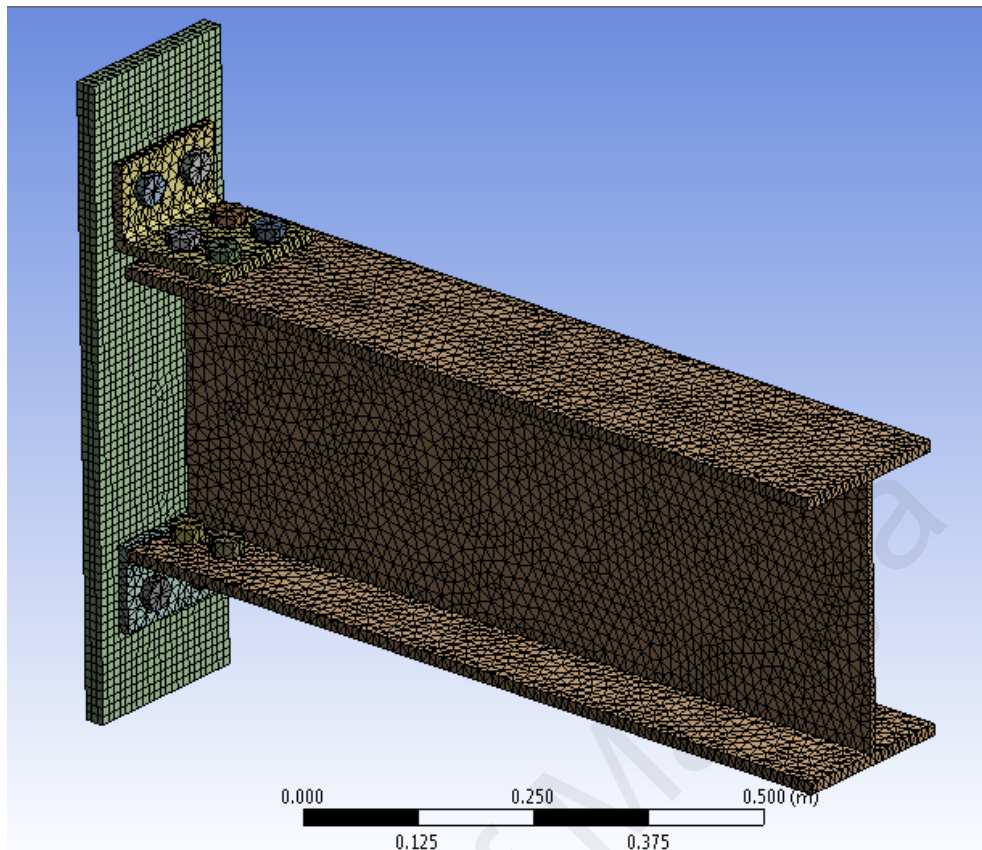


Figure 4.18 Meshing pattern result for the model

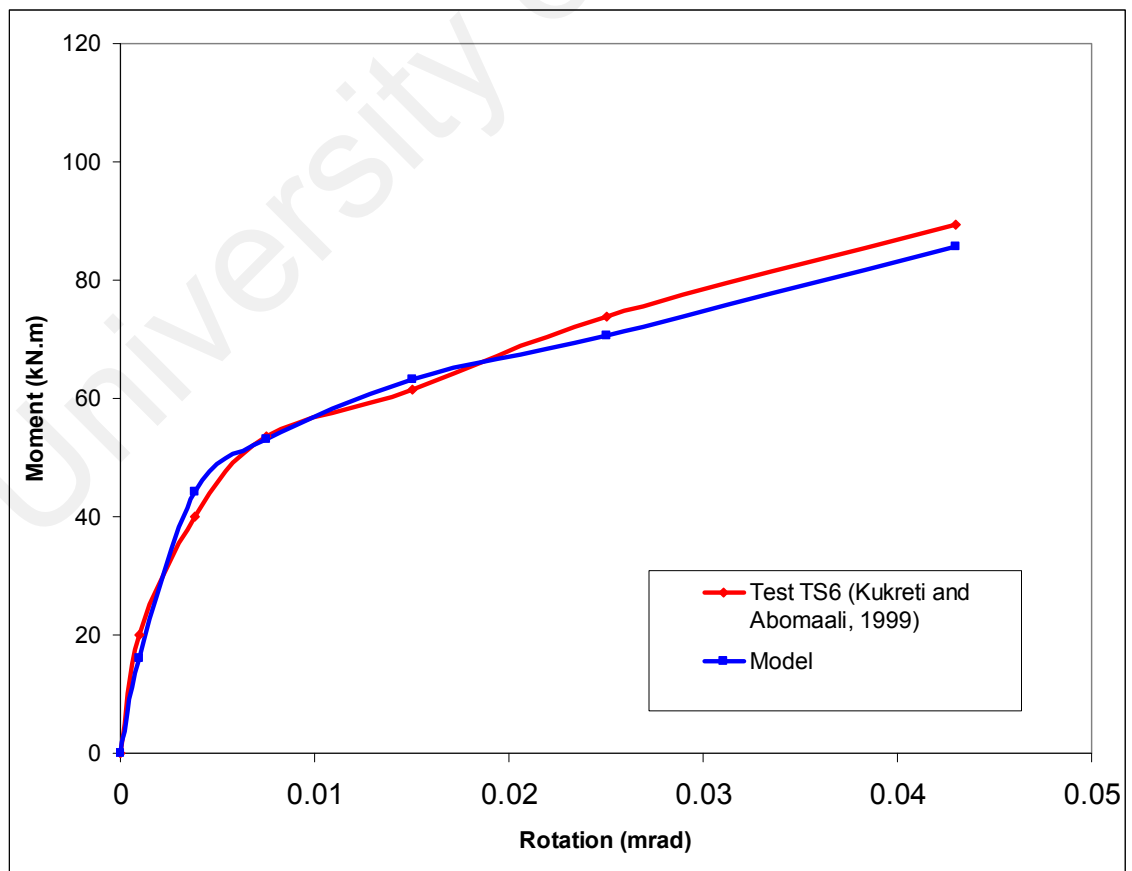
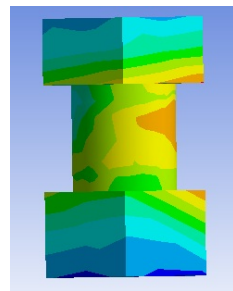


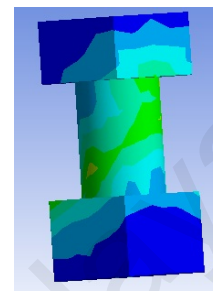
Figure 4.19 Behavior of model and TS6 (Kukreti and Abomaali, 1999)

Stress patterns for model Kukreti and Abomaali (1999) is in a diagonal pattern where the plane is from the area near the bolt head to the nut while for model validated with Azizinamini (1982), stress is focused on the side nearer to the column. A comparison is made between the stress patterns as shown in Figure 4.20. Possible cause would be the complex effect of the gaps of the connection on the beam leg bolts.



(a) Azizinamini (1982)

validation model



(b) Kukreti and Abomaali (1999)

validation model

Figure 4.20 Stress pattern comparisons for bolts

#### 4.2.2 Elevated Temperature Models

A beam model is validated first followed by the validations of three top-seat angle connections in elevated temperature. Validations of the behavior of beam at elevated temperature is based on the study by Liu et al. (2002) while in terms of elevated temperature experimental results, there exists only one test available for top-seat angle connections, which is conducted by Saedi and Yahyai (2009a).

Considering that there are no other recent experimental tests of top-seat angle connections in elevated temperatures, this experimental test by Saedi and Yahyai (2009a) has been selected as the major validation reference. Although this, a number of issues with the models are raised, including the bolt distance between the beam face nearest to column and the first bolt row at beam leg.

#### 4.2.2.1 Beam Behavior in Elevated Temperatures

As a precursor to studies on the steel connection in elevated temperatures, another study is conducted on the behavior of steel beam under elevated temperatures with the fact that analysis on models with temperature loads can be conducted using the dynamic structural or static structural component of ANSYS. As dynamic analysis is dependant on the time factor, there are other considerations to be taken such as having the time to reflect the full analysis duration or if a representation is sufficient.

Closer time reflection would result in an increase in computational time and effort due to the additional load steps to cater for each second of the test duration. With the additional resources required, it is predicted that this method may not be sufficiently efficient to solve model analysis for elevated temperature conditions.

Conducting a static structural analysis is advantageous for the elevated temperature analysis as load steps can be defined by stages and the number of load steps is less comparatively to dynamic analysis and therefore saves computational power. The simplest solution would be to validate a static structural model with experimental results. Subsequently the study by Liu et al. (2002) on the behavior of beams in elevated temperature has been selected for this validation purpose. Although this, the usage of static structural analysis for elevated temperature condition analysis has been previously done by Dai et al. (2010).

Consisting of a single simply supported I-beam with concrete slab cast on top of the beam, the beam is loaded and the deformation at the center span of the beam is determined. The mechanical properties of the steel and concrete materials considered for the study is as shown in Figure 4.21 and Table 4.12 respectively. Meanwhile the concrete slab has a width of 650mm and 130mm thick that spans between the 4m supports. Relations between the concrete and the steel are considered to be “bonded” as to avoid considerations of the interface between the two components which are not part of the study. Model loadings and mesh is as shown in Figure 4.22 and 4.23 respectively.

On the other hand, the cantilever end was not considered in the model as it is assumed that the cantilever portion does not provide any structural contributions to the behavior. The behavioral comparison is made and shown in Figure 4.24. From the figure, the initial stiffness of the model relates closely to the experimental results, however, the end-result of the model diverts from the experimental results starting from the nonlinear portion of the behavior.

One of the possible reasons that lead to the difference in results would be the inaccurate definition for concrete materials degradation under elevated temperature conditions as well as imperfections and the interaction between the concrete and steel elements which are not considered in the model. In addition, the temperature has been assumed to be uniform throughout the steel member in contrast to the different temperature distribution reported. Early behavior comparison of the model is sufficient to conclude that the static temperature method can be utilized for elevated-temperature related studies.

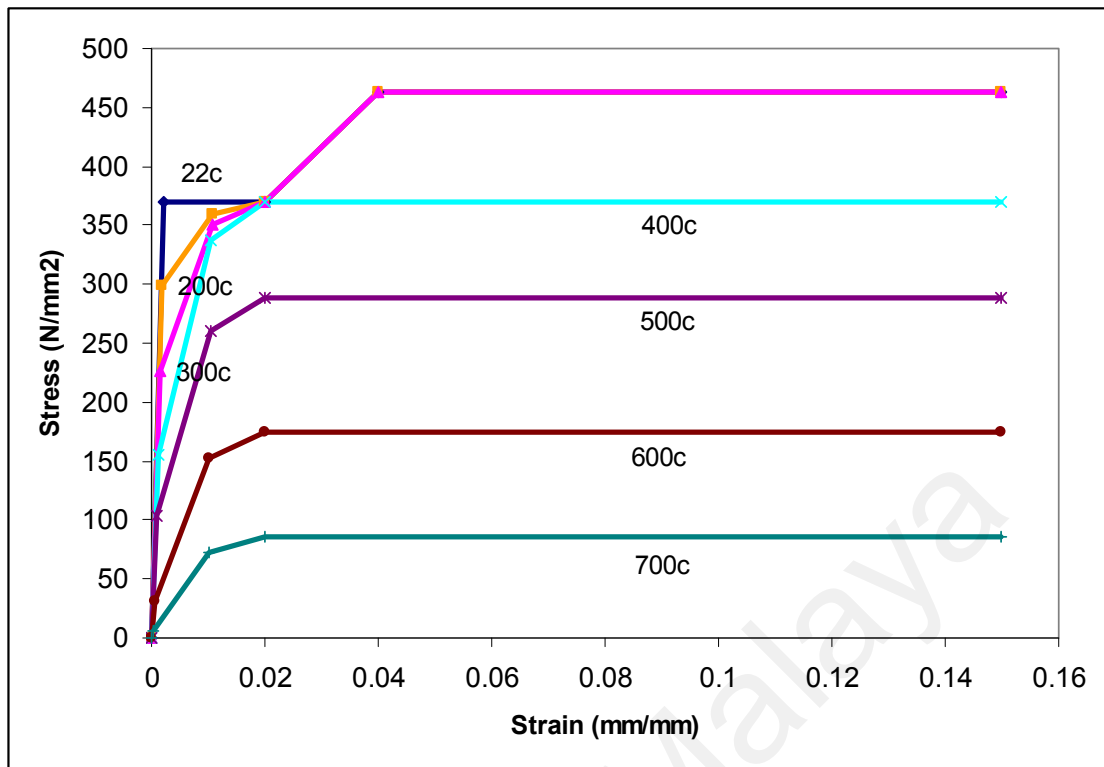


Figure 4.21 Material properties of steel used in the model

Table 4.12 Material properties of concrete used in the model

Properties	Value
Yield Stress	0 N/mm <sup>2</sup>
Elastic Modulus	1.8 x 10 <sup>5</sup> N/mm <sup>2</sup>
Tensile Strength	5 N/mm <sup>2</sup>
Compressive Strength	41 N/mm <sup>2</sup>

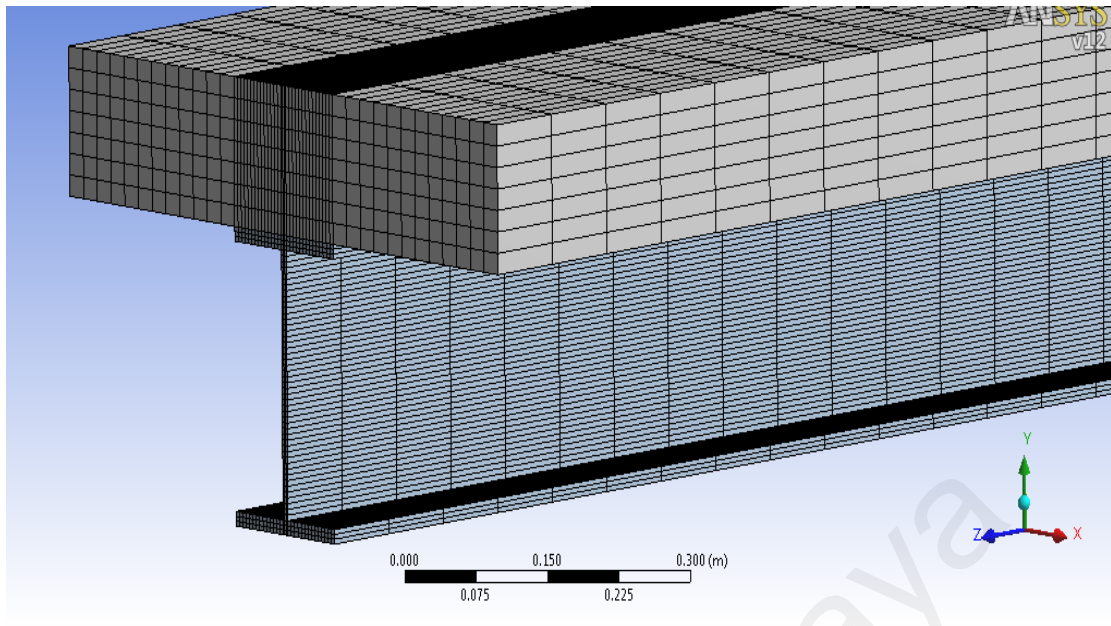


Figure 4.22 Mesh pattern of the model

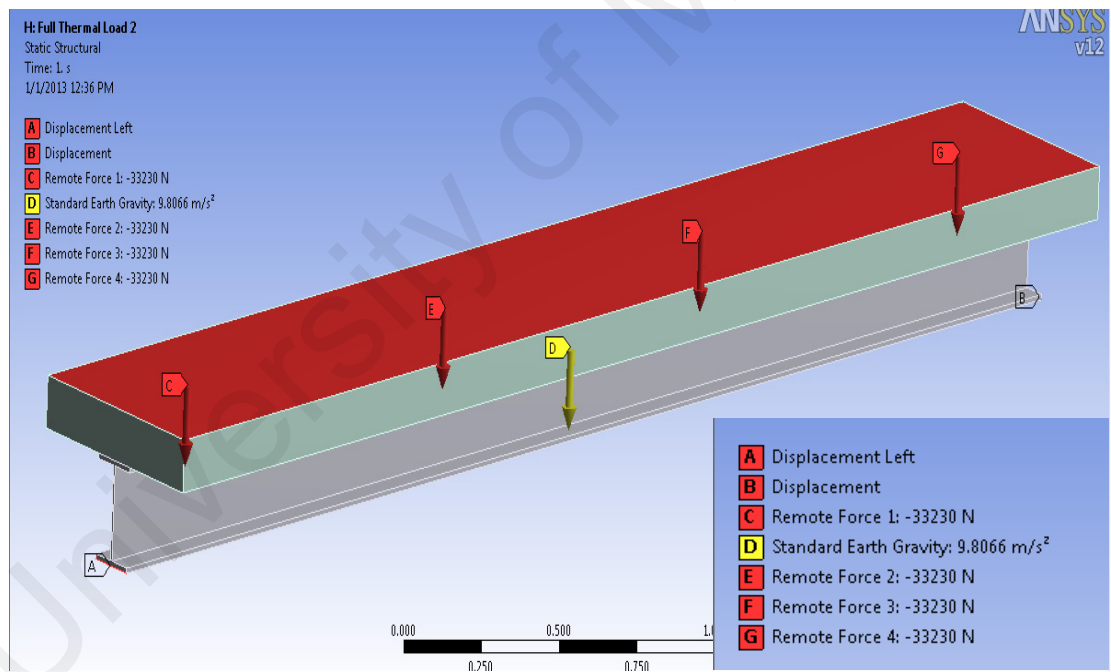


Figure 4.23 Loading and Boundary Conditions of the model

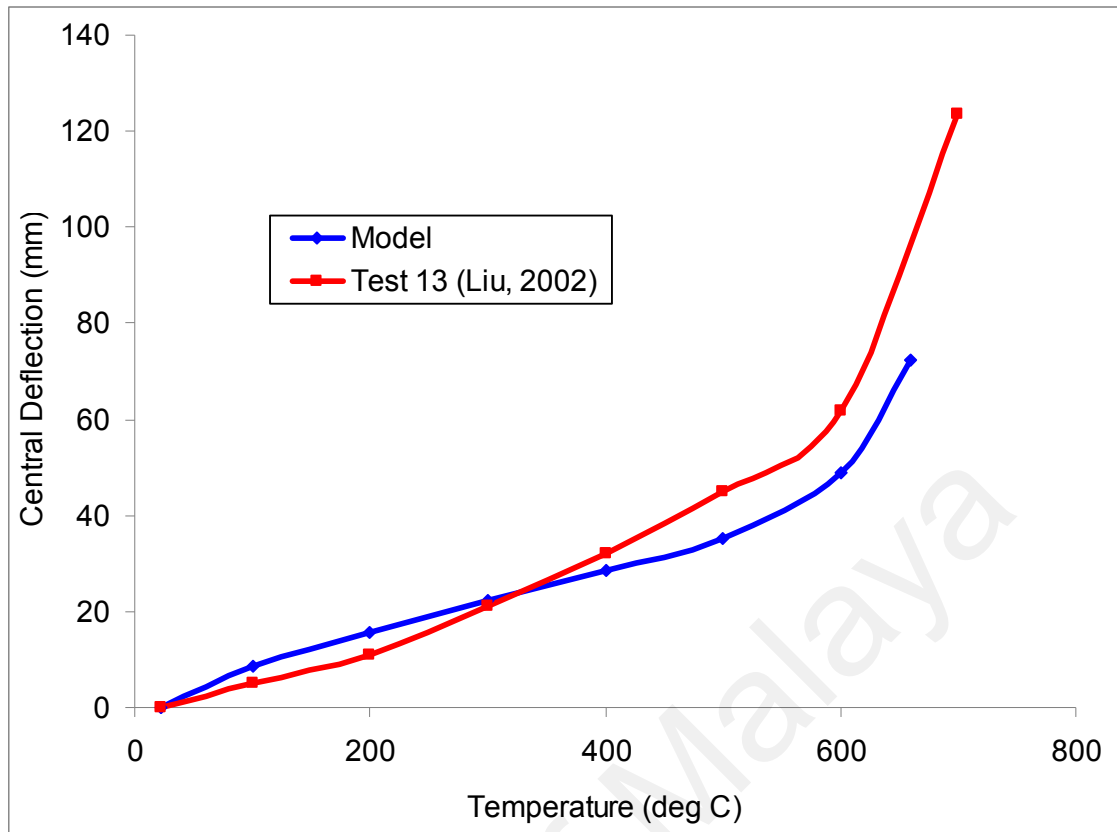


Figure 4.24 Comparison between the model and test results

#### 4.2.2.2 Validation of Joint Model at Elevated Temperatures

Among the total of 18 tests conducted by Saedi (2009), three tests have been selected for the validation of the models in ANSYS Workbench, namely tests S3, S4 and S9. Test S3 is selected due to the fact the failure mode of the connection has been clearly shown in the published journal which would assist in providing a clear picture of the failure and behavior of the model. Meanwhile, test S4 is selected due to the increased thickness and may therefore also provide a highlight the behavioral difference for the analysis model. On the other hand, test S9 to highlight on the difference in bolt distances effect at the beam leg for the top angle section.

The dimensions of the geometrical model applied for the analysis models are as shown in Table 4.13, while the material model details are as shown in Figure 4.25 for steel members and Figure 4.26 for the bolt used in the study. Nodal connectivity check has been ensured for the meshing of the model, where the element nodes are determined to be at point with the mesh nodes of the connecting member (e.g. angle section element mesh nodes with beam flange mesh nodes).

In comparison to the studies conducted by Saedi and Yahyai (2009a), material properties for the steel model are taken as; Young's Modulus value is  $2.06 \times 10^5$  MPa, and yield stress of steel at 235 Mpa while the yield stress for Grade 8.8 bolts is 640. Material curve parameters and reduction factors are based on those specified by Eurocode 3: 2005 Part 1-2 for both bolts and member materials. Although this, for simplifications, only partial of the curve is simulated, as shown in Figure 4.27. Not only that the full curve required increased computational effort, but may be redundant since the simplification provides similar or comparative connection behavior.

Table 4.13 Details of the models in elevated temperatures

Specimen	S3	S4	S9
Model	ELM3	ELM4	ELM9
Applied Moment Loads	8.48 kN.m	8.51 kN.m	8.52 kN.m
Angle Section	L 100x100x10	L 100x100x15	L 100x150x15
Pretension Force	7.5 kN each bolt		
Column	IPE 300		
Beam	IPE 220		

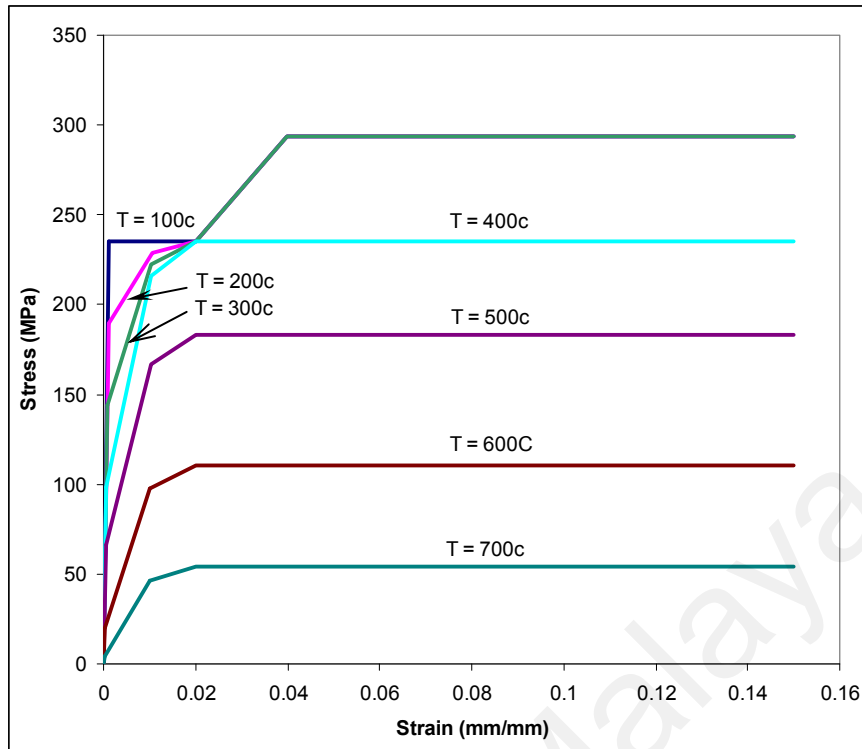


Figure 4.25 Material Models for Elevated Temperature Models of Steel Members

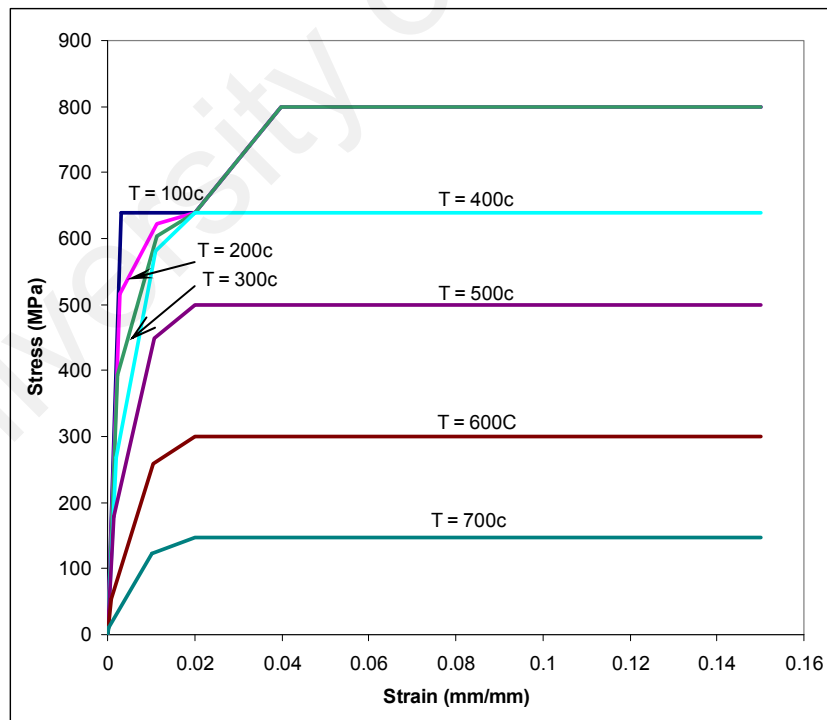


Figure 4.26 Material Models for Elevated Temperature Models of Steel Bolts

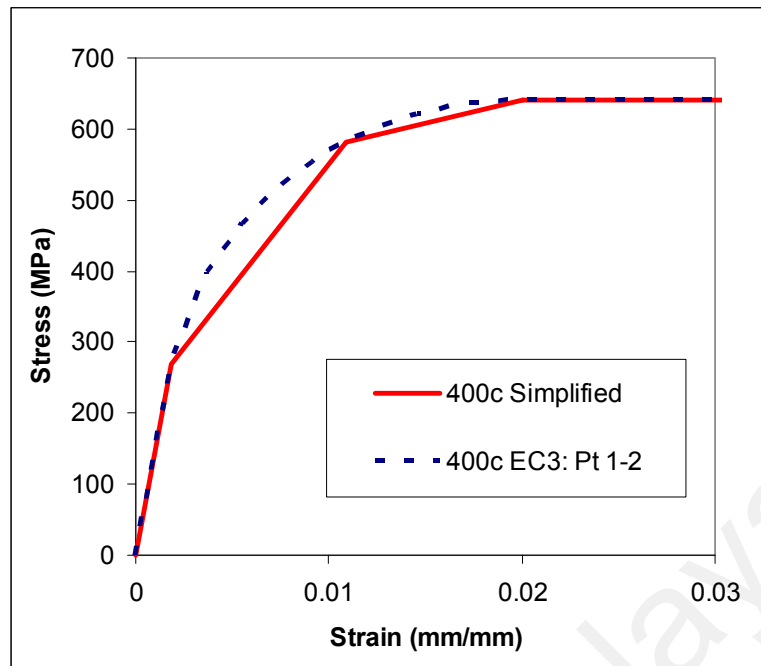


Figure 4.27 Sample of the simplified material properties adopted in the model

Moment force loads are used to apply loadings on to the beam which value is constant throughout the analysis. Due to the fact that the connections are symmetrical, only half of the connection is modeled and analyzed to reduce computational effort. Boundary conditions for connection is defined to be fixed at the base of the column and left free at the top. The symmetrical simplification of the model results in the surface of the symmetry axis being defined with the “symmetry” option in ANSYS Workbench which essentially is a simply support option that prevents the area to have any separation deformation away from the axis plane.

Meshing of the model was done using Hypermesh with the size of  $5 \times 10^{-3}$  m and the meshing end result is as shown in Figure 4.28 for the bolts and Figure 4.29 for the beam and angle sections. Mesh metric is given by Table 4.14. Thermal loadings are applied via a series of load steps under the static structural component where time is not a dependant factor and the thermal loadings are in the form of temperature variation.

Typical boundary conditions and thermal loadings for the models are as shown in Figure 4.30 and 4.31 respectively. While it is the actual case for the temperature to vary between the components of the connection due different exposure levels to the source of heat, the temperature has been assumed to be uniform throughout the analysis for simplification purposes. In comparison to the ambient temperature models, the moment loads and the rotation of the model is computed using Equations 4.1 and 4.2 outlined in previous sections. It is assumed that the rotational values will be sufficiently small that is will not be affected by the degree and radians conversion.

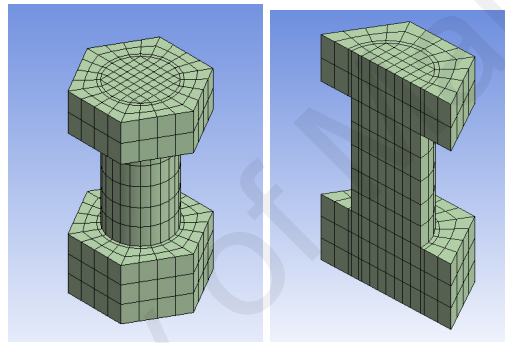
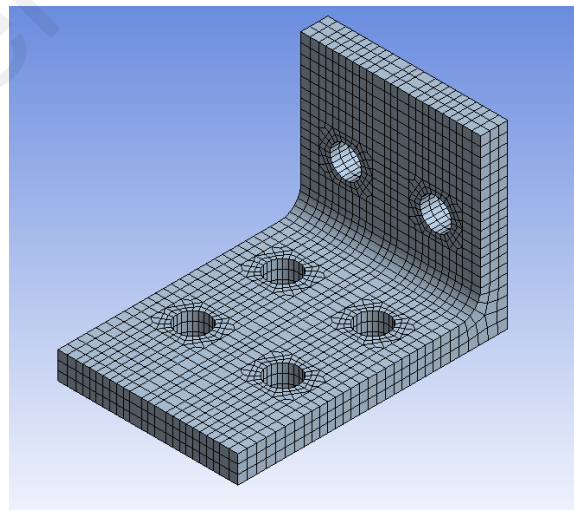
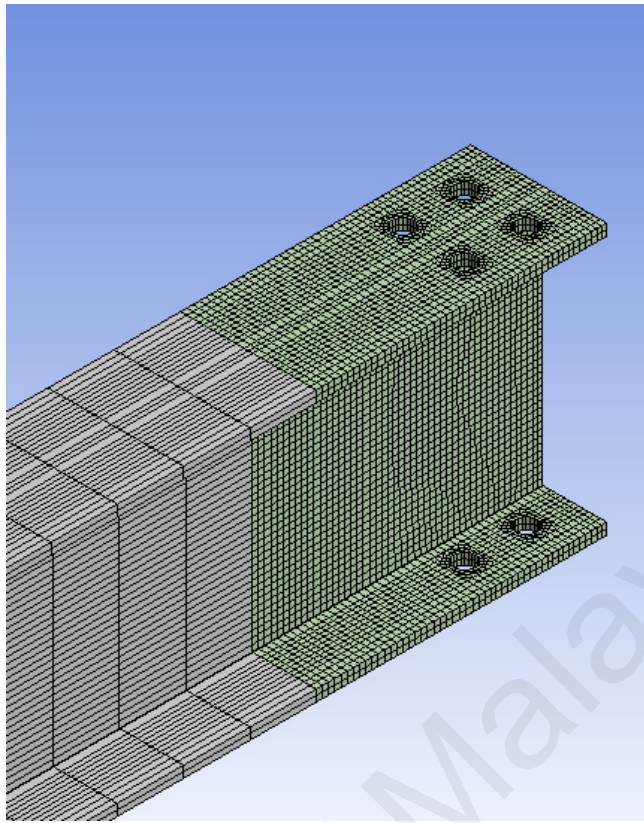


Figure 4.28 Meshing result for bolts



(a) Angle Section Meshing

Figure 4.29 Meshing results Steel Sections



(b) Beam Member Meshing

Figure 4.29 Meshing results Steel Sections (Continued)

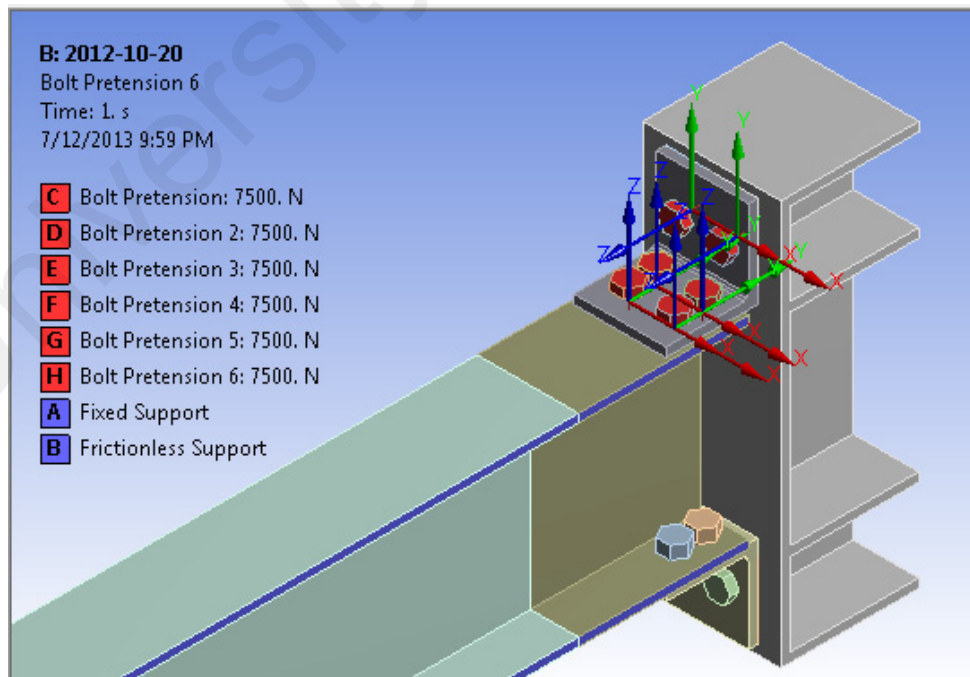


Figure 4.30 Typical boundary conditions of elevated temperature models

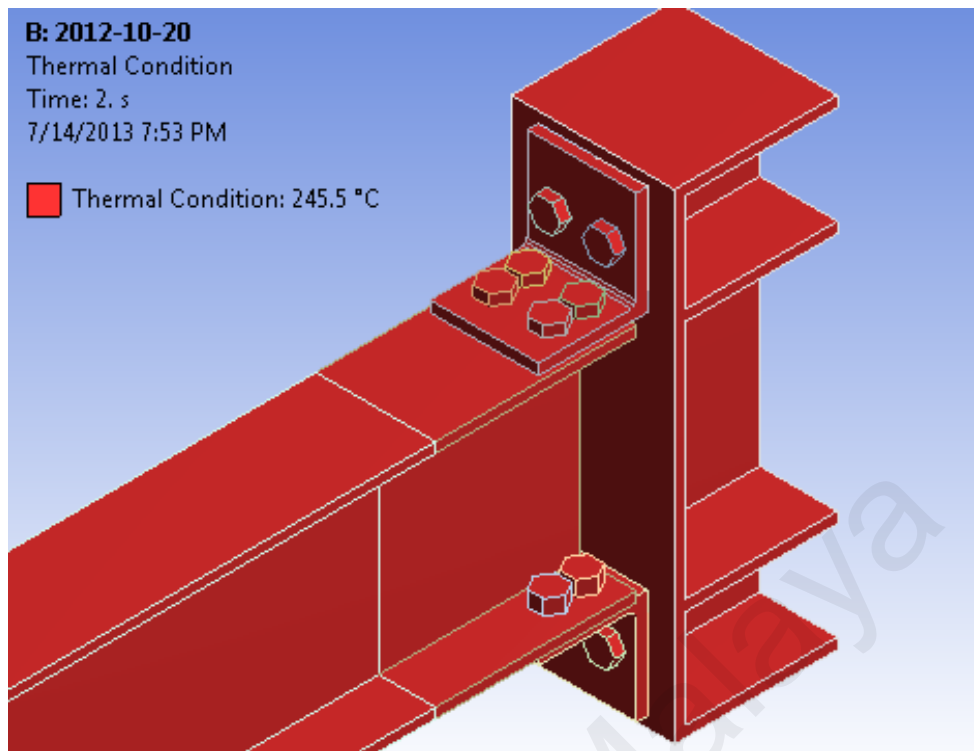


Figure 4.31 Typical thermal loading areas applied on the models

Table 4.14: Mesh criteria for models

Criteria	Minimum	Maximum	Average
Skewness	0.01	0.5	0.05
Jacobian Ratio	1	3.86	1.13
Aspect ratio	1.01	146.7	3.96
Element Quality	0.004	0.99	0.76

The major differences between the models where ELM3 is the control as comparison, is that ELM4 has thicker angle sections while ELM9 has a longer beam leg. Both ELM4 and ELM9 have the same 15mm thick angles but different beam leg length. With this comparison as the reference, difference between ELM3 and ELM4 would provide greater understanding on the effect of angle thickness while comparing ELM4 with ELM9 increases understanding on the effect of the beam leg bolt gauge variation.

Behavior of models ELM3 and ELM4 as compared to tests S3, and S4 are as shown in Figures 4.32 and 4.33 respectively. Meanwhile, Figure 4.34 shows the behavior of the model ELM9 with comparison to results of test S9. From the analysis results, it is clear that for all three models, the early stiffness have shown good agreement with the test results.

Meanwhile, behavior at the elasto-plastic region shows that the model is stiffer than the actual behavior. In the plastic region, good agreement is obtained for models ELM4 and ELM9. For model ELM3, the end behavior for the model deviates from the actual testing result and is behaving in a more flexible manner. In terms of stress, concentration of the Von-Mises stress is concentrated at the root radius of the top angle, between the first bolt row of the beam leg and the areas surrounding the column leg bolt. At the bottom of the top angle, stress is generated by the force of the beam “bearing” against the bottom of the angle, creating a leverage or fulcrum where the top angle is being “sheared” by the edge of the beam.

As shown in Figure 4.35 for model ELM3, measured at 600°C, the continuity of the stress at the beam leg and coupled with the plastic strain locations, would eventually lead to failure of the top angle. This is also supported by the value of stress at this point, which is generally 109 MPa, where the yield stress at 600°C is computed to be 110 MPa which justifies the assumption of the angle failure possibility.

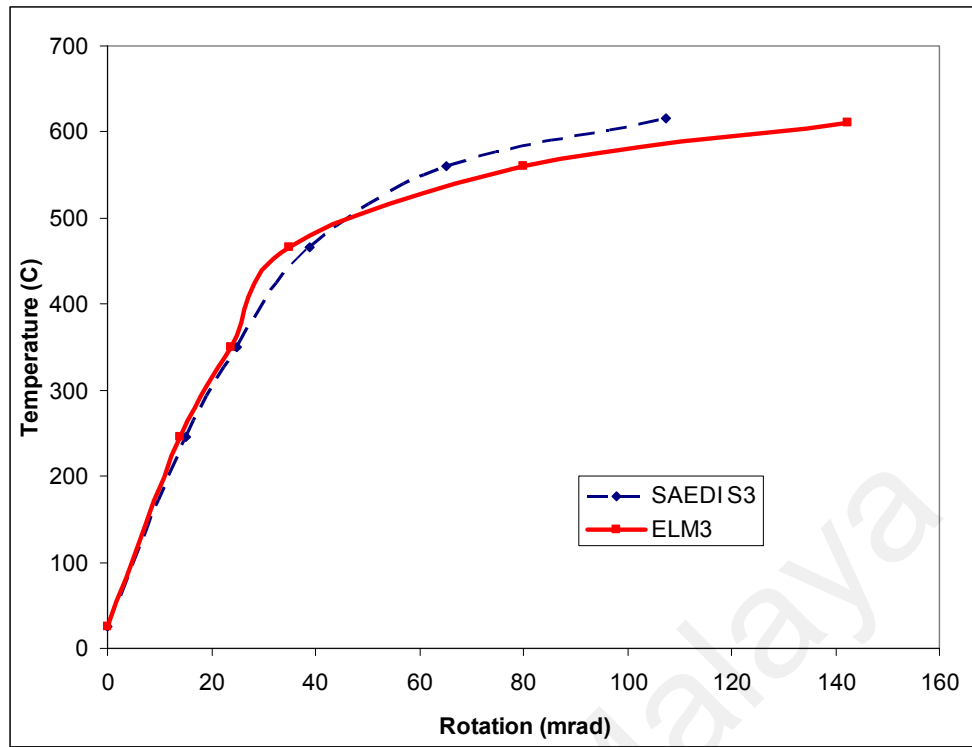


Figure 4.32 Behavior of Model ELM3 compared to test S3 (Saedi and Yahyai, 2009a)

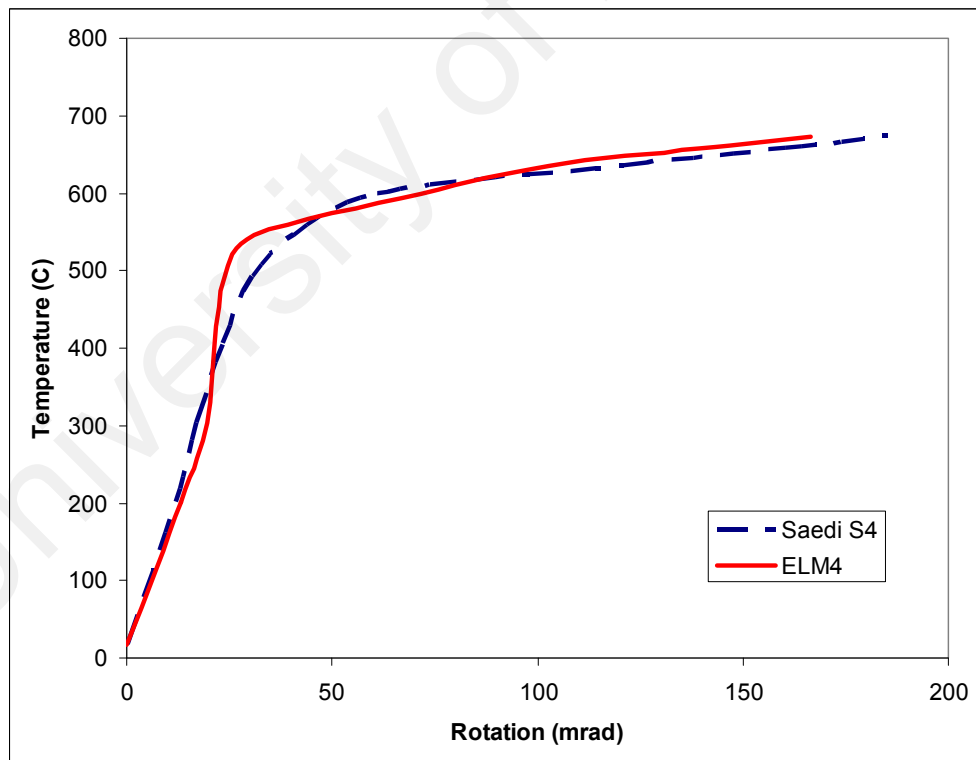


Figure 4.33 Behavior of Model ELM4 compared to test S4 (Saedi and Yahyai, 2009a)

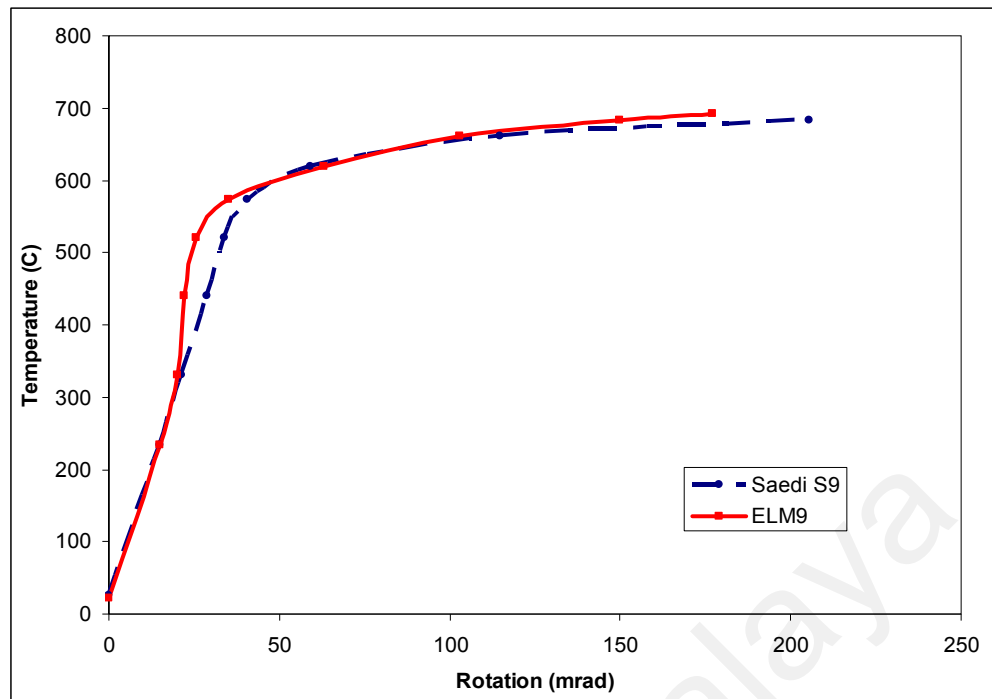


Figure 4.34 Behavior of Model ELM9 compared to test S9 (Saedi and Yahyai, 2009a)

On the other hand, for model ELM4, at 673°C, nearing the failure temperature of the connection, the stress values at the beam leg is valued at 63.01 MPa where the yield stress for the materials at 700°C is 54.1 MPa. Effectively, this would lead to the conclusion that the angle has already achieved failure at this stage. With reference to an earlier temperature level, stress at this point for the top angle is valued at 109 MPa, similar to the value at model ELM3. Although this, the stress pattern is not continuous at the beam leg as those observed in model ELM3, which therefore implicates that the material may have begun to yield, but the stress has not propagated through the component, delaying failures.

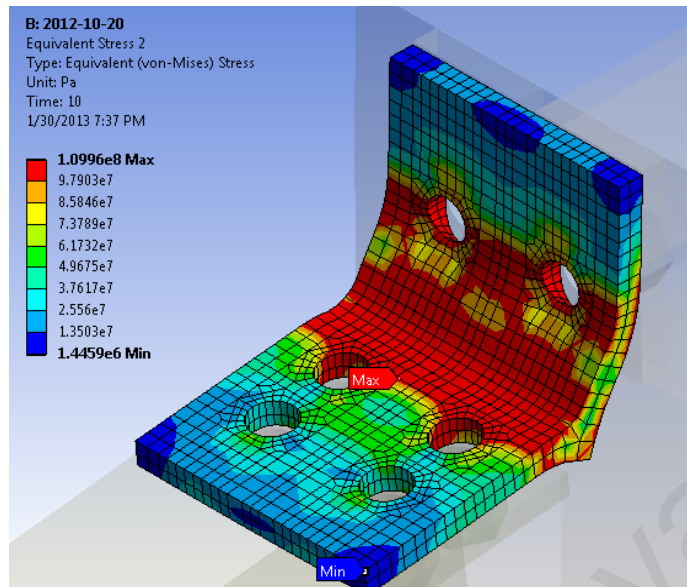


Figure 4.35 Stress pattern for ELM3 at 600°C

The deformation of the models is being compared through Figure 4.36 for the bolts at the top angle. Meanwhile, deformation of the top angle is compared using Figure 4.37 for the models in terms of plastic strains and Figure 4.38 for the top angle stress patterns. Stress patterns for the bottom angle are as compared in Figure 4.39 and Figure 4.40 for bolts at the bottom angle stress patterns.

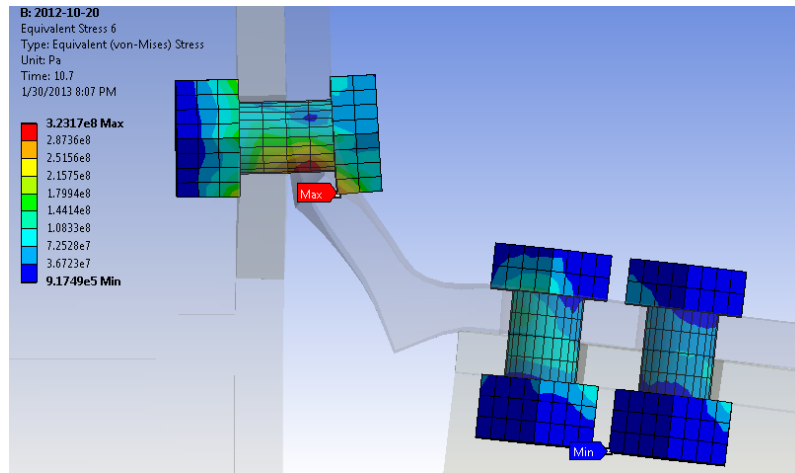
However, as the Static Structural analysis component used in this study, is a part of the implicit method series, the component cannot be used for failure analysis and instead, explicit analysis must be used to analyze the accurate failure of the components. This issue would not be elaborated further as it requires a more detailed study. Although this, implicit analysis such as this is able to provide a clear idea on the deformation sequence of the connection and the possible stress concentration after analysis that would help in the design of components for the connection. While the explicit method is able to display clearly the failure of the connection, however, it is usually reserved for more critical conditions such as that the actual location of the failure must be known.

### 4.3 Parametric Studies at Ambient Temperatures

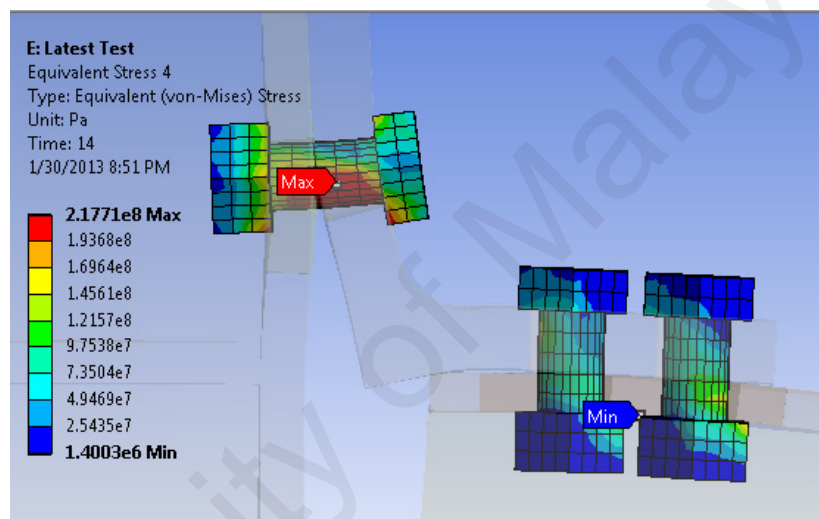
From literature reviews, numerous studies have been conducted using ANSYS with the classical interface while the usage of ANSYS Workbench as the analysis platform is relatively less common. Subsequently, the viability of using ANSYS Workbench as the reliable analysis platform is not known. There is no doubt that using ANSYS Workbench presents some disadvantages due to the fact that not all options are available and may not be as flexible as the classical interfaces. However, ANSYS Workbench do provide a 'ready' interface where parameters are defined within lists instead of having to define each item separately in the classical interface, where specific procedures must be completed to ensure all parameters are defined or the effort would be pointless.

It is known that certain settings or parameters may not be available and therefore there might be some difference in the outcome of the model validation. In the worst case scenario, the parameter is not available in Workbench and must be defined through command leading to another series of trials-and-error. In the course of the study, a number of parametric studies have been conducted to study of most of the software settings encountered, including the effects of contact settings, variation of non-linear and linear material properties on behavior as examples.

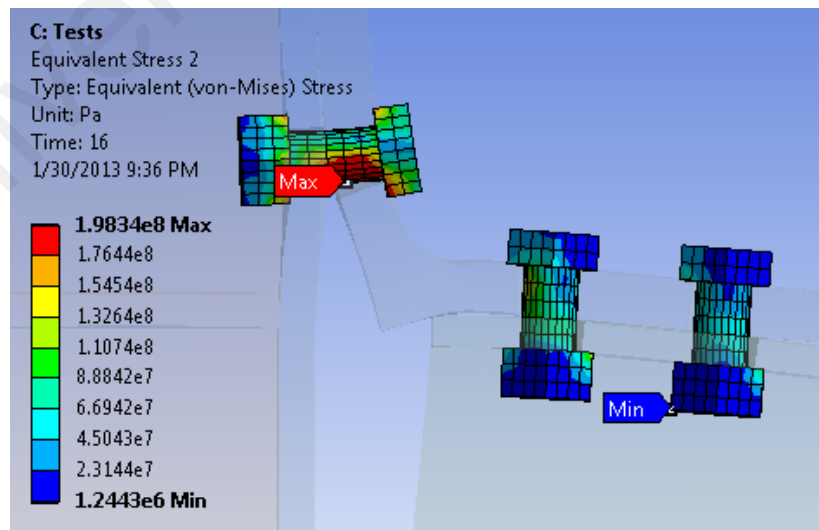
On the other hand, some of the parametric studies were conducted to understand the effect of certain parameters that may define the response of the connections and also to verify the guidelines provided by EC3: Part 1-8 on the design for angle connections especially for top-seat angle connections.



(a) Model ELM3

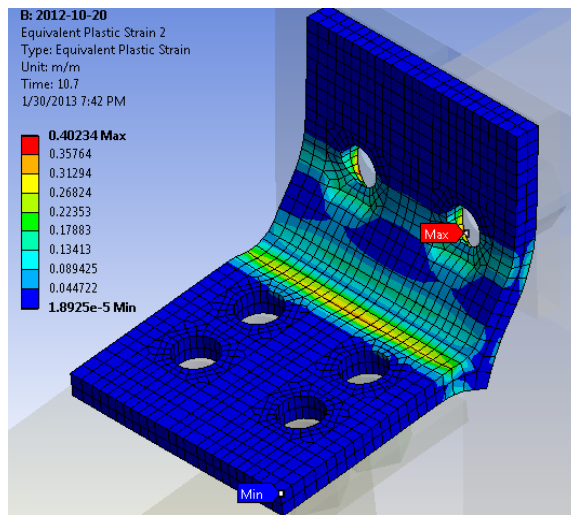


(b) Model ELM4

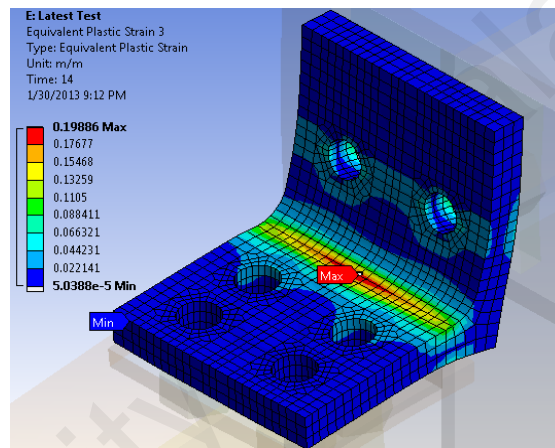


(c) Model ELM9

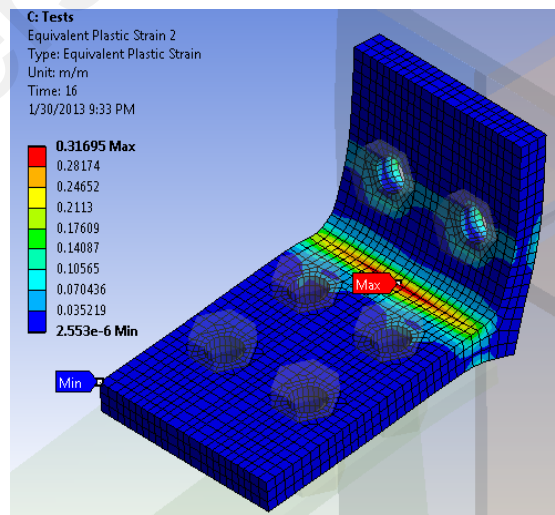
Figure 4.36 Top angle bolt stress for models at elevated temperature



(a) Model ELM3

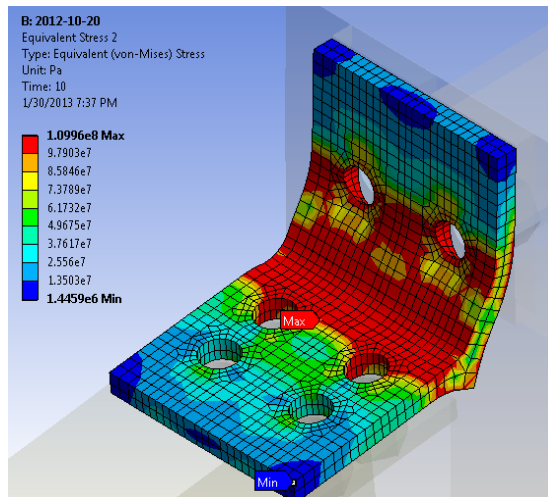


(b) Model ELM4

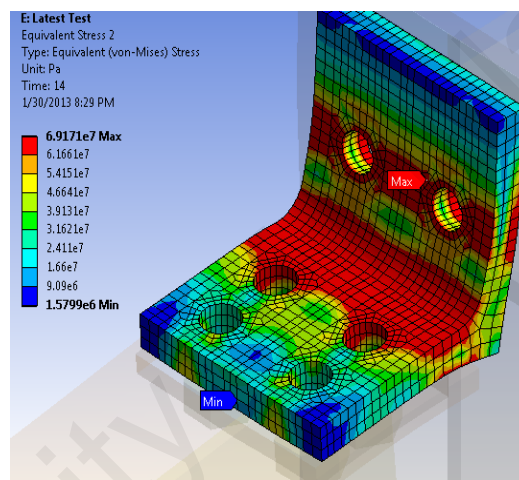


(c) Model ELM9

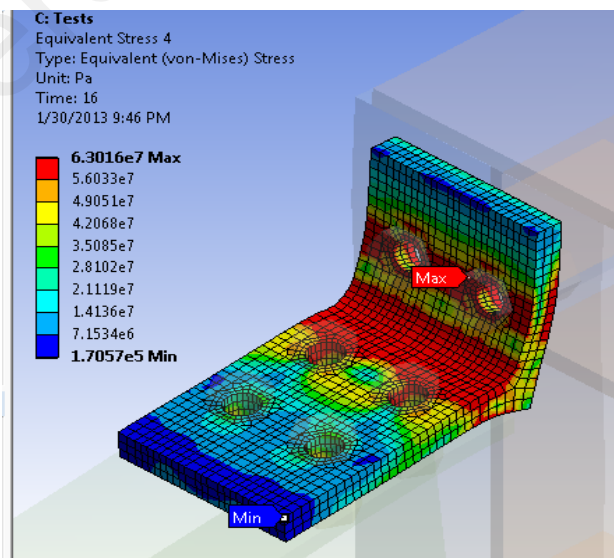
Figure 4.37 Top Angle Plastic Deformation patterns of models at elevated temperatures



(a) Model ELM3

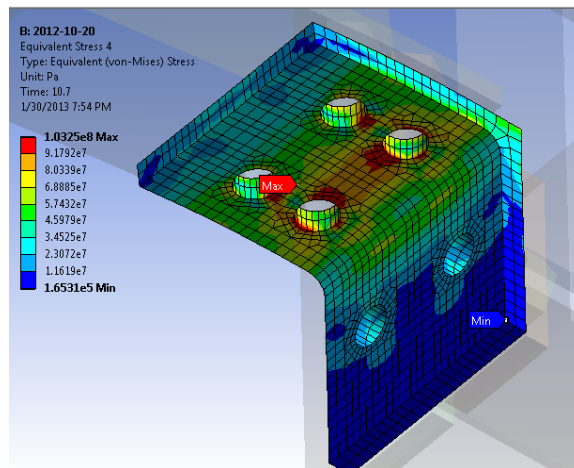


(a) Model ELM4

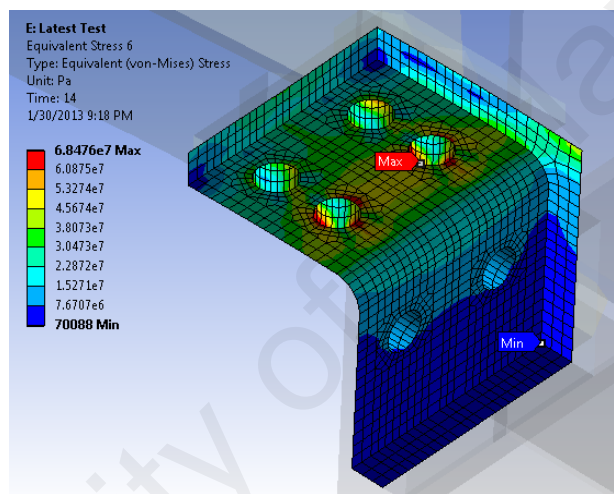


(a) Model ELM9

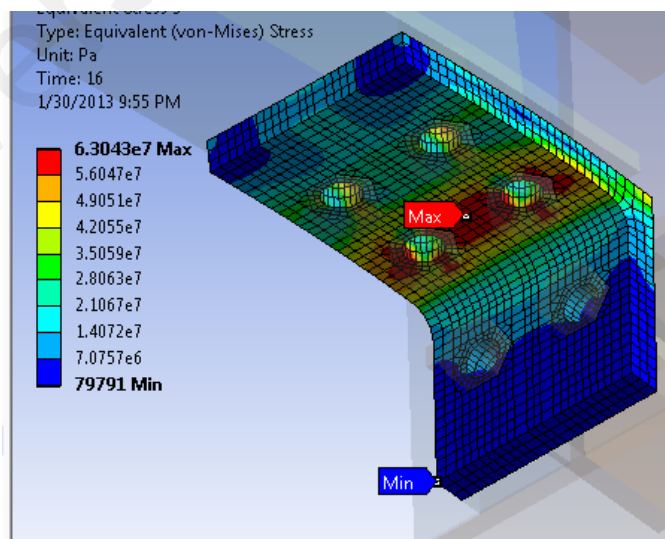
Figure 4.38 Top Angle Stress patterns of Models at elevated temperatures



(a) Model ELM3

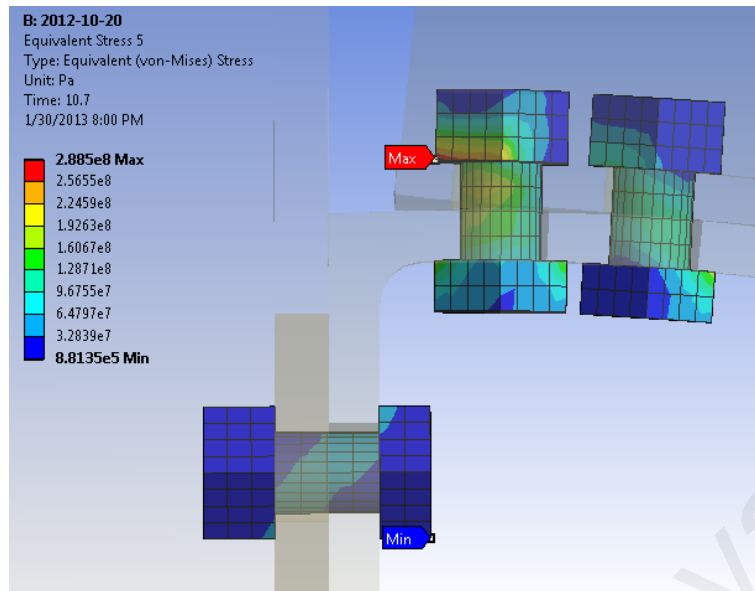


(b) Model ELM4

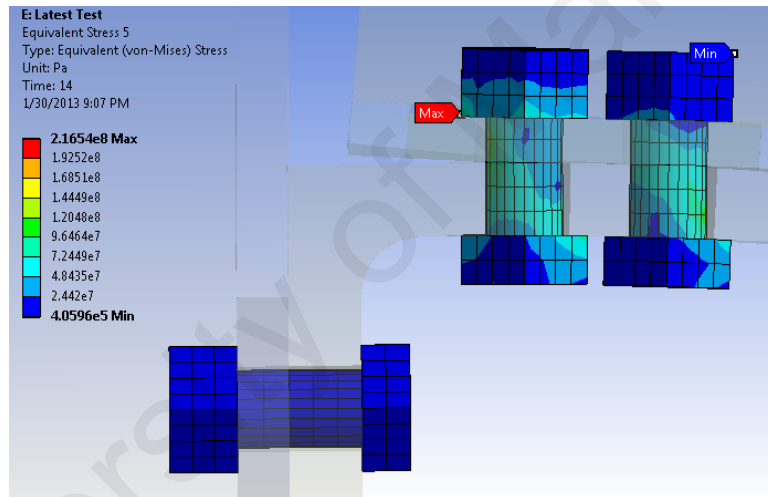


(c) Model ELM9

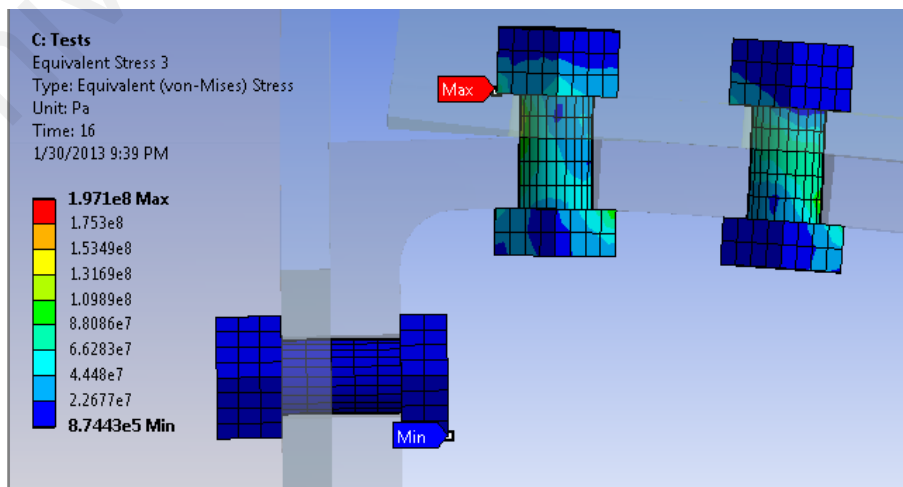
Figure 4.39 Bottom Angle Stress patterns of models at elevated temperature



(a) Model ELM3



(b) ELM4



(c) Model ELM9

Figure 4.40 Bottom angle bolt stress of models at elevated temperatures

### 4.3.1 Effect of Seat Angle

It is generally assumed that in the design of top-seat angle connections, loads from floors are transferred to the beams via vertical line loads. These line loads are then transferred to the connections and finally to the bolts and column. Design assumptions made include that the loads have an eccentricity and therefore a lever arm which results in a moment force acting onto the connection. The moment force is then distributed into a tension / compression force within the depth of the beam, where the lever arm is the depth of the beam section. Subsequently, design is based on the shear force of bolts at the beam leg with tension forces at the bolts of column leg at the top angle section. With this concept, in theory, the seat angle itself does not have a major contribution to the behavior and capacity of the connection.

Based on Pirmoz and Danesh (2009b), the effect of the seat angle on the connection behavior is studied by varying the length of the beam and deductions are made on the assumption that the increased beam length would result in a higher a load, in which the behavior is directly affected by the seat angle. The simplification of the concept is as shown in Figure 4.41 and Equations 4.5 to Equations 4.6 as proposed by Pirmoz and Danesh (2009b). The study concluded that the seat angle contribution to the connection behavior cannot be neglected.

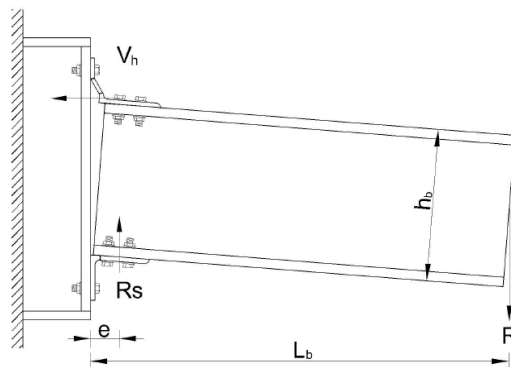


Figure 4.41 Illustration of the effect of seat angle concept. (Pirmoz, 2009b)

$$M = R.L_b = V_h.h_b + R_s.e \quad (\text{Eqn. 4.4})$$

$$R = R_s \quad (\text{Eqn. 4.5})$$

$$V_h.h_b = R.(L_b - e) \quad (\text{Eqn. 4.6})$$

However, for this study, instead of having theoretical calculations or logical deductions, the effect of seat angles are studied through a series of geometrical changes in the model and analyzed using Ansys Workbench. The basis for the model, including assumptions, material properties, supports and loads are based on the validated model AMS1 as the behavior of AMS1 relates closer to the experimental results compared to AMS2. Among the geometrical parameter studied for the seat angle including the reduced bolt numbers, gauges distances for column and beam leg, seat angle thickness and the gap distance between beam face closest to column and the column flange face.

#### **4.3.1.1 Effect of Seat Angle Thickness**

In comparison to the model AMS1, the thickness of the seat angle is modified and analyzed. With the seat angle thickness modified, the bending capacity of the seat angle is altered. This would then result in a higher capacity / stiffness of the connection. Results of the analysis from ANSYS Workbench are as shown in Figure 4.42. Thickness of the seat angle has been increased from 3/8 in. (9.53 mm) to 7/8 in. (22.23 mm) thick in AMS1 and AMBT1 respectively. AMBT2 on the other hand, has thickness of 0.625in. (15.78mm). Results shown in Figure 4.42 clearly reflect the concept that the seat angle does not behave by transfer of shear forces alone, but the contribution of the seat angle to the connection behavior is by the bending capacity of the angle.

From the results, the stiffness of the connection is increased by 7.8% and moment capacity increased to 54kN.m from 48kN.m, which is a 12.5% increase in moment capacity. The increase in stiffness is relatively minor as the elastic behavior of the connection is dependence on the elastic value of the materials while the post yield behavior is dependence on the geometrical properties of the model. Comparing the beam end deformation at 36mm deflection or rotation of 24mrad for a 1.5m beam, would result in a higher capacity for connection with higher bottom angle thickness.

Studies on the bottom angle thickness have also been done by Yang and Chen (1999) on the effect of seat angle connections without the top-angle. While without the top-angle and the study focuses on the seat angle, however, the results from the study and has shown similar results where the moment capacity of the connection was dependent on the angle thickness, similar to the results shown in this study.

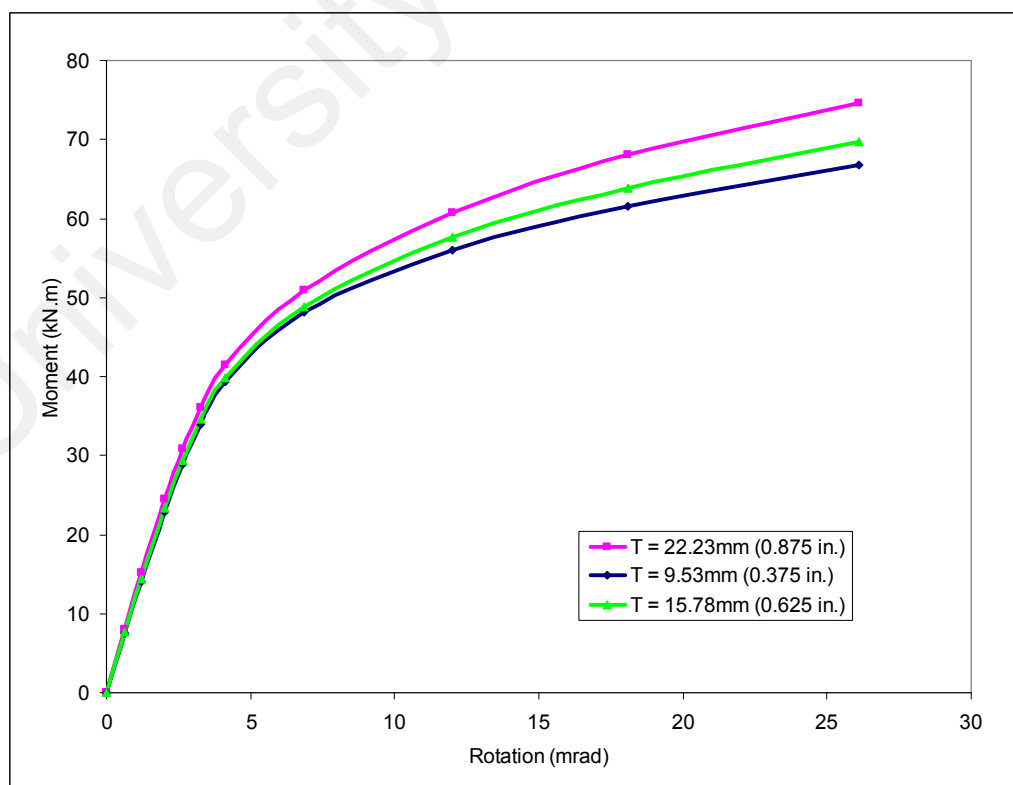


Figure 4.42: Effect of Bottom Angle Thickness

#### 4.3.1.2 Effect of Seat Angle Gauge Length

In the design of top-seat angle connections, the connection behavior is often governed by the top-angle in bending deformation. Bending of the top-angle is affected by the gauge distance, or the parameter  $m$  in EC3: Part 1-8. Although this, the gauge length for the seat angle has not been studied. Both behaviors are as shown in Figures 4.43 and 4.44 respectively. It is shown separately as to highlight the comparison with the validated models. From the graphs, by varying the gauge length at the seat angle, a higher gage length, or increase of the distance between the first bolt row and the root of the angle would slightly increase the end-moment capacity of the connection. Only minor differences in the stiffness of the connection was observed and considered to be negligible.

Meanwhile, having a decrease in gage length displays no prominent difference in behavior in comparison with the original model AMS1. Possible explanation on this is that the bolt row at the bottom angle for the column leg was unaffected or provided little contribution to the behavior of the connection on the whole. The slight increase in moment capacity when the gage length at the column leg was increased may be a result of an increase in the lever arm distance.

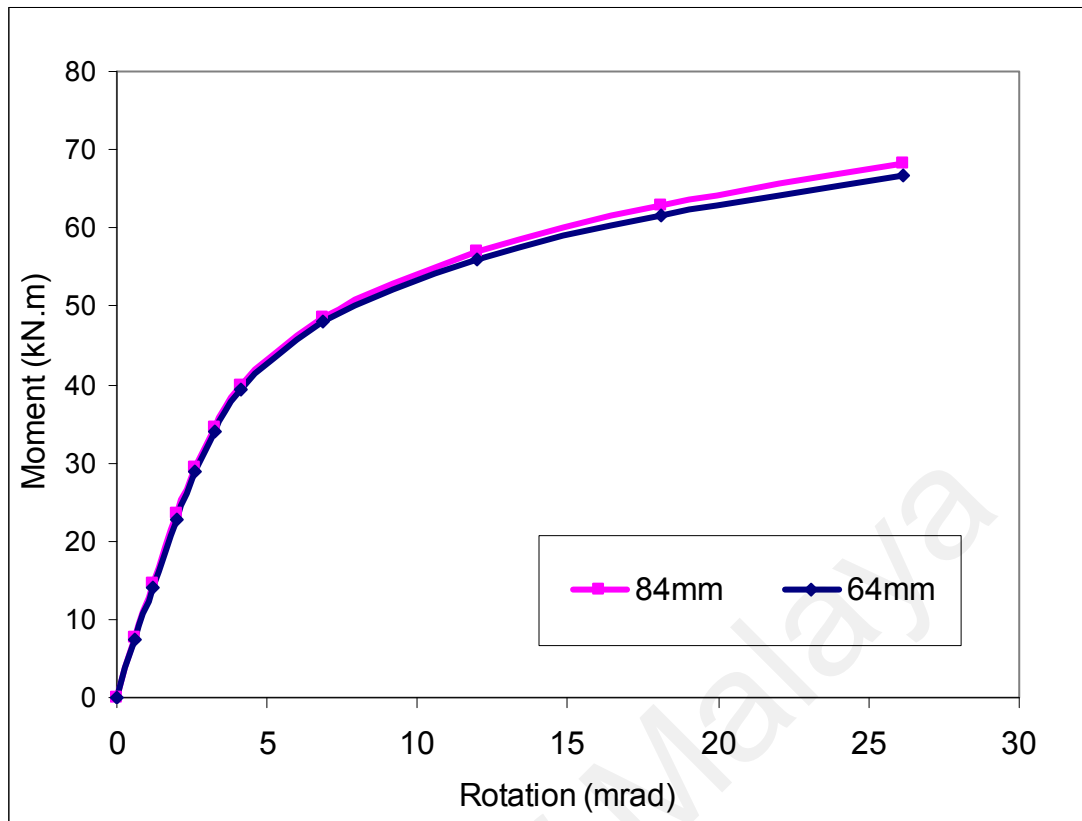


Figure 4.43: Effect of Increased Gage Length at Bottom Angle

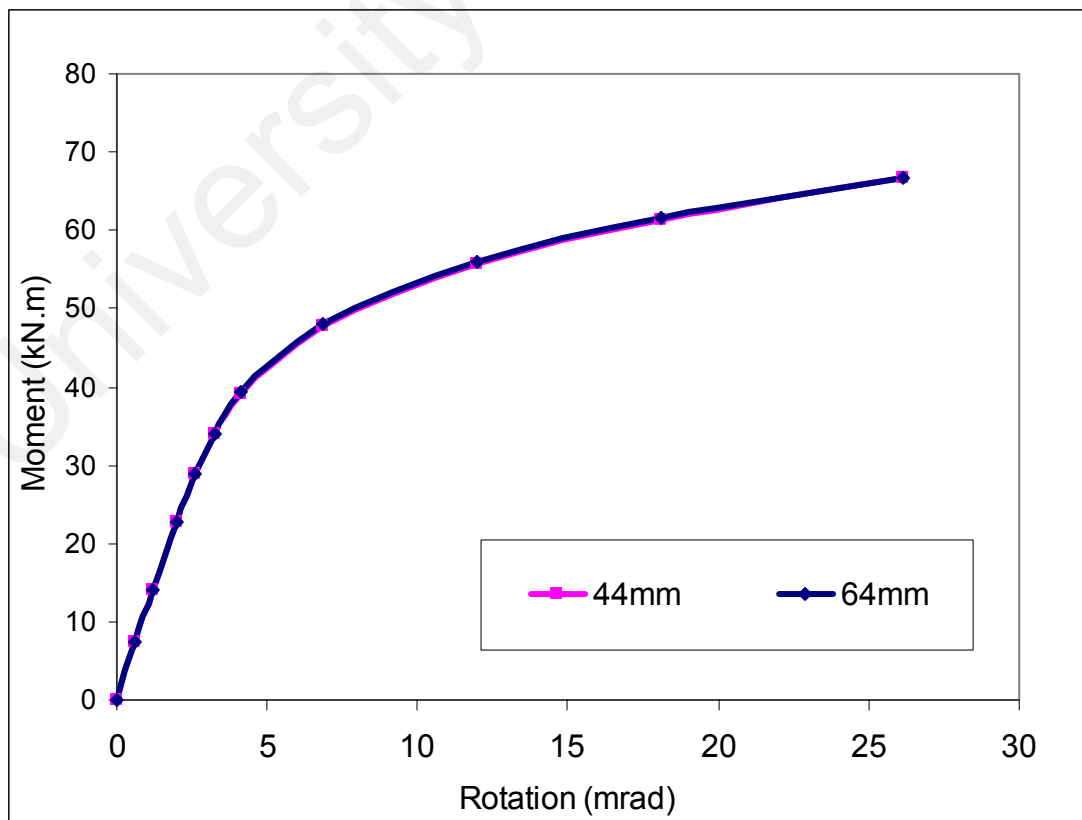
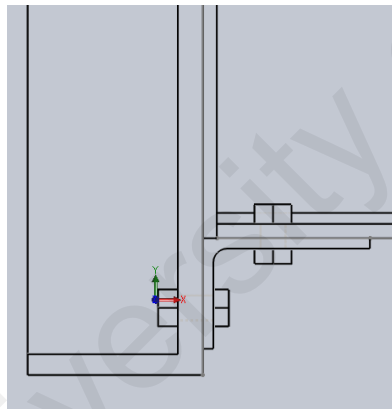


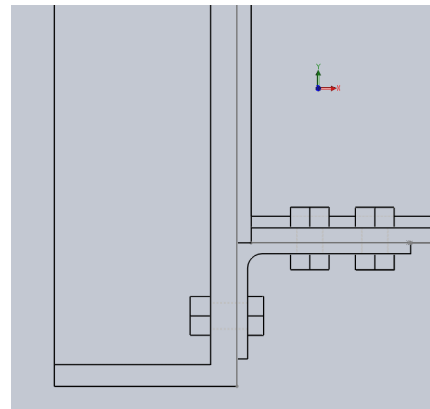
Figure 4.44: Effect of Decreased Gage Length at Bottom Angle

### 4.3.1.3 Effect of Seat Angle Bolt Rows

With consideration that the behavior of the top-seat angle connection at the seat angle is not dependence on the shear of the bolts at the seat angle, the behavior is studied with only a single bolt row at the seat angle, as shown in the comparison in Figure 4.45. Results as shown in Figure 4.46 indicate that reducing the seat angle bolt rows would have minor effect on the connection behavior. Reducing the bolt row would have reduced the capacity to limit the rotation of the angle by increasing the length of the seat angle available for bending capacity, which results in the minor differences seen in the behavioral results.



(a) Reduced bolt row model with 1 bolt row



(b) Normal model with 2 bolt rows

Figure 4.45 Reduced Bolt Row comparisons

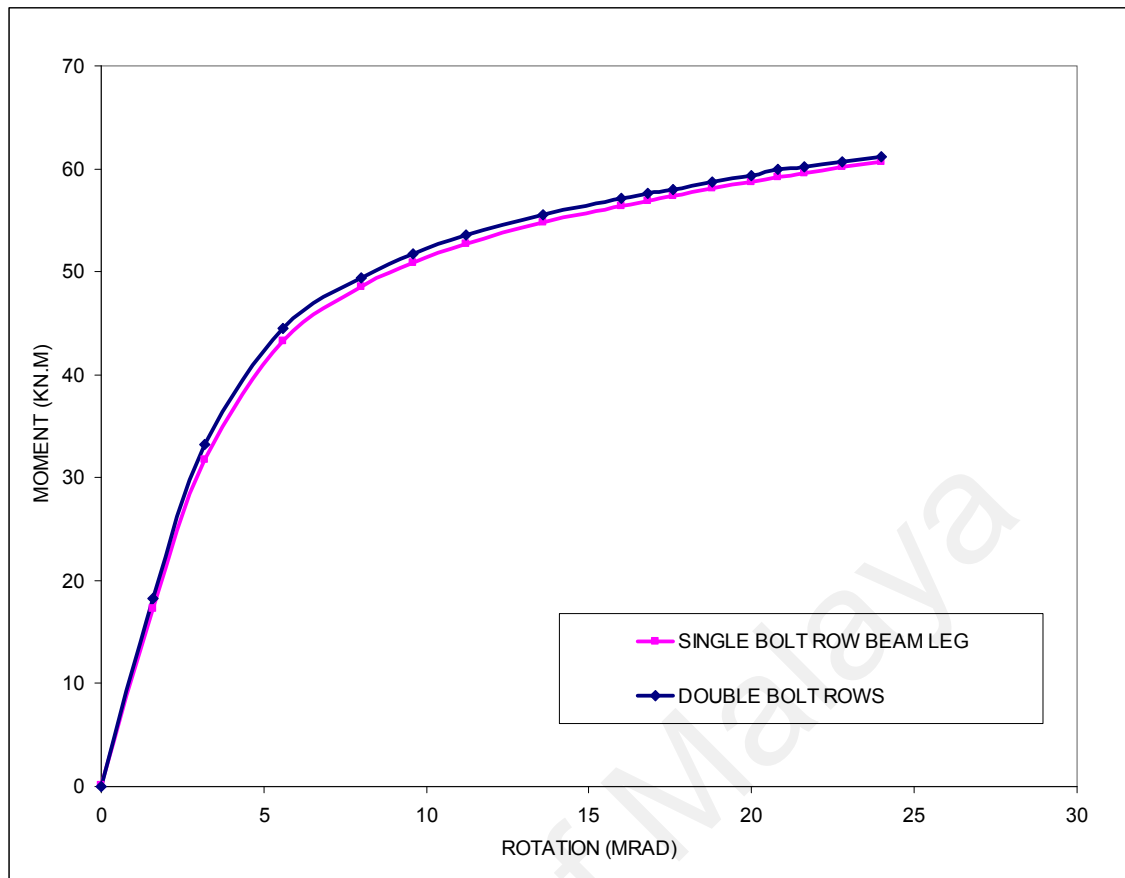


Figure 4.46 Effect of Reduced Bolt Row at Seat Angle

### 4.3.2 Effect of Gap

On the effect of gaps on the behavior of the connection, this study is conducted to highlight on the bearing effect of top edge of the beam on the bottom of the top angle under the condition where a vertical load is applied, creating a moment load on connection and with the top beam leg as the fulcrum, having a prying effect on the top angle due to the different deformation patterns of beam and top angle. Effect of gap has been studied in elevated temperature conditions by Saedi and Yahyai (2009a) and it was found that the decrease in gap resulted in a higher connection stiffness in the elastic range and shows negligible difference in the plastic range due to the contacting beam edge to the column flange limitation.

With the geometrical properties similar with model AMS1, models are created with lower and higher gap values of 38.1mm and 6.35mm gap in comparison with the gap value of 12.7mm used for model AMS1. Analysis is conducted and from the results compared shown in Figure 4.47, it can be deduced that the reduced gap increases the moment capacity significantly while an increase in the gap distance reduces the moment capacity or the after yield behavior. In comparison to the study by Saedi and Yahyai (2009a), the gap has not been affected by the beam bottom contacting the column flange but instead sufficient space is still available, as depicted in Figure 4.48 for the deformation of the seat angle at 26 mrad connection rotation value.

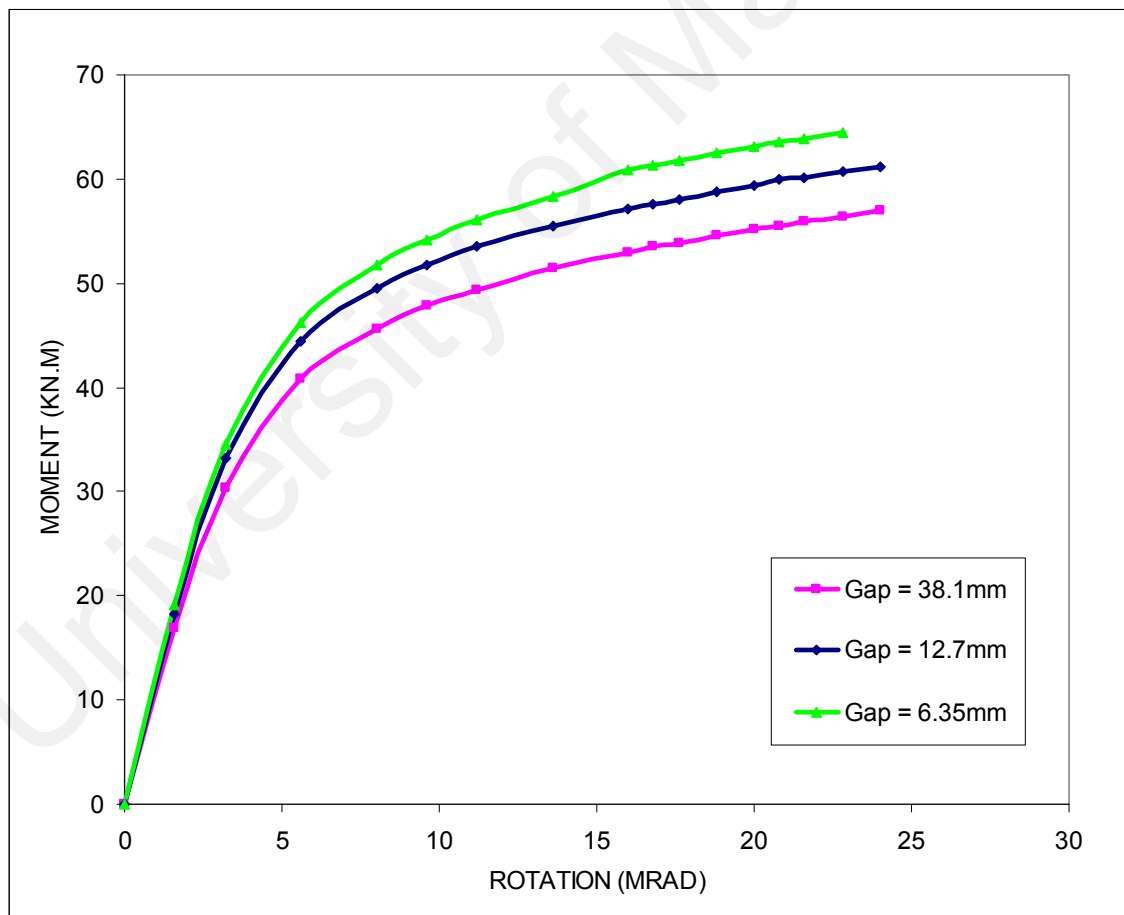


Figure 4.47: Effect of Gap values on the behavior of connection

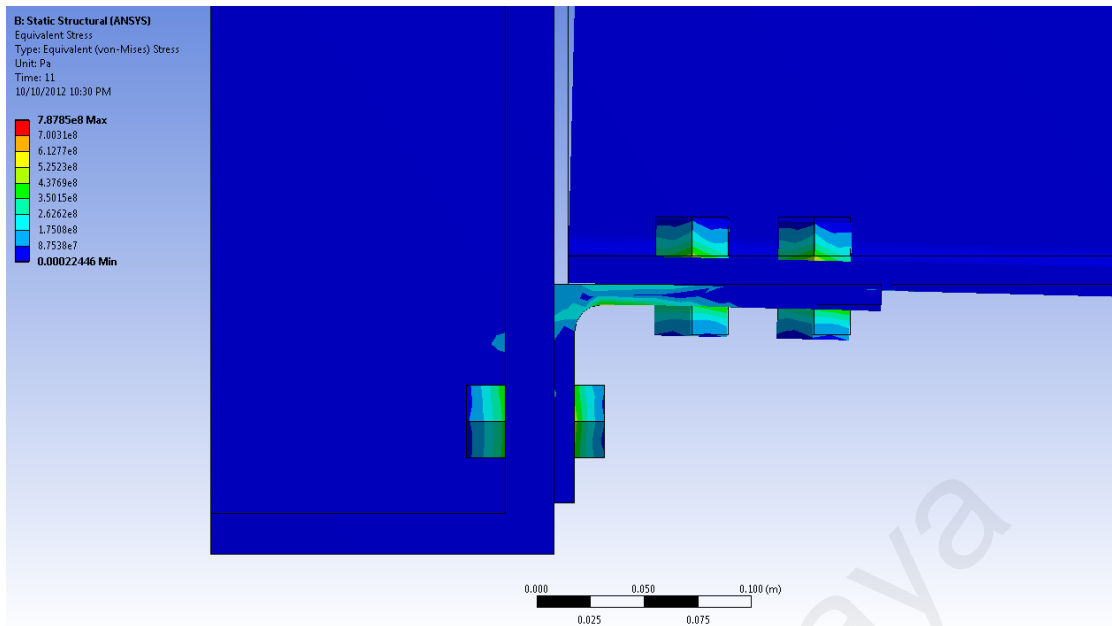
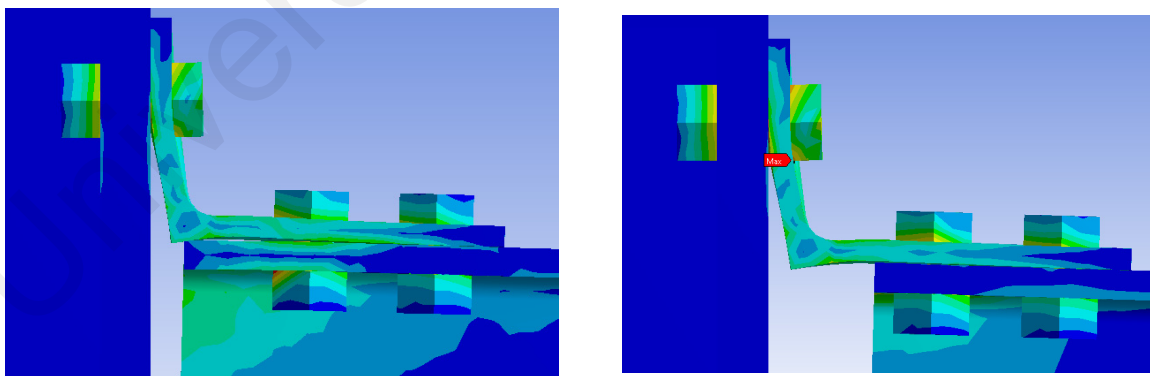


Figure 4.48 Deformation of Seat Angle for reduced gap (6.35mm) model

The prying effect is clearly shown when a comparison is made between models, as depicted in Figure 4.49. Analysis results have also shown that the bearing behavior contributes to the behavior of the connection by providing a limitation to the deformation of the beam, therefore increasing moment capacity of the connection.



(a) Decreased gap model (6.35mm)

(b) Increased gap model (38.1mm)

Figure 4.49 Comparison of top angle deformation for effect of gap

### 4.3.3 Effect of Angle Length

From previous analysis results, the plastic strain for top-seat angle connections commonly occur across the angle sections. This pattern has lead to the assumption that the loads are transferred across the angle section, especially the top angle section in case of moment loads. With this notion, a study is conducted to examine the effects of angle length on the connection behavior. Model basis is model ASM1 validated earlier. Other than the angle section length, the other parameters are similar to the previously validated model.

In terms of the angle length, due to the fact that the bolt to bolt distances on the column leg angle section are wide apart, it is only permissible to reduce the length by 10% to avoid the angle section being shorter than the bolt head sizes and distances. Length of the angle section in model AMS1 is 203.2mm while the length used for this study is 304.8mm, 254mm, 223.52mm and 182.88mm which accounts for 50%, 25%, 10% in angle length increase and 10% in length reduction. Summary of the models is given Table 4.15 while the models connection response when compared to AMS1 is as shown in Figure 4.50

Table 4.15 Summary of angle length study models

Model	Length Percentage	Length (mm)
AMS1	-	203.2
ALGTH50	+50%	304.8
ALGTH25	+25%	254.0
ALGTH10	+10%	223.52
ALGTH10R	-10%	182.88

Response of the analysis shows that the increase in angle length increases the moment capacity of the connection. However, the stiffness of the connection does not increase while the elastic-plastic curve changes accordingly. One of the possible reasons for this behavior is that the increase in angle length leads to the increase in bending capacity, due to the fact that bending capacity is determined by the moment of inertia area which increases with the length, therefore increasing the moment capacity.

On the other hand, the comparison of failure modes for each of the lengths studied is as compared in Figure 4.51. Similar to model AMS1, the deformation is concentrated at the bolt locations on the column and the beam leg near the angle section heel area. However, the increased length has decreased the loads resisted by the angle per unit length while the reduced length has the opposite effect as shown by the concentration of plastic deformation on the angle heel.

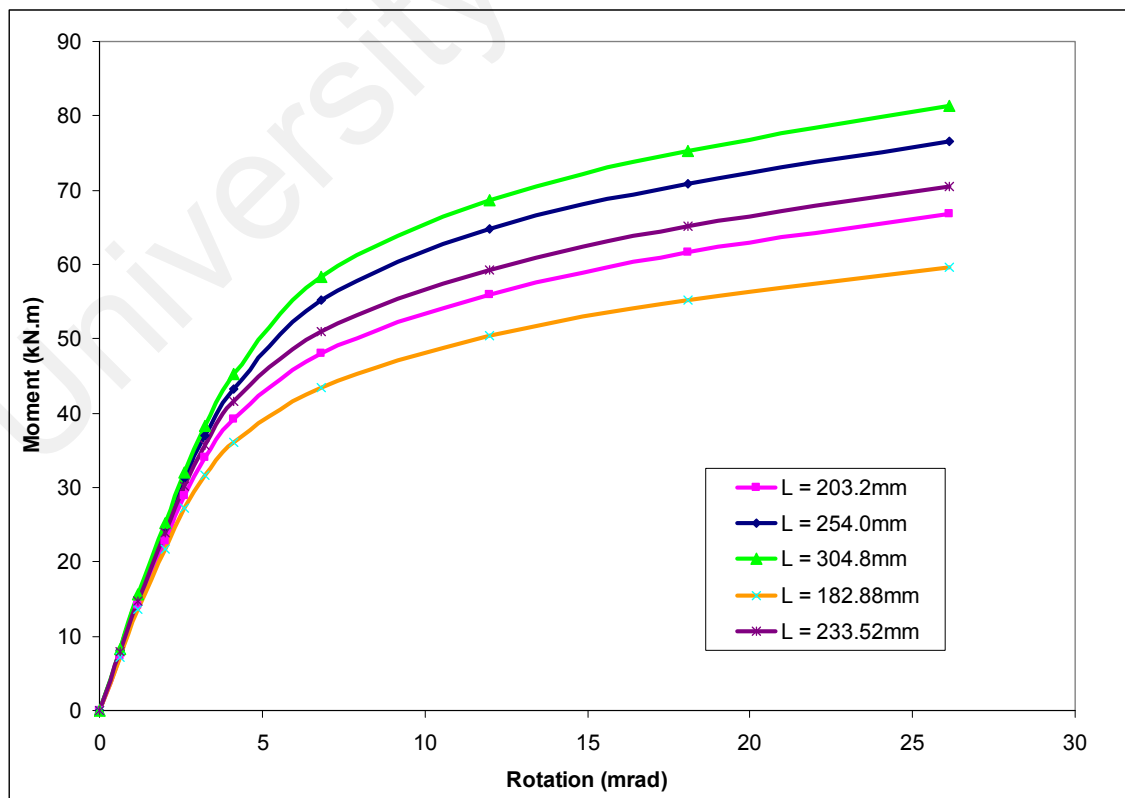
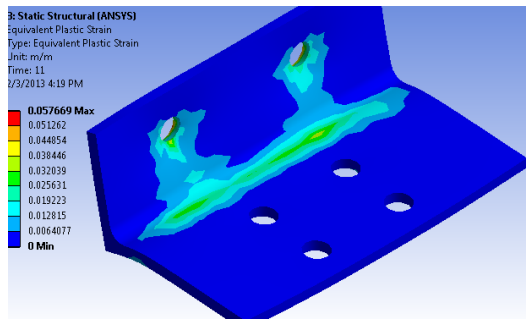
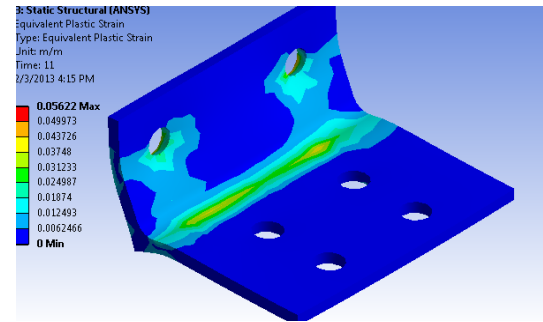


Figure 4.50 Effect of Angle Length on Connection Behavior



(a) Model ALGTH50



(b) ALGTH10R

Figure 4.51 Plastic Deformation Pattern due to Effect of Angle Length

#### 4.3.4 Effect of Coefficient of Friction

Friction occurs due to the interaction between surfaces, where surfaces move in parallel directions or where the edges of an object collide with another. Undoubtedly, all objects fall under the governance of friction, but the difference is whether the levels are high that large forces are still unable to displace the object or the friction is negligible. In the study of structural steel connections, for simplicity, the effect of friction contact is at times assumed negligible. Smoother surfaces results in a lower value of friction coefficient while a rough surface otherwise.

A study is conducted to examine the effect of friction on the connection response and behavior in effort to determine if the coefficient of friction has any noticeable effect. Basis of the study is the validated ambient temperature models of AMS1. From the analysis, the response of the connection is as given in Figure 4.52 and the results show that the coefficient of friction plays a major contribution in determining the response of the connection.

Higher coefficient values increases the moment capacity while lower values decrease the moment capacity by a large amount. On the preset “rough” contact surface, the coefficient value of 0.5 is unable to match the response of the connection under the rough contact setting which means that the value of friction is relatively much higher than 0.5.

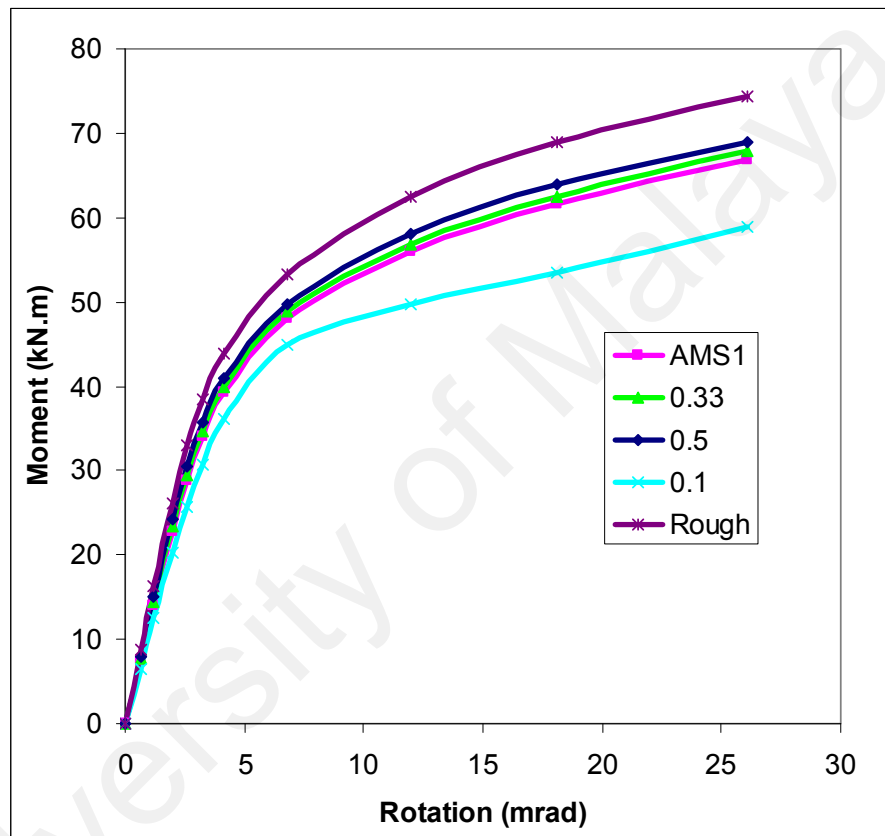


Figure 4.52 Effect of Coefficient of Friction

#### 4.3.5 Effect of Contact Settings

In the analysis of structural steel connections using finite-element analysis software, the contacts between the components involved are often one of the major considerations to be examined. In actual testing conditions, the contacts between the components contribute to the connection response.

Although this, in simulation terms, the contacts are usually the main factor that results in the non-convergence of the model analysis, due to the software unable to solve the discrepancies in load distribution, from the various deformation patterns of the components which therefore causes the failure of the analysis.

In ANSYS Workbench, there are five types of contacts being: no separation, frictionless, rough, frictional and bonded. While bonded and no separation contact is particularly similar, the no separation contact still do allow for displacements but the defined parts for the contact cannot be separated. On the other hand, rough and frictionless are the extremes of the frictional contact, where frictionless would result in almost zero friction while rough have infinite friction. Only ambient temperature conditions are studied as it is assumed that the contacts do not change with elevated temperature conditions.

A list of locations where the contact settings are generally defined is as shown in Table 4.16. Response of the connection under the different contact settings, shown in a moment-rotation graph is as given in Figure 4.53. With bonded contacts, the connection requires higher loads to achieve similar deformation levels of the beam edge when compared to other contact settings. Due to the similarity in conditions with bonded contact, the “no separation” contact is not analyzed in the study with the assumption that the behavior would be similar.

On the other hand, frictionless contact causes the connection to fail entirely in terms of model deformation where the angle sections “slip” without any rotational effect on the connection, as shown in Figure 4.54 with the outline of the un-deformed model wire frame shown for comparison.

The deformation distance corresponds to the displacement loads applied onto the model, similar to the values applied during the validation process. Meanwhile, the response of the connection under rough contact settings have the basic curve similar to frictional contacts, however, the connection is stiffer with higher moment capacity.

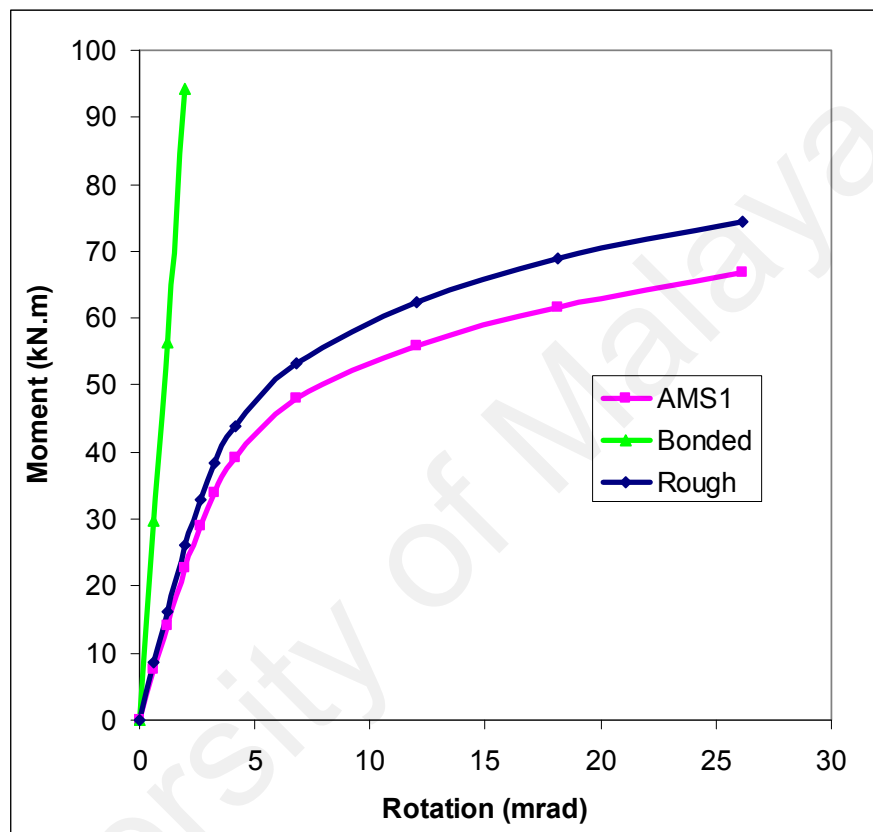


Figure 4.53 Effect of Contact Settings on connection

Table 4.16 Contact Settings Locations

Bolt Head to Angle Section-Column Leg
Bolt Nut to Column Flange
Bolt Head to Angle Section-Beam Leg
Bolt Nut to Beam Flange
Angle Section Surface to Column Flange
Angle Section Surface to Beam Flange

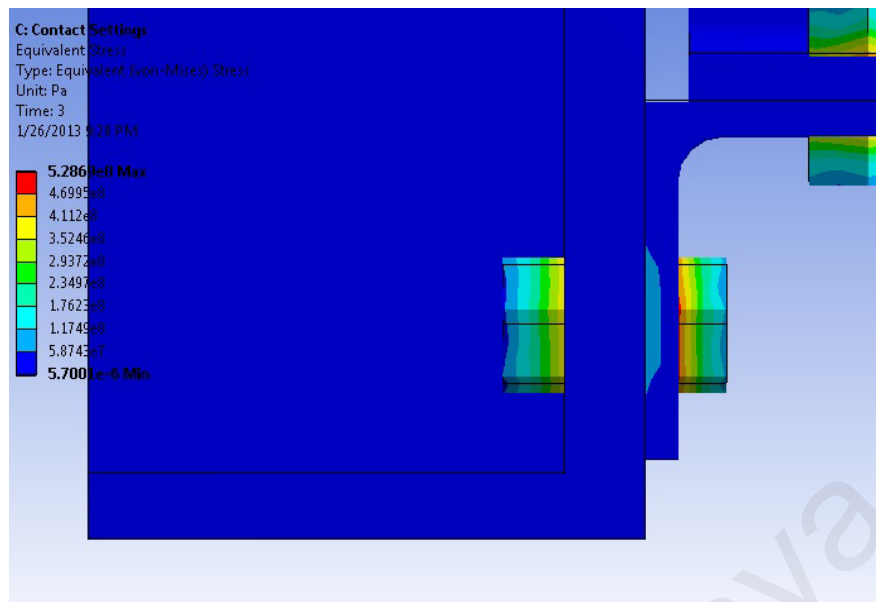


Figure 4.54 Slip of bottom angle – column leg bolt under frictionless contact

#### 4.3.6 Effect of Axial Loadings At Ambient Temperature

For ambient temperature conditions, axial loadings that occur in the connection may not be due to the nearby members but due to the internal force generated from loads at other locations or connecting components. An example would be in the case of truss members or roof rafters. Loads are applied onto the beams, while at the same time, loads on other members are causing the beam to resist axial loads and therefore, resisted by the connection arrangement. Compression in the member would result in axial restraint loads while tensional forces result in the axial release condition.

As specified by the guidelines provided by Eurocode 3 (2005): Part 1-8, the axial loadings to be limited to 5% for applications of the moment resistance calculations where the 5% accounts for the cross-section capacity of the member, which in this case is the connecting beam member.

Although this, another question is raised on the application of forces onto the beam. The methods in concern, is either by (1) Applying the load that continuously change directions with beam cross-section as the connection deforms, where the load maintains to be in the direction normal to the cross-section even as deformation occurs or (2) To apply axial loadings in the direction parallel to the original orientation of the beam before any deformation occurs and remain the same throughout the analysis, regardless of the deformation occurred on the beam. No study has been conducted which has been recorded of the either case in which actual conditions are occurring in the members during the loading process.

However, due to the fact that the axial restraint reduces the deformation of the connection, either Method (1) or Method (2) is expected to produce similar results. The lack of deformation limits the beam in a horizontal position which can be assumed to be either in the horizontal axis or where the beam axis remains horizontal. On the other hand, deformation of the connection is amplified by the axial release; therefore the different methods involved would result in different connection responses. A simpler definition would be where Method (1) is expected to affect the beam leg bolts while Method (2) would be affecting the column leg bolts.

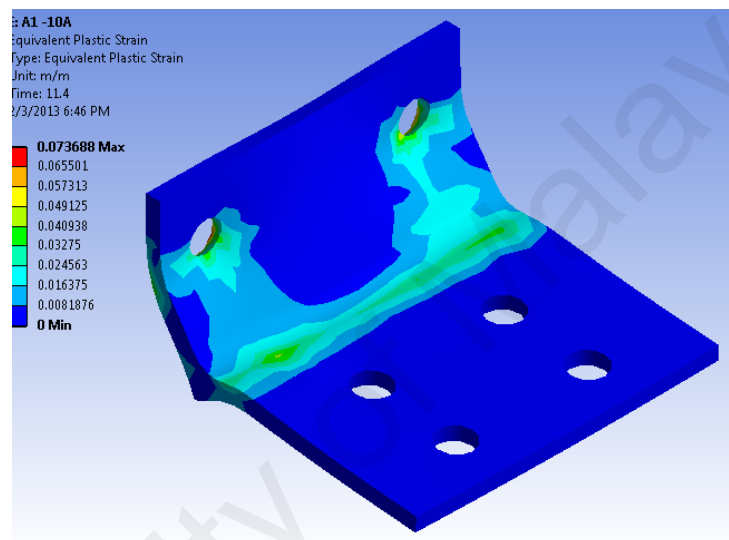
For ambient temperature models, model AMS1 is used as the basis for the model considering that the model has been validated with good agreement when compared with experimental results. In this study, both effect of axial restraints and axial release under ambient temperature conditions are analyzed with 2.5%, 5% and 10% of the cross sectional axial capacity. With the material yield stress valued at  $365 \text{ N/mm}^2$  due to the material properties published, a pressure of  $3.65 \times 10^7 \text{ Pa}$  is applied onto the beam at the 10% levels,  $1.825 \times 10^7 \text{ Pa}$  at 5% axial levels and  $9.125 \times 10^7 \text{ Pa}$  at 2.5% axial loadings.

In terms of loadings precedence, without any displacements, the pretension loads on the bolts are applied at the first step followed by the axial loadings in the next step. Beam displacements are applied as the controlling deformation in the subsequent steps after the axial loading step has been completed where the axial loadings remain constant while the beam displacement increases.

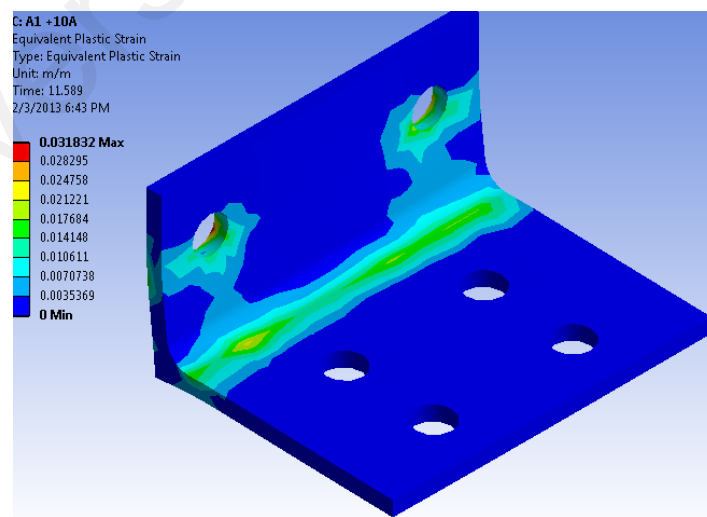
From Figure 4.55(a), it is shown that the axial release forces or the axial tension is supported largely by the column leg bolts with the plastic deformation concentrated at the beam leg at areas directly below the bolts location. On the other hand, axial restraint forces are resisted by the whole length of the angle section, generally uniform across the length of the section. In comparison to the plastic deformation patterns at zero axial loadings as shown in Figure 4.10 of the earlier sections, the patterns under axial loadings, as given Figure 4.55(b), differs in terms that the plastic deformation under axial restraints is more uniform and the pattern more evident.

Models have been marked as AM1A10 or AM1AR10 where 'A' for restraints and 'R' for release conditions and '10' being the axial percentage level applied onto the connection studied. Behavior of the models under compression loads or axial restraints is as shown in Figure 4.56 and the results indicate that at low level of axial restraints, the axial force is capable of increasing the connection stiffness and moment capacity. However, for axial restraints higher than 5%, the response pattern of the connection are observed to be increasingly higher in the plastic regions in comparison to the response at lower than 5% axial restraints where the plastic regions remain parallel throughout the different levels of axial restraints.

On the other hand, the connection response under axial release conditions or tensional connection loads is as shown in Figure 4.57 for AM1R series. The effect of axial release has been expected, where the connection has reduced stiffness and moment capacity. At higher axial restraint levels, elastic-plastic difference is not evident and the connection behaves almost linearly with the loads applied. Plastic deformation patterns under the 10% level of axial loadings are as shown in Figure 4.36 for both restraint and release.



(a) At 10% Axial Release



(b) At 10% Axial Restraint

Figure 4.55 Plastic Deformation at Ambient Models under 10% Axial Loadings

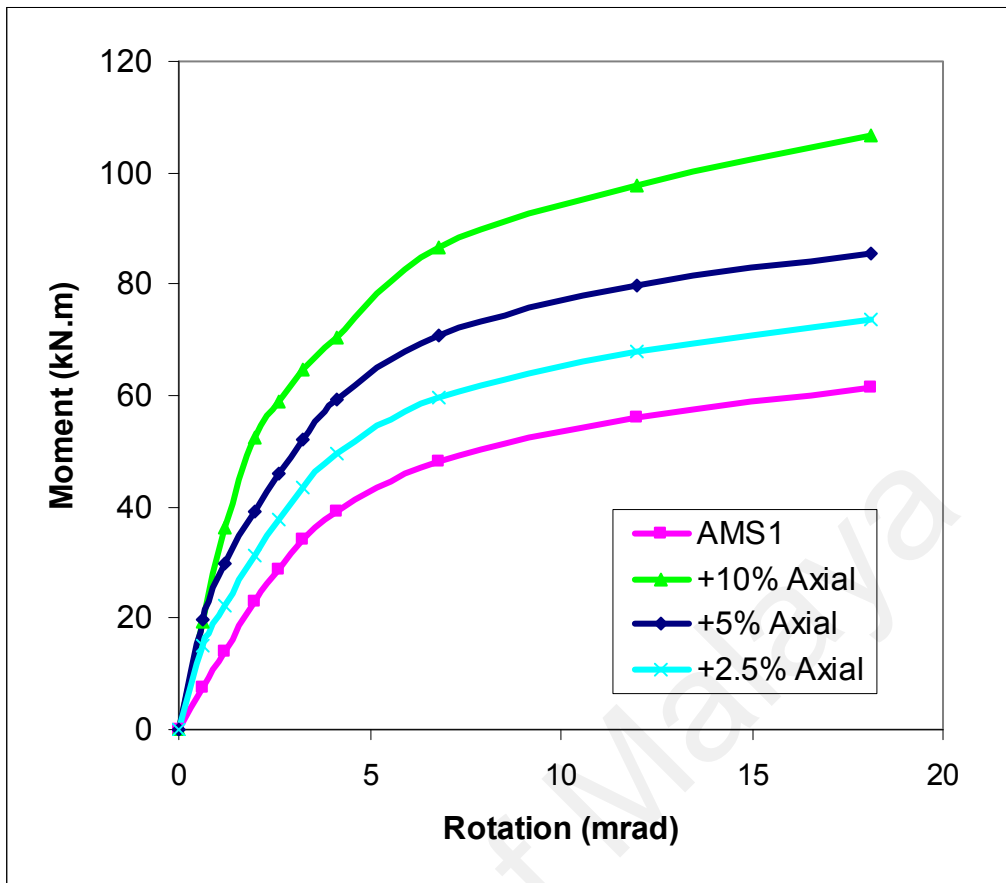


Figure 4.56 Effect of Axial Restraint on Model AMS1

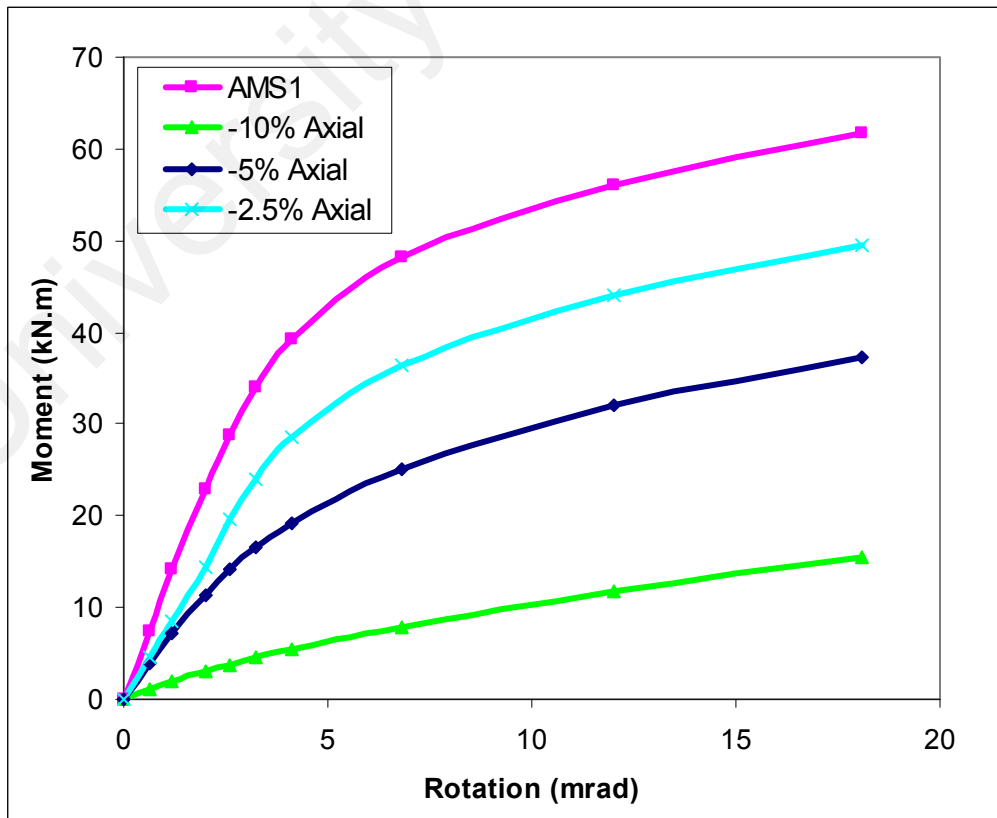


Figure 4.57 Effect of Axial Release on Model AMS1

## **4.4 Parametric Studies at Elevated Temperatures**

### **4.4.1 Connection Behavior at Isothermal Conditions**

Isothermal condition describes uniform temperatures throughout and gradual loadings being applied. Although anisothermal conditions analysis is essential in understanding the behavior of connection under elevated temperature, however, isothermal conditions analysis would provide understanding of the behavior and response of the connection generally under different temperatures and would assist in the design of the connection at elevated temperatures.

In addition, material properties specified in the guidelines provided by Eurocode 3 (2005): Part 1-2 is based on tests conducted in isothermal conditions and due to the effect of different heating rates. In comparison to the anisothermal behavior where only the maximum resistive temperature, which is the intersection between the straight lines formed by the plastic region and elastic region, similar in concept to the moment capacity, can be determined, isothermal behavior provides information on the maximum moment capacity of the connection at the particular designed temperature. With knowledge of the isothermal behavior connection response, the connection can be reinforced according to the designed temperature and applied moment loads.

A study has been conducted under isothermal conditions where the temperatures selected for the study being ambient temperature at 20°C, 200°C, 300°C, 400°C, 500°C and 600°C. Temperatures of 100°C are not included in the study due to the fact that at 100c, the material properties specified in EC3: Part 1-2 has no difference with ambient temperature properties, where it is assumed that the behavior will have minor and negligible difference.

Model ELM3 is used as the basis for the study and similar to the validation of models in elevated temperature conditions, the temperature load is applied uniformly on all the components. Force applied onto the connection is through displacements of the beam end. A maximum displacement of 30mm, providing a rotation of 125 mrad, is specified in this study which is beyond the considered deflection failure of a cantilever beam. Material properties for both steel material and bolts are as specified previously in the ELM3 model. Behavior of the connection at the various studied temperatures is as shown in Figure 4.58.

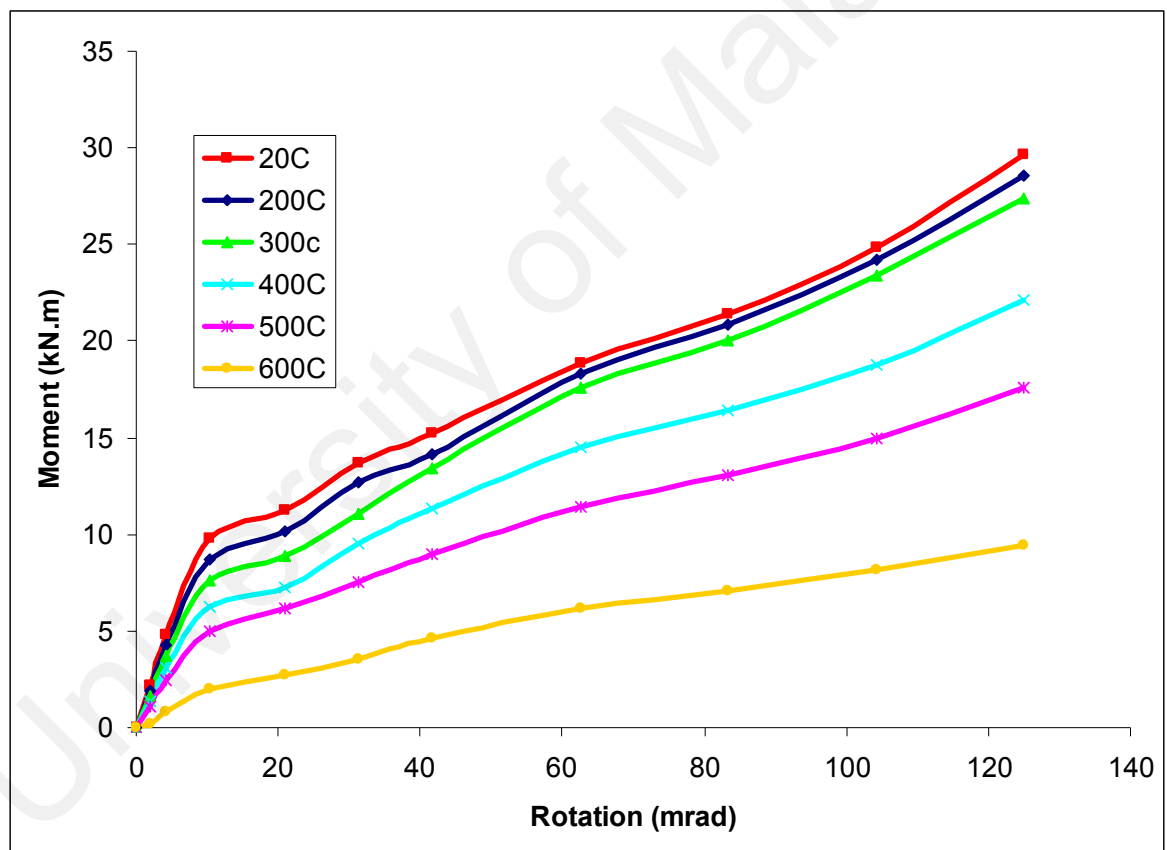
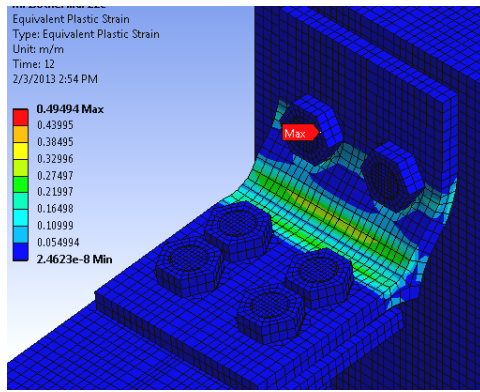


Figure 4.58 Model ELM3 Response under Isothermal conditions

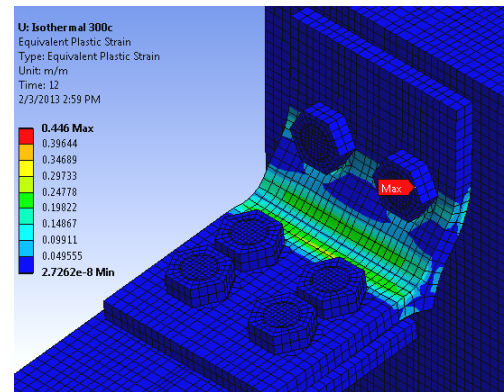
As shown in Figure 4.50, the moment capacity of the connection is reduced with the increase in temperatures. Major differences are seen between 500°C and 600°C where from Table 4.17 obtained from EC3: Part 1-2 shows that the yield, proportional limit and the elastic modulus values are reduced by 50%. Meanwhile the amount of time for a fire to achieve 600°C from 500°C is approximately three minutes according to the standard ISO834 curve, which is a sufficiently short time considering the human factor when handling fire conditions.

On the other hand, yield curve area of the behavior of the connection has been shown to be the difference between the response at 200°C and 300°C. The differences in material properties between 200°C and 300°C temperatures are the proportional limit and minor differences in terms of elastic modulus reduction and no difference in terms of yield reduction factor. This fact combined with the results of the analysis show that the stiffness of the connection is governed by the elastic modulus, elasto-plastic curve area is governed by the proportional limit while the end behavior is governed by the yield value of the materials.

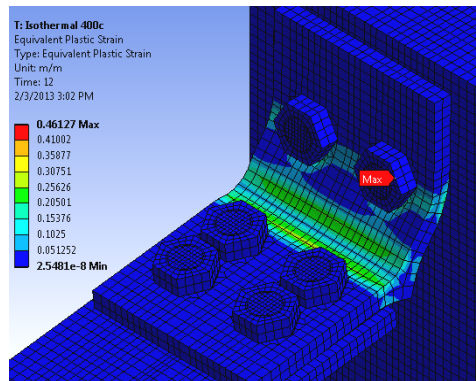
In terms of end deformation response, the different temperatures show variation in the location of the plastic regions, where the comparison is shown in Figure 4.59, while the stress patterns are as shown in Figure 4.60. At ambient temperature, the plastic deformation pattern is evident at the heel of both column leg and beam leg, however, as the temperature gradually increases; the plastic deformation at the column leg is reduced and becomes evident at the beam leg near the heel area. Stress patterns on the other hand, remains virtually unchanged even with the increase in temperatures, however the values only slightly varied among the temperatures.



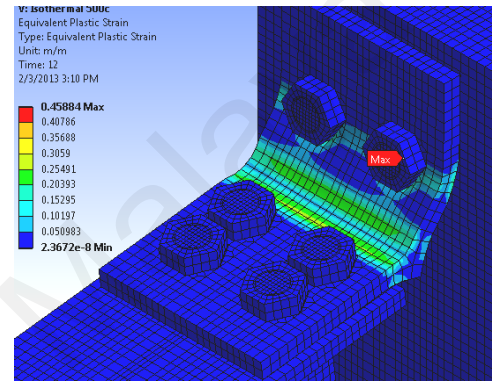
(a) Ambient Temperature



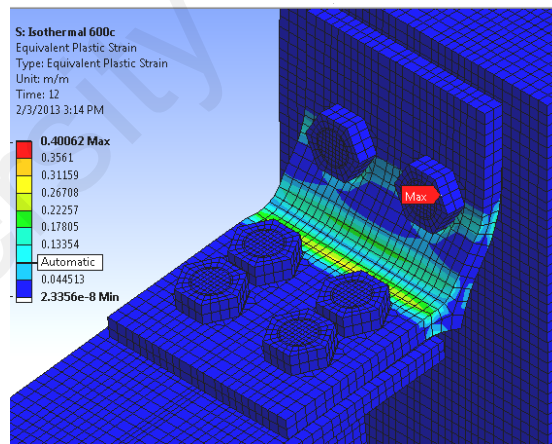
(b) 300°C



(c) 400°C

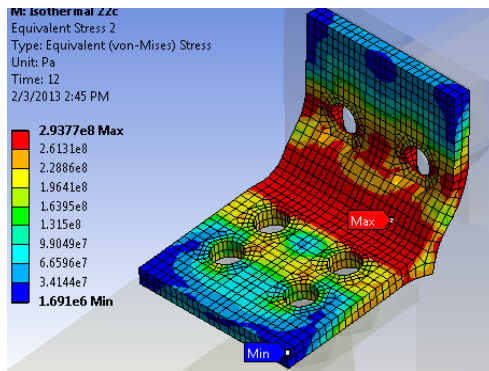


(d) 500°C

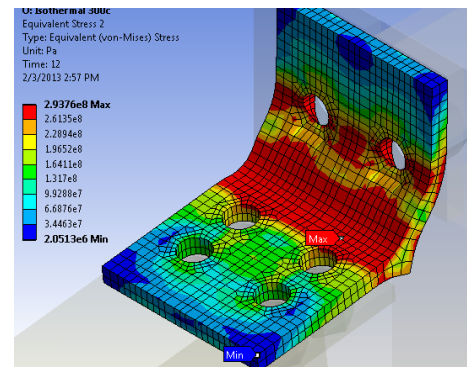


(e) 600°C

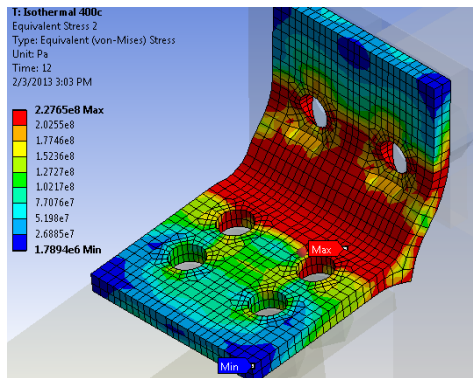
Figure 4.59 Plastic Deformation Pattern under Isothermal Conditions



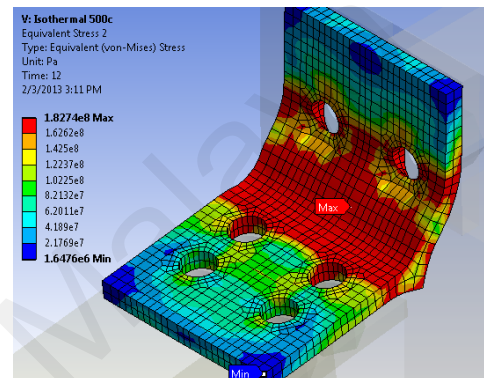
(a) Ambient Temperature



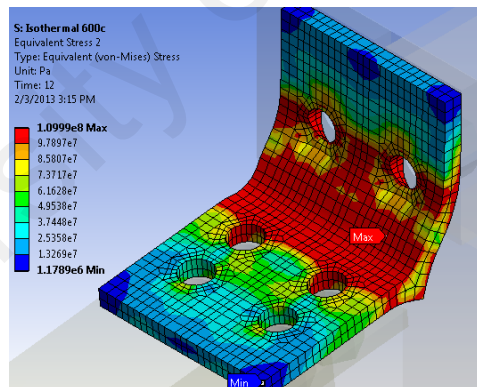
(b) 300°C



(b) 400°C



(b) 500°C



(b) 600°C

Figure 4.60 Stress Distribution Pattern under Isothermal Conditions

In comparison to the studies done by Saedi and Yahyai (2009b), the response of the connection differs greatly in stiffness, elasto-plastic and plastic behavior, as shown in Figure 4.61. The response of the connection by Saedi and Yahyai (2009b) has higher stiffness and the response pattern as a higher curve shape factor in comparison with the model.

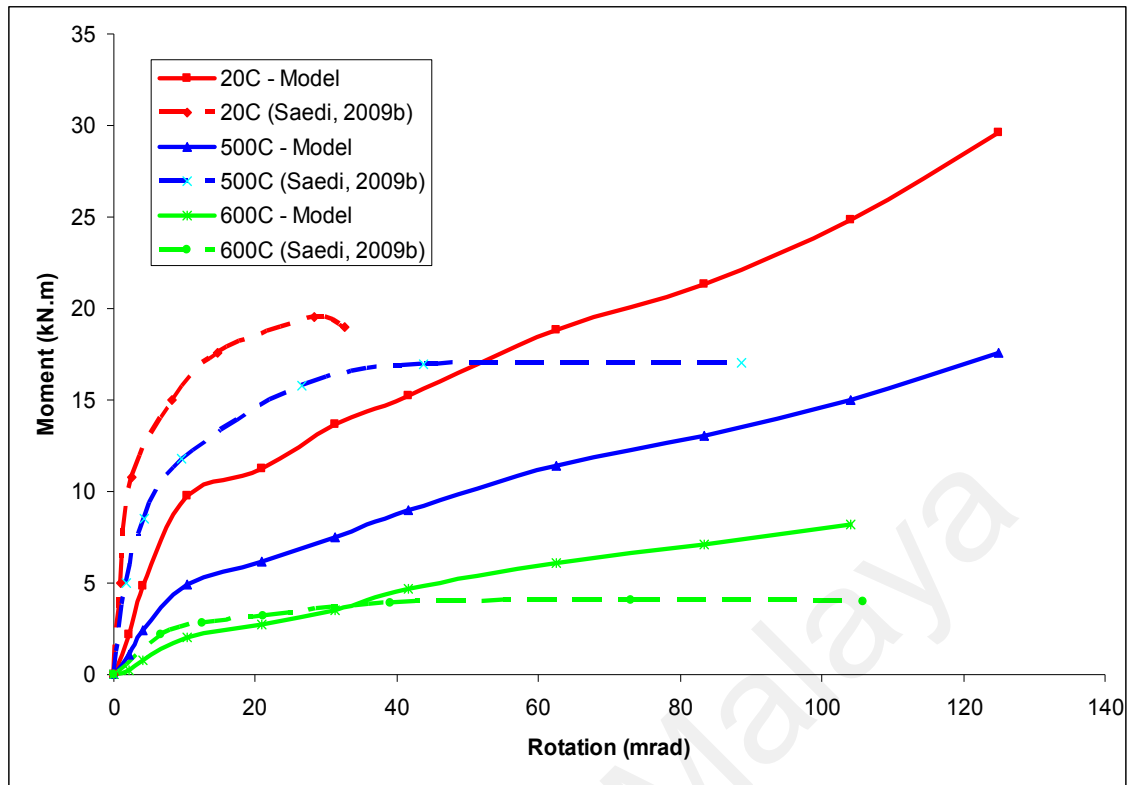


Figure 4.61 Comparison of isothermal behavior with Saedi and Yahyai (2009b)

However, at 600°C, the behavior of the connection has some similarities in terms of the initial stiffness, but continues to deviate after the elasto-plastic regions. The possible justifications being that the definition of the material properties by Saedi and Yahyai (2009b) is based on the incorporation of the stiffness and strength of the materials alone, as elastic-plastic materials. While that, the degradation of materials is based on EC3: Part 1-2. It can be assumed from the difference in the isothermal behavior that the material properties defined by Saedi and Yahyai to be higher stiffness than those in this study. Further validations with other tests in elevated temperatures are generally required with further study to understand the connection better.

Table 4.17 Reduction factors under elevated temperatures

Steel Temperature $\theta_a$	Reduction factors at temperature $\theta_a$ relative to the value of $f_y$ or $E_a$ at 20°C		
	Reduction factor (relative to $f_y$ ) for effective yield strength $k_{y,\theta} = f_{y,\theta}/f_y$	Reduction factor (relative to $f_y$ ) for proportional limit $k_{p,\theta} = f_{p,\theta}/f_y$	Reduction factor (relative to $E_a$ ) for the slope of the linear elastic range $k_{E,\theta} = E_{a,\theta}/E_a$
20°C	1,000	1,000	1,000
100°C	1,000	1,000	1,000
200°C	1,000	0.807	0.900
300°C	1,000	0.613	0.800
400°C	1,000	0.420	0.700
500°C	0.780	0.360	0.600
600°C	0.470	0.180	0.310
700°C	0.230	0.075	0.130
800°C	0.110	0.050	0.090
900°C	0.060	0.0375	0.0675
1000°C	0.040	0.0250	0.0450
1100°C	0.020	0.0125	0.0225
1200°C	0.000	0.0000	0.0000

On the other hand, assumption that the deformation of the connection in anisothermal conditions would reflect in isothermal results can be given consideration. A comparison of values is being made between Figure 4.58 and 4.32 (in section 4.2.2.2 of this document) reveals that relatively minor difference in rotation values the same temperatures compared. From Figure 4.48, at 8.48 kN.m moment loads, the rotation of the connection for the temperature studied at 400°C as an example has connection response of approximately 29 mrad while for anisothermal results at Figure 4.32; the rotation reaches up to 30 mrad for temperature of 400°C with moment load of 8.48 kN.m as applied.

This has shown that the from the anisothermal behavior of the connection, it would possible to extract the particular isothermal response at a specific temperature and moment loads applied since the anisothermal behavior is reflected in the isothermal response considering the same material properties used.

#### **4.4.2 Effect of Axial Loadings**

##### **4.4.2.1 Anisothermal Temperature Condition**

Using the validated elevated temperature model ELM3, the effect of axial loadings on the connection behavior is being studied. Axial loadings on the beam under elevated temperature conditions occur during the event of a fire due to the heating and cooling effect of the adjacent members in the full cycle of fire loadings.

Specifically, axial loadings due to the beam cooling are considered to be axial release or a negative axial load while the effect of steel elongation is considered to be axial restraints as a positive valued axial load. Coupled with the fact that the steel beams tend to display catenary actions under load, the axial effect is critical. Studies have been conducted by Liu (2001) on the effect axial restraints on steel beams while the effect on steel fin plate connections by Li et al. (2012). However, the effect of axial restraints on top seat angle connections in elevated temperature have yet to be recorded in any publications identified. With the yield stress defined as  $235 \text{ N/mm}^2$  in the material models, the resulting axial force is valued at 78.49 kN at the 10% level, which is applied as a pressure of  $2.35 \times 10^7 \text{ Pa}$ , normal to the cross-section of the beam section. Other percentage levels of the axial loadings follow accordingly.

As there are two methods for the application of axial forces, either method could be applied which the behavior of the method be representative of the effect on axial loadings onto the connection, as there is no actual tests conducted for the effect of axial loadings on the top-seat angle connection in elevated temperatures

Due to the fact that model ELM3 has the best behavioral shape and good agreement with comparative test behavior results, model ELM3 is used for the parametric studies in order to examine the effect of the axial loading. Axial studies model in anisothermal temperature conditions are labeled as a series of EL1A10 or EL1R10, similar to the marking pattern used for ambient temperature models on the effect of axial loading studies. The resulting behavior utilizing method (1) for axial loadings is as shown in Figure 4.62 for the connection with axial restraints and Figure 4.63 for axial release behaviors on the connection. Meanwhile, behavior models utilizing method (2) are being shown in Figure 4.64. Axial restraints behavior utilizing either method displays minor differences after study is conducted.

Early stiffness for Method 1 axial restraints remain consistent across the axial levels, with only 10% level axial restraints having a higher stiffness. Meanwhile, connection yielding behaviors differ after the 250°C mark for axial restraints of 2.5% and 5%. The connection has also increased in capacity. Between 0 - 5% of the axial restraint levels, the effect is only felt under in the later stages of deformation. In simplification, moment loads are assumed to be distributed with a lever arm, therefore resulting in a compression and tension areas. Axial restraints increase the effect of compression and reduce the effect of the tension forces, which is more prominent under high loads or degradation of materials under elevated temperature conditions.

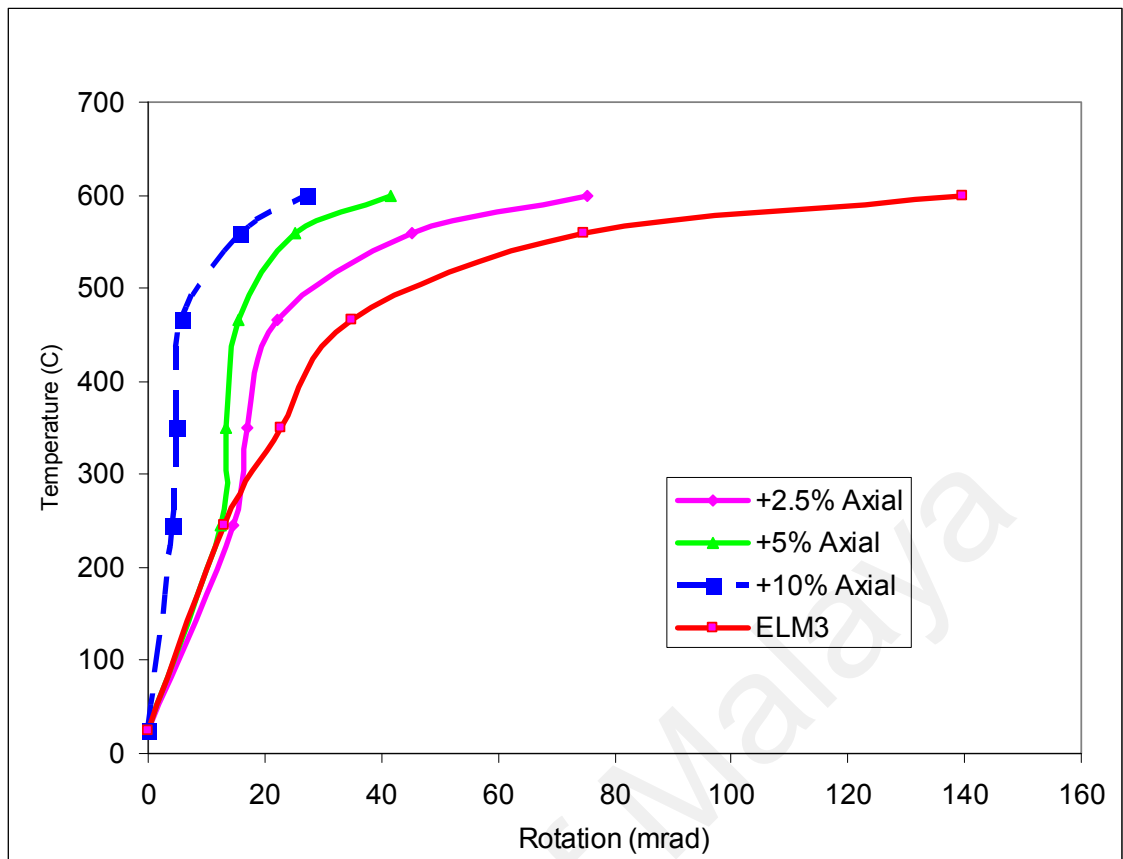


Figure 4.62 Effect of axial restraints on the connection with Method 1

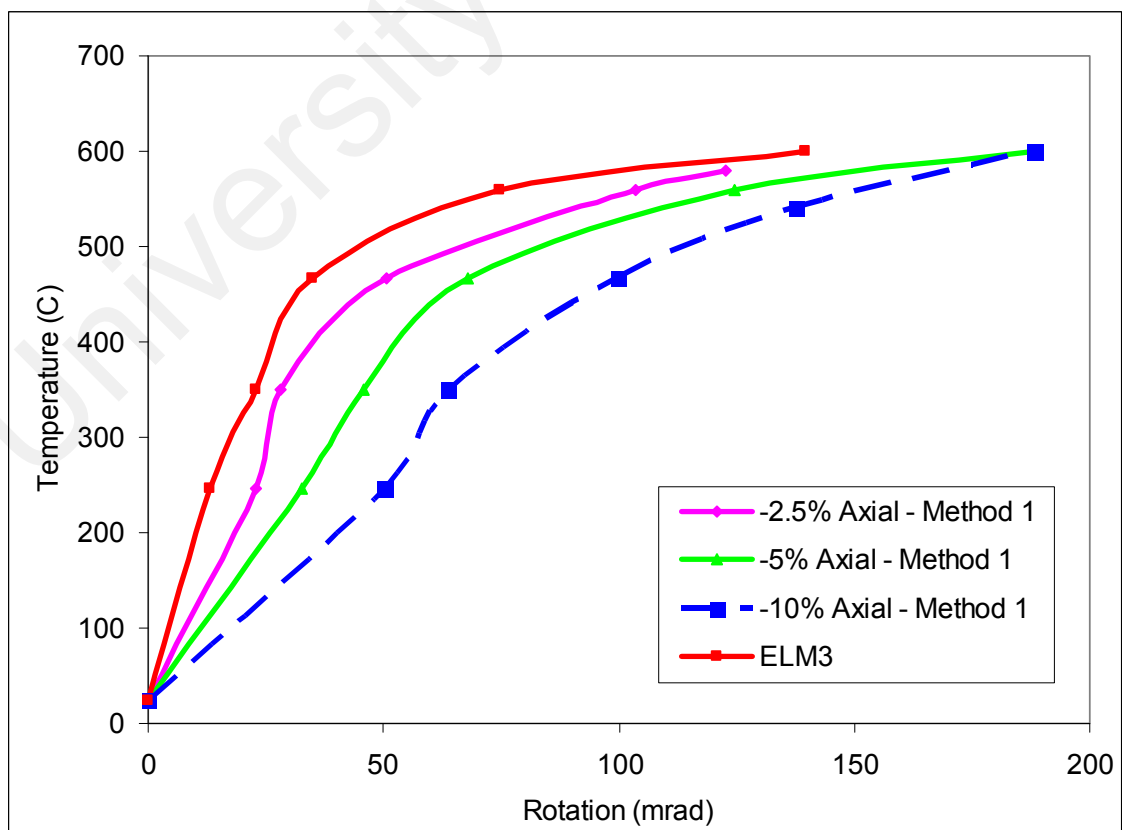


Figure 4.63 Effect of axial release on the connection with Method 1

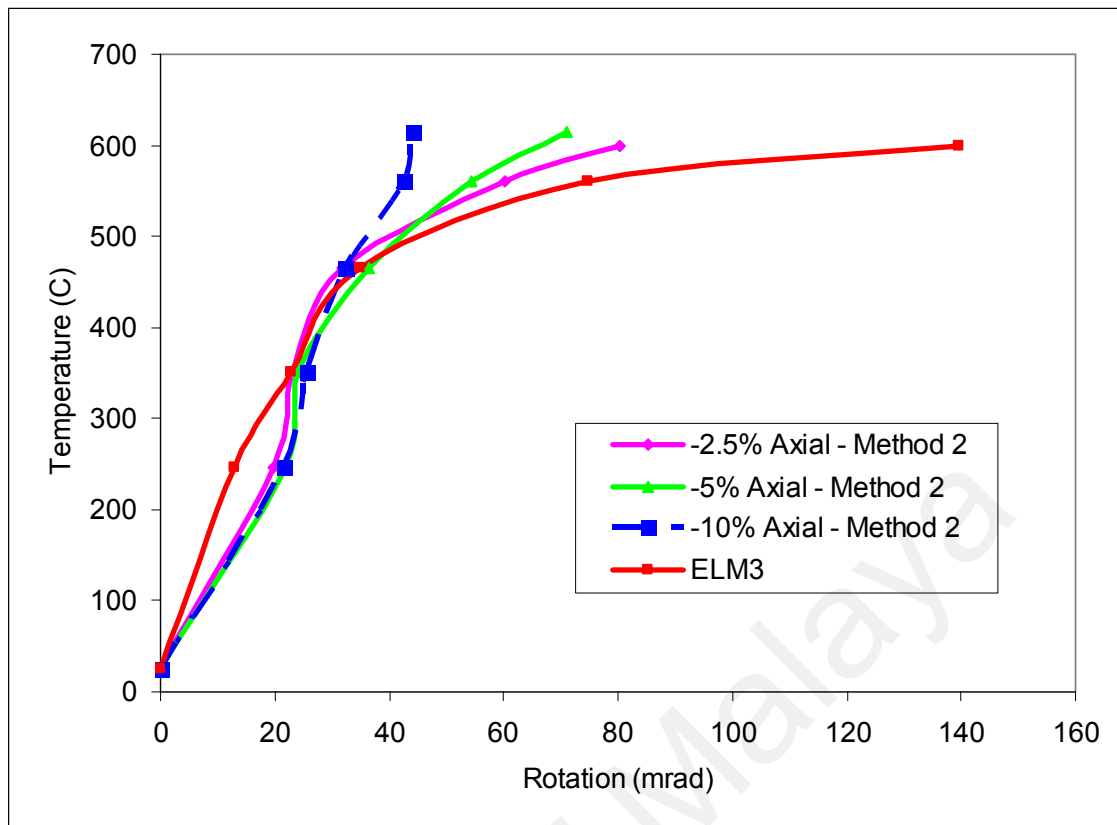


Figure 4.64 Effect of axial release on the connection with Method 2

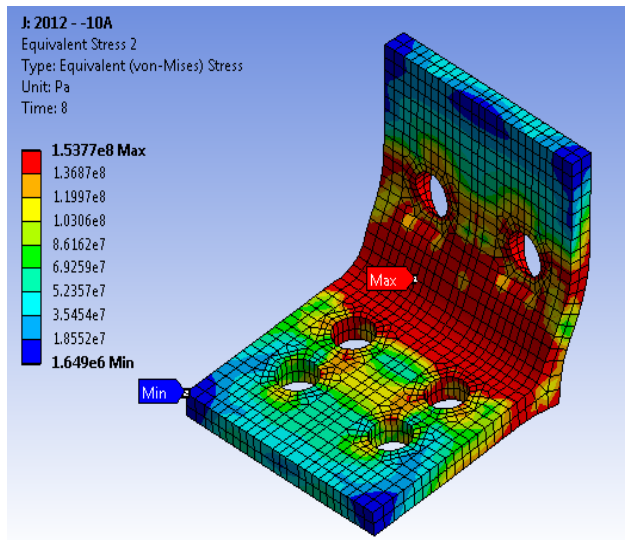
Axial release on the other hand, increases the effect of the tensional loads which is the major forces that cause the deformation of the top-seat angle connections. Axial release also reduces the compression levels distributed by the lever arm from the moment loads. The resulting behavior is an increased flexibility and reduced connection moment capacity. While Method 1 of axial release decreases the connection stiffness and reduces the moment capacity, Method 2 shows a different behavior response.

While the axial release of Method 2 decreases stiffness of the connection at lower temperatures, the elasto-plastic region remains unchanged while in the plastic region, the connection response is less flexible and the connection rotation have only minor changes at 10% axial release level.

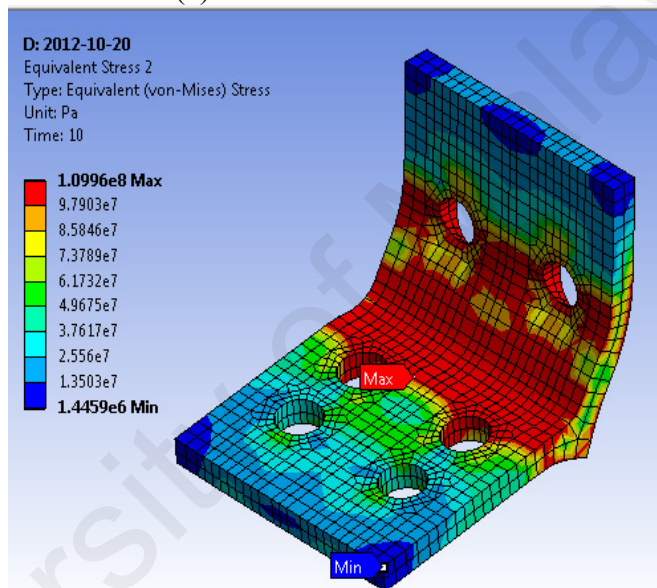
With Method 1, the axial loadings constantly act on the cross-section of the beam area as it deforms while Method 2 only act in the horizontal axis. The response results in the Method 1 being considered as the axial loading, utilizing the whole interaction of the connection to resist the moment loads while Method 2 shifts the loading resistance of the connection, from the connection to relying entirely on the shear of the bolts, therefore increasing the capacity.

In comparison between axial restraints and release, stress concentration for the top angle, as shown in Figure 4.65, is less for the axial restraints while relatively similar to the connection without axial loadings for the model with axial restraints. Stress concentration for the seat angle is as shown in Figure 4.66 and as assumed, axial releases results in additional stresses on both the top and seat angles while the behavior of a connection under axial restraints are governed by bolts as evident by the stresses caused by the bolts on the angle sections.

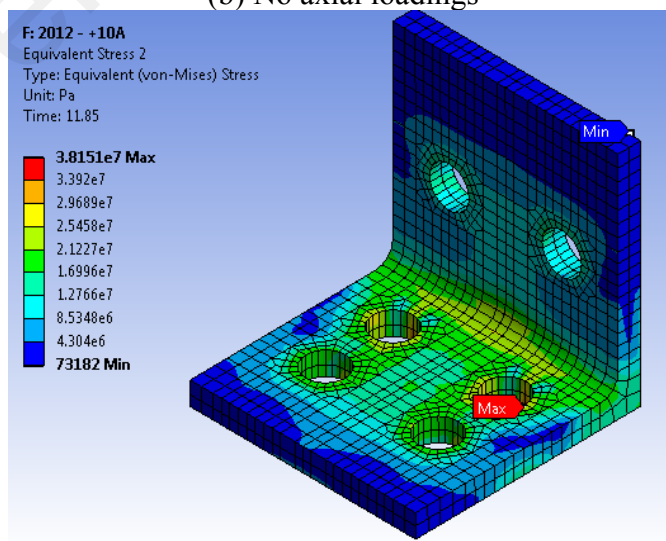
A noticeable difference in behaviors for the methods used for axial release is the deformation in the angles. Fixed axis direction or Method 2 axial loading at 10% level have resulted in the angles being pulled in a single direction as seen in Figure 4.67. The resulting behavior is that the components of the connection do not interact in accordance with the connection under zero axial loadings. At minor axial releases, at the lowest level studied of 2.5%, this behavior is still major as highlighted by the moment-rotation behavior shown. Evidently, this case is not beneficial to the design of the connections although the difference of stiffness is relatively not large.



(a) At 10% Axial Release

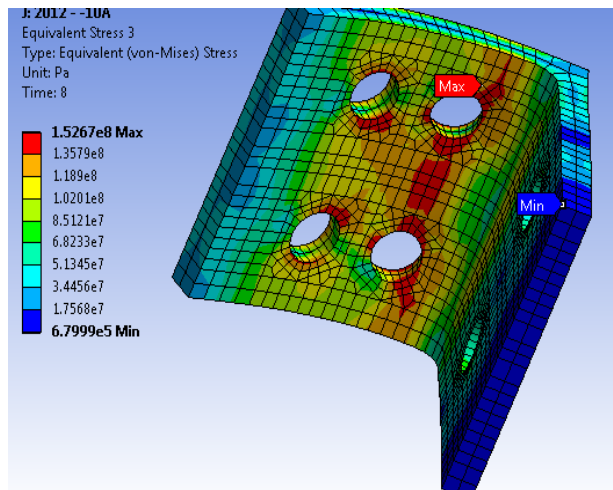


(b) No axial loadings

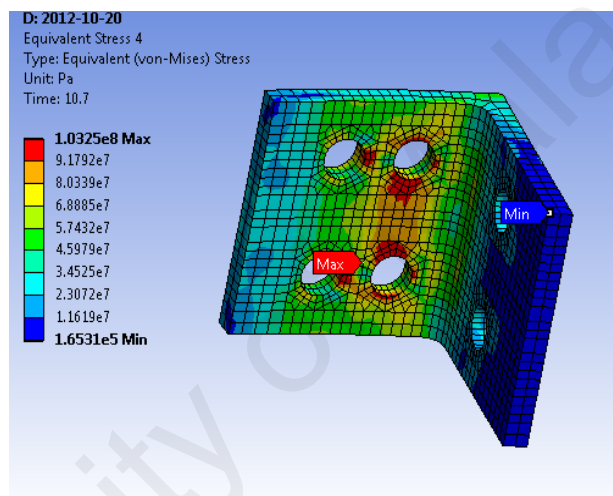


(c) At 10% Axial Restraint

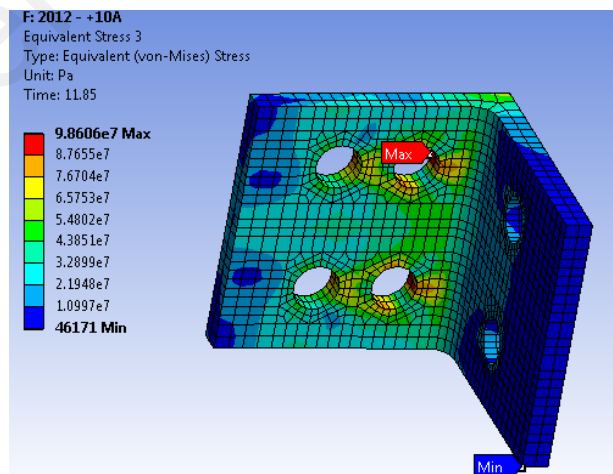
Figure 4.65 Top Angle stress concentration of model ELM3 due to effect of axial loadings



(a) At 10% Axial Release



(b) No axial loadings



(c) At 10% Axial Restraint

Figure 4.66 Bottom Angle stress concentration of model ELM3 due to effect of axial loadings

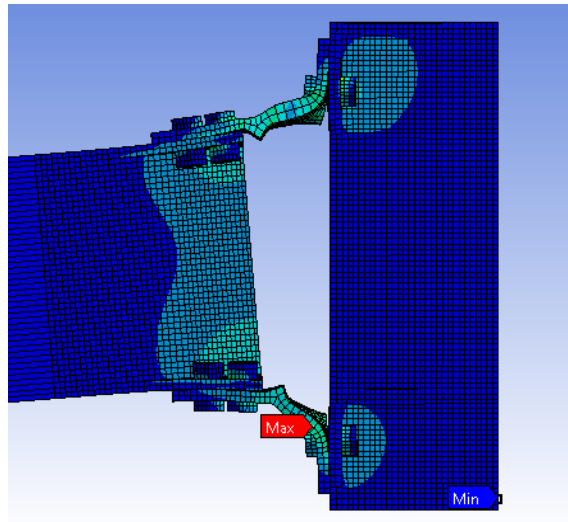


Figure 4.67 Deformations of Angles at 10% Axial Release Method 2

#### 4.4.2.2 Isothermal Temperature Condition

In comparison to anisothermal condition, isothermal conditions focus on the moment rotation response of the connection under different temperatures. Studying on the effect of axial loadings under different temperatures would result in the understanding on the different patterns of deformation and if any differences between the temperatures exist.

As shown in the earlier section on the effect of axial restraints on connections under anisothermal conditions, the comparison with ambient temperatures response shows that the effect of axial restraints are different in the terms of stiffness and moment capacity effect. This therefore warrants a study of the effect of axial restraints towards the connection response under isothermal conditions.

With the vast range in possible study temperatures, temperatures of 20°C, 400°C and 600°C has been selected as the common temperatures. The ambient temperature of 20°C is selected due to the fact that the difference in behavior with anisothermal and the different material models with the models used in the effect of axial restraints on ambient temperature models. Having results in the ambient temperature with the isothermal models would ease the comparisons in connection response. With that, model ELM3 is used as the basis, where the concepts and procedural in isothermal analysis has been described in earlier sections of this chapter.

In this study, the effect of axial release has not been studied with the justifications that there is no cooling effect with isothermal conditions. Isothermal conditions are considered to controlled environments and therefore the temperatures are to be maintained accordingly. Comparatively, in anisothermal or fire conditions is not controlled and most of the members would be engulfed in the fire, but otherwise localized in isothermal conditions. With this, therefore, only axial restrain effect exists while axial release conditions do not. Subsequently, the levels of axial restraints follow of that which has been applied in anisothermal model analysis for axial restraints.

For the individual temperatures at 2.5%, 5% and 10% axial restraints, the behavior of the models are as shown in Figures 4.68 to Figure 4.70. The effect of the axial restraints on the connection stiffness in isothermal conditions is not evident for axial restraints at 2.5%, but at 5% and 10% axial restraint levels, the stiffness increases. On the other hand, moment capacity of the connection increases throughout the axial restraint levels.

Meanwhile, a comparison is being made on the response of the connections under 10% axial restraints levels under various temperatures which is as given in Figure 4.71, while the plastic deformation regions of the connection at 10% axial restraint is as given in Figure 4.72.

At lower temperatures, plastic deformation forms near the top angle section heel area at the column leg and beam leg, while at high temperatures, plastic deformation patterns is more evident at the beam leg in comparison to the column leg. Due to the lower properties at higher temperatures, plastic deformation occurs earlier and before the second plastic deformation can occur on the column leg, and the deformation of the connection has reached the limit.

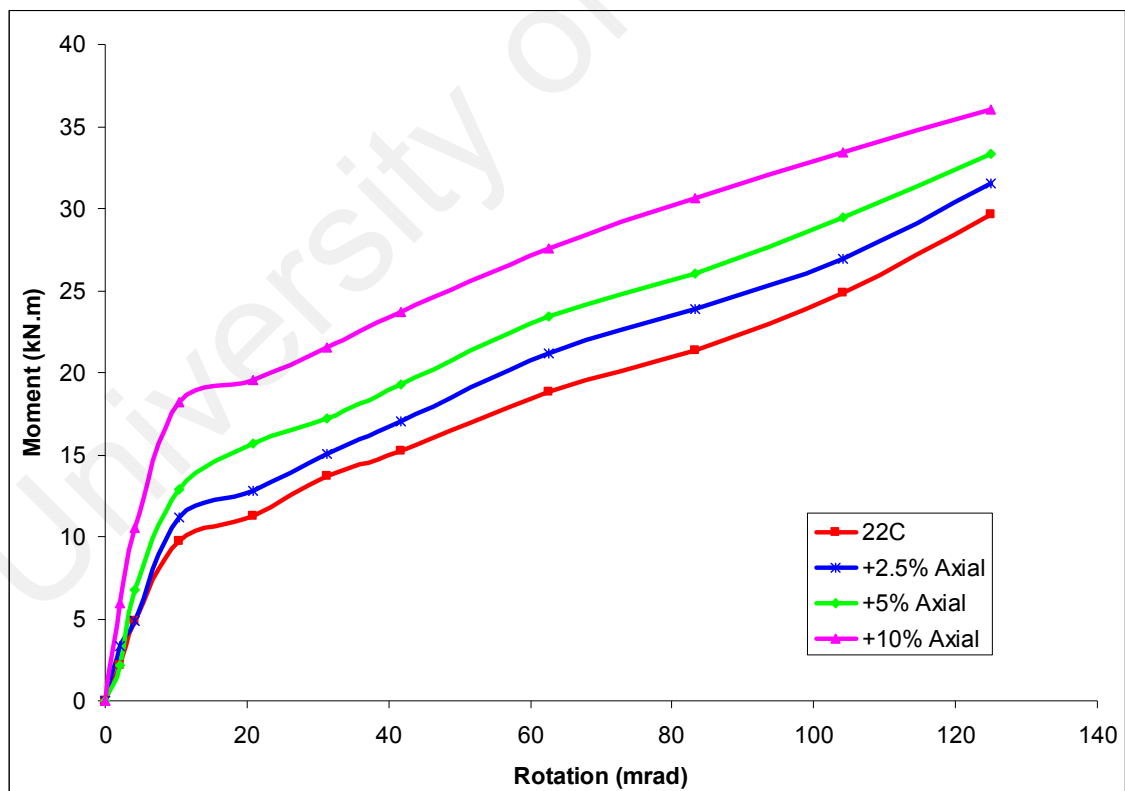


Figure 4.68 Effect of axial restraints on Isothermal Model at 22°C

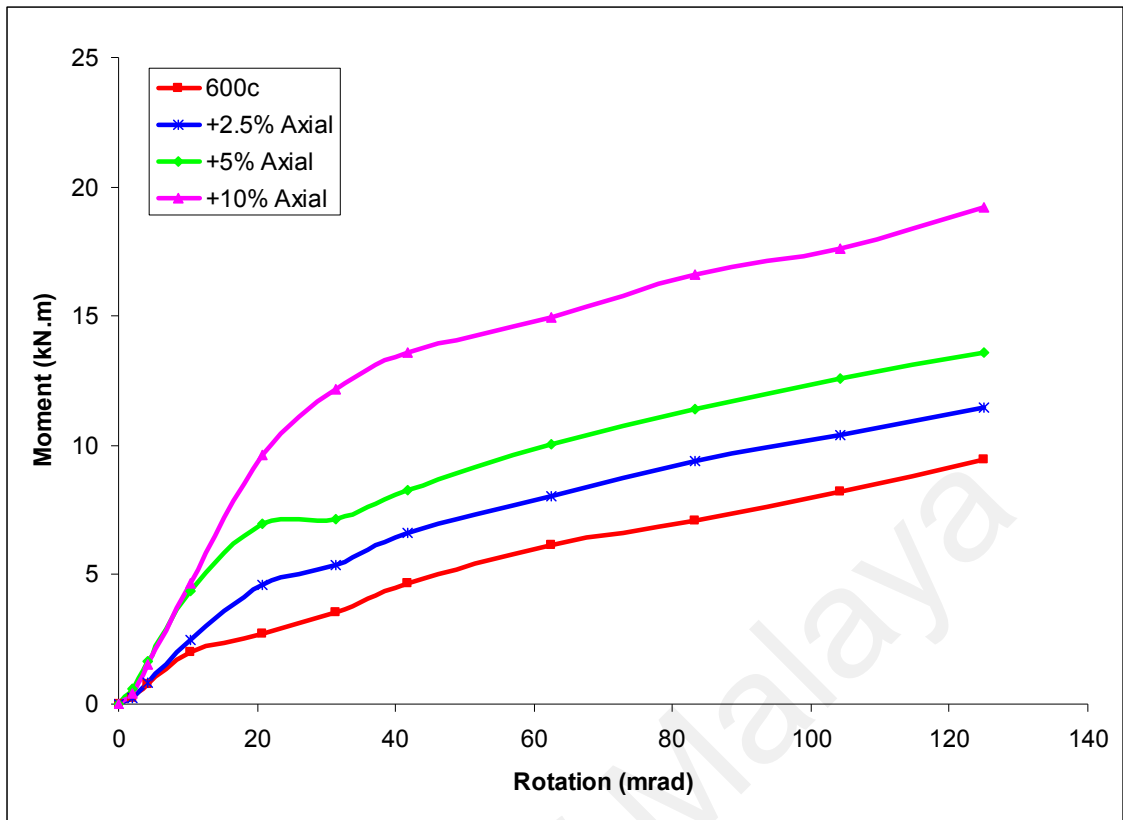


Figure 4.69 Effect of axial restraints on Isothermal Model at 600°C

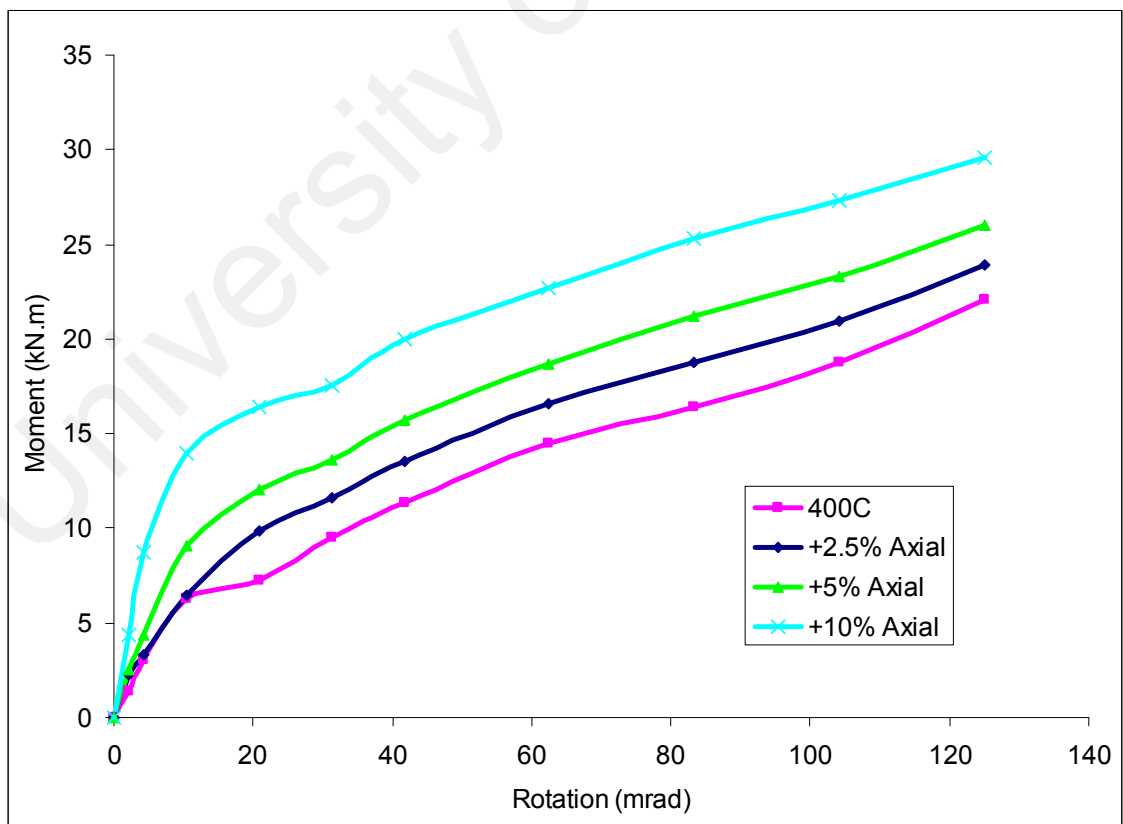


Figure 4.70 Effect of axial restraints on Isothermal Model at 400°C

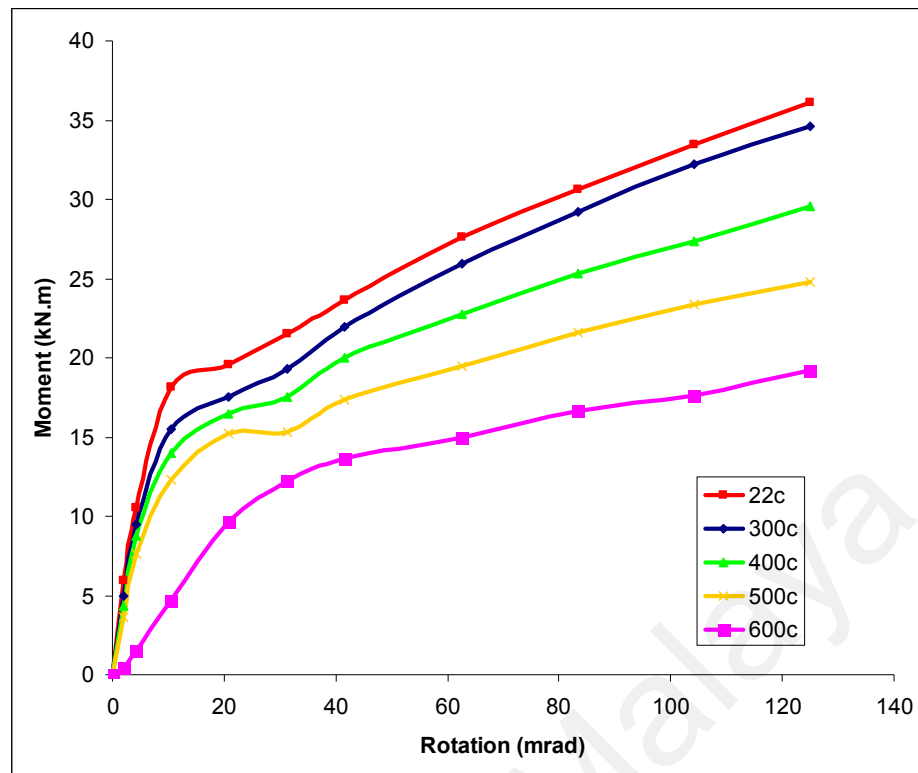
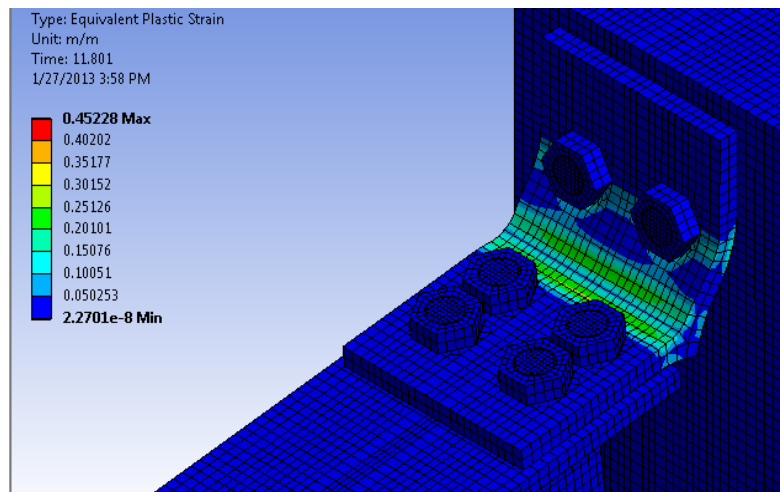


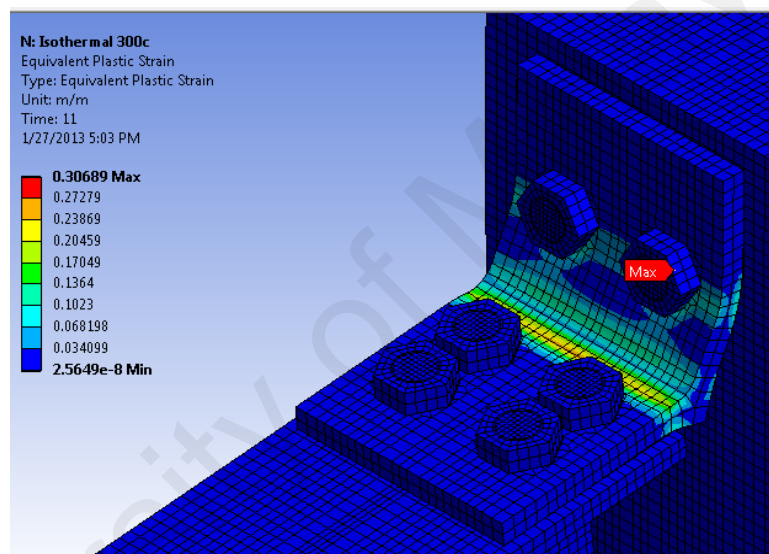
Figure 4.71 Behavior of Isothermal Models at 10% Axial Restraints

#### 4.4.3 Effect of Pretension Loads

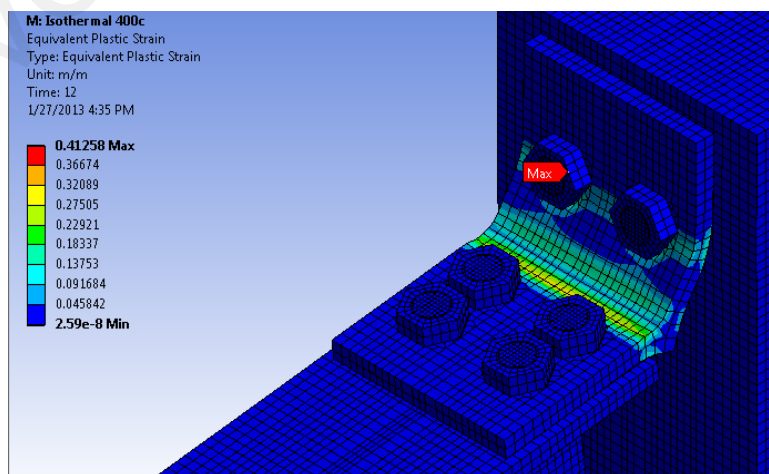
In structural steel joint terms, pretension loads are internally generated loads in bolts or members which are caused by the compression action from the tightening of bolts of a connection. The effect of pretension on connection behavior has been discussed in various literatures, such as studies conducted by Saedi and Yahyai (2009a). However, the effect of pretension has not been studied for bolted joints in elevated temperature conditions especially top-seat angle connections. It is common for the values of the pretension to be not reported and thus, often, the effect of pretension must be studied to determine the best suitable values that best fit the connection response.



(a) At 22°C with 10% Axial Restraint

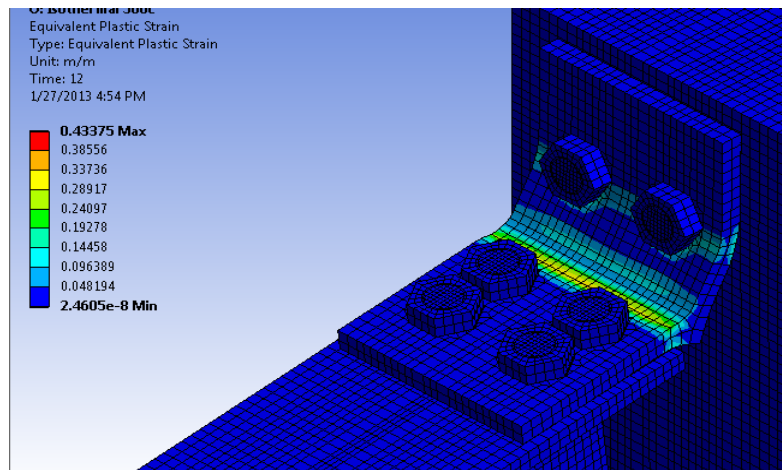


(b) At 300°C with 10% Axial Restraint

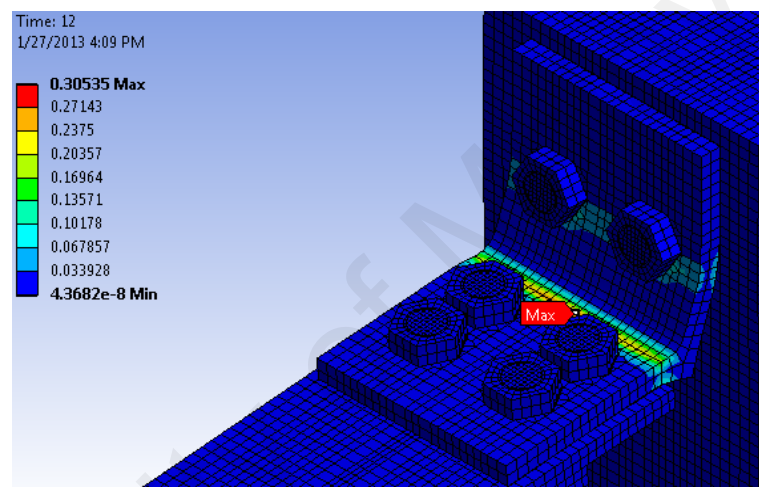


(c) At 400°C with 10% Axial Restraint

Figure 4.72 Plastic Regions for isothermal models at 10% Axial Restraints (Continued)



(d) At 500°C with 10% Axial Restraint



(e) At 600°C with 10% Axial Restraint

Figure 4.72 Plastic Regions for isothermal models at 10% Axial Restraints (Continued)

The parametric study on the effect is conducted in both elevated temperatures and ambient temperature conditions and models AMS1 and ELM3 are used as the comparison basis. Pretension loads studied are at a percentage increase levels from the finalized and validated values. The comparison response of the connection is as shown in Figure 4.73 for elevated temperature conditions and Figure 4.74 in ambient temperature conditions.

Results of the analysis show that the connection behavior changes accordingly to the value of pretension loads applied. In elevated temperature conditions, the stiffness of the connection reduces with the reduction of pretension values, while the end-behavior does not change whether the pretension loads have been increased or decreased. Meanwhile, under ambient temperature conditions, both connection stiffness and moment capacity change accordingly, however the changes are relatively minor.

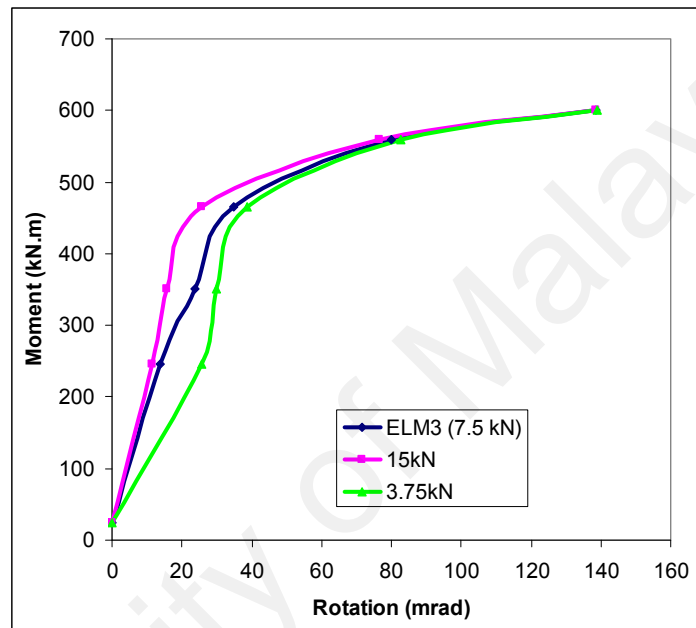


Figure 4.73 Effect of Pretension on Anisothermal Model ELM3

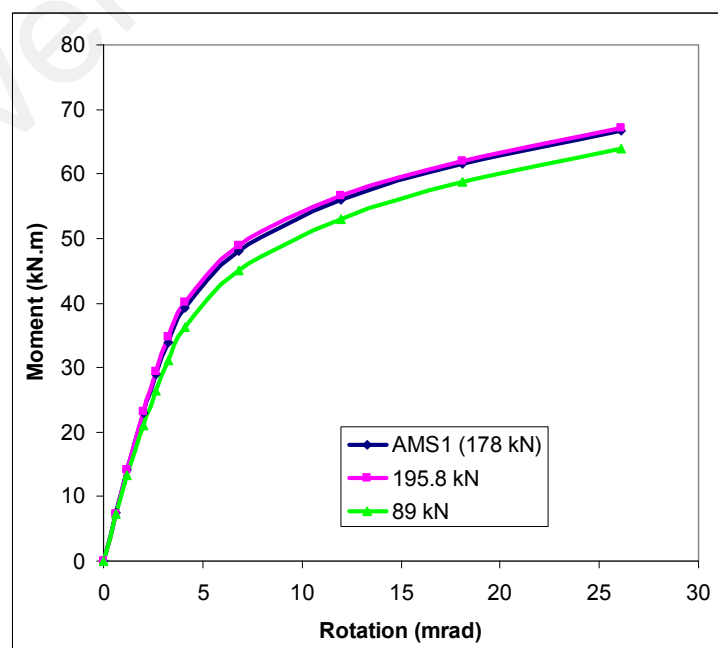


Figure 4.74 Effect of Pretension on Ambient Temperature Models

## 4.5 Design Implications

For designs of connections, the Eurocode 3 (2005): Part 1-8 provided guidelines on the analysis of connections using the component method basis. The component method which was examined in the literature review chapter focuses on arranging the component in series so that the related possible failure modes or deformation pattern for each component to be aligned with the supporting lever arm distance to the connection rotational point. Each component related to the connection must be checked for each individual local component parameters involving the design resistance, rotation capacity and stiffness coefficients. Determining the values of these parameters would result in the determination of the moment-rotation response of the connection. Besides that, the stiffness of the flange cleat connection is to be taken from the combination of the components:-

- Column Web in Transverse Compression,  $k_2$
- Column Web in Transverse Tension,  $k_3$
- Column Flange in Bending,  $k_4$
- Flange Cleat in Bending,  $k_6$
- Bolts in Tension,  $k_{10}$
- Bolts in Shear,  $k_{11}$
- Bolts in Bearing,  $k_{12}$

From the modeling and analysis conducted in this study, some comparisons are made between the results of this study with the guidelines provided by Eurocode 3, including on the seat angle effect, axial loading effect, angle length effect and the elevated temperature design of the connection.

#### 4.5.1 Seat Angle Design Effect

In EC3: Part 1-8, the major type of connection specified are end-plate connections, welded connections, column base plates and the flange cleat connections, and for each of these connection types, the design moment resistance is determined according to (Figure 6.15) of the code. With reference to (Figure 6.15 (b)) of EC3: Part 1-8 for the moment resistance of flange cleat angles, the lever arm is provided to be the distance between the centre of the top-tensional bolt to the mid-thickness of the bottom angle beam leg, as shown in Figure 4.75, with the total design resistance  $F_{Rd}$  multiplied by the lever arm to result in the resistance of moment loads.

One angle is assumed to be the rotational pivot of the connection and therefore, the angle section furthest from the pivot resists the tensional loads while the other on the compression loads distributed from the moment loads. This concept therefore results in the bolts of the bottom angle at the beam leg to resist shear forces while the seat angle contributing only the bearing resistance and the force transfer to the column. Assumingly, the shear forces at the seat angle would be significant and using smaller size bolts would lead to the bottom angle shear capacity being the critical component of the connection.

However, studies conducted on the variation of seat angle geometrics and parameters have shown that the seat angle has significant contribution on the behavior of the connection and that the distribution of moment loads is different than previously assumed. The basic concept outlined by Pirmoz (2009a) clearly illustrates the concept where the seat angle provides contribution to the connection response.

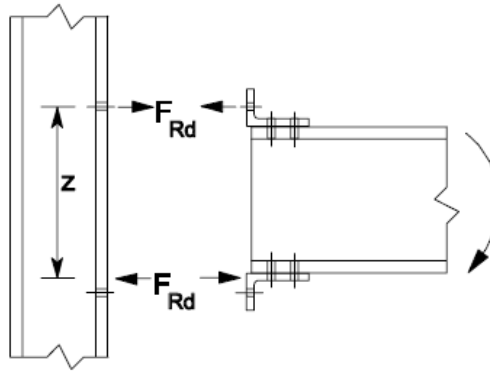


Figure 4.75 Moment load distribution to EC3: Part 1-8 for flange cleat connections.

A number of parameters have been explored in this study in attempt to highlight this issue, being: - the effect of reduced bottom bolt rows, effect of seat angle thickness and the effect of bottom angle gauge lengths. Detailed explanations are as outlined below:

i) Reduced Bolt Rows

Studies on the reduction of bolt rows at the bottom angle beam leg have shown that the bolts have little effect on the response of the connection. The minor difference in behavior is caused by the reduced clamping capacity on the beam leg of the bottom angle section, decreasing connection deformation resistance capacity. Results from the study have shown that the reduced shear capacity do not affect the response of the connection and thus eliminating the fact that the moment loads are distributed as shear forces on the bottom angle bolts on the beam leg.

ii) Increased Bottom Angle Thickness

In terms of bottom angle thickness, an increase in angle thickness increases the section bending capacity. According to the concept outlined in EC3: Part 1-8 or from common logical distribution methods, increasing the bottom angle thickness would have only shown that the bearing capacity of the angle is acceptable in resisting the forces caused. However the results of analysis in this case show that the increased bending capacity has provided increased moment capacity towards the connection response.

iii) Bolt Gage Length

Study shows that a decrease in bottom angle gage length reduces the moment capacity response of the connection while an increase in the gage length raises the moment capacity. While for the top angle, EC3: Part 1-8 provides the guidelines on obtaining the  $e_{\min}$  and  $m$  value which is determined by the gage length of the top bolts, there are no guidelines providing the determination of the values or its significance in the code which thus results in assumption that the location of the lever arm,  $z$  is possibly at the bottom angle column leg bolts center, therefore, corresponds to the changes in moment capacity. However, the change is considerably minor due to the limited distance.

This shows that the effect of seat angle and its relevant parameters are rather significant and considerations of the seat angle to the design of top-seat angle connection would expected to increase the accuracy of the design. Not only that, greater understanding of the behavior of the connection assists in providing reinforcements to resist greater loads.

#### 4.5.2 Axial Loading Design Effect

For design of bending moment capacity of the joint, EC3: Part 1-8 specifies that the moment resistance calculations are only valid if the axial loadings do not exceed 5% of the beam cross-sectional capacity. Cross sectional capacity varies due to beam sectional area and the specified material yields. In terms of elevated temperature condition designs, neither EC3: Part 1-2 nor EC3: Part 1-8 provides detailed design guidelines especially for this area.

Although a 5% limit is mentioned, it does not specify if the axial loadings should be positive axial as restraints or negative axial for axial release as described earlier. Studies have been done on the effect of axial loadings in both ambient and elevated temperatures with different axial loading levels. In terms of axial restraints under ambient temperatures, 10% level of axial restraints double the rotational stiffness and moment capacity of the connection. Axial release on the other hand, reduces the moment capacity of the connection.

At ambient temperature conditions, 10% of axial restraints causes the moment capacity to increase by 89%, 38% increase of moment capacity at 5% axial restraints and 11% under 2.5% axial restraints. On the other hand, the reduction patterns are similar for the response of the connection under axial release conditions, being 89% reduction under 10% axial release level and 22% moment capacity reduction for 2.5% of axial release level. It is clear that the axial release is a critical design component as a low level axial release is capable of reducing the moment capacity, even at axial loadings below the set limitations.

Meanwhile for elevated temperature conditions, there are two possible study situations, with anisothermal setting with axial loadings and isothermal setting with axial loadings. Under the anisothermal settings, the 5% axial restraint limitations have minimal effect over the response of the connection. This is due to the fact that moment loads applied on the connection have the same values across the temperature variation. On closer examination, the introduction of axial restraints in the analysis did alter the response pattern, however the resistive temperatures remains unchanged at approximately 460°C~480°C across the axial restraint levels.

On the other hand, with the axial release Method 1, there is an approximately 8% reduction in resistive temperature as a result of the 2.5% level axial release. Meanwhile, having 5% and 10% of axial release being applied on the connection, would result in 12% and 28% reduction in resistive temperatures respectively. Method 2 of axial release results is comparatively similar and considerably negligible difference in resistive temperatures due to the undefined deformation response of the connection. Due to the fact that the loadings remain constant through the anisothermal analysis, the effect of axial restraints under anisothermal conditions is difficult to measure through moment capacity of the connection.

In terms of isothermal behavior, axial restraint effects have caused the moment capacity of the connection at ambient temperatures using the Eurocode 3 material models to increase by 40% under 5% while 60% increase at 10% axial restraints respectively. Meanwhile at temperatures of 600°C, the moment capacity doubles and triples the value at 5% and 10% axial restraints respectively.

Other than at 2.5%, the stiffness has been increased with the increment of axial restraint levels. The higher effect of the axial restraints at 600°C has been caused by the amplified effects due to the decrease in material properties without the proportionate decrease in axial restraint levels.

In comparison to the guidelines provided by EC3, for end-plate connections, there is a possibility of beam member failure due to high axial restraints. At higher axial loadings, the conservative ratios, in which the total to be less than 1.0, of the resistance moment of the connection and applied moments with the axial resistance of the member with and the applied axial loads onto the connection / beam, coupled with the centenary action of the beam, as studied by Wang et al. (2011).

This is considering that the end plate serves as the load transfer component to the columns and also as the boundary condition for the beam. The resulting condition is that the beam member under axial loadings may result in buckling or local crushing failure. Possible failures in a top-seat angle connection under axial loadings only include the bolt shear, bearing failures and the angle bearing failure.

In the study of end-plate connections under elevated temperatures, the effect of axial restraints has an opposite effect, lowering the connection moment capacity as shown in the studies by the Li et al. (2012) and also in the studies by Qian et al. (2008). This therefore shows that the guidelines provided by EC3: Part 1-8 has basis in end-plate connections, however, these studies have shown that at less than 5% of axial restraint levels, the moment capacity still differ from the response when no axial restraints are applied. With the additional loads and the boundary conditions, failure of the beams contributed to the lower response of the connection.

Conclusively, the axial loadings guidelines are insufficient for designs of top-seat angles. In comparison to end-plate connections, the top-seat angle connections benefit from the axial loadings due to the reduction of effects from the moment loads and at the same time, the beams do not experience similar failures as such in end-plate connections, such as shown in the study by Qian et al. (2008) where out of plane deformations occur in the beam. The 5% limitations have been shown to be conservative while under axial restraint conditions. With axial release conditions, the limitation have only overestimated the connection capacity and therefore further definitions on the axial loading limitations needs to be made.

#### **4.5.3 Angle Length Design Effect**

Eurocode 3 (2005): Part 1-8 specifies that the bending of angle and tension capacity of bolts for the top angle to be computed using the T-stub method similar to the concept used for end-plate connections. With this concept, the effective length used in the calculation,  $l_{\text{eff}}$  is to be taken as 0.5 of the angle section length used regardless of bolt positions on the column leg. Three modes of failures are specified for the T-stub, which is shown in Table 4.18, and similar to Table 6.2 in the code. Other parameters involved are determined from Figure 4.75.

From the guidelines provided, with the change in angle length, the values of  $l_{eff}$  changes linearly and therefore in a linear change of the resistance capacity. From the results graph of Figure 4.51 (Section 4.3.3), it is evident that the increase in the angle length increases the moment capacity with minor effect on the stiffness of the connection, which also similar effect for the reduction in length where reduced length would result in the reduction of moment capacity and relatively minor effect on the connection stiffness.

An increase in 10% of the length would expectedly result in 10% increase in the moment capacity of the connection and the similar expected behavior for 50% change in the angle section length. As summarized in Table 4.19, the approximate values of the moment capacities of the connections with different angle section length used is shown. However, the analysis results have shown that the 10% increase in angle length only results in 8% moment capacity change, while 10% decrease results in 12.5% in moment capacity reduction. On the other hand, at the highest change studied, at 50% in length, changes are approximately 29.2%, which is less than the expected 50% increase.

Table 4.18 T-Stub Failure Mode Computation for Angle Connections

Mode 1	$F_{T,1,Rd} = \frac{\sum l_{eff} \cdot t_f^2 \cdot f_y}{m}$
Mode 2	$F_{T,2,Rd} = \frac{(0.5 \cdot \sum l_{eff} \cdot t_f^2 \cdot f_y) + (n \cdot \sum F_{t,Rd})}{m + n}$
Mode 3	$F_{T,3,Rd} = \sum F_{t,Rd}$
$F_{t,Rd}$	– Design Tension Resistance of Bolt
$l_{eff}$	– 0.5 of Angle Section Length
$n$	– $e_{min}$ (Refer Figure 4.76 ), < 1.25m
$m$	– Refer Figure 4.76

Table 4.19 Moment capacity of Joints with different angle lengths

Model Mark	Percentage Length Difference	Angle Length (mm)	Moment Capacity (kN.m)	Percentage Change
AMS1	-	203.2	48	-
ALGTH50	+50%	304.8	62	+29.2%
ALGTH25	+25%	254.0	55	+14.6%
ALGTH10	+10%	223.52	52	+8.3%
ALGTH10R	-10%	182.88	42	-12.5%

This therefore has shown that the parameter assuming  $l_{eff}$  can be taken as 0.5 of the angle length utilized requires further study. It is considered to be conservative to be taking the length of angle as 0.5 of the length. Other parameters may also be considered such as the bolt-bolt gauge length at the column leg of the angle section.

#### 4.5.4 Gap Design Effect

From the results of the study on the effect of gap, which is the distance between the column flange and the starting edge of the beam, on connection behavior, gap distance values have been shown to affect the response of the connection. An increase in gap distance lowers the moment capacity of the connection while the decreasing the gap distance has an opposite effect. This does not apply to the point where the gap is close enough that the bottom edge of the beam is liable to be in contact with the column flange after deformation occurs.

In the study, an angle section of 9.53mm thickness was used. Variation of the gap distances are valued at 6.35mm, 12.7mm and 38.1mm corresponding to 0.25in, 0.5in and 1.5in. With the same displacement loads and other similar parameters and properties of materials, the effect of the gap has been studied. From figure 4.76(b) as provided in the guidelines, the gap distances is more than 0.4 of the angle thickness; therefore, the value of  $m$  parameter is still similar. With reference to Table 4.18 in the previous section, resistance force,  $F_{T,Rd}$  can be assumed to be similar due to the same  $m$  value encountered.

With the resulting increase in moment capacity of the connection, the value of  $F_{T,Rd}$  is higher to obtain the level of moment capacity, therefore, due to the fact that the values of the other parameters do not change, the value of  $m$  would have to be lower. This therefore shows that the condition for the gap values would have to be further revised with better understanding on the values for more accurate connection designs.

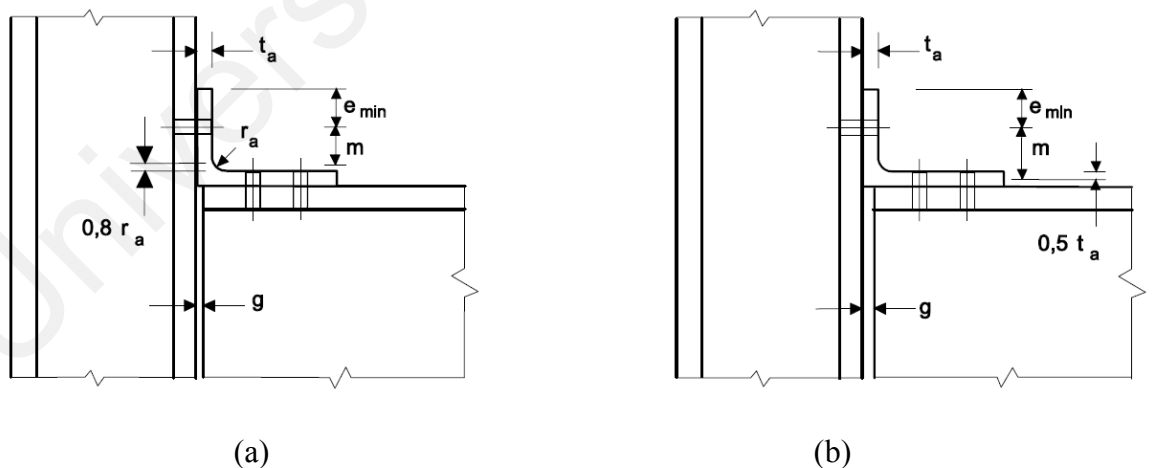


Figure 4.76 Determination of parameters  $e_{min}$  and  $m$   
(a)  $Gap \leq 0.4t_a$  (b)  $Gap > 0.4t_a$

#### 4.5.5 Implications on Design Summary

From the detailed explanation of the previous sections, it is clear that the guidelines provided by EC3 is insufficient to cater for the design of the top and seat angle connections for both ambient and elevated temperature conditions. Implications of the model towards the design guidelines of Eurocode 3: Part 1-8 (2005) is as shown in Table 4.19 below. Undoubtedly, further studies are necessary to validate the implications and effect on the design guidelines.

Table 4.19 Implications of the model results to EC3

<b>Aspect</b>	<b>Implications</b>
Bottom Angle Effect	<ul style="list-style-type: none"><li>• Bottom angle bending governs the connection behavior. The concept of lever arm <math>z</math> must be reconsidered for top-seat angle connection as the effect is not major. Thickness of the bottom angle section is among main contributor to the capacity of the connection.</li><li>• Bolt shear does not affect the behavior of the connection, thus, increasing the number of bolts at the seat angle does not change the behavior as in previously assumed design method.</li></ul>

<p>Axial Loading Design Effect</p>	<ul style="list-style-type: none"> <li>• Axial loadings are not specified in EC3 in terms of the release or restraint. For axial restraint, 5% is considered to be conservative while for release to be under-designed of the connection capacity.</li> <li>• In comparison to end plate connections, top-seat angle connections benefit from axial restraints as there are no boundary conditions which results in the beam buckling failure.</li> </ul>
<p>Angle Length Effect</p>	<p>EC3 provided guidelines has assumed that half length of the angle section to be considered as the effective length for design purposes. The models in study have confirmed that the value taken can be considered as conservative and suitable for design purposes.</p>
<p>Gap Distance Effect</p>	<p>Increase of gap would reduce the connection capacity but the value for the parameters has only been given a general guidelines. Therefore, it would be possible to have capacities lower than based on EC3 design guidelines capacity. In the study, values chosen for the gap is still larger than 0.4 of the angle thickness. The value of m should not change based on this. However as the model results show, the moment capacity maybe lower as seen with 38.1mm gap compared to 12.75mm with angle 9.5mm thick.</p>

#### 4.6 Concluding Remarks

In this chapter, the ambient temperature models are validated through a series of analysis using ANSYS Workbench. Due to the complexity of finite-element analysis, T-stub models in ambient temperature conditions are validated first followed by the actual simulation models. Results of the analysis have shown that the behavior of the model is agreeable with the behavior result of the test specimens. This therefore has shown that the combination of parameter assumptions utilized, such as the contact, convergence parameters and the material model type results in a model which closely reflects the actual conditions of the modeled state.

Subsequently the contribution of seat angles is studied by varying the geometrical properties of the seat angle. Seat angle thickness has been shown to provide the most influence over the behavior of top-seat angle connections. This not only provides an insight on the deformation sequence and pattern of the top-seat angle connection, but also revisions on the possible mechanism which contributes to the strength and stiffness of the connection.

On the other hand, a minor study on the effect of the gap highlights the bearing behavior of the beam which increases the capacity of the connection significantly. This behavior has not been considered in other studies prior. With the ambient temperature models validated, the elevated temperature models are then validated accordingly. The assumptions made during the validation of ambient temperature models are reapplied accordingly. Although this, the material models are different due to clear guidelines provided by Eurocode 3: Part 1-8(2005), which is followed accordingly but simplified to avoid inefficient increase in computational effort.

Another major difference in comparison with the ambient temperature models, which is logical, is the application of temperatures on the model. Temperature gradients across the components of the connections are ignored, again for simplification purposes. Temperature are not considered loadings such as with forces, moment loads or self-weight but temperatures in this study relate highly to conditions that changes the material strength instead of an external agent that acts as a direct physical force onto the connection.

With the experimental tests behavior comparison, the elevated temperature models are shown to be in a good agreement. As a result, the concept of load steps for elevated temperature analysis is a viable method in comparison to time based dynamic analysis. Not only that, the parameters and guidelines outlined by Eurocode 3: Part 1-2 (2005) (EC3) has been considered to be representative of steel materials. Subsequently, the validation of elevated temperature models provided for a platform for further studies on the behavior of top-seat angle connections in elevated temperatures including the behavior in isothermal conditions, effect of axial loadings for both positive and negative valued axial loadings and also on the design comparisons with EC3 provided guidelines.

## CHAPTER 5

### CONCLUSION AND RECOMMENDATIONS

#### 5.1 Conclusions

In this study, the top-seat angle connection was thoroughly studied in both ambient and elevated temperature conditions. Literature review has shown that the understanding of the top-seat angle is relatively low considering the fact that the number of studies on the subject matter is low comparatively to end-plate connection types. This however does not justify the fact that top-seat angle connections have significant benefits. In terms of construction, crane usage time is reduced and thus the cost reduced. In addition, as studies by Shen and Astaneh (1999) show, top-seat angle connections have higher cyclic energy dissipation in comparison to other connection types where higher cyclic energy dissipation are considered beneficial for earthquake resisting connections.

Based on the findings of this study, the following conclusion can be withdrawn:

(a) Models were produced and validated against the studies by Shen and Astaneh (1999) for T-stub models, and Azizinamini (1982), Kukreti and Abomaali (1999), including Komuro et al. (2003) for the full top-seat angle connections at ambient temperature models. For elevated temperature models, validations are done with the studies Liu (2002) for the beam models and full connection models validated with the experimental study by Saedi and Yahyai (2009a). In most cases the early stiffness behavior has minor differences in comparison to the experimental test results of 1-5%.

Meanwhile, end behavior comparison varies between 5-15% for the comparison between model and experimental test results. Connection response of the models show good agreement with the experimental results referred. From the validation of the models, it can be concluded that static structural analysis is sufficient for elevated temperature model analysis and there is a close relationship between the response of the connection in anisothermal conditions and isothermal conditions.

(b) With the validated models, the effect of axial restraints on the connection response is studied by applying 2.5%, 5% and 10% of the beam cross-sectional capacity as axial restraints. Besides anisothermal and isothermal conditions, the effects are also studied for ambient temperature condition models. Axial loadings are described with two possible modes, being the compression and tensional modes. Axial restraints refer to the compression mode while axial release refers to the tensional forces. In terms of axial restraints, the effect has been determined that higher axial restraints levels have beneficial effect over the behavior of connections, increasing stiffness and moment capacity. A 40% increase in moment capacity has been recorded for 5% axial restraints level while at 10% axial restraint level, a 60% increase in moment capacity was computed. As expected, the axial release levels directly affect the connection stiffness and moment capacity by reducing these values.

This is due to the amplification and reduction effect on the connection from the distribution moment forces on a connection, for compression or tensional loads. Axial restraint loadings reduce the tensional effects of the distribution from the moment loads as axial restraints are classified as compression forces, thus reducing deformation, while the axial release loadings increase the tensional effects while reducing the compression component of the load distribution which results in an increase of deformation, as axial release is essentially tension force in the connection.

(c) At ambient temperatures, the role of the seat angle cannot be ignored in the top-seat angle connection configuration. The earlier assumption is that the top-angle played the major role in the determination of the connection. However, the parametric variation of the seat angle geometrics has shown that the seat angle has major contribution to the connection response, affecting the moment capacity of the connection, especially when the thickness of the bottom angle is increased. The increase in moment capacity has been computed to be 4% with 60% thickness increase and with 200% increase in thickness; moment capacity is raised by 12%. At the same time, the effect of gauge length at the column leg, gaps and reduced bolt numbers has been studied for the seat angle effect.

(d) The studies have shown that the design of the connection, when based on logical deduction, have shown to be different in terms of design assumptions. Previous values and limitations set out by the code have been compared and the result is that further validations must be made on the design standards. Design implications that has been determined includes on the effect of seat angles, gaps, angle length and the axial loadings effect on connection response.

These design parameters or conditions have been found to be affecting design values and guidelines. In terms of axial restraint effects, low axial restraint levels of less than the 5% limitations set by EC3 guidelines have been shown to be conservative in axial restraint cases while for design in axial release cases to be too high, leading to higher moment capacity than the actual response. Gap values of the connection, where parameter  $m$  is affected, is shown to affect the connection, in terms that the guidelines provided by EC3 is insufficient in determining the moment capacity of the connection, although conservatively. However, parameters such as the angle section length used and the effect of the seat angle requires further verification studies for any further guidelines proposal.

## **5.2 Recommendations**

From the literature review of this study and also the results of the study put forth, it is recommended for further studies that more experimental tests of top-seat angle connection in elevated temperature to be done. This is due to the fact that, the benefits of the connection justifies the fact that more understanding is needed on this connection type. Validations of models are limited due to this, and no other comparison can be done. With other experimental tests conducted on the top-seat angle, further validation can be done and thus, increased accuracy for the design guidelines.

On the other hand, numerical and component method studies can also be done for the top-seat angle connection. While the finite-element model is the closest study to the experimental tests, however, the computational effort required is comparatively huge. This would be very much time consuming and only suitable for research purposes. For actual design applications, the more robust component method strengthened with numerical models for each of the component to be outlined has lower time consumption and less computational effort. No doubt that there have been numerous studies being conducted for this, however, the elevated temperature condition has received little attention, while that the risk of fire is comparatively critical.

University of Malaya

## REFERENCES

- Ali Ahmed, Norimitsu Kishi, Kenichi Matsuoka, Masato Komuro (2001) "Nonlinear Analysis on Prying of Top and Seat Angle Connections". *Journal of Applied Mechanics* (4): p. 227-236.
- Ang, K.M., and Morris, G.A. (1984) "Analysis of Three-Dimensional Frames with Flexible Beam-Column Connections", *Canadian Journal of Civil Eng*(11), p245-254
- Agerskov H. (1976) "High strength bolted connections subject to prying." *Journal of the Structural Division* (102): p.161–75.
- Al-Jabri, K. S. (1999). The Behaviour of steel and composite Beam-Column Connections in fire. *PhD thesis*, Department of Civil and Structural Engineering, University of Sheffield.
- Al-Jabri, K. S., Burgess, I. W., & Plank, R. J. (2004). Prediction of the degradation of connection Characteristics at elevated temperature. *Journal of Constructional Steel Research*, 60, 771-781.
- Al-Jabri, K. S. (2004). Component-based model of the behaviour of flexible end-plate connections at elevated temperatures. *Composite Structures*, 66(1-4), 215-221.
- Al-Jabri, K. S., Burgess, I. W., Lennon, T., & Plank R. J. (2005). Spring-stiffness model for flexible end-plate bare-steel joints in fire. *Journal of Constructional Steel Research*, 61, 1672–1691.
- A. Saedi Daryan, Mahmood Yahyai (2009a) "Behavior of bolted top-seat angle connections in fire". *Journal of Constructional Steel Research* (65): 531-541.
- A. Saedi Daryan, Mahmood Yahyai (2009b) "Modeling of Bolted Angle Connections in Fire". *Fire Safety Journal* (44): p. 976-988.
- Azizinamini A. (1982) "Monotonic Response of semi-rigid steel beam to column connections". *Master Thesis*. University of South Carolina: Columbia.
- Cabrero, J.M., Bayo, E. (2007) "Evaluation of the semi-rigid behaviour of three-dimensional extended end-plate steel joints in the framework of the component method". *6th International Conference on Steel and Aluminium Structures (ICSAS'07)*. Oxford.

- Cafer, Harun Uslu (2009) “3-D Finite Element Analysis of Semi-Rigid Steel Connections”. *Master Thesis*. Middle East Technical University: Turkey.
- Calado, L. , G. De Matteis, R.Landolfo (2000) “Experimental Response of top and seat angle semi-rigid steel frame connections”. *Materials and Structures* (33): p. 499-510.
- Chen, L. and Y.C. Wang (2012) “Efficient modelling of large deflection behaviour of restrained steel structures with realistic endplate beam/column connections in fire.” *Engineering Structures*(43): p. 194-209.
- Chen, W. F., & Lui, E. M. (1991). *Stability design of steel frames*. CRC Press.
- Dai, X.H., Y.C. Wang, C.G. Bailey (2010) “Numerical modelling of structural fire behaviour of restrained steel beam–column assemblies using typical joint types.” *Engineering Structures* (32): p. 2337-2351.
- Davison, J. B., Kirby, P. A., and Nethercot, D. A. (1987). "Rotational Stiffness Characteristics of Steel Beam-to-Column Connections." *Journal of Constructional Steel Research* (8): p. 17-54.
- Danesh, F; A. Pirmoz, A. Saedi Daryan (2007) “Effect of shear force on the initial stiffness of top and seat angle connections with double web angles”. *Journal of Constructional Steel Research* (63): p. 1208-1218.
- Del Savio, A.A., Nethercot, D.A., Vellasco, P.C.G.S., Andrade, S.A.L., Martha, L.F. (2009) “Generalised component-based model for beam-to-column connections including axial versus moment interaction”. *Journal of Constructional Steel Research* (65): p.1876-1895.
- Díaz, C., Victoria, M., Marti, P., Querin, O.M. (2011) “FE model of beam-to-column extended end-plate joints” *Journal of Constructional Steel Research*(67): p. 1578-1590.
- Eurocode 3 (2005) “Design of steel structures – Part 1-2: General Rules-Structural Fire Design”. British Standards Institution: United Kingdom.
- Eurocode 3 (2005) “Design of steel structures – Part 1-8: Design of Joints”. British Standards Institution: United Kingdom.

- Faella C, Piluso V, Rizzano V. (2000) "Structural steel semi-rigid connections: Theory, design and software". FL (US): CRC Press LLC.
- Federal Emergency Management Agency (FEMA 2002). World Trade Center building performance study. FEMA, USA
- Frye, M.J., and Morris, G.A. (1975), "Analysis of flexibly connected steel frames," Canadian J. Civil Eng., 2(3): 280-291.
- Galambos, T.V. (1988) "Guide to Stability Design Criteria for Metal Structures" 4th Edition, John Wiley & Sons:New York
- Heidarpour, Amin, and Mark A. Bradford (2008) "Behavior of T-stub assembly in steel beam-to-column connections at elevated temperatures". Engineering Structures (30): 2893-2899.
- Heidarpour, Amin, and Mark A. Bradford (2009) "Generic Nonlinear Modeling of restrained steel beams at elevated temperatures". Engineering Structures (31): 2787-2796.
- Hong, K., JG. Yang, SK. Lee (2002) "Moment-rotation behavior of double angle connections subjected to shear load". Engineering Structures (24): 125-132.
- Huang, Z., (2011) "A connection element for modelling end-plate connections in fire". Journal of Constructional Steel Research(67): p. 841-853.
- Izzudin, BA (1991) "Nonlinear Dynamic Analysis of Framed Structures" Imperial College of Science, Technology and Medicine: London.
- Jaramillo TJ. (1950) "Deflections and moments due to a concentrated load on a cantilever plate of infinite length" *Journal of Applied Mechanics* (17): p.67-72.
- Komuro, M., Kishi, N., and R.Hasan (2003). Quasi-static loading tests on moment rotation behavior of top- and seat-angle connections, *Proceedings of the Conference on Behaviour of Steel Structures in Seismic Areas*, Naples, Italy: p.329-334.

- Komuro, M; N.Kishi; W.F Chen (2004) "Elasto Plastic FE Analysis On Moment Rotation Relations of Top-Seat Angle Connections. *Proceedings of the Fifth International Workshop on Connections in Steel Structures: Behaviour, Strength and Design: Netherlands.*
- Kukreti, A.R., and Abolmaali, A., (1999) "Moment-Rotation Hysteresis Behavior of Top and Seat Angle Steel Frame Connections," *Journal of Structural Engineering, ASCE* (125): 810-820.
- Lee, C.H., Chiou Y.J., Chung, H.Y., Chen, C.J, (2011) "Numerical modeling of the fire-structure behavior of steel beam-to-column connections". *Journal of Constructional Steel Research*(67): p. 1386-1400.
- Lee Sang-Sup, Mun Tae-Sup (2002) "Moment-rotation model of semi-rigid connections with angles." *Engineering Structure* (24): 227-237.
- Lemonis, Minas E., Gantes, Charis J., (2009) "Mechanical Modeling of the Non-linear Response of beam-to-column joints". *JCSR* (65): 879-890.
- Leston-Jones, L. C., Burgess, I. W., Lennon, T, Plank R. J. (1997). Elevated-temperature moment-rotation tests on steelwork connections. *Proceedings of the Institution of Civil Engineers: Structures and Buildings* (122): p. 410-419.
- Li, G.Q., Chen, L.Z., Li, J.T., Lou, G.B. (2012) "Modeling of end-plate bolted composite connection in fire considering axial force effects". *Journal of Constructional Steel Research* (76): p. 133-143.
- Lima LRO, de Simoes da Silva L, Vellasco PCGS, de Andrade SA. (2004) "Experimental evaluation of extended end-plate beam-to-column joints subjected to bending and axial force." *Engineering Structures* (26): p.1333-1347.
- Liu, T.C.H; M.K Fahad; J.M Davies (1996) "Finite Element Modeling of Behaviors of Steel Beams and Connections in Fire". *Journal of Constructional Steel Research* (36): 181-199.
- Liu, T.C.H; M.K Fahad; J.M Davies (2002) "Experimental investigation of behaviour of axially restrained steel beams in fire". *Journal of Constructional Steel Research* (58): 1211-1230.
- Mao, C.J, Y.J Chiou, P.A Hsiao, M.C Ho (2009) "Fire response of steel semi-rigid beam-column moment connections". *Journal of Constructional Steel Research* (65): 1290-1303.

- Mao, C.J., Chiou, Y.J., Hsiao, P.A., Ho, M.C., (2010) "The stiffness estimation of steel semi-rigid beam-column moment connections in a fire." *Journal of Constructional Steel Research* (66): p. 680-694.
- Michal Strejček, Jan Řezníček, Kang-Hai Tan, František Wald (2011) "Behavior of column web component of steel beam to column joints at elevated temperatures". *Journal of Constructional Steel Research* (67): 1890-1899.
- M. R. Bahaari and A.N. Sherbourne (1994) "Computer Modeling of an Extended End-Plate Bolted Connection." *Computers and Structures (An Intl. Journal)*, Vol. 52(5): .879-893.
- Nelson, Thomas; Wang, Erke (2004) "Reiable FE Modeling with ANSYS". Paper presented in the International ANSYS Conference 2004.
- N.Kishi, A.Ahned, N.Yabuki (2001) "Nonlinear finite-element analysis of top-and seat angle with double web angle connections". *Structural Engineering and Mechanics* (12): 201-214.
- Pakala, P., V. Kodur, M. Dwaikat (2012) "Critical factors influencing the fire performance of bolted double angle connections." *Engineering Structures* (42): p. 106-114.
- Pirmoz, Akbar, Amir Saedi Daryan, Ahad Mazaheri, Hajar Ebrahim Darbandi (2008) "Behavior of bolted angle connections subjected to combined shear force and moment". *Journal of Constructional Steel Research* (64): 436-446.
- Pirmoz, Akbar, Amir Seyed Khoei, Ebrahim Mohammadrezapour, Amir Saedi Daryan (2009a) "Moment rotation behavior of bolted top-seat angle connections". *Journal of Constructional Steel Research* (65): p. 973-984.
- Pirmoz, Akbar, F.Danesh (2009b) "The seat-angle role on the moment-rotation response of Bolted Angle Connections". *Journal of Structural Engineering* (9): p.73-79.
- Pirmoz, Akbar, Danesh, Fakhroodin, Farajkhah, Vahid (2011) "The effect of axial beam force on moment-rotation curve of top and seat angle connections". *The Structural Design of Tall and Special Buildings*. Vol 20(7): p.767-783.
- Ramli Sulong, N. H. (2005). Behaviour of steel connections under fire conditions. PhD thesis, Imperial College London, University of London.

- Ramli-Sulong, N.H., A.Y. Elghazouli, B.A. Izzuddin (2007) "Behavior and design of beam-to-column connections under fire conditions". *Fire Safety Journal* (42): p.437-451.
- Rathburn J.C (1936) "Elastic Properties of Riveted Connections" *Trans. ASCE*, Paper No.1933, 101, 524-563.
- Reinosa, José Manuel, Alfonso Loureiro, Ruth Gutiérrez, Alicia Moreno (2008) "Nonlinear elastic-plastic 3D Finite Element Modeling - Top and seat angle connections with double web angle". Eurosteel 2008. 5th European Conference on Steel and Composite Structures.
- Sarraj Marwan (2007) "The behavior of steel fin plate connections in fire". Ph.D. thesis. University of Sheffield.
- Selamet, S. and M.E. Garlock (2010) "Robust fire design of single plate shear connections." *Engineering Structures* (32): p. 2367-2378.
- Shen. J & Astaneh (1999) "Hysteretic Behavior of Bolted Angle Connections". *Journal of Constructional Steel Research*(51): 201-218.
- Silva, L. Simões, Aldina Santiago, Paulo Vila Rael (2001) "A component model for the behaviour of steel joints at elevated temperatures". *Journal of Constructional Steel Research* (57): 1169-1195.
- Spyrou S. (2002) "Development of a component based model of steel beam-to-column joints at elevated temperatures". Ph.D thesis. University of Sheffield.
- Spyrou, S., J.B Davison, I.W Burgess, R.J Plank (2004a) "Experimental and analytical investigation of the 'tension zone' component within a steel joint at elevated temperatures". *Journal of Constructional Steel Research* (60): 867-896.
- Spyrou, S., J.B Davison, I.W Burgess, R.J Plank (2004b) "Experimental and analytical investigation of the 'compression zone' component within a steel joint at elevated temperatures". *Journal of Constructional Steel Research* (60): 841-865.
- Steenhuis, M., Jaspart, J.P., Gomes, F., Leino, T., (1998) "Application Of The Component Method To Steel Joints." *Proceedings of the Control of the Semi-Rigid Behaviour of Civil Engineering Structural Connections Conference*, Liege, Belgium: p.125-143.

- Tahir, Mahmood Md., Hussein, Mohd.Azman, Sulaiman, Arizu, Sharin Mohamed (2009) “ Comparison of Component Method with Experimental Tests for Flush End-Plate Connections using Hot-Rolled Perwaja Steel Sections”. *Steel Structures* (9): p.161-174.
- Theodore V. Galambos (1988) “Guide to Stability Design Criteria for Metal Structures”. 4th Edition, John Wiley & Sons: New York.
- Qian, ZH, Tan KH, Burgess IW (2008) “Behavior of steel beam-to-column joints at elevated temperature: Experimental investigation”. *Journal of Structural Engineering* (34): p.713-726.
- Qian, ZH, KH-Tan, I.W. Burgess (2009) “Numerical and analytical investigations of steel beam-to-colum joints at elevated temperatures”. *JCSR* (65): 1043-1054.
- Wang, M. and P. Wang, (2013) “Strategies to increase the robustness of endplate beam–column connections in fire”. *Journal of Constructional Steel Research*(80): p. 109-120.
- Wang, Wei Yong, Guo-Qiang Li, Yu-li Dong (2007) “Experimental study and spring-component modeling of extended end-plate joints in fire”. *Journal of Constructional Steel Research* (63): p. 1127-1137.
- Wang, Y.C., X.H. Dai, C.G. Bailey (2011) “An experimental study of relative structural fire behaviour and robustness of different types of steel joint in restrained steel frames.” *Journal of Constructional Steel Research* (67): p. 1149-1163.
- Yang, J.G, T.M Murray, R.H Plaut (2000) “Three-dimensional finite element analysis of double angle connections under tension and shear”. *JCSR* (54): p. 227-244.
- Yang, J.G, G.Y Lee (2007) “Analytical models for the Initial Stiffness and ultimate moment of a double angle connection”. *Engineering Structures* (29): p. 542-551
- Yang, J. G. and Jeon, S. S. (2009) “Analytical models for the initial stiffness and plastic moment capacity of an unstiffened top and seat angle connection under a shear load”. *International Journal of Steel Structures* (9): p. 195-205.
- Yang, J.G., Choi, J.H., Kim, S.M., (2011) A Finite Element Model for the Prediction of the Behavior of an Unstiffened Top and Seat Angle Connection with Various Top Angle Bolt Gage Distances”. *Journal of Asian Architecture and Building Engineering* (10): p. 367-374.

- Yang, KC, SJ-Chen, MC-Ho (2009) "Behavior of beam-to-column moment connections under fire load". *Journal of Constructional Steel Research* (65): 1520-1527.
- Yang, W.H., Chen, W.F., (1999) "Experimental Study On Bolted Unstiffened Seat Angle Connections". *Journal of Structural Engineering* (125): p.1224-1231.
- Yu, H., Burgess, I. W., Davison, J. B., & Plank, R. J. (2008). Experimental investigation of the tying capacity of web cleat connections in fire. *EUROSTEEL*, Graz, Austria.
- Yu, Hong-xia, I.W Burgess, J.B Davison, R.J Plank (2009a) "Tying capacity of web cleat connections in fire, Part 1: Test and finite element simulation". *Engineering Structures* (31): 651-663.
- Yu, Hong-xia, I.W Burgess, J.B Davison, R.J Plank (2009b) "Experimental investigation of the behavior of fin plate connections in fire". *Journal of Constructional Steel Research* (65): 723-736.
- Yuan, Zhen; K.H, Tan; K.T, Seng (2011) "Testing of composite steel top-and-seat-and-web angle joints at ambient and elevated temperatures, Part 1: Ambient tests". *Journal of Engineering Structures* (33): 2727-2743
- Zoetemeijer P. (1974) "A design method for the tension side of statically loaded bolted beam-to-column connections." *Heron*; 20(1):1-59.